

Characterization of the Poxviral Encoded Ubiquitin Ligase p28

by

Bettina Jessica Lehman

A thesis submitted in partial fulfillment of the requirements for the degree of

Doctor in Philosophy

in

Virology

Medical Microbiology and Immunology

University of Alberta

© Bettina Jessica Lehman, 2015

## **ABSTRACT**

Many cellular processes are regulated by the ubiquitin proteasome system (UPS), which utilizes the polypeptide ubiquitin to mark proteins for destruction via the 26S proteasome. Since the UPS plays an important role in cellular homeostasis, many viruses have evolved strategies to regulate the process of ubiquitination to their own advantage. Poxviruses also manipulate the UPS by encoding E3 ubiquitin ligases to target cellular or viral proteins for ubiquitination. This allows poxviruses to exploit the UPS and manipulate a wide range of cellular processes.

p28, a poxvirus encoded ubiquitin ligase, was first described in ectromelia virus (ECTV). p28 contains an N-terminal Kila-N DNA binding domain and a C-terminal RING-domain that is necessary for the ubiquitin ligase activity. Buller and colleagues demonstrated that deletion of p28 from ECTV results in a dramatic reduction in virus virulence, indicating its importance during viral infection. p28 is a highly conserved ubiquitin ligase that is expressed in a wide range of poxviruses, including Avipoxviruses. One distinguishing feature of the Avipoxviruses is their large genome, as exemplified by the prototypical members of fowlpox virus (FWPV) (288 kbp) and canarypox virus (CNPV) (365 kbp), encoding a number of yet uncharacterized proteins. FWPV and CNPV each contain two p28-like ubiquitin ligases. In contrast, non-Avipoxviruses encode only one p28-like ubiquitin ligase. FWPV and CNPV also encode additional Kila-N only genes lacking a RING domain; an observation not seen in other members of the poxvirus family. The data presented in this thesis demonstrate that both p28 homologues in FWPV, FWPV150 and FWPV157 are functional ubiquitin ligases located at the virus factories. Intriguingly, expression of FWPV150 started early in infection,

while FWPV157 was expressed late. We further demonstrated that each of the eight Kila-N domain-containing proteins were expressed during FWPV infection. Since many cellular and viral ubiquitin ligases are regulated through ubiquitination, we investigated whether this was true of p28. Our data confirmed a role for the RING domain for the self-ubiquitination of p28, but we further found that p28 is also regulated by another E3 ubiquitin ligase(s). It remains to be investigated whether ubiquitination changes p28 activity or if the ubiquitination is solely required for the proteasomal degradation of p28 at a certain stage during infection.

Finally, we conducted a mass spectrometry screen for p28 substrates, and identified heat shock protein 70 (HSP70) as an interaction partner of p28 during VACV infection. While we were unable to show that HSP70 is a substrate of p28, we demonstrated HSP70 enrichment at the virus factory in the presence of p28 when compared with VACVCop infected cells alone. This effect of HSP70 enrichment was conserved within the investigated p28 homologues. We further found that p28 residues 184-204 were important for recruiting HSP70 from the cellular nuclear and cytoplasmic pool to the virus factory. The importance of the p28 mediated HSP70 recruitment to the virus factory is to be determined.

In summary, this thesis characterized the expression, cellular localization and ubiquitin ligase activity of p28 homologues in FWPV. In addition, p28 RING and Kila-N mutants were characterized in terms of their ubiquitin ligase activity and interaction with ubiquitin and the UPS; in the end a mass spectrometry screen and follow up validation confirmed HSP70 as an interaction partner of p28.

## ACKNOWLEDGEMENTS

I would like to thank my initial supervisor, Dr. Michele Barry, for taking me into her lab and for this very interesting project. I would like to thank members of the Barry lab, especially Robyn-Lee Burton for all our therapeutic rant sessions, but also for sharing her accurate protocols and troubleshooting experiments. Thank you Dr. John Thibault for all the funny memories. You will be deeply missed. Thank you Ninad Metha; we've been though a lot together. Furthermore, I am very grateful for all the help and support from Dr. Ryan Noyce during his brief time in the Barry lab and continuing in the Evans lab, who went over and beyond his job description.

I especially would like to thank my current supervisor, Dr. Rob Ingham, for taking care of me in the last year and welcoming me into his lab. Thank you for all the support and guidance, but also for the freedom to develop and grow as a scientist. I really enjoyed working in your lab and I appreciate the inspiring and pleasant work environment. I have learned a lot during my time working for you, and I am forever grateful for this experience.

Next I would like to thank my committee members, Dr. David Evans and Dr. Edan Foley, for their helpful suggestions and reagents. Thank you Drs. David Evans, Mary Hitt, Maya Shmulevitz and Troy Baldwin and their labs for helpful discussions during lab meeting. Special thanks to Dr. Chad Irwin for all his help and knowledge. Thanks to Dr. Stephen Ogg and Greg Plummer for help with microscopy and to the office staff (Anne, Debbie and Tabitha) not only for their technical help but also for their kind words and support.

I am very fortunate to have made amazing friends in this department. Especially Kinola, Uli and Nancy; I would have not survived this experience without you. Thank you for all the crazy memories and for helping me to shake off the everyday nonsense with humor and/or a glass of wine.

Most importantly I would like to thank my family for all their encouragement and belief in me, which allowed me to succeed. I would like to thank my husband Scott, whom I admire and am insanely proud of. Your support and inspirational spirit has given me the strength to accomplish more than I ever thought possible.

## TABLE OF CONTENT

<b>ABSTRACT</b> .....	<b>i</b>
<b>ACKNOWLEDGEMENTS</b> .....	<b>i</b>
<b>TABLE OF CONTENT</b> .....	<b>v</b>
<b>LIST OF FIGURES</b> .....	<b>ix</b>
<b>LIST OF TABLES</b> .....	<b>xi</b>
<b>LIST OF ABBREVIATIONS</b> .....	<b>xii</b>
<b>CHAPTER 1: INTRODUCTION</b> .....	<b>1</b>
<b>1.1 Poxviruses</b> .....	<b>2</b>
<b>1.2 The <i>Poxviridae</i> family</b> .....	<b>2</b>
1.2.1 Orthopoxviruses .....	5
1.2.2 Avipoxviruses .....	8
<b>1.3 Poxviral genome structure</b> .....	<b>8</b>
<b>1.4 Virus life cycle/replication</b> .....	<b>10</b>
<b>1.5 Animal models of poxvirus infection</b> .....	<b>16</b>
<b>1.6 Poxvirus manipulation of host immune response</b> .....	<b>17</b>
<b>1.7 The Ubiquitin system</b> .....	<b>22</b>
1.7.1 Types of E3 ubiquitin ligases.....	24
1.7.2 Types of ubiquitination .....	25
1.7.3 Regulation of E3 ubiquitin ligases.....	28
1.7.4 Substrate regulation by ubiquitination .....	28
1.7.5 De-ubiquitinating enzymes .....	29
1.7.6 The 26S Proteasome .....	30
<b>1.8 Viruses manipulate the ubiquitin-proteasome system</b> .....	<b>33</b>
<b>1.9 Importance of ubiquitination and a functioning proteasome during poxvirus infection</b> .....	<b>35</b>
<b>1.10 Poxviral E3 ubiquitin ligases and adapter proteins</b> .....	<b>35</b>
<b>1.11 p28 and homologues</b> .....	<b>39</b>
<b>1.12 Hypothesis and study objectives</b> .....	<b>44</b>
<b>CHAPTER 2: MATERIALS AND METHODS</b> .....	<b>46</b>
<b>2.1 Cell Culture and Viruses</b> .....	<b>47</b>
2.1.1 Cell Lines .....	47
2.1.2 Viruses .....	47
<b>2.2 DNA Methodology</b> .....	<b>50</b>
2.2.1 Polymerase Chain Reaction .....	50
2.2.2 Agarose Gel Electrophoresis.....	57
2.2.3 Gel Extraction .....	57
2.2.4 Restriction Digests.....	58
2.2.5 DNA Ligation .....	58

2.2.6 Bacterial Transformation .....	59
2.2.7 Plasmid DNA Isolation .....	59
2.2.8 DNA Sequencing and Computer Analysis .....	60
2.2.9 Plasmids .....	60
2.2.10 Generation of pSC66-FLAG-FWPV150, pSC66-FLAG-FWPV157, pSC66-FLAG-FWPV075, and pSC66-FLAG-FWPV124.....	<b>Error! Bookmark not defined.</b>
2.2.11. Generation of pSC66-FLAG-FWPV150(C196S/C199S) and pSC66-FLAG-FWPV157(C218S/C221S).....	63
2.2.12 Generation of pSC66-FLAG-p28(1-184) and pSC66-FLAG-p28(1-204).....	64
<b>2.3 Transfections .....</b>	<b>64</b>
2.3.1 General Transfection Protocol .....	64
2.3.2 General Infection/Transfection Protocol.....	65
<b>2.4 Virus Generation and Manipulation.....</b>	<b>65</b>
2.4.1 General Virus Infection Protocol .....	65
2.4.2 Preparation of Virus Stocks .....	66
2.4.3 Virus Titre Determination.....	66
2.4.4 Preparation of Virus Genomic DNA.....	68
<b>2.5 Protein Methodology .....</b>	<b>69</b>
2.5.1 Antibodies .....	69
2.5.2 SDS Polyacrylamide Gel Electrophoresis .....	69
2.5.3 Semi-Dry Transfer .....	73
2.5.4 Western Blotting .....	73
2.5.5 Immunoprecipitation to detect ubiquitination.....	74
2.5.6 Acetone Precipitation of Cell Lysates.....	75
2.5.7 <i>In vitro</i> ubiquitination assay.....	76
2.5.8 Infection and immunoprecipitation for Mass Spectrometry .....	77
2.5.9 Coomassie Staining.....	77
2.5.10 Mass Spectrometry.....	78
<b>2.6 Bioinformatics .....</b>	<b>79</b>
2.6.1 Analysis of Functional Annotation Clustering .....	79
2.6.2 Protein sequence alignments.....	79
<b>2.7 Assays .....</b>	<b>79</b>
2.7.1 Reverse Transcription PCR to Detect Virus Gene Expression.....	79
2.7.2 Confocal Microscopy.....	80
2.7.3 Flow cytometry .....	81
2.7.4 Proteasome assay .....	82
<b>CHAPTER 3: FOWLPOX VIRUS ENCODES TWO P28-LIKE UBIQUITIN LIGASES THAT ARE EXPRESSED EARLY AND LATE .....</b>	<b>84</b>
<b>3.1 Introduction.....</b>	<b>85</b>
<b>3.2 Results .....</b>	<b>86</b>
3.2.1 FWPV and CNPV encode p28-like ubiquitin ligases.....	86
3.2.2 FWPV150 and FWPV157 localize to viral factories.....	88
3.2.3 FWPV150 and FWPV157 are ubiquitinated during infection and act as ubiquitin ligases .....	95
3.2.4 K48-linked ubiquitin localizes to viral factories in association with FWPV150 and FWPV157.....	100

2.3.5 FWPV150 and FWPV157 are expressed at different times during infection	103
<b>3.3 Summary and Brief Discussion</b>	<b>110</b>
<b>CHAPTER 4: THE POXVIRUS ENCODED UBIQUITIN LIGASE P28 IS REGULATED BY PROTEASOMAL DEGRADATION AND AUTOUBIQUITINATION</b>	<b>115</b>
<b>4.1 Introduction</b>	<b>116</b>
<b>4.2 Results</b>	<b>117</b>
4.2.1 Mammalian poxviruses and <i>Avianpoxvirus</i> FWPV do not inhibit the proteasomal system	117
4.2.2 p28 homologues co-localize with conjugated ubiquitin at the virus factory	119
4.2.3 The Kila-N DNA binding domain plays a critical role in localizing p28 to the virus factory, but does not affect the accumulation of conjugated ubiquitin at the virus factory	123
4.2.4 p28 RING mutants lost ubiquitin ligase activity	129
4.2.5 Both the Kila-N and RING domains of p28 are ubiquitinated in the presence of MG132	130
4.2.6 p28 catalytic non-functional RING mutants are still stabilized in the presence of MG132	134
4.2.7 An additional ubiquitin ligase promotes the accumulation of conjugated ubiquitin at the virus factory	137
<b>4.3 Summary and Brief Discussion</b>	<b>141</b>
<b>CHAPTER 5: IDENTIFICATION OF P28 INTERACTION PARTNERS</b>	<b>146</b>
<b>5.1 Introduction</b>	<b>147</b>
<b>5.2 Results</b>	<b>148</b>
5.2.1 Numerous cellular and viral proteins co-immunoprecipitate with FLAG-p28	148
5.2.2 Identification and functional grouping of p28 mass spectrometry hits	150
5.2.3 Verification of viral and cellular p28 mass spectrometry hits with co-immunoprecipitation studies	154
5.2.4 Confocal studies reveal that p28 leads to the enrichment of HSP70 at virus factories	159
5.2.5 p28 does not promote the ubiquitination of HSP70	<b>Error! Bookmark not defined.</b>
5.2.6 p28 homologues in MYXV and FWPV show a trend to trigger enrichment of HSP70 at the virus factory	172
5.2.7 Residues 1-204 within p28 are necessary for recruiting HSP70 to the virus factory	175
<b>5.3 Summary and Brief Discussion</b>	<b>178</b>
<b>CHAPTER 6: DISCUSSION AND FUTURE DIRECTIONS</b>	<b>181</b>
<b>6.1 Poxviruses modulate the UPS</b>	<b>182</b>
<b>6.2 p28 homologues in FWPV</b>	<b>182</b>
<b>6.3 Speculations on the origin of the p28 gene</b>	<b>185</b>
<b>6.4 Regulation of p28</b>	<b>186</b>
<b>6.5 Substrate identification of p28</b>	<b>188</b>
6.5.1 Limitations of mass spectrometry approach in this thesis	188

6.5.2 Alternative mass spectrometry approaches.....	189
6.5.3 Choice of cell lines and virus.....	191
6.5.4 Validation of poxvirus proteins as substrates of p28.....	192
6.5.5 p28 interaction with HSP70.....	194
<b>Conclusions.....</b>	<b>199</b>
<b>References.....</b>	<b>202</b>
<b>Appendix: Supporting methodology and data.....</b>	<b>242</b>

## LIST OF FIGURES

### CHAPTER 1: INTRODUCTION

Figure 1.1 Poxvirus structure and virus. ....	4
Figure 1.2 The genome of poxviruses (central and variable regions).....	12
Figure 1.3 Poxvirus life cycle. ....	15
Figure 1.4 ECTV pathogenesis. ....	19
Figure 1.5 Ubiquitination of target proteins. ....	27
Figure 1.6 The 26S Proteasome. ....	32
Figure 1.7 Poxviral E3 ubiquitin ligases and adapter proteins. ....	37
Figure 1.8 p28 E3 ubiquitin ligase. ....	43

### CHAPTER 3: Fowlpox Virus Encodes Two p28-Like ubiquitin Ligases That are Expressed Early and Late in Infection

Figure 3.1 Alignment of p28 homologues in FWPV and CNPV demonstrates conservation of the Kila-N and RING domains.....	87
Figure 3.2 FWPV150 and FWPV157 localize to viral factories. ....	89
Figure 3.3 FWPV150 and FWPV157 co-localize with conjugated ubiquitin to viral factories. ....	91
Figure 3.4 FWPV150 and FWPV157 localize with conjugated ubiquitin at virus factories in quail cells. ....	94
Figure 3.5 FWPV150 and FWPV157 are regulated by ubiquitination. ....	97
Figure 3.6 Ubiquitin ligase activity of p28, FWPV150, and FWPV157. ....	98
Figure 3.7 FWPV150, FWPV157 and double-cysteine mutants co-localize with HA-Ub and HA-K48-Ub.....	102
Figure 3.8 FWPV150 is expressed early and FWPV157 is expressed late during FWPV infection. ....	104
Figure 3.9 <i>Avipoxviruses</i> encode multiple Kila-N domains. ....	108
Figure 3.10 <i>Avipoxviruses</i> encode multiple Kila-N domain proteins that are expressed early during FWPV infection. ....	112

## **CHAPTER 4: The poxvirus encoded ubiquitin ligase p28 is regulated by proteasomal degradation and autoubiquitination.**

Figure 4.1 Mammalian poxviruses and <i>Avianpoxvirus</i> FWPV do not inhibit the proteasomal system.....	118
Figure 4.2 Alignment of p28 homologues.....	120
Figure 4.3 p28 homologues co-localize to the virus factory with conjugated ubiquitin in HeLa cells.....	122
Figure 4.4 p28 homologues co-localize to the virus factory with conjugated ubiquitin in macrophage cell lines.....	125
Figure 4.5 The KIL-A-N DNA binding domain plays a critical role in p28 localization to the virus factory, but does not affect the accumulation of conjugated ubiquitin at the virus factory.....	128
Figure 4.6 <i>In vitro</i> ubiquitin ligase activity of p28 and p28 mutants.....	131
Figure 4.7 p28 is regulated by ubiquitination.....	133
Figure 4.8 Mutations in the RING domain stabilize p28 (Kelly Mottet).....	136
Figure 4.9 RING mutants localize to virus factories with conjugated ubiquitin. ....	<b>Error!</b> <b>Bookmark not defined.</b>
Figure 4.10 p28 RING mutants demonstrate variable patterns of ubiquitination.....	140

## **CHAPTER 5: IDENTIFICATION OF P28 INTERACTION PARTNERS**

Figure 5.1 FLAG-p28 and FLAG-p28(C173S/C176S) mutant-interacting proteins.....	149
Figure 5.2 Analysis of functional annotation clustering for p28 mass spectrometry hits.....	153
Figure 5.3.1 Verification of viral and cellular p28 mass spectrometry hits with co-immunoprecipitation studies.....	156
Figure 5.3.2 Verification of cellular p28 mass spectrometry hits belonging to.....	157
Figure 5.4.1 p28 does not affect the cellular localization of MSH2, ATM, Exportin-1, and HSP90, but leads to enrichment of HSP70 at the virus factory.....	165
Figure 5.4.2 HSP70 does not co-localize with FLAG control protein.....	168
Figure 5.5 p28 does not lead to the ubiquitination of HSP70.....	171
Figure 5.6 p28 homologues in MYXV and FWPV show a trend to trigger enrichment of HSP70 at the virus factory.....	174

Figure 5.7 Residues 1-204 within p28 are necessary for recruiting HSP70 to the virus factory. ....	177
--	-----

## LIST OF TABLES

### CHAPTER 1: INTRODUCTION

Table 1.1 The poxvirus family.....	6
Table 1.2 Poxviridae Immunomodulators.....	21
Table 1.3 p28 homologues .....	41

### CHAPTER 2: MATERIALS AND METHODS

Table 2.1 Cells and viruses used in this study .....	49
Table 2.2 Oligonucleotides used in this study .....	56
Table 2.3 Plasmids used in this study .....	62
Table 2.4 Antibodies used in this study .....	72

## LIST OF ABBREVIATIONS

ANOVA	Analysis of variance
ALCAM	activated leukocyte cell adhesion molecule
APC	anaphase-promoting complex
APC11	anaphase promoting complex subunit 11
AraC	b-D-arabinofuranoside hydrochloride
ATCC	American type culture collection
ATM	ataxia telangiectasia mutated
ATP	adenosine triphosphate
BGMK	baby green monkey kidney cells
BLAST	Basic Local Alignment Search Tool
BrdU	5-bromo-2'-deoxyuridine
BSA	bovine serum albumin
BSL4	biosafety level 4
BTB	Bric-a-brack/tram-track/broad complex protein domain
CAS	cellular apoptosis susceptibility protein
CD4	cluster of differentiation 4
CD95	cluster of differentiation 95
CDC	Centres for Disease Control and Prevention
CMC	carboxyl-methyl cellulose
CNPV	canarypoxvirus
CMV	Cytomegalovirus
CPXV	cowpox virus
CRL	Cullin-RING ubiquitin ligases
Crm	Cytokine response modifier
CV-1	African green monkey kidney cells
CYLD	cylindromatosis
DAPI	4', 6' diamidino-2-phenylindole
DAVID	Database for Annotation, Visualization and Integrated Discovery
DMEM	Dulbecco's minimal essential media
DMSO	dimethyl sulphoxide
DNA	deoxyribonucleic acid
dNTP	deoxyribonucleotide triphosphate
DUB	deubiquitinating enzyme
DUF	domain of unknown function
dsDNA	double-stranded deoxyribonucleic acid
dsRNA	double-stranded ribonucleic acid
DTT	dithiothreitol
E1	Ubiquitin activating enzyme
E2	Ubiquitin conjugating enzyme
E3	Ubiquitin ligase

E6AP	E6-associated protein
EBNA1	Epstein–Barr nuclear antigen 1
EBV	Epstein-Barr virus
ECL	enhanced chemiluminescence
ECTV	Ectromelia virus
EDTA	ethylenediaminetetraacetic acid
EEV	extracellular enveloped virus
EGFP	Enhanced green fluorescent protein
EV	enveloped virus
Fwd	Forward
FWPV	fowlpox virus
GAPDH	Glyceraldehyde 3-phosphate dehydrogenase
GFP	green fluorescence protein
MCV	Molluscum contagiosum virus
HA	Hemagglutinin
HBV	Hepatitis B virus
HC	heavy chain
HCMV	Human cytomegalovirus
HECT	homologues to E6-associated protein carboxy terminus
HI-FBS	heat inactivated foetal bovine serum
HIV	Human immunodeficiency virus
HPV	Human papilloma virus
HRP	Horse radish peroxidase
HSP	Heat shock protein
HSV	Herpes Simplex Virus
IBD	Institute for Biomolecular Design
ICAM-1	Intercellular Adhesion Molecule 1
ICP0	infected-cell polypeptide 0
ICTV	International Committee on the Taxonomy of Viruses
IFI16	gamma-interferon-inducible protein 16
IFN	interferon
IL	interleukin
IMP	inflammation modulatory proteins
IP	immunoprecipitate
IPTG	isopropyl $\beta$ -D-1-thiogalactopyranoside
IRF3	interferon regulatory factor 3
ITR	inverted terminal repeat
IV	immature virus
JAMM	Jab1/MPN domain-associated metalloisopeptidase
kbp	kilobase pairs
kDa	kilodaltons
LacZ	$\beta$ -galactosidase
LB	Luria-Bertani broth
LC	light chain
LC-MS/MS	liquid chromatography-tandem mass spectrometry
LMB	Leptomycin B

LMP	low melting point
LMP1	latent membrane protein 1
LMP2A	latent membrane protein 2A
LUBAC	linear ubiquitin chain assembly complex
MARCH	membrane associated RING-CH
MCMV	murine cytomegalovirus
MCP	Molecular and Cellular Proteomics guidelines
Mdm2	Mouse double minute 2 homolog
mg	milligram
MHC	major histocompatibility complex class I
MJD	Machado-Josephin-domain
mL	milliliter
mM	milimolar
MOI	multiplicity of infection
MPXV	monkeypox virus
mRNA	messenger ribonucleic acid
MSH2	DNA mismatch repair protein 2
MSH6	DNA mismatch repair protein 6
MVA	Modified vaccinia Ankara
MYXV	myxoma virus
MV	mature virus
MVA	modified vaccinia Ankara
MyD88	myeloid differentiation primary response 88
N/A	not applicable
NCBI	National Centre for Biotechnology Information
NCS	newborn calf serum
NEM	N-Ethylmaleimide
NES	nuclear export signal
NLS	nuclear localization signal
ns	non significant
NBF	neutral-buffered formalin
NFκB	nuclear factor kappa B
ORF	open reading frame
OUT	ovarian tumor domain proteins
PAGE	polyacrylamide gel electrophoresis
PARG	Poly(ADP-ribose) glycohydrolase
PBS	phosphate buffered saline
PCNA	Proliferating cell nuclear antigen
PCR	polymerase chain reaction
PECAM-1	Platelet endothelial cell adhesion molecule 1
pE/L	synthetic poxviral early/late promoter
PKR	protein kinase R
PML	Promyelocytic leukemia protein
PVDF	polyvinylidene fluoride
PFA	paraformaldehyde
PFU	plaque forming unit

Rev	Reverse
RING	Really Interesting New Gene
RIPA buffer	Radioimmunoprecipitation assay buffer
RLU	relative light units
RNA	ribonucleic acid
RNF8	ring finger protein 8
RNF168	ring finger protein 168
ROI	Region of interest
Rpm	rotations per minute
RT-PCR	Real time polymerase chain reaction
SCF	Skp-1/Cullin-1/F-box
SDS	sodium dodecyl sulfate
Serp1	stress-associated endoplasmic reticulum protein 1
SILAC	Stable isotope labeling of amino acids in cell culture
SOC	super optimal broth with catabolite repression
SPI	serpin
SSC	standard saline citrate
SPICE	smallpox inhibitor of complement enzymes
ssDNA	single-stranded DNA
STAT1	Signal Transducers and Activators of Transcription family of transcription factors 1
SUMO	Small Ubiquitin-like Modifier
TAGC	The Applied Genomics Centre
TAE	Tris-acetate buffer
TBK1	TANK-binding kinase 1
TBST	tris-buffered saline plus Tween 20
TCC	Training Consulting Centre
TK	thymidine kinase
TNF	tumor necrosis factor
TMRE	tetramethylrhodamine ethyl ester
TRAF6	tumor necrosis factor receptor-associated factor 6
tRNA	transfer RNA
U	Unit
Ub	ubiquitin
Ubc13	Ubiquitin-conjugating enzyme 13
UCH	ubiquitin C-terminal hydrolase
UPS	ubiquitin-proteasome system
USP	ubiquitin specific protease
v/v	volume per volume
VACV	vaccinia virus
VACVCop	vaccinia virus copenhagen
VARV	variola virus
VCP	valosin-containing protein
vFLIPs	viral Fas-associated death domain-like interleukin-1 $\beta$ converting enzyme inhibitory protein
vCD30	viral cluster of differentiation 30

w/v	weight per volume
WB	Western blotting
WCL	whole cell lysates
WGA	wheat germ agglutinin
WHO	World Health Organization
WR	Western Reserve
WT	wild type
X-Gal	5-Bromo-4-chloro-3-indolyl- $\beta$ -D-galactosidase

## **CHAPTER 1: INTRODUCTION**

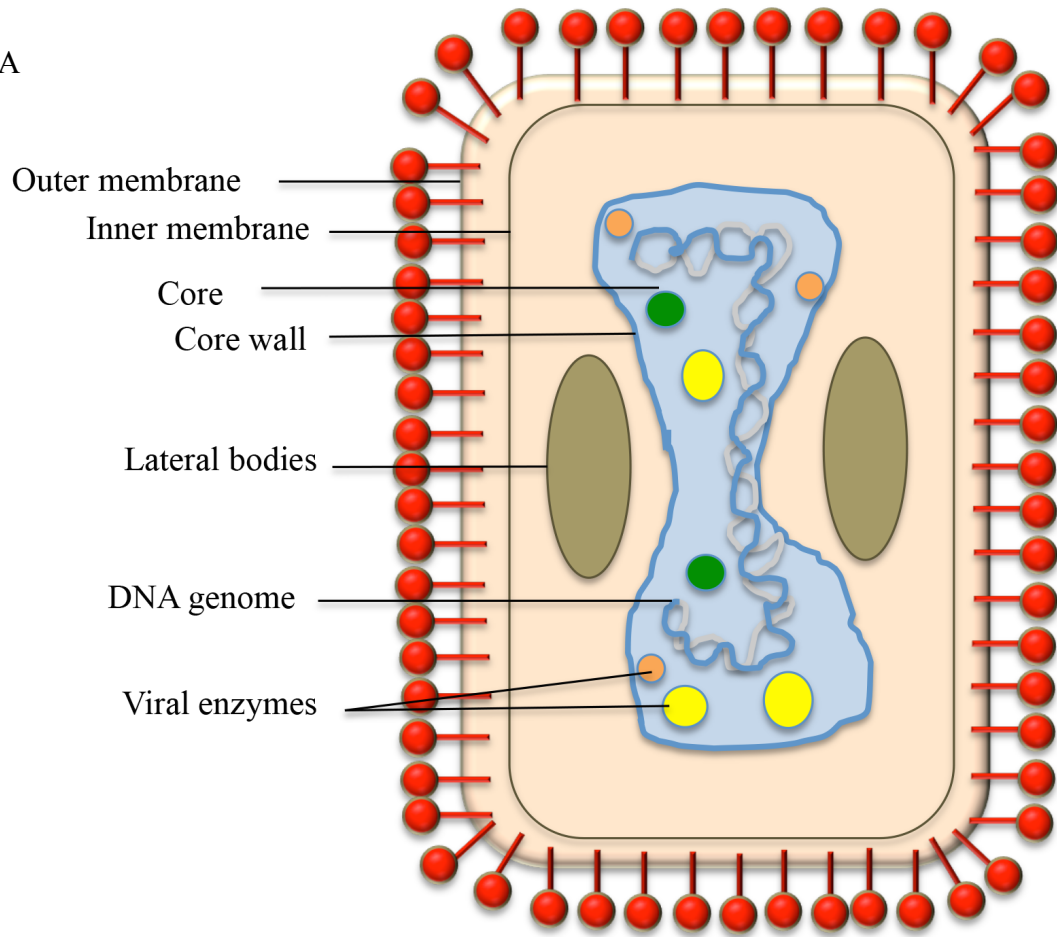
## 1.1 Poxviruses

*Poxviridae* are double-stranded DNA (dsDNA) viruses capable of infecting a wide range of hosts (1). Viruses within this family are enveloped and large in size, with dimensions of 200 nm x 300 nm, and appear brick-shaped under an electron microscope. Unlike most other families of DNA viruses, poxviruses replicate exclusively in the cytoplasm in so-called virus factories (**Figure 1.1**) (1). Since poxviruses complete their life cycle in the cytoplasm, their genomes encode the majority of the structural proteins and enzymes needed for gene expression and replication (2). The rest of the poxviral genome is dedicated to host-specific virulence factors, which are crucial for infection *in vivo* and dictate host range, immune evasion strategies and host cell manipulation in general (2, 3). Studying poxviral virulence factors is a powerful way to understand the complexity of virus-host interactions, host immune response and cellular pathways. This work focuses on characterizing a poxviral virulence factor called p28 and the role it plays during infection.

## 1.2 The *Poxviridae* family

The *Poxviridae* family contains over forty-six different poxviruses, which infect a wide range of hosts, both vertebrate and invertebrate (1). The International Committee on the Taxonomy of Viruses (ICTV) divided poxviruses into two subfamilies, called *Chordopoxvirinae* and *Entomopoxvirinae* (4). The *Entomopoxvirinae* subfamily consists of fewer members and exclusively infects invertebrates. The more intensively studied

A



B

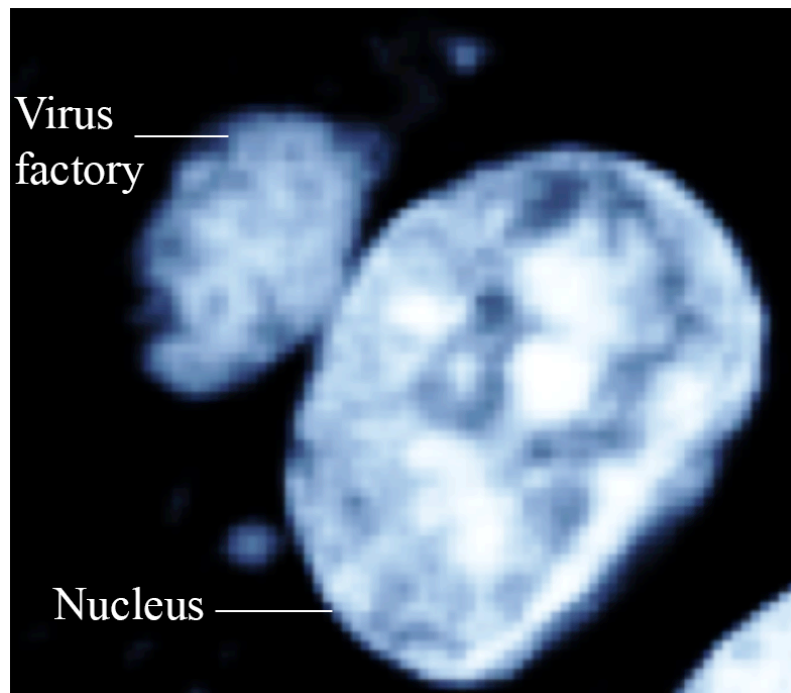


**Figure 1.1 Poxvirus structure and virus.** (A) Virion structure of poxviruses. The poxviral dsDNA genomes are enclosed in a dumbbell shaped viral capsid. Lateral bodies, which are protein rich structures, containing enzymes necessary for initiating the next round of infection, are found besides both sides of the core. The virion contains an inner and outer membrane. (B) Poxviruses replicate in the cytoplasm in so-called virus factories. Here, we infected HeLa cells with VACVcop for 12 hours, and then fixed and stained with DAPI (4',6-diamidino-2-phenylindole), a fluorescent stain that binds strongly to A-T rich regions in DNA, to visualize nuclei and virus factories.

*Chordopoxvirinae* subfamily infects vertebrates and can be subdivided into the *Avipoxvirus*, *Capripoxvirus*, *Cervidpoxvirus*, *Leporipoxvirus*, *Molluscipoxvirus*, *Orthopoxvirus*, *Parapoxvirus*, *Suipoxvirus*, and *Yatapoxvirus* genera. These genera are classified based on host range, serological cross-reactivity between members, disease pathology and genetic similarity (**Table 1.1**) (1, 4). Two genera are of particular interest to our work on characterizing homologues of the virulence factor p28: Orthopoxviruses and Avipoxviruses.

### **1.2.1 Orthopoxviruses**

Orthopoxviruses contain the most medically relevant poxviruses for humans including variola virus (VARV, discussed more in Section 1.2.1.1), Vaccinia virus (VACV) and monkeypox virus (MPXV) (1). In total, there are fourteen species classified as Orthopoxviruses with different host ranges and severity of disease (1, 5). Orthopoxviruses encode many genes that are homologous between members in this genus including those necessary for virus replication and immune modulation. However, there are still differences, which define their host tropism. VARV and ECTV are restricted to a single host, human and mice, respectively, causing severe symptoms with high mortality rates (6). In contrast, VACV, MPXV, and cowpox virus (CPXV) can infect a variety of hosts (1, 3). While VACV and CPXV cause mild diseases in humans, MPXV has been reported to cause outbreaks of smallpox-like symptoms in the Democratic Republic of the Congo (7-11). Today, VACV is the prototypical member of Orthopoxviruses and serves as an excellent model to study virus-host interactions.

Subfamily	Genus	Member
<i>Chordopoxvirinae</i>	<i>Avipoxvirus</i>	Canarypox virus Fowlpox virus Penguinpox virus
	<i>Capripoxvirus</i>	Goatpoxvirus Lumpy skin disease virus Sheeppox virus
	<i>Cervidpoxvirus</i>	Deerpoxvirus
	<i>Leporipoxvirus</i>	Myxomavirus Shope fibroma virus
	<i>Molluscipoxvirus</i>	Molluscum contagiosum virus
	<i>Orthopoxvirus</i>	Camelpox virus Cowpox virus Ectromelia virus Monkeypox virus Taterapox virus Vaccinia virus Variola virus
	<i>Parapoxvirus</i>	Bovine papular stomatitis virus Orf virus
	<i>Suipox virus</i>	Swinepox virus
	<i>Yatapoxvirus</i>	Tanapox virus Yaba-like disease virus Yaba monkey tumour virus
<b>Entomapoxvirinae</b>	<i>Entemopoxvirus alpha</i>	<i>Melontha melontha</i>
	<i>Entemopoxvirus beta</i>	<i>Amsacta moorei</i> <i>Melanoplus sanguinipes</i>
	<i>Entemopoxvirus gamma</i>	<i>Chrionimus luridus</i>

**Table 1.1 The poxvirus family.** The Poxvirus family infects vertebrates and invertebrates. The *Entomapoxvirinae* subfamily infects invertebrates and includes three genera. The *Chordopoxvirinae* subfamily contains nine genera, which infect a wide range of vertebrates. The genus *Avipoxvirus* infects birds. The genus *Capripoxvirus* infects sheep, cattle and goats. The members of the *Cervidpoxvirus* genus infect deer. *Leporipoxvirus* members infect rabbits. Members of the *Molluscipoxvirus* can infect humans. *Orthopoxvirus* members can infect camels, cows, mice, monkeys, humans, and other small mammals. *Parapoxvirus* infect sheep, cattle, or goats. *Suipox virus* infects swine, and *Yatapoxvirus* infects humans and non-human primates (12).

### **1.2.1.1 Variola virus**

Historically, VARV is the most infamous member of the Orthopoxviruses, which caused a devastating disease known as smallpox (3, 13). Smallpox is an ancient disease, with smallpox lesions reported as early as 5000 years ago on the remains of Egyptian mummies (14). VARV is a strict human pathogen and has not been reported in non-human hosts (15). It is transmitted via inhalation, which leads to infection of epithelia and respiratory mucosa. In the next stage, VARV infects lymphoid organs, which is followed by viraemia and skin lesions (1). There are two strains of VARV: variola major and variola minor. VARV has a mortality rate of up to 30-40%, while the minor strain is the milder form and has a death rate of less than 1% (1).

### **1.2.1.2 Orthopoxviruses used as a vaccination strains**

At the end of the 18<sup>th</sup> century, Dr. Edward Jenner used a CPXV strain for vaccination against smallpox. This was the first recorded demonstration of vaccination, which made Dr. Jenner the “Father of Vaccination” (16). Thanks to an extensive vaccination program, the World Health Organization (WHO) declared that smallpox was eradicated in 1979 (16). Over the years, the smallpox vaccine components switched from CPXV and HPXV to VACV. However, the origin of VACV remains unknown and controversial. Some argue that VACV arose from vaccine farms during the eradication campaign (1, 13, 17). VACV is closely related genetically to VARV; however, it rarely causes disease in healthy individuals (17). With a wide host range, VACV provides protective immunity against smallpox. All variola virus stocks were collected in 1978 after a laboratory outbreak in the UK and are currently contained in only two BSL4 facilities worldwide

(The Vector Institute in Russia and the Centres for Disease Control and Prevention (CDC) in Atlanta) (18-21). Today, VACV and other members of the *Poxviridae* family are used as a tool to study host-virus interactions.

### **1.2.2 Avipoxviruses**

Avipoxviruses are evolutionally more divergent from Orthopoxviruses and generally infect birds (**Table 1.1**). Fowlpox virus (FWPV) and canarypox virus (CNPV) are the best-characterized members of the *Avipoxvirus* family (22, 23). FWPV infection in poultry leads to lesions and scabs on the skin, or in severe cases, to lesions in the upper gastrointestinal and respiratory tracts (24). Typically, transmission depends on contact and shedding from lesions due to increased stress (24). FWPV poses a serious agriculture problem in poultry houses, as it leads to decreased flock performance and egg production, resulting in significant economic loss (24). Luckily, vaccines are available in the form of attenuated FWPV (25, 26). Furthermore, Avipoxviruses like FWPV and CNPV are also suitable candidates for safe vaccination vectors in humans since they infect mammalian cells. In mammalian cells they only express early proteins, but are unable to replicate due to restricted host range (27). Even though FWPV is a prototypical member of Avipoxviruses with applications for vaccines, most of their host range and immune evasion genes still remain unexplored.

### **1.3 Poxviral genome structure**

Poxviruses contain some of the largest viral genomes with sizes ranging from 150-300 kbp, encoding 150 to 350 ORFs (1). The poxviral dsDNA is connected by hairpin loops

at the inverted terminal repeats (ITR) that contain AT-rich regions (1). The VACV genome was originally characterized via a *HindIII* restriction enzyme digestion of the VACV genome, which was used to define genomic fragments. The resulting DNA fragments were alphabetically named (A to P) based on the *HindIII* digested fragment length and were assigned a number reading from the left to the right hand side (**Figure 1.2**). Furthermore, depending on the direction in which the ORF was transcribed, it was named “R” for right or “L” for left (e.g. F1L). The genome consists of a central region with highly conserved genes, including transcription factors, polymerases, factors important for viral replication, and structural proteins (28). Collectively, these gene products allow poxviruses to replicate in cytoplasmic compartments known as viral factories, mostly independent from the host replication machinery (2). Around 100 of these central genes are conserved within the *Orthopoxvirus* genus, while 50 are conserved across all poxviruses (28, 29). Poxvirus genes do not contain introns and the viral mRNA is not spliced, which allows further independence of poxvirus transcription from the host transcription machinery. Two variable regions flank the central region of the poxviral genome. Typically, these variable regions contain less conserved genes. Many are unique and non-essential ORFs to the individual virus and are typically important for host range, virulence, and immune evasion capabilities (20, 30, 31). Deletion of genes within the variable region usually does not affect the ability of the virus to replicate in cell culture *in vitro*. Rather, these genes are usually important *in vivo* for immune evasion strategies and host range (2, 29). Interestingly, there are no genes within the variable region of the genome that are found in all known members of the

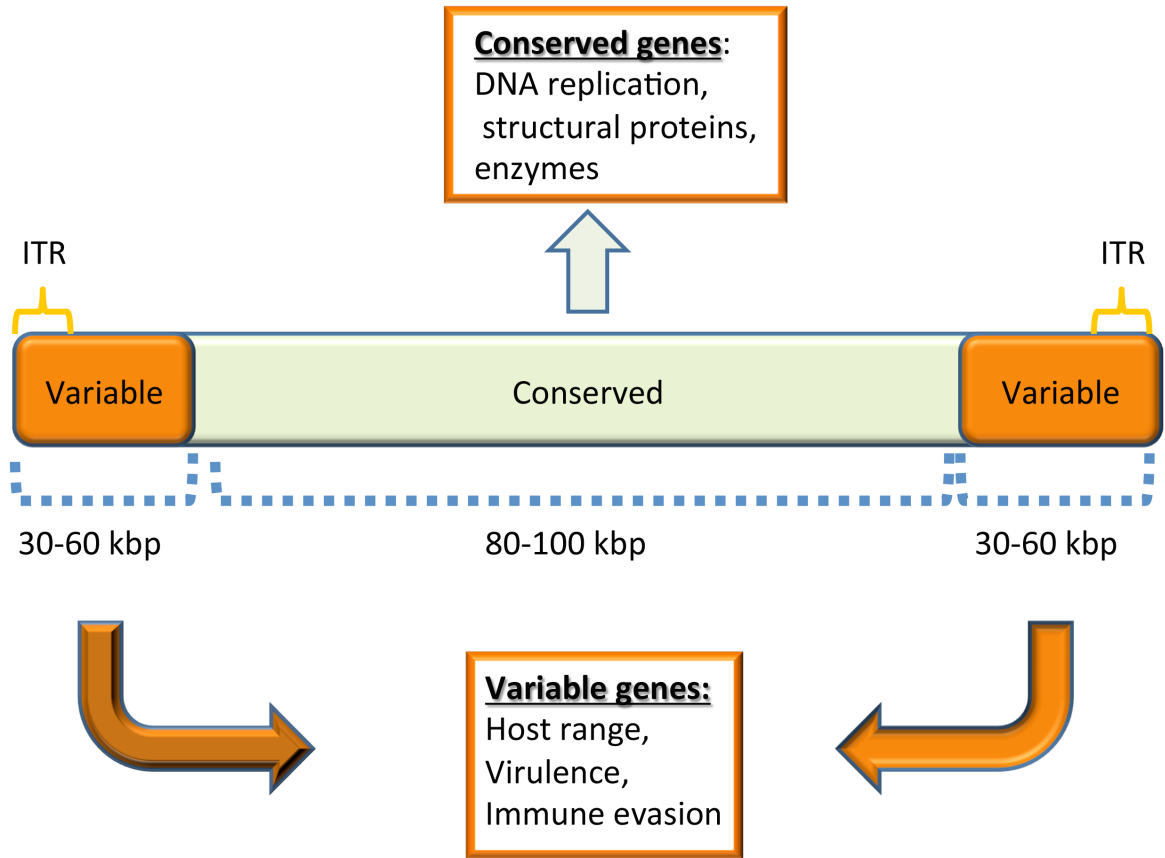
Orthopoxviruses (28, 29). This presents a contrast with genes in the central region, which are crucial for virus replication.

#### **1.4 Virus life cycle/replication**

Poxviruses can enter their host cell by binding to a number of different cell surface molecules. These include heparan sulfate, glycosaminoglycans, laminin, or chondroitin sulfate (32-35). In the case of VACV, the entry-fusion complex involves proteins A21, A28, H2 and L5 on the outer membrane, which allows fusion and cell entry via endocytic uptake of the virus particle (36-41). Following internalization of the poxvirus core into the cytoplasm, cores travel via microtubules to sites near the nucleus, where virus replication is initiated (**Figure 1.3**). Unlike other DNA viruses, poxviruses replicate exclusively in the cytoplasm in structures known as virus factories (42-44).

Virus factories are perinuclear DNA rich regions, which allow for viral replication, transcription, translation, and viral progeny formation. The number of virus factories is proportional to the multiplicity of infection (MOI) and can originate from a single virion (45, 46). The virus factory is structured and surrounded by cellular endoplasmic reticulum early during infection. This membrane disappears during virus assembly (47). Furthermore, there are subdomains within the virus factories, which provide distinct areas for viral gene transcription and translation (45).

A



B

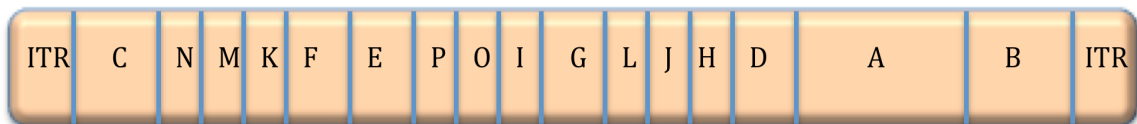


**Figure 1.2 The genome of poxviruses (central and variable regions).**

**(A)** The poxvirus genome contains a conserved region in the center of the genome, which is flanked by variable regions. At both the ends of the genome are inverted terminal repeats (ITR), which form hairpin loops to connect the double stranded DNA. **(B)** The genome is organized in letters, which represent the fragments after *Hind*III digestion of the VACVcop genome, A being the biggest and P, being the smallest fragment (48). The genome of poxviruses contains a central conserved region consisting of genes that are important for viral replication as well as structural proteins and enzymes. The terminal variable regions contain numerous genes that are important for tropism, immune evasion, and host range.

Poxvirus replication is organized into temporally distinct steps. These steps are dependent on the type of promoter and comprise early, intermediate, and late gene expression (49, 50). Early genes are transcribed and translated first, even before the virus core reaches the site of establishing a virus factory (2, 51). Early genes comprise roughly half of the genes encoded by the VACV genome and include genes that are important for uncoating, immune evasion, host tropism, expression of intermediate genes, and DNA replication (30, 52, 53). Early transcripts can be detected as early as 20 minutes and up to 4 hours post-infection. After transcription of early genes, intermediate genes are expressed, which encode for proteins that are crucial for DNA replication. DNA replication occurs between early and intermediate stages. Following DNA replication, late genes are expressed, which encode structural proteins required for virion assembly, transcription factors for early genes, RNA polymerase, transcript capping and methylation enzymes and budding from the host cell (2). Some of these late proteins are packed into virions for the next round of infection (2, 29). It is noteworthy that there is a distinct promoter sequence for each class of viral genes (50, 54). However, some genes are driven by promoters, which combine early, intermediate, or late promoters in tandem, upstream of the ORF, so that some genes are expressed during more than one stage of infection (50). A hybrid early/late promoter is used in this study to express transgenes from a vector, called pSC66, which was further used to create recombinant poxviruses that express transgenes from this hybrid promoter (54). After late protein synthesis, poxviruses begin the stage of virion morphogenesis, which is a maturation process that involves structural changes at the virus factory. It is still controversial whether the outer poxviral membrane of the virion is produced, or if it arises from an intermediate

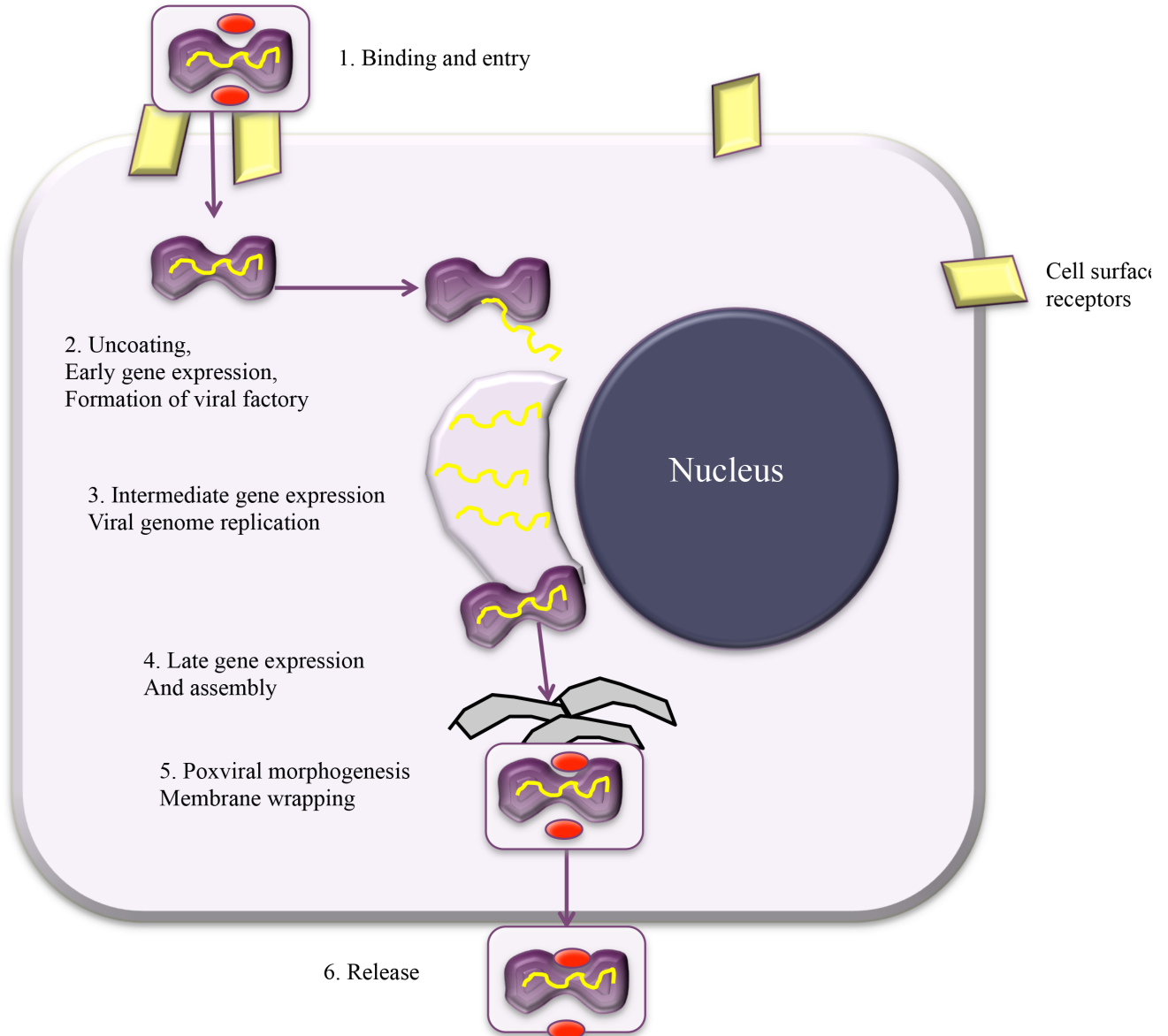


### **Figure 1.3 Poxvirus life cycle.**

**1.** Poxviruses bind to cell surface receptors, followed by a fusion event or endocytosis that leads to the release of the virion core into the host cell cytoplasm. **2.** The early genes are transcribed, which provide viral factors for immune evasion and uncoating. The virus factory is formed. **3.** Intermediate genes are expressed and the viral genome replicates. **4.** Late poxviral genes are transcribed, which encode structural proteins and enzymes that are packaged into virions, **5.** During poxviral morphogenesis, the genome is packaged into the new cores, which is followed by the formation of crescent shaped structures. **6.** Mature virions (MV) can be released via lysis or budding. MV can also acquire lipid membranes from the endosome or the Golgi-complex to form wrapped virus (WV), which release extracellular enveloped virions (EV) via fusion with the plasma membrane.

compartment of the Golgi apparatus and endoplasmic reticulum (44, 55). Following this first morphogenetic step, the immature virus particles develop into mature virions (MV) with a genome-containing core (2, 33). MVs constitute the majority of infectious poxviruses and are released from the host cell via lysis (33). In addition, some MVs undergo additional wrapping into a double-membrane derived from the endosome or trans-Golgi network to produce wrapped virions (WV), which leave the host cell before cell lysis (56-59). WV are transported to the cell surface through actin filaments. They fuse with the plasma membrane and release extracellular enveloped virions (EV) (33, 60, 61). EV can form actin projectiles, which can push the EV away from the cell to infect neighboring cells. This is crucial *in vivo* for lethal viral infection. In fact, many viral factors are investigated via knockout viruses in an ECTV mouse model to investigate their function during infection in a natural host (7, 62, 63).

### **1.5 Animal models of poxvirus infection**

ECTV infection of mice provides an excellent animal model to study poxvirus infection in a natural host, since it causes severe symptoms and disease in susceptible mouse strains (**Figure 1.4**) (7). Susceptible mouse strains include CBA, A/J, BALB/c and DBA/Z. Resistant mouse strains include C57/BL6 and AKR (3, 64). Resistance seems to correlate with the ability of the mouse strain to evoke a Th1-polarized immune response (65). In support of this, Jackson *et al.* demonstrated that a recombinant ECTV strain expressing interleukin-4, a Th2 cytokine, was lethal in non-susceptible mouse strains (66). This further implies the importance of a Th1 immune response against ECTV infection (66). Natural infection in mice begins following abrasions on the skin; with

virus replication occurring in the skin layers of the epidermis, followed by poxviral spread to the lymph nodes and bloodstream (**Figure 1.4**) (64). ECTV is carried by infected macrophages and replicates and disseminates within the host (67, 68). Macrophages play an important role in controlling virus infection, but can also be used as a tool for virus dissemination. ECTV uses macrophages to gain access to the liver through the bloodstream, where it is taken up by the liver macrophages called Kupffer cells. This leads to an infection of hepatocytes, extensive liver necrosis and death (69-71). Since ECTV belongs to the same *Orthopoxvirus* family as VARV and VACV, it contains a large number of similar immune modulator homologues, which makes it a great tool to study poxvirus virulence factors and pathogenesis (7, 20).

### **1.6 Poxvirus manipulation of host immune response**

Viruses have co-evolved with their hosts for millions of years. Hosts have developed both innate and adaptive immune responses to defeat viral infection and disease (72). In response, viruses have established mechanisms to evade the immune response in numerous ways (**Table 1.2**) (2, 20). Their large genome allows poxviruses to encode a multitude of immune evasion proteins that can inhibit the immune response at both extracellular and intracellular levels. Extracellular mechanisms include poxviral encoded secretory proteins, such as chemokine homologues, cytokine decoy receptors, and poxviral proteins that bind cytokines, chemokines, or complement factors (**Table 1.2**). Consequently, an inflammatory response in the host is inhibited. Poxviruses also encode proteins that inhibit the induction of intracellular immune signaling and apoptosis, disrupt receptor-ligand interactions and viral antigen presentation (30).

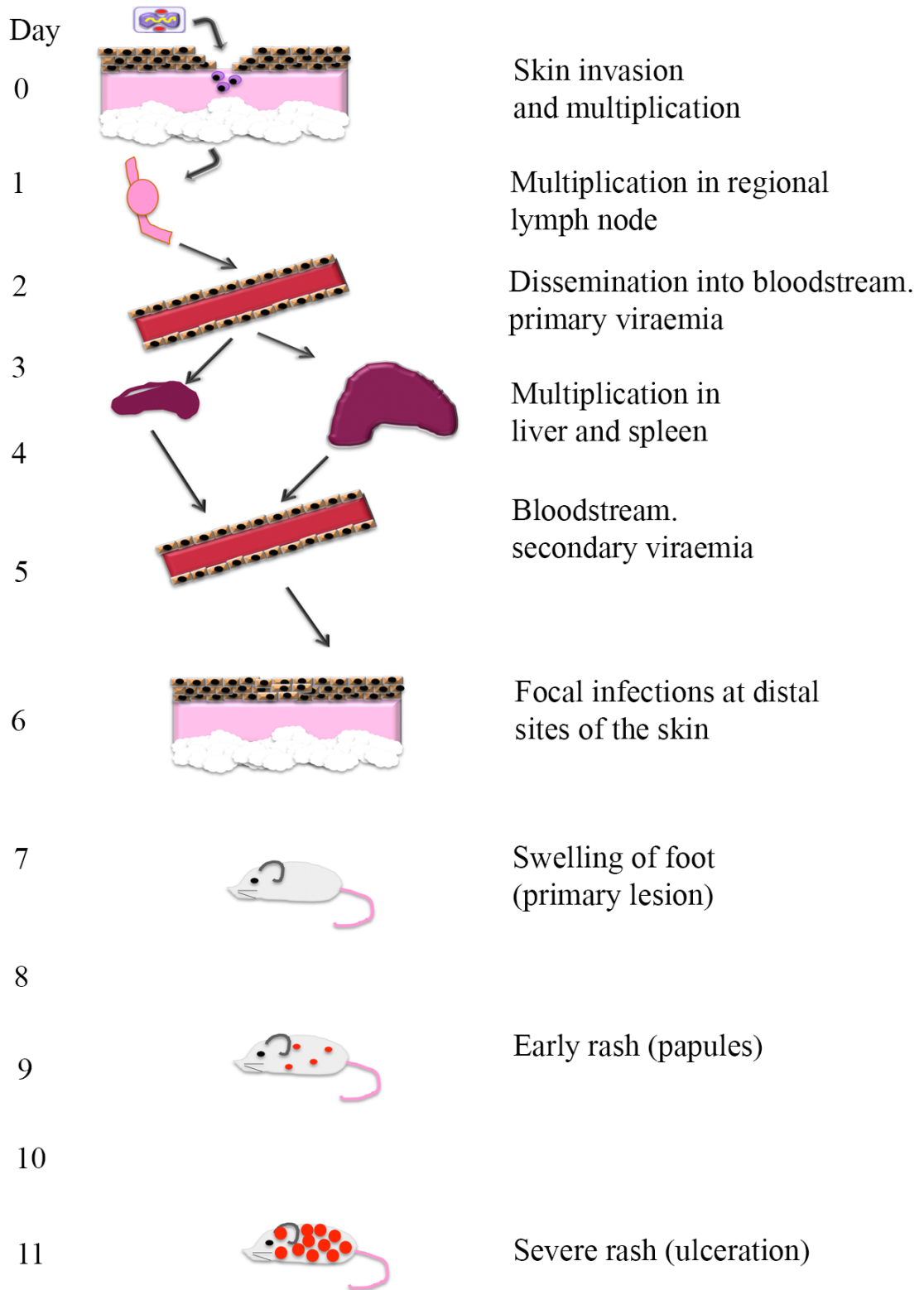


**Figure 1.4 ECTV pathogenesis.**

Adapted from Esteban et al. (7). ECTV infects the mouse through the skin in the footpad. The virus replicates and disseminates into the lymphatic system. Once ECTV spreads into the bloodstream, primary viraemia begins. This event allows viral infection of liver, spleen and other organs. When the virus is released from the organs, secondary viraemia starts. This results in infection of distal sites of the skin.

<b>Virostealth Genes</b>	<b>Virus</b>	<b>Mode of action</b>	<b>Reference</b>
M153R	Myxoma	Ubiquitin ligase; Down-regulation of MHC class I, CD4, ALCAM, CD95	(73, 74)
<b>Virotransducer</b>			
E3L	Vaccinia	dsRNA binding protein, inhibits PKR-induced IFN response	(75, 76)
H1L	Vaccinia	De-phosphorylates STAT1; prevents IFN response	(77)
K3L	Vaccinia	Prevents PKR-induced IFN response	(78)
K7L	Vaccinia	Prevents TBK1/IKK $\epsilon$ activation of IFN	(79)
CrmA, SPI-1, SPI-2	Cowpox	Intracellular serine protease inhibitors	(80-83)
F1L, M11L, FWPV039, DPV022	Vaccinia, Myxoma, Fowlpox, Deerpox	Anti-apoptotic proteins	(84-86)
vFLIPs	Molluscum	Signal transduction inhibitors	(87)
A46R	Cowpox	Toll-like receptor inhibitor	(83)

<b>Virokines</b>			
SERP-1, SPI-3	Vaccinia, Myxoma	Extracellular serine proteases	(88, 89)
D7L	Ectomelia	Il-18 binding proteins	(90, 91)
M-T7, M-T1	Myxoma	Chemokine binding proteins	(92-94)
VCP, IMP, SPICE	Vaccinia Cowpox Variola	Complement binding proteins	(95-97)
<b>Viroceptors</b>			
B15R	Vaccinia	IL-1 $\beta$ receptor homologue	(98)
B18R, B8R	Vaccinia	IFN receptor homologues	(18, 99)
M-T2, CrmB, CrmC, CrmD, CrmE, vCD30	Myxoma, Cowpox	TNF receptor homologs	(100-104)

**Table 1.2 Poxviridae Immunomodulators**

Poxvirus immunomodulatory proteins can be categorized as virostealth, virotransduction, and viromimicry (30). Virostealth proteins can mask virus infected cells, for example, by reducing cell surface molecules and subsequently preventing recognition by cytotoxic T cells. Virotransduction proteins can modulate cell signaling networks, which aids in minimizing effects of proinflammatory signaling and to create a favourable cellular environment for virus replication. Viromimicry include virokines, which mimic host cytokines or viroreceptors, mimicking cytokine receptors, to block extracellular immune signaling.

Poxviruses also encode a large number of proteins that inhibit NF- $\kappa$ B activation, and subsequent anti-viral mechanisms, including A46, A52, B13, B14, B15, E3, M2, N1, K1, and K7 (79, 98, 105-115). Furthermore, VACV proteins E3 and K3 prevent the host cell sensing of dsRNA (76, 78, 98). To further establish a cellular environment for optimal poxviral replication, poxviruses encode proteins to manipulate the UPS (116, 117).

### **1.7 The Ubiquitin system**

Ubiquitin is a highly conserved 76 amino acid protein with only three amino acid changes between the yeast and human homologue (118, 119). It is a globular protein, which is added post-translationally to lysine residues on the target protein. The C-terminus of ubiquitin contains a di-glycine motif, which forms a covalent bond with the lysine residue of the target protein. This modification is called ubiquitination and is important for a wide array of cellular functions such as cell cycle control, DNA repair, signal transduction, antigen processing and apoptosis (120-122). Ubiquitination can have diverse effects on the target protein depending on the type of labeling. Ubiquitin contains seven distinct lysine residues, K6, K11, K27, K29, K33, K48, and K63 (123). Any of these seven allows for the formation of ubiquitin chains. Furthermore, chemical structure and length of the ubiquitin chain can influence signalling outcomes (122). Monoubiquitination with the addition of a single ubiquitin molecule can lead to histone modification, and regulate endocytosis, protein trafficking, or function of substrates (120). Polyubiquitin chains can lead to different outcomes depending on the type of chain linkage (120). Chains are connected by isopeptide bonds between a specific lysine residue of one ubiquitin and the carboxyl group of the next ubiquitin. Chains linked

through lysine 48 and lysine 63 are well-characterized (122, 124). Lysine 63 chains can modulate protein function in a non-proteolytic manner, including regulation of intracellular trafficking, DNA repair, and signal transduction pathways. In contrast, lysine 48 ubiquitin chains typically mark the proteins for degradation by the 26S proteasome to destroy old proteins or proteins with altered functions so their components can be recycled (120, 122, 125). Tight regulation of ubiquitination, which maintains a fine balance in the amount of proteins in cells, is crucial for avoiding cellular dysfunction that may result in diseases such as neurodegenerative disorders and cancer (120-122).

Regulation occurs through an enzymatic cascade including enzymes E1, E2, and E3 (**Figure 1.5**). E1 catalyzes formation of a thiol-ester bond in an ATP-dependent manner between itself and the carboxyl terminal glycine of ubiquitin, leading to the activation of ubiquitin (126). The E1 ubiquitin-activating enzyme is highly conserved and there is only one copy in most eukaryotic genomes (126). Activated ubiquitin is then transferred from E1 to the E2 ubiquitin conjugating enzyme (127). The human genome encodes at least 25 E2 conjugating enzymes, which interact with a distinct group of E3 ubiquitin ligases (122). The E2 enzymes contribute to the chain type and length of ubiquitin chain formed. For example, the E2 enzyme Ubc13 is important for K63-linked ubiquitin chains (128). In the final step, the E3 ubiquitin ligase binds both the target protein and E2 thioesterified with ubiquitin, and mediates the transfer of activated ubiquitin onto the target protein (122). Genes encoding hundreds of putative E3 ubiquitin ligases have been identified in the human genome. It is thought that every E3 ligase has its own unique set of target proteins for ubiquitination.

### 1.7.1 Types of E3 ubiquitin ligases

Two major types of E3 ligases are found in eukaryotes: homologues to E6-associated protein carboxy terminus (HECT) and Really Interesting New Gene (RING) proteins (129). HECT domain E3s were first discovered in Human papilloma virus (HPV) infection, where viral E6 proteins redirect cellular E6-AP to ubiquitinate and degrade p53 (130). HECT domains usually form thiol-ester intermediates with ubiquitin and transfer it onto the substrate, whereas RING domain E3 ligases transfer ubiquitin from E2 directly to the target protein. RING domains are conserved from yeast to humans and contain a highly conserved motif of 7 cysteines and one histidine buried in the 3D structure in the domain's core. This is important for maintaining the overall structure through binding of two zinc atoms (131). Only one quarter of RING domain E3 ligases contain the substrate-binding site in the same protein. The majority of RING E3 ligases act in multi-subunit protein complexes, where substrate recognition is mediated by a separate subunit (131). Examples of multi-subunit E3 ligases include the Skp-1/Cullin-1/F-box (SCF) complex and other Cullin-RING ubiquitin ligases (CRL) with diverse substrate-recognition subunits, like F-box or BTB domains (132). There are further subfamilies of RING ubiquitin ligases (133), including U-box and RING-CH domain-containing proteins, which are structurally similar, but have variations within the RING domain (134, 135). The U-box is structurally similar to the RING domain, but the zinc ions are replaced by hydrogen bonds to hold the structure in shape (136). The RING-CH domain, or membrane associated RING-CH (MARCH) domain, has a C4HC3 configuration in its RING domain (137). MARCH E3 ligases are predominantly membrane bound and are

associated with down-regulation of cell surface proteins (135). In this thesis, I will focus only on RING domain E3 ligases.

### **1.7.2 Types of ubiquitination**

Ubiquitination can occur in the form of mono-, multi-mono-, or poly-ubiquitination. Mono or multi-mono-ubiquitination can initiate the internalization of cell surface receptors and subsequent degradation in lysosomes (138, 139). Polyubiquitination chains can form through any of the seven lysine residues in ubiquitin (K6, K11, K27, K29, K33, K48, K63) (140). Furthermore, linear polyubiquitin chains can be formed by the catalytic activity of the linear ubiquitin chain assembly complex (LUBAC) (141). Since different ubiquitin chains have distinct structures, the type of ubiquitin chain dictates the fate of the target protein (138). To date, most investigations have focused on K48 and K63 (142-144). K63-linked chains are elongated, while K48-linked are compact chains (142, 143). A K48 tetramer chain is the minimal signal for proteasomal degradation (145). While the K48-linked chain is mostly known for proteasomal degradation, K11-linked chains can also lead to the degradation of target proteins. Targets for K11-linked chains include proteins that are involved in the cell cycle, and ER-associated proteins (146, 147). K29-linked chains play a role in lysosomal protein degradation (148). K63-linked chains are involved in NF- $\kappa$ B activation, DNA damage response, and down-regulation of cell

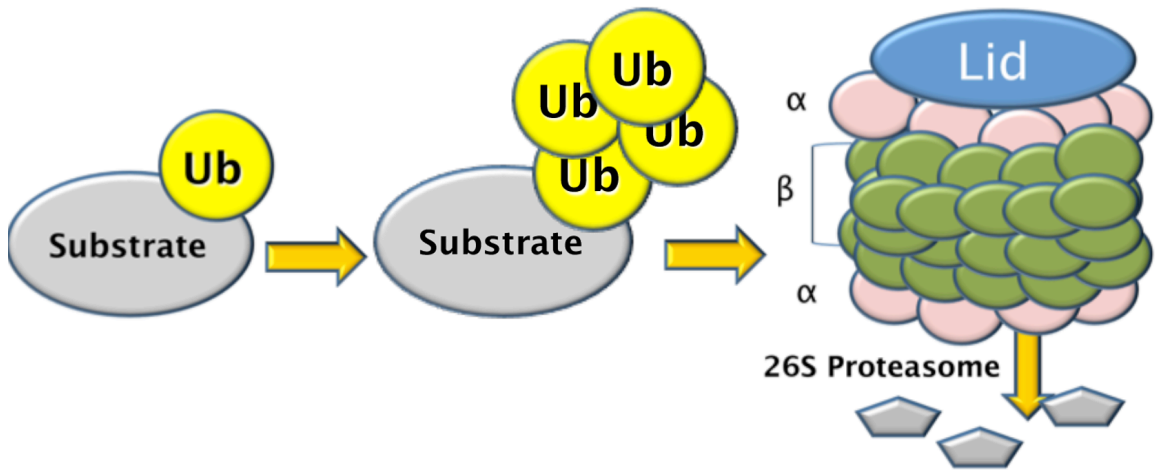
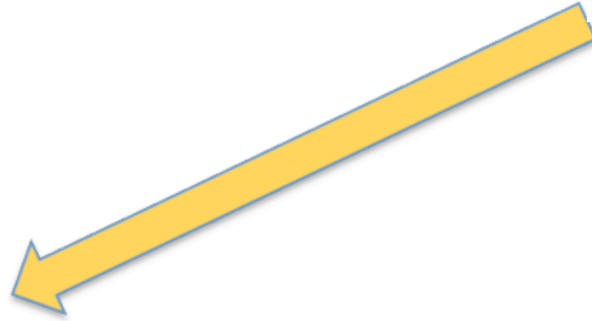
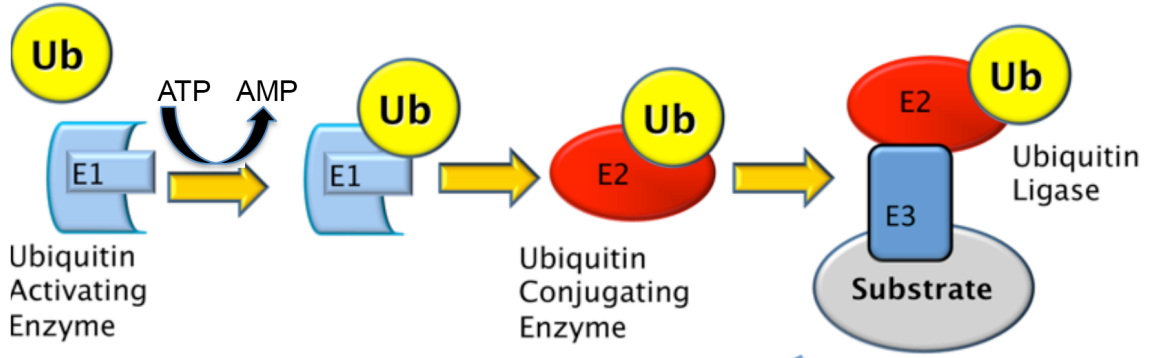


**Figure 1.5 Ubiquitination of target proteins.**

Free ubiquitin (Ub) is activated by the E1 activating enzyme in an ATP-dependent manner. Ub is transferred to the E2 ubiquitin conjugating enzyme. The E3 ubiquitin ligase interacts with both E2 and the protein substrate and mediates the transfer of activated Ub onto the target protein. In the case of K48-linked polyubiquitination, the labeled protein is targeted to the 26S proteasome for degradation.

surface receptors (128, 149-151). Recently, head to-tail-linked linear polyubiquitin chains formed by LUBAC has been demonstrated to be a critical regulator of the NF- $\kappa$ B pathway (152).

### **1.7.3 Regulation of E3 ubiquitin ligases**

Ubiquitin ligases are the key regulators of target proteins and therefore have to be tightly regulated (139). Post-translational modifications can target a protein for ubiquitination, but can also influence E3 ubiquitin ligase activity. For example, when the yeast E3 ubiquitin ligase APC is phosphorylated, there is increased ubiquitin ligase activity compared to the non-modified APC (153). Commonly, ubiquitin ligases are themselves regulated by ubiquitination as a feedback regulatory mechanism. This can occur through autoubiquitination or via another ubiquitin ligase (139). TRAF6 is an example of autoubiquitination, which occurs during stimulation of the NF- $\kappa$ B signal transduction pathway (154). When enough of a substrate is present for the ubiquitin ligase, it tends to be protected from autoubiquitination. In the absence of substrates, autoubiquitination serves as a regulatory mechanism, since their service is not needed (139, 155).

### **1.7.4 Substrate regulation by ubiquitination**

Most intracellular and many extracellular proteins experience regular turnover (156). Old or misfolded proteins are hydrolyzed down to amino acids and new proteins are built to replace them. This process is regulated by ubiquitin ligases and is very important for homeostatic functions. Either excessive breakdown, or accumulation of proteins can lead

to diseases (157). Deregulation of ubiquitination can lead to abnormal activation or shutdown of pathways, which can play a role in oncogenesis (158, 159). Furthermore, incorrect assembly of protein complexes can result in interference with inflammatory responses or impairment of DNA repair (160). Moreover, impaired ubiquitination can lead to accumulation of misfolded proteins, which is thought to play a role in neurodegenerative diseases and mislocalization of proteins (161).

The turnover rate for a given protein varies from minutes for some regulatory enzymes, to days/weeks for actin and myosin in skeletal muscle, to months for hemoglobin in erythrocytes (156). In some instances, ubiquitination is used to rapidly degrade specific proteins to permit adaptation to new physiological conditions. This includes the regulation of many transcription factors in order to modulate gene transcription (162). Ubiquitination of transcription factors can lead to their removal or re-location (163, 164). Monoubiquitination typically does not lead to proteolysis, but can lead to internalization of cell surface proteins (165) or regulation of transcription factors (166).

Different types of post-translational protein modification can stimulate ubiquitination. One of the most common is phosphorylation of the target protein. However, there are other mechanisms, which recruit E3 ubiquitin ligases to substrates, including glycosylation, nitrosylation, and deacetylation (156).

### **1.7.5 De-ubiquitinating enzymes**

De-ubiquitinating enzymes (DUB) play a further regulatory role by removing ubiquitin chains from the target protein and opposing the action of ubiquitin ligases. There are over

90 DUBs found in the human genome, which can be grouped into two families, including cysteine proteases and ubiquitin-specific metalloproteases (167). The former comprise the ubiquitin specific protease (USP), ubiquitin C-terminal hydrolase (UCH), ovarian tumor domain proteins (OTU), Machado-Josephin-domain (MJD), while the metalloproteases contain JAMM domain proteins (167-170).

USP7 is an example of a DUB, which targets ubiquitin ligases Mdm2, ICP0, MARCH7, and RING1B and regulates their stability (171). CYLD and A20 are DUBs that both have an inhibitory effect on the NF- $\kappa$ B pathway, via removing K63 ubiquitin chains from TRAF6 (172-174). Some DUBs have important roles as tumor suppressors and are mutated in a number of cancers (158, 159, 175).

### **1.7.6 The 26S Proteasome**

Many polyubiquitinated proteins are targeted to the 26S proteasome for degradation (176, 177). The 26S proteasome is a multi-protein complex, which consists of a barrel shaped 20S core particle with a 19S regulatory particle at either or both ends (**Figure 1.6**) (178, 179). Substrate entry is catalyzed by the 19S particle. This outer lid can bind the polyubiquitin chains and disassemble the ubiquitin chain to recycle ubiquitin for degradation of other proteins (180). The target proteins are then unfolded and translocated into the 20S core, which contains the catalytic activity of the proteasome (178, 179). The 20S core consists of four stacked rings. The outer two rings consist of non-catalytic  $\alpha$  subunits, while the inner two rings consisting of  $\beta$  subunits have the catalytic activity. All proteins that are targeted to the proteasome are subsequently processed and degraded into small peptides (181). An estimated 80-90% of intracellular

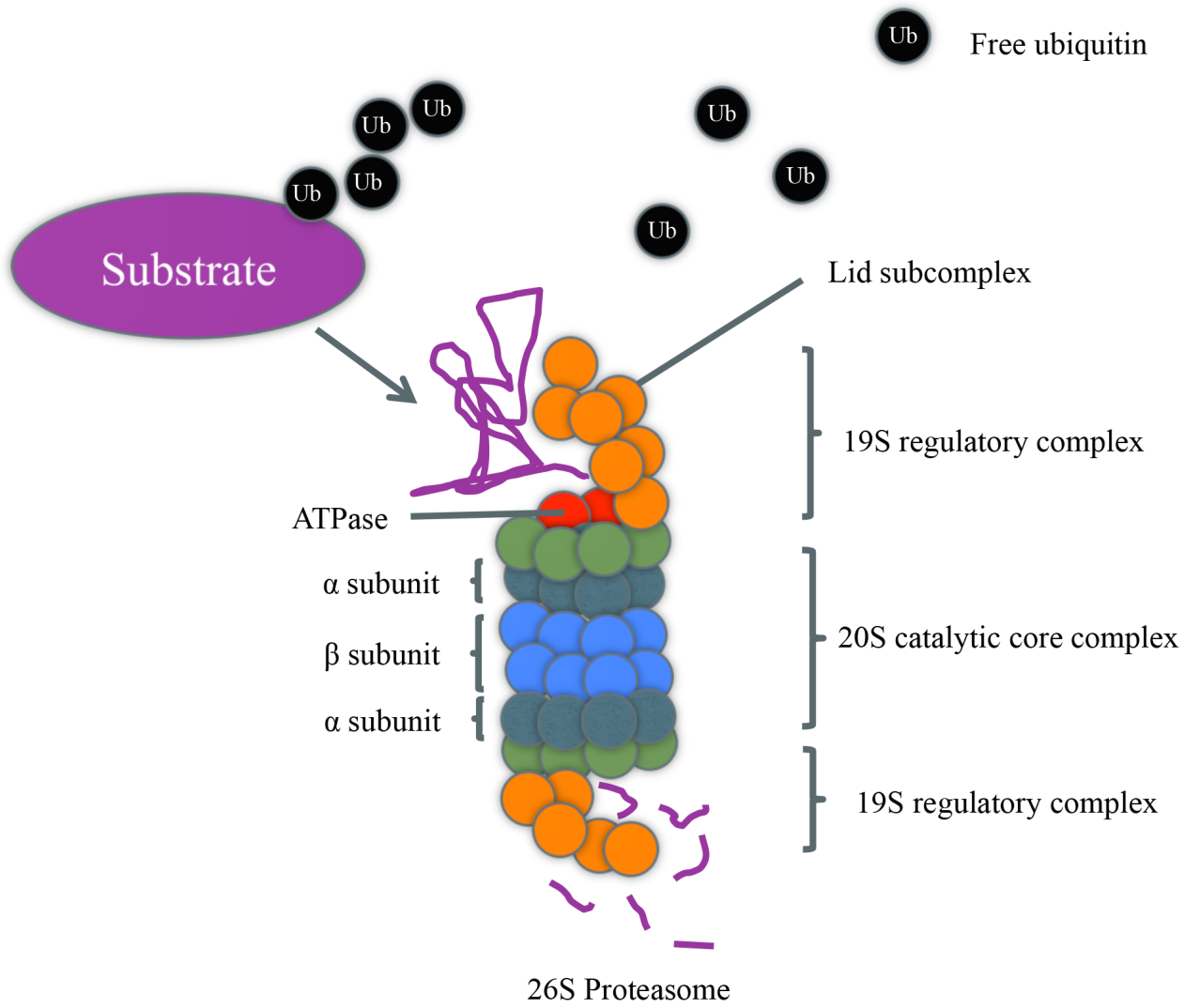


**Figure 1.6 The 26S Proteasome.**

Polyubiquitinated substrate proteins are targeted for proteolysis by the 26S proteasome. The ubiquitinated proteins are recognized by the lid subcomplex of the 19S regulatory complex and are deubiquitinated to reuse free ubiquitin for ubiquitination of other targets. Proteins are then unfolded and translocated into the 20S catalytic core complex. The 20S core consists of non-catalytic  $\alpha$  subunits and catalytic  $\beta$ -subunits.

proteins are degraded by the 26S proteasome (182). There are numerous chemical inhibitors of the 26S proteasome (183, 184). One of the most widely used proteasome inhibitors for cell biology experiments is the synthetic peptide aldehyde MG132, which inhibits the proteasome by targeting the chymotrypsin-like  $\beta 5$  subunit (93, 185). Some inhibitors are used in clinical settings, especially in cancer research (186, 187).

### **1.8 Viruses manipulate the ubiquitin-proteasome system**

Since viruses have adapted to interfere with cellular pathways, it is not surprising that many viruses have developed ways to manipulate the ubiquitin-proteasome pathway to their own advantage (116, 117, 188-199). It has been extensively shown that proteasome inhibitors interfere with the replication cycle of numerous human pathogens, such as herpesviruses (188, 189), adenoviruses (191), influenza viruses (192), coronaviruses (196), picornaviruses (198), hepadnaviruses (190), retroviruses (193-195), paramyxoviruses (197), rotaviruses (199), and poxviruses (116, 117). This underlines the importance of a functional ubiquitin-proteasome system for viruses. One of the first examples was discovered in HPV, where the viral E6 protein interacts with a cellular ubiquitin ligase E6AP (UBE3A), which leads to the ubiquitination and subsequent degradation of p53 to prevent apoptosis of the host cell (130). In addition to inhibition of apoptosis, ubiquitination is required for functional gene expression during infections such as with Epstein-Barr virus (EBV) and human immunodeficiency virus-1 (HIV-1) (200-202). EBV proteins LMP2A and LMP1 regulate replication by interacting with ubiquitin ligases or DUBs (203, 204). Viruses also exploit ubiquitination for manipulation of the immune response, downregulation of immune signaling proteins, inhibition of MHC

Class I antigen presentation, inhibition of viral induced apoptosis, modulation of NF- $\kappa$ B activation, interferon regulatory factor 3 (IRF3), and type I interferon (IFN) responses (205-212).

Some large DNA viruses encode their own ubiquitin ligases or adapter proteins. Kaposi's Sarcoma-Associated Herpesvirus encodes viral E3 ligases K3 and K5 that are responsible for immune evasion strategies. These target MHC class I antigen presentation to cytotoxic T cells and modulation of ICAM-1 and PECAM-1 to diminish antiviral cytokine release (213, 214). Another example is Herpes Simplex Virus (HSV) protein ICP0, which contains a RING finger domain and acts directly as an E3 ligase responsible for ubiquitination of cellular proteins PML, SUMO, IFI16, MyD88, NF- $\kappa$ B, I $\kappa$ B, PARG, RNF168, RNF8, and USP7 (215, 216). Furthermore, ICP0 is an important mediator for reactivation of HSV from its latent state to a state of lytic infection.

Furthermore, there are several reports of viral proteins interacting with cellular de-ubiquitinating enzymes (DUBs). HSV protein ICP0 and EBV protein EBNA1 interact with the cellular DUB USP7 (217, 218). This leads to the removal of ubiquitin chains from cellular p53, subsequently preventing its degradation (219, 220). Moreover, ICP0 is a substrate of USP7, which leads to ICP0 stabilization. In general, EBV infection leads to an increase in activity of cellular DUBs, including USP5, USP7, USP9, USP13, USP15, and USP22 (221). Measles infection leads to the upregulation of the cellular DUB, A20, which removes ubiquitin from TRAF6 and interferes with NF- $\kappa$ B activation (222). Some viruses encode their own DUBs including HSV-1, EBV, MCMV, and HCMV (223-226). Overall, viruses extensively use the ubiquitin-proteasome system for their life cycle and immune evasion.

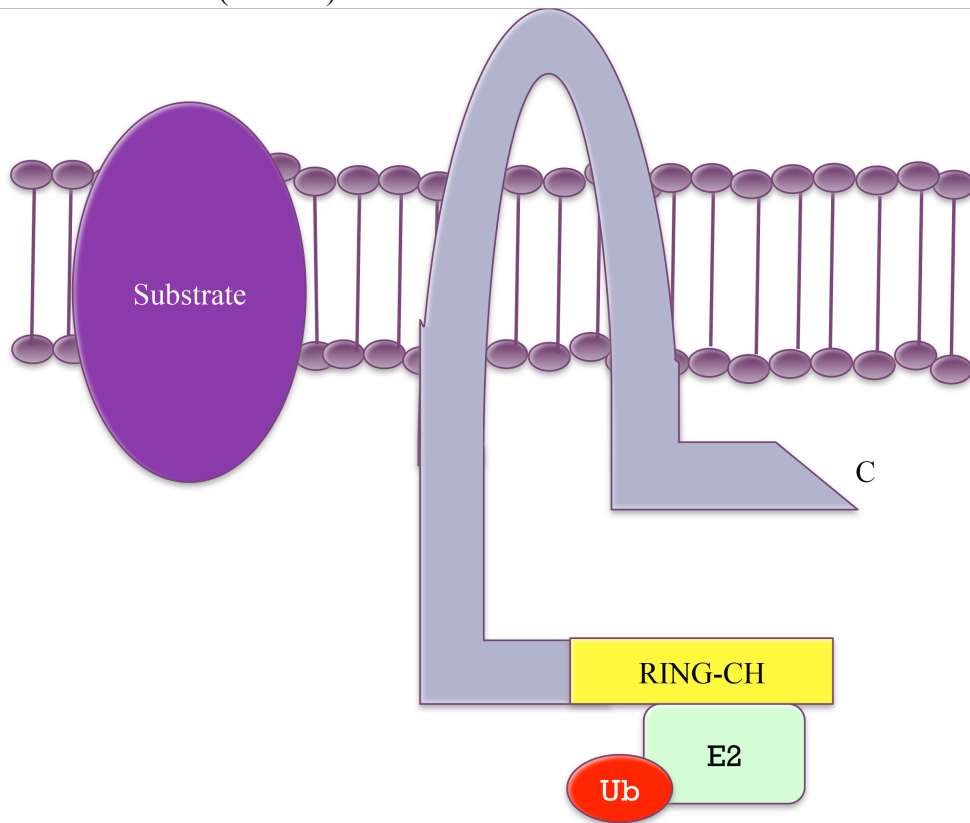
## **1.9 Importance of ubiquitination and a functioning proteasome during poxvirus infection**

Like other virus families, poxviruses encode a variety of proteins to manipulate the ubiquitin-proteasome pathway. The importance of the ubiquitin-proteasome system during poxviral infection was recently highlighted by the observation that poxviruses require a functional ubiquitin-proteasome system for replication and late gene expression (116, 117). Interestingly, some poxviruses, including canarypox and entomopoxvirus, encode a homologue to human ubiquitin (22, 23). However, the role of poxvirus-encoded ubiquitin remains unknown, since poxviruses also incorporate host cell ubiquitin into their virions (180, 227, 228). Additionally, poxviruses contain a putative DUB I7L, although its activity remains to be confirmed (229). Below, I will discuss some of the better characterized mechanisms of manipulation of the ubiquitin-proteasome pathway by poxviruses.

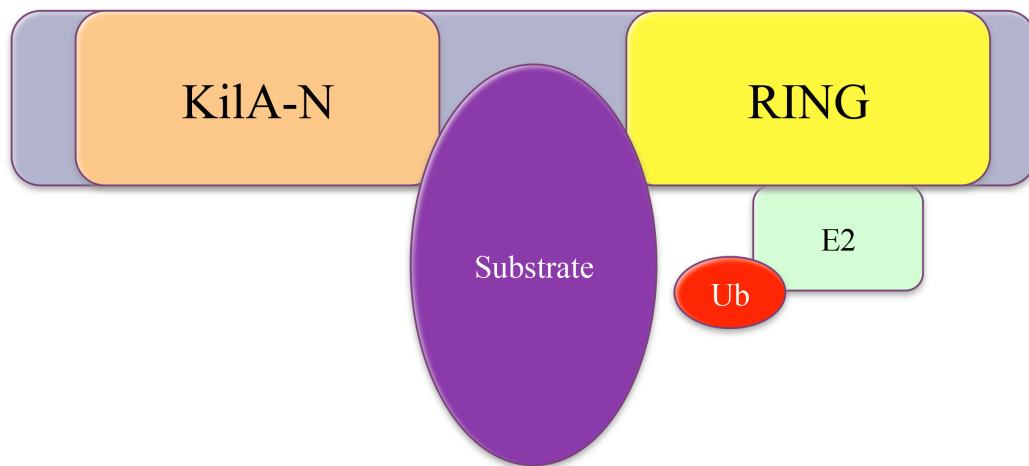
## **1.10 Poxviral E3 ubiquitin ligases and adapter proteins**

Poxviruses encode a variety of proteins to manipulate the UPS (**Figure 1.7**). One of the first described poxviral E3 ligases was M153R, found in MYXV, a poxviral strain that infects rabbits. M153R is a Membrane-Associated RING-CH (MARCH) E3 ligase (73, 74). MARCH has a modified RING domain at its N-terminus combined with a transmembrane domain, which keeps it localized to the membrane. At the plasma membrane, M153R is involved in down-regulating cell surface immune molecules like MHC class I, MHC class II, and CD4 coreceptor (73, 74, 230-232). This prevents

A MARCH (M153R)



B RING (p28)



C BTB/Kelch

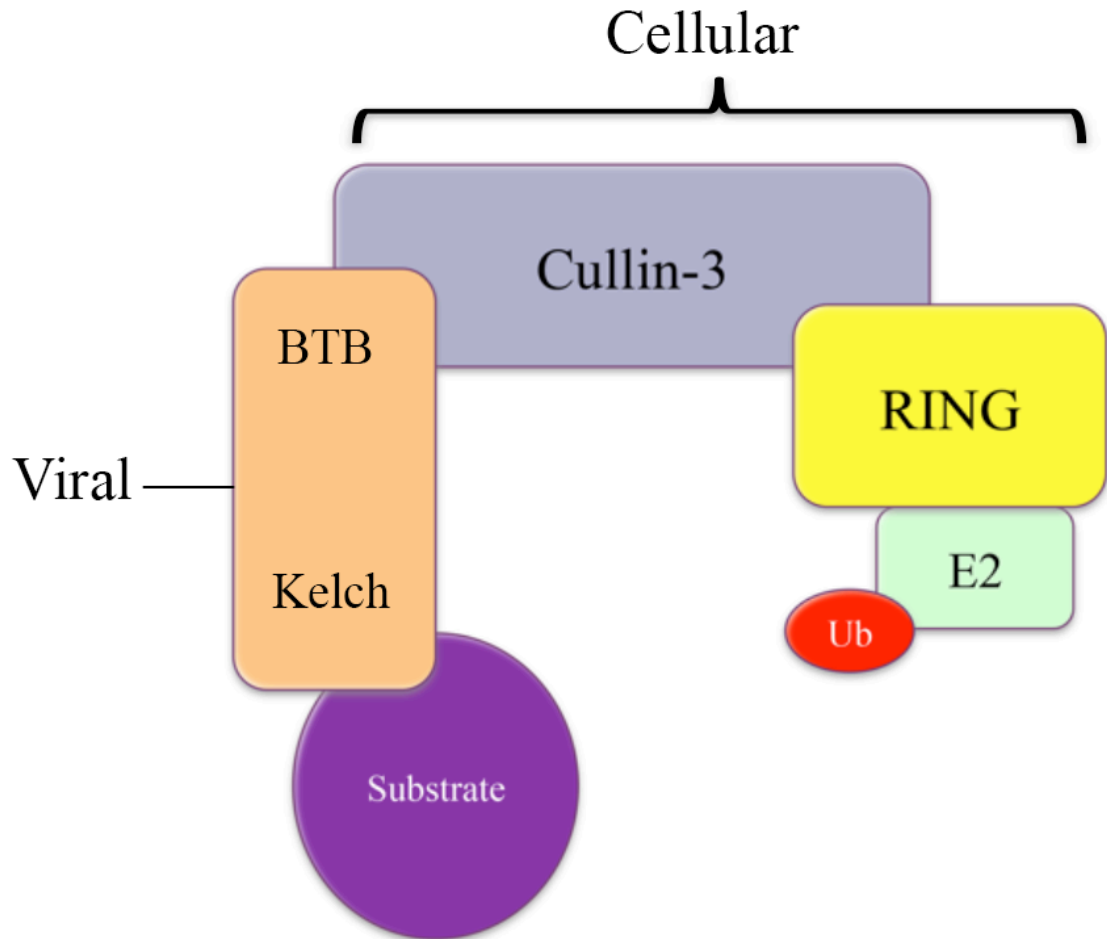


**Figure 1.7 Poxviral E3 ubiquitin ligases and adapter proteins.**

Adapted from Barry *et al.* (233). **(A)** MARCH (membrane-associated RING-CH) has an N-terminal RING domain and a C-terminal trans-membrane domain. **(B)** p28 is a single subunit ubiquitin ligase with an N-terminal Kila-N DNA binding domain and a C-terminal RING domain. **(C)** Multi-subunit ubiquitin ligase. This is a member of the cullin protein family, which interacts with linker protein and RING finger protein.

the presentation of viral peptides to T cells and subsequently suppresses the adaptive immune response.

*Parapoxviruses*, *Molluscipoxviruses*, crocodilepox and squirrelpox viruses are also known to express APC11 homologues with similarity to RING-finger proteins (234). However, this thesis will focus on the poxviral E3 ligase p28 and its homologues in FWPV.

In addition to encoding E3 ubiquitin ligases, the family of Orthopoxviruses expresses adapter proteins that facilitate recruitment of substrates to multi-subunit cullin-based ubiquitin ligases. These adapter proteins can contain BTB/Kelch (Broad-complex, Tramtrack and Bric-a-Brac) domains or Ankyrin/F-box proteins (208, 229, 233). The Barry laboratory (University of Alberta, Edmonton, Canada) has demonstrated that ECTV encodes four Ankyrin/F-box proteins (EVM002, EVM005, EVM154 and EVM165), which interact with the cellular SCF ubiquitin ligase to inhibit NF- $\kappa$ B activation (235, 236). Of note, EVM005 can inhibit NF- $\kappa$ B activation through manipulation of the host SCF ubiquitin ligase complex, but also acts as an NF- $\kappa$ B-independent virulence factor (237). Furthermore, ECTV encodes four BTB/kelch adaptor proteins, EVM018, EVM027, EVM150, and EVM167, which are associated with the cellular cullin-3 ubiquitin ligase complex (233, 238-240). It was recently demonstrated that EVM150 inhibited both TNF- $\alpha$ - and IL-1 $\beta$ -induced NF- $\kappa$ B nuclear translocation, without blocking the degradation of I $\kappa$ B $\alpha$  (241). In addition to the role of EVM150 as an adapter for cullin-3-based ubiquitin ligases, the BTB domain of EVM150 was sufficient to suppress NF- $\kappa$ B activation (241).

### 1.11 p28 and homologues

While poxviruses utilize several strategies for manipulating the ubiquitin pathway, this thesis is mainly focused on characterization of the poxviral encoded p28 E3 ligases. p28 is a 28 kDa protein found in diverse members of the poxvirus family. It was first described in VACV and ECTV (242, 243), but homologues are also found in myxoma virus (MYXV), Shope fibroma virus, VARV and birdpoxviruses (**Table 1.3**). p28 is the first RING domain protein demonstrated to be associated with virulence. Interestingly, p28 is mostly found in highly pathogenic poxviruses, but is absent in the attenuated VACV strains used for vaccination. p28 is not essential for replication in tissue culture (242, 244, 245). The first indication that p28 acts as a virulence factor was demonstrated by the Buller group (244). Mice survived infection with ECTV devoid of p28, demonstrating a dramatic reduction in virus virulence compared to WT ECTV infection. This was due to the fact that the p28 knockout virus could no longer replicate in macrophages, which is important for viral dissemination from skin lesions to lymph nodes and the liver (244, 245).

p28 consists of two highly conserved functional domains (**Figure 1.8**). The C-terminus has a RING domain, which defines its E3 ligase activity. The N-terminal domain is a DNA binding domain named Kila-N domain, which is largely uncharacterized. Kila-N domains were previously found in large DNA viruses, bacteria and bacteriophages and seem to bind non-specifically to DNA (246). p28 is the only known protein to our knowledge which pairs a Kila-N DNA binding domain with a RING domain. Previous work with N1R, the p28 homologue in Shope fibroma virus, revealed that the Kila-N domain seems to be responsible for localizing p28 to the viral

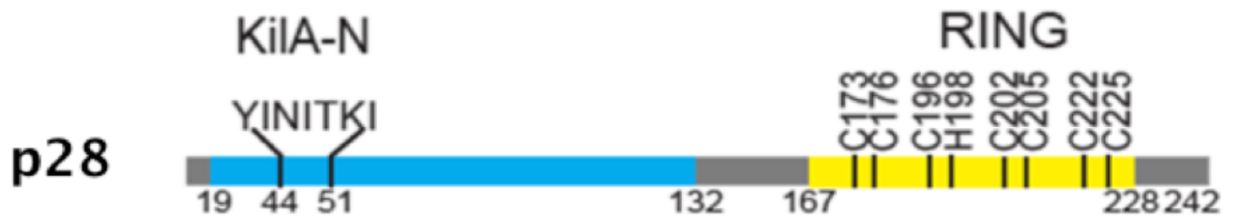
factories where the virus replicates (247). Dissection of diverse parts of the KIL-A-N domain revealed that this 112 amino acid KIL-A-N domain contained a highly conserved 7 amino acid area from residue 44-50 (YINITKI), which is crucial for this localization **(Figure 1.8)**.

The VACV-WR strain contains only a truncated version of p28 lacking the RING domain, while VACV-Cop completely lacks p28. Previous work in the laboratory of Dr. Barry in collaboration with Dr. Klaus Frueh (Oregon Health and Science University, Beaverton, OR) demonstrated the E3 ligase activity of p28 in an *in vitro* ubiquitination assay. It was also shown that the first two highly conserved cysteines C173 and C176 within the RING domain were crucial for E3 ligase activity. When these two cysteines were mutated to serines, the E3 ligase activity of p28 was abolished, since the mutations disrupted the ability of the RING domain to form a complex with zinc (243). Even though p28 was demonstrated to be a virulence factor during viral infection, no substrates for p28 have been identified to date. Previous reports suggest that p28, and the p28 homologue in Shope fibroma virus (N1R) might be involved in inhibition of apoptosis, which leads to the speculation that p28 might target pro-apoptotic proteins for ubiquitination and proteasomal degradation (20, 247, 248). However, this awaits confirmation.

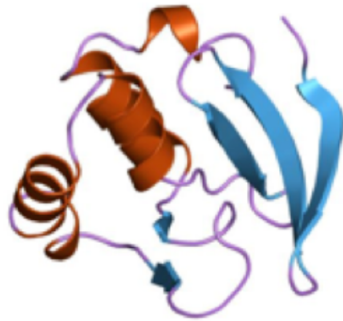
Since p28 localizes to viral factories, potential substrates might be located there as well. It is known that p28 expression starts early during infection before the virus factories are formed (245, 249). Therefore, other substrates might be found in the cytoplasm of the host cell as well.

<b>Genus</b>	<b>Virus</b>	<b>Gene/Protein</b>	<b>Length</b>	<b>Accession</b>	
<b>Avipoxvirus</b>	CNPV	CNPV197	275	VP0043670	
		CNPV205	318	VP0043678	
	FWPV	FWPV150	276	VP0037882	
		FWPV157	311	VP0037889	
<b>Capripoxvirus</b>	GTPV-Pellor	127	240	VP0044947	
	LSDV-Nee	140	240	VP0040345	
	SPPV-A	136	240	VP0044645	
<b>Leporipoxvirus</b>	MYXV-Lau	M143	234	VP0038572	
	RFV-Kas	gp143R (N1R)	234	VP0038740	
<b>Orthopoxvirus</b>	CMLV-CMS	14R	242	VP0041112	
	CPXV-GRI	C7R	242	VP0042678	
	ECTV-Mos	12	241	VP0040932	
	MPXV-ZAR	D5R	242	VP0040369	
	VACV IHD-W	p28	243	N/A	
	VARV-BGD75major	D6R	242	VP0038767	
	RPXV-Utr	8	242	VP0041370	
	<b>Suipoxvirus</b>	SWPV-Neb	138	246	VP0040694
	<b>Yatapoxvirus</b>	TANV-COD	143R	234	VP0067759
YMTV-Amano		143R	236	VP0043181	

**Table 1.3 p28 homologues**



**DNA Binding Domain:**  
Localizes to viral factories



**RING Domain:**  
E3 Ligase activity

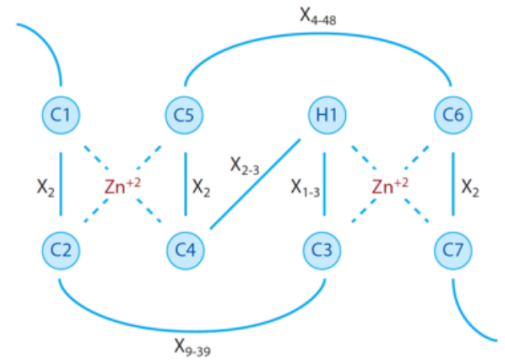


**Figure 1.8 p28 E3 ubiquitin ligase.**

A schematic representation of p28 illustrates the N-terminal KilA-N DNA binding domain and the C-terminal RING domain; The KilA-N domain is an illustration of the related APSES DNA binding domain, adapted from Iyer *et al.* (246). The p28 KilA-N domain contains a YINITKI motif, which is necessary for localization to the virus factory. The highly conserved cysteine and histidine residues are further highlighted in the RING domain; adapted from Deshaies *et al.* (139).

Interestingly, p28 has been associated with K63 ubiquitin chains, since a yeast-2 hybrid associated p28 with E2 conjugating enzyme Ubc13, an enzyme that is solely utilized for formation of K63-linked chains (242). This suggests that p28 could be responsible for either targeting proteins for proteasomal degradation, or altering their functions.

### **1.12 Hypothesis and study objectives**

Previous work from our group and other labs suggested that p28 acts as an important E3 ligase. We were also interested in investigating homologues of p28 in other members of the poxviruses family and determining their role in host cell infection. Unlike other members of the poxvirus family, both Avipoxviruses FWPV and CNPV contain two homologues of p28. In FWPV p28 homologues were named after their ORF number FWPV150 and FWPV157, and had not been studied at the time I began my thesis. Notably, the critical key residues within RING domains (seven cysteines and one histidine motif) and Kila-N domains (YINITKI motif) are conserved in both FWPV150 and FWPV157, suggesting that these proteins likely function as ubiquitin ligases as well. However, the rest of the sequences do not contain high sequence homology. Protein sequence identity between FWPV150 and FWPV157 is 36%, whereas sequence identity between p28 and FWPV150 is 24% and between p28 and FWPV157 is 43%. FWPV also encodes eight Kila-N domain-containing proteins lacking the RING domain and canarypox virus encodes twenty-three Kila-N only proteins. The function of these Kila-N domains during virus infection were unknown at the time that my thesis work began. The substrates of p28 and its homologues were also unknown. I was interested in

characterizing the mechanism by which these proteins function as virulence factors during virus infection.

**Hypotheses:**

My working hypotheses are:

- 1) FWPV150 and FWPV157 act as E3 ligases due to their domain similarity to p28
- 2) p28 targets cellular and/or viral targets for ubiquitination during viral infection.

I will test these hypotheses by pursuing the following objectives.

**Thesis Objectives:**

Objective 1: Characterize the ubiquitin ligase activity, expression and cellular localization of FWPV150 and FWPV157 in FWPV.

Objective 2: Characterize p28 RING and KILAN mutants, their interaction with ubiquitin, and their ability to act as ubiquitin ligases.

Objective 3: Identify interaction partners and potential substrates for p28.

## **CHAPTER 2: MATERIALS AND METHODS**

## 2.1 Cell Culture and Viruses

### 2.1.1 Cell Lines

The cell lines and viruses used in this study are listed in **Table 2.1**. Human fibroblasts (HeLa), CV-1, J774, Raw 264, baby green monkey kidney (BGMK), and HuTK<sup>-/-</sup>-143B cells were obtained from the American Type Culture Collection (ATCC, Burlington, ON, Canada) and maintained at 37°C and 5% CO<sub>2</sub>. HeLa, CV-1, J774, Raw 264 and HuTK<sup>-/-</sup>-143B cells were cultured in Dulbecco's modified Eagle's Medium (DMEM; Invitrogen, Grand Island, NY) supplemented with 10% heat-inactivated fetal bovine serum (HI-FBS; Invitrogen), 50 U/mL penicillin, 50 µg/mL streptomycin, and 200 µM L-glutamine (Invitrogen). HuTK<sup>-/-</sup>-143B cell media additionally contained 25 µg/mL 5-bromo-2'-deoxyuridine (BrdU; Sigma-Aldrich, Oakville, ON, Canada). BGMK cells were cultured in DMEM supplemented with 10% newborn calf serum (NCS; Invitrogen), 50 Units (U) of penicillin/ml, 50 µg/mL streptomycin, and 200 µM L-glutamine. Quail fibrosarcoma (QM5) cells were a generous gift from R. Duncan (Dalhousie University, Halifax, NS) and maintained in Dulbecco's Modified Eagle medium supplemented with 10% heat inactivated fetal bovine serum (HI-FBS) (Invitrogen), 50 U of penicillin/ml (Invitrogen), and 200 µM glutamine (Invitrogen).

### 2.1.2 Viruses

VACVCop (no endogenous p28), VACVWR (truncated version of endogenous p28(1-184)), and CPXV were provided by G. McFadden (University of Florida, Gainesville,

<b>Cell Line</b>	<b>Cell Type</b>	<b>Characteristics</b>	<b>Source</b>
<b>HeLa</b>	Human Fibroblast		ATCC
<b>BGMK</b>	Baby Green Monkey Kidney		ATCC
<b>CV-1</b>	Monkey Kidney Fibroblast		ATCC
<b>HuTK<sup>-/-</sup>-143B</b>	Human 143B Osteosarcoma	Deficient in Thymidine Kinase	ATCC
<b>QM5</b>	Quail Fibroblast		D. Evans
<b>J774</b>	Mouse Macrophage		ATCC
<b>Raw 264</b>	Mouse Macrophage		ATCC
<b>Viruses</b>	<b>Strain</b>	<b>Characteristics</b>	<b>Source</b>
<b>VACV(Cop)</b>	Copenhagen	No endogenous p28	G. McFadden
<b>VACVWR</b>	Western Reserve	Truncated p28	G. McFadden
<b>VACV-IHDW</b>	IHDW	Endogenous p28	D. Evans
<b>VACV-FLAG-M143R</b>	Copenhagen	Expresses FLAG-M143R instead of TK	K. Früh (243)
<b>VACV-HA-Ubiquitin</b>	Copenhagen	Expresses HA-Ubiquitin in place of TK	K. Früh (243)
<b>VACV-FLAG-p28</b>	Copenhagen	Expresses FLAG-p28 in place of TK	K. Früh (243)

<b>VACV-FLAG-p28(C173S/C176S)</b>	Copenhagen	Expresses FLAG-p28(C173S/C176S) in place of TK	K. Fröh (243)
<b>VVT7lacOI</b>	WR		B. Moss (250)
<b>VACVΔF1L-FLAG-FWPV039</b>	Copenhagen	Expresses FLAG-FWPV039 instead of TK; lacks endogenous F1L	L. Banadyga (84)
<b>CPXV</b>	Brighton Red		G. McFadden
<b>ECTV</b>	Moscow		M. Buller

**Table 2.1 Cells and viruses used in this study**

FL). FWPV and VACV-IHDW were generously provided by D. Evans (University of Alberta, Edmonton, AB). Recombinant VACV-FLAG-M143R, Recombinant VACV-HA-Ubiquitin and VACV-FLAG-p28, and VACV-FLAG-p28(C173S/C176S) were previously described (243). VACV strain Western Reserve expressing T7 polymerase VACVT7lacOI (VACVT7) and ECTV were a generous gift from B. Moss (National Institute of Allergy and Infectious Diseases, Bethesda) (251) Recombinant VACV $\Delta$ F1L-FLAG-FWPV039 was generated as previously described (84) All viruses were propagated in BGMK cells and purified as previously described, except for FWPV, which was propagated in QM5 cells (252).

## **2.2 DNA Methodology**

### **2.2.1 Polymerase Chain Reaction**

Polymerase chain reactions (PCR) were carried out in volumes of 50  $\mu$ l containing 60 mM Tris-SO<sub>4</sub>, 20 mM (NH<sub>4</sub>)<sub>2</sub>SO<sub>4</sub>, 2 mM MgSO<sub>4</sub>, 3% glycerol, 0.06% NP-40, and 0.05% Tween-20 (pH 9.0 at 25°C). Each reaction contained 1 pmole of each primer, 10 mM deoxyribonucleotide triphosphates (dNTPs; Invitrogen), 2.5 U of LongAmp Taq DNA polymerase (New England Biolabs, Whitby, ON, Canada) and either 10 ng of plasmid DNA or 100 ng of viral DNA template. All primers used in this study are listed in **Table 2.2**. Temperature cycles were performed with a C1000 thermal cycler (BioRad, Mississauga, ON, Canada) using the following parameters: Initial denaturation for 5 minutes at 95°C followed by 30 cycles of denaturation at 95°C for 1 minute, primer annealing at 55°C for 30 seconds, and primer elongation at 65°C for 1 minute/kilobase

<b>Primer Name</b>	<b>Primer Sequence (5' – 3')</b>	<b>Restri ction Site</b>	<b>Description</b>	<b>Source</b>
<b>FLAG- FWPV150 <i>SalI</i> Fwd</b>	GTCGACATGGACTAC AAAGACGATGACGAC AAGTCACATCTTCATC TTAAT	<i>SalI</i>	Used to clone pSC66-FLAG- FWPV150 and RT- PCR test for gene expression	This study
<b>FWPV150 <i>NotI</i> Rev</b>	GCGGCCGCTTAACAT GATTTTATATATAC	<i>NotI</i>	Used to clone pSC66-FLAG- FWPV150 and RT- PCR test for gene expression	This study
<b>FLAG- FWPV157 <i>SalI</i> Fwd</b>	GTCGACATGGACTAC AAAGACGATGACGAC AAGAAGGAGGACGAC TCATCA	<i>SalI</i>	Used to clone pSC66-FLAG- FWPV157 and RT- PCR test for gene expression	This study
<b>FWPV157 <i>NotI</i> Rev</b>	GCGGCCGCTTATATTT TTATTGTTCTTAT	<i>NotI</i>	Used to clone pSC66-FLAG- FWPV157 and RT- PCR test for gene expression	This study

<b>FWPV150(C1 96S/C199S) Fwd</b>	CGATAAATCCGGTATT TCTTTGGATGC	N/A	Used as overlapping primer for site directed mutagenesis	This study
<b>FWPV150(C1 96S/C199S) Rev</b>	GCATCCAAAGAAATA CCGGATTTATCG	N/A	Used as overlapping primer for site directed mutagenesis	This study
<b>FWPV157(C2 18S/C221S) Fwd</b>	CCAGTAAAAAGTCTG GCATATCCATAGAAG	N/A	Used as overlapping primer for site directed mutagenesis	This study
<b>FWPV157(C2 18S/C221S) Rev</b>	CTTCTATGGATATGCC AGACTTTTTACTGG	N/A	Used as overlapping primer for site directed mutagenesis	This study
<b>FLAG-p28- <i>SalI</i>-(Fwd)</b>	GTCGACATGGACTAC AAGGACGACGACG	<i>SalI</i>	Used to clone pSC66-FLAG- p28(1-184) and pSC66-FLAG- p28(1-204)	This study
<b>p28(1-184) <i>NotI</i> Rev</b>	GCGGCCGCTCAGCGC TTGCTG	<i>NotI</i>	Used to clone pSC66-FLAG- p28(1-184)	This study
<b>p28(1-204) <i>NotI</i> Rev</b>	GCGGCCGCTCAGGTG ATGCCA	<i>NotI</i>	Used to clone pSC66-FLAG- p28(1-204)	This study

<b>FWPV085</b>	TGGAAATAGCTAGAG	N/A	RT-PCR late gene	This
<b>Fwd</b>	AAACGCTAA		control	study
<b>FWPV085</b>	AAACGAAGTATTCTTC	N/A	RT-PCR late gene	This
<b>Rev</b>	CTGCTG		control	study
<b>FWPV037</b>	GAATTCATGACGCTAT	N/A	RT-PCR early gene	This
<b>Fwd</b>	TCGAATATATA		control	study
<b>FWPV037</b>	GGATCCGATTGTGACT	N/A	RT-PCR early gene	This
<b>Rev</b>	TTTCAGACTTTTTACT		control	study
<b>GAPDH Fwd</b>	TGATGACATCAAGAA GGTGGTGAAG	N/A	RT-PCR housekeeping gene	This study
<b>GAPDH Rev</b>	TCCTTGGAGGCCATGT GGGCCAT	N/A	RT-PCR housekeeping gene	This study
<b>FWPV075</b>	GTCGACATGGACTAC	N/A	RT-PCR test for	This
<b>Fwd</b>	AAAGACGATGACGAC AAGGAGTTTGTACCTA ACACC		gene expression	study
<b>FWPV075</b>	GCGGCCGCTTATTTTA	N/A	RT-PCR test for	This
<b>Rev</b>	TGGATAAACC		gene expression	study
<b>FWPV124</b>	GTCGACATGGACTAC	N/A	RT-PCR test for	This
<b>Fwd</b>	AAAGACGATGACGAC AAGGACTTCTCGGATC TCGTT		gene expression	study
<b>FWPV124</b>	GCGGCCGCTTAACCG	N/A	RT-PCR test for	This

<b>Rev</b>	ATTAAAACAGG		gene expression	study
<b>FWPV155</b> <b>Fwd</b>	GTCGACATGGACTAC AAAGACGATGACGAC AAGATGTTTAATAGTA TGATA	N/A	RT-PCR test for gene expression	This study
<b>FWPV155</b> <b>Rev</b>	GCGGCCGCTTAGTTAT CTGAAAATAT	N/A	RT-PCR test for gene expression	This study
<b>FWPV159</b> <b>Fwd</b>	GTCGACATGGACTAC AAAGACGATGACGAC AAGTCTACTATTACCT GTTAT	N/A	RT-PCR test for gene expression	This study
<b>FWPV159</b> <b>Rev</b>	GCGGCCGCTTAGATG AAAAAAATTAGCTT	N/A	RT-PCR test for gene expression	This study
<b>FWPV161</b> <b>Fwd</b>	GTCGACATGGACTAC AAAGACGATGACGAC AAGGATAAAAGATAT ATATCA	N/A	RT-PCR test for gene expression	This study
<b>FWPV161</b> <b>Rev</b>	GCGGCCGCCTACATGT TGTATGAATT	N/A	RT-PCR test for gene expression	This study
<b>FWPV163</b> <b>Fwd</b>	GTCGACATGGACTAC AAAGACGATGACGAC AAGAATACCTTACCGT ATATT	N/A	RT-PCR test for gene expression	This study

<b>FWPV163</b> <b>Rev</b>	GCGGCCGCTTATTTAG ATTTTCTGAATGTTAG	N/A	RT-PCR test for gene expression	This study
<b>FWPV236</b> <b>Fwd</b>	GTCGACATGGACTAC AAAGACGATGACGAC AAGAAATTTAAGGAA GTTAGA	N/A	RT-PCR test for gene expression	This study
<b>FWPV236</b> <b>Rev</b>	GCGGCCGCCTATTCGT AATTATTCGCTACCGC TGG	N/A	RT-PCR test for gene expression	This study
<b>FWPV248</b> <b>Fwd</b>	GTCGACATGGACTAC AAAGACGATGACGAC AAGGAAATCAAAGTA GAATCG	N/A	RT-PCR test for gene expression	This study
<b>FWPV248</b> <b>Rev</b>	GCGGCCGCCTACATAT TG TTATCATCGTTTAA	N/A	RT-PCR test for gene expression	This study
<b>TK- Fwd</b>	GATCTACTTCCTTACC GTGC	N/A	Sequencing of pSC66 vector, confirmation of purity of recombinant viruses	R. Burton
<b>TK- Rev</b>	GGAACGGGACTATGG ACGC	N/A	Sequencing of pSC66 vector,	R. Burton

			confirmation of purity of recombinant viruses	
--	--	--	---	--

Fwd – Forward, Rev – Reverse, N/A – not applicable

**Table 2.2 Oligonucleotides used in this study**

(kb). Alternatively, PCR reactions were done in 50µl volumes containing 200 mM Tris-HCl pH 8.4, 500 mM KCl, 50 mM MgCl<sub>2</sub>, 1 pmole each primer, 10 mM dNTPs, 10 ng template DNA, and 2.5 U of Taq DNA polymerase (Invitrogen). Temperature cycles were performed as described above, except that elongations were performed at 72°C.

### **2.2.2 Agarose Gel Electrophoresis**

DNA products of PCR and endonuclease digestion (described in section 2.2.4) were purified and isolated by agarose gel electrophoresis followed by gel extraction. DNA was suspended in a sample loading dye containing 30% glycerol (Fisher Scientific, Ottawa, ON, Canada) and 0.25% Bromophenol blue (BioRad). DNA products were separated by gel electrophoresis in gels made of 1% weight per volume (w/v) UltraPure Agarose (Invitrogen) in 1X TAE buffer (40 mM Tris, 20 mM acetic acid, and 1 mM ethylenediaminetetraacetic acid (EDTA)). To visualize DNA bands, SYBR Safe DNA gel stain (Invitrogen) was added to the agarose gels at a 1:100 dilution. Electrophoresis was performed in 1X TAE running buffer in a Mini-Sub Cell GT (BioRad) at 100V. DNA bands were visualized using a Gel Doc EZ Imager (BioRad). Bands of interest were excised and subjected to gel extraction as described in Section 2.2.3.

### **2.2.3 Gel Extraction**

Gel extraction was performed using a QIAquick gel extraction kit (Qiagen, Toronto, ON, Canada) according to the manufacturer's protocol. In brief, excised DNA bands were suspended in 3 volumes of solubilization buffer per 1 volume of gel (300 µl per 100 mg) and incubated at 50°C for 10 minutes, or until the gel was completely dissolved. One gel

volume of isopropanol was then added before being run on a QIAquick DNA column followed by an ethanol wash. Bound DNA was eluted in 25  $\mu$ l of 10 mM Tris-HCl (pH 8.5) or ddH<sub>2</sub>O. The extracted DNA was assessed by agarose gel electrophoresis.

#### **2.2.4 Restriction Digests**

Restriction digests were performed according to the manufacturer's instructions with endonuclease restriction enzymes from Invitrogen or New England Biolabs. In general, restriction digests were performed in a total volume of 50  $\mu$ l for 1 hour at 37°C. The resulting DNA fragments were isolated by agarose gel electrophoresis.

#### **2.2.5 DNA Ligation**

DNA fragments produced by PCR were ligated into the T-A vector pGEM-T (Promega, Madison, WI), PCR was done using LongAmp Taq DNA polymerase to add a single deoxyadenosine to the 3'-end of the fragments. T-A cloning was done in 20  $\mu$ l reactions containing 2  $\mu$ l of gel extracted DNA, 50 ng of pGEM-T vector, 3 U of T4 DNA ligase, and 5  $\mu$ l of 2X rapid ligation buffer containing 60mM Tris-HCl (pH 7.8), 20mM MgCl<sub>2</sub>, 20mM dithiothreitol (DTT), 2mM ATP, and 10% polyethylene glycol. Ligation reactions were incubated at 4°C overnight. For ligation into pSC66, or pEGFP reactions were done in 20  $\mu$ l volumes containing 4 U T4 DNA ligase (New England Biolabs), 50 mM Tris-HCl (pH 7.5), 10 mM MgCl<sub>2</sub>, 1 mM ATP, and 10 mM DTT. Vector to insert ratios of 1:3, 1:6, or 1:9 were tested for the best ligation efficiency and reactions were incubated at 16°C overnight. Ligations were transformed into competent *E. coli* cells as described in Section 2.2.6.

### **2.2.6 Bacterial Transformation**

Competent *E. coli* DH5 $\alpha$  cells (Invitrogen) were transformed with ligation reactions using a heat shock method. Fifty  $\mu$ l of competent DH5 $\alpha$  cells were incubated with 5  $\mu$ l of ligation reactions on ice for 30 minutes followed by heat shock at 42°C for 45 seconds and a 2 minute recovery on ice. Two hundred fifty  $\mu$ l of super optimal broth with catabolite repression (253) media containing 20 mg/mL tryptone, 5 mg/mL yeast extract, 0.5 mg/mL NaCl, and 2.5 mM KCl (pH 7.0) was added and cells were incubated at 37°C for 1 hour. Transformed bacteria were plated on Luria-Bertani (LB) agar plates supplemented with the appropriate antibiotic, either 100  $\mu$ g/mL ampicillin (Sigma-Aldrich) or 30  $\mu$ g/mL kanamycin (Sigma-Aldrich). *E. coli* transformed with pGEM-T plasmids were plated on LB agar plates containing 100  $\mu$ g/mL ampicillin, 80  $\mu$ g/mL 5-bromo-4-chloro-3-indolyl- $\beta$ -D-galactopyranoside (X-gal; Rose Scientific, Edmonton, AB, Canada) and 0.5 mM isopropyl  $\beta$ -D-1-thiogalactopyranoside (IPTG; Rose Scientific) to allow for blue/white screening of recombinants.

### **2.2.7 Plasmid DNA Isolation**

To prepare plasmids used for expression in mammalian cells or sequencing, 200 mL of LB broth containing the appropriate antibiotic (100 mg/mL ampicillin or 60 mg/mL kanamycin) was inoculated with *E. coli* DH5 $\alpha$  cells containing the desired plasmid and incubated overnight at 37°C. For low copy plasmids, such as pSC66, cultures were incubated for 8 hours followed by treatment with 170 mg/mL chloramphenicol (Sigma-Aldrich) for another 18 hours. Plasmid DNA was prepared using a Plasmid MaxiPrep kit (Qiagen) according to the manufacturer's protocol. DNA yields and optical densities at

280 nm were determined using a NanoVue Plus spectrophotometer (GE Healthcare, Mississauga, ON, Canada).

### **2.2.8 DNA Sequencing and Computer Analysis**

Sanger sequencing was performed by either The Applied Genomics Centre (TAGC) in the Faculty of Medicine at the University of Alberta, or at the McGill University and Génome Québec Innovation Centre. DNA sequence analyses were performed using the Basic Local Alignment Search Tool (BLAST) provided by the National Centre for Biotechnology Information (NCBI).

### **2.2.9 Plasmids**

All plasmids used in this study are listed in **Table 2.3**. All T-A cloning was done in the pGEM-T vector (Promega), and the pEGFP-C3 vector (Clontech, Mountain View, CA) was used to generate all N-terminal enhanced green fluorescent protein (EGFP)-tagged proteins. pSC66, which contains a synthetic poxviral early/late promoter (pE/L), was provided by Dr. E. Long (National Institute of Allergy and Infectious Disease, Bethesda, MB) (54).

<b>Plasmid</b>	<b>Characteristics</b>	<b>Source</b>
<b>pGEM-T</b>	TA cloning vector; CMV promoter	Promega
<b>pEGFP-C3</b>	Empty EGFP vector with a CMV promoter	Clontech
<b>pSC66</b>	Synthetic poxviral early/late promoter; VACV thymidine kinase sequence flanks LacZ and promoter, and multiple cloning site; Used to generate VACV recombinants	Dr. E. Long (54)
<b>pSC66-FLAG-p28</b>	Full length FLAG-p28	C. Milne
<b>pSC66-FLAG-p28(1-152)</b>	FLAG-p28, only KIL-A-N domain	C. Milne
<b>pSC66-FLAG-p28(153-242)</b>	FLAG-p28, only RING domain	C. Milne
<b>pSC66-FLAG-p28(<math>\Delta</math>44-51)</b>	FLAG-p28, lacking virus factory localization signal	C. Milne
<b>pSC66-FLAG-p28(C173S/C176S)</b>	FLAG-p28, double cysteine mutant	B. Nerenberg (243)
<b>pSC66-FLAG-p28(1-184)</b>	FLAG-p28, truncated	This study
<b>pSC66-FLAG-p28(1-204)</b>	FLAG-p28, truncated	This study
<b>pSC66-FLAG-FWPV150</b>	FLAG-FWPV150	This study
<b>pSC66-FLAG-FWPV157</b>	FLAG-FWPV157	This study

<b>pSC66-FLAG-FWPV150(C196S/C199S)</b>	FLAG-FWPV150(C196S/C199S), double cysteine mutant	This study
<b>pSC66-FLAG-FWPV157(C218S/C221S)</b>	FLAG-FWPV157(C218S/C221S), double cysteine mutant	This study
<b>pSC66-FLAG-FWPV075</b>	FLAG-FWPV075, Kila-N only domain	This study
<b>pSC66-FLAG-FWPV124</b>	FLAG-FWPV124, Kila-N domain with Domain of unknown function	This study
pSC66-FLAG-A50	FLAG-A50	D. Evans
<b>pEGFP-p28</b>	EGFP-p28 for flow cytometry	K. Mottet
<b>pEGFP-p28(C173S/C176S)</b>	EGFP-p28(C173S/C176S) for flow cytometry	K. Mottet
<b>pEGFP-p28(1-184)</b>	EGFP-p28(1-184) for flow cytometry	K. Mottet
<b>pEGFP-p28(1-204)</b>	EGFP-p28(1-204) for flow cytometry	K. Mottet

**Table 2.3 Plasmids used in this study**

### **2.2.10 Generation of pSC66-FLAG-FWPV150, pSC66-FLAG-FWPV157, pSC66-FLAG-FWPV075, and pSC66-FLAG-FWPV124**

QM5 cells ( $1 \times 10^5$ ) were infected with FWPV, at a multiplicity of infection (MOI) of 5 and genomic FWPV DNA was extracted as described in Section 2.5.8. The FWPV150 gene was amplified from FWPV DNA and FLAG-tagged by PCR using the primers 5`-GTCGACATGGACTACAAAGACGATGACGACAAGTCACATCTTCATCTTAAT-3`(forward) and 5`-GCGGCCGCTTAACATGATTTTATATATAC-3`(reverse). The *SalI* restriction site was included in the forward primer and the *NotI* restriction site was included in the reverse primer. The FWPV157, FWPV075, and FWPV124 genes were amplified using the primers listed in **Table 2.2**. PCR products were subcloned into pGEM-T (Promega) and the constructs were verified by sequencing at TAGC at the University of Alberta. FLAG-FWPV150, FLAG-FWPV157, FLAG-FWPV075, and FLAG-FWPV124 were subcloned into the pSC66 vector, using *SalI* and *NotI*, placing the FLAG-tagged genes under the control of a synthetic early/late poxviral promoter provided by Dr. E. Long (National Institute of Infectious Diseases, Bethesda) (54).

### **2.2.11. Generation of pSC66-FLAG-FWPV150(C196S/C199S) and pSC66-FLAG-FWPV157(C218S/C221S)**

The double cysteine mutants pSC66-FLAG-FWPV150(C196S/C199S) and pSC66-FLAG-FWPV157(C218S/C221S) were generated by overlapping PCR using primers listed in **Table 2**, following the instructions from the site-directed mutagenesis kit (Stratagene, La Jolla, CA). Mutations were verified by sequencing the resulting plasmids (see Section 2.2.8).

### **2.2.12 Generation of pSC66-FLAG-p28(1-184) and pSC66-FLAG-p28(1-204)**

FLAG-p28(1-184) and FLAG-p28(1-204) were generated using pSC66-FLAG-p28 vector as a template using FLAG-p28(1-184) Fwd along with p28(1-184) Rev, or FLAG-p28(1-204) Fwd along with p28(1-204) Rev, respectively. The PCR products were ligated into pGEM-T and sub-cloned into pSC66 as *SalI/NotI* digested fragments to place them under the control of a synthetic poxviral early/late promoter.

## **2.3 Transfections**

### **2.3.1 General Transfection Protocol**

Transfection of  $1 \times 10^6$  HeLa or QM5 cells was accomplished using Lipofectamine 2000 (Invitrogen) according to the manufacturer's specifications. Five  $\mu$ l of Lipofectamine reagent and 2  $\mu$ g of plasmid DNA were added to separate 500  $\mu$ l aliquots of OptiMEM media (Invitrogen) and incubated for 5 minutes. Lipid and DNA suspensions were gently mixed together and allowed to incubate for another 20 minutes. Following incubation, the DNA-lipid mixture was added to cell monolayers along with another 0.5 mL of OptiMEM for a total of 1 mL. Transfections were incubated at 37°C and 5% CO<sub>2</sub> for 2 hours followed by supplementation with recovery DMEM media containing 20% HI-FBS and 2 mM L-glutamine. The cells were incubated at 37°C and 5% CO<sub>2</sub> for an additional 12-16 hours.

### **2.3.2 General Infection/Transfection Protocol**

Twelve hour infection/transfections were performed to express proteins from pSC66 in the context of VACVCop infection. HeLa cells were infected in 500  $\mu$ l to 5 mL of OptiMEM with the appropriate virus at an MOI of 5, rocking every 10 minutes for 1 hour. During this time, 2-5  $\mu$ g of plasmid DNA and 5-25  $\mu$ l of Lipofectamine 2000 were incubated in 500  $\mu$ l to 5 mL of OptiMEM, as described in 2.3.1. Following the 1 h infection, cells were washed with OptiMEM and the DNA-Lipid mixture was added to the cell monolayer. After 2 hours at 37°C and 5% CO<sub>2</sub>, an equal volume of recovery media was added to the existing transfection media, and the cells were maintained at 37°C and 5% CO<sub>2</sub> for another 10 hours.

## **2.4 Virus Generation and Manipulation**

### **2.4.1 General Virus Infection Protocol**

Typically, virus stocks were thawed at 37°C and sonicated using a Sonic Dismembrator (Misonix Inc., Farmingdale, NY) for 20 seconds at 0.5 second pulses (on/off cycle) prior to use. To infect cell monolayers in 6-well plates or 12-well plates with 18mm coverslips, 500  $\mu$ l of appropriate culture media containing the appropriate virus at the indicated MOI was added. The plates were incubated at 37°C and 5% CO<sub>2</sub> for 1 hour with gentle rocking every 10 minutes to allow for virus attachment to cells. An additional 1 mL of culture media was then added for a total of 2 mL. For cell monolayers in 10 cm dishes, 5 mL of culture media containing virus was added to the dishes, incubated at 37°C and 5% CO<sub>2</sub> for 1 hour. Dishes were gently rocked every 10 minutes, followed by the addition of 5

mL of cell culture media. Infections were allowed to progress for the indicated amounts of time at 37°C and 5% CO<sub>2</sub>.

#### **2.4.2 Preparation of Virus Stocks**

Viruses were amplified in roller bottles containing  $3 \times 10^8$  BGMK cells by infecting at an MOI of 5 for 12-24 hours. Infected cells were harvested in saline-sodium citrate (SSC), centrifuged at 1000 x g for 5 minutes to pellet the cells, and the pellet was re-suspended in 5 mL of ice cold swelling buffer (10 mM Tris, pH 8.0, 2 mM MgCl<sub>2</sub>). The infected cells were lysed by 3 freeze-thaw cycles (see Section 2.5.5). Virus was isolated by dounce homogenization on ice using a “B” pestle (Bellco Biotechnology, Gilroy, CA) to lyse the cell membranes but not the virus membranes. After 100 strokes, the homogenate was centrifuged (1000 x g, 10 min) to pellet membranes while freed virus remains in the supernatant. After collecting the supernatant, pellets were re-suspended in 10 mL swelling buffer and dounce homogenized again with 60 strokes. After centrifugation at 1000 x g, 10 minutes, supernatants were collected and centrifuged at 10,000 x g for 1 hour at 4°C to pellet the virus. Virus pellets were re-suspended in DMEM and viral titres were determined as described in Section 2.5.7.

#### **2.4.3 Virus Titre Determination**

To determine the number of plaque-forming units per mL (PFU/mL) of virus in a stock, serial dilutions were used to infect BGMK monolayers. In brief, 10 µl of the original stock was added to 990 µl of 1X PBS (phosphate-buffered saline) for a 10<sup>-2</sup> dilution. One hundred µl of this dilution was serially diluted into 900 µl of 1X PBS 6 times for a series

of dilutions from  $10^{-3}$  to  $10^{-8}$ . Four hundred  $\mu\text{l}$  of each dilution was added to 6-well plates of sub-confluent BGMK monolayers in duplicate, and infections were incubated ( $37^{\circ}\text{C}$  and  $5\% \text{CO}_2$ ) for 12-24 hours. Infected wells were then fixed in neutral-buffered formalin (NBF) (37% (w/v) formaldehyde (Sigma-Aldrich), pH 7.4, 100 mL 10X PBS) and stained with a solution of 0.1% (w/v) crystal violet (Sigma-Aldrich) and 20% (v/v) ethanol. Single infectious virions, or PFU, are seen as visible regions of cell-clearing that can be counted and, with the known dilution of each well, can be used to calculate the original virus titre. The number of visible PFU multiplied by the reciprocal of the dilution of the well that was counted, divided by the total volume of that dilution added to the well, gives the stock concentration in PFU/mL. The average of the two duplicates was taken as the stock concentration.

To determine what volume was required for a given MOI, the following calculation was performed: the number of cells to be infected was multiplied by the desired MOI to give the total number of PFU required. This value was then divided by the stock concentration to give the volume of virus stock, which contains the desired number of PFU.

Calculation of the concentration of FWPV stocks required a separate protocol, since FWPV does not replicate in non-bird cells and does not form plaques at 24 hours post infection. To titer stocks of FWPV, the virus was serially diluted 10-fold in PBS. A 450  $\mu\text{l}$  volume of the dilutions ( $10^{-3}$  to  $10^{-8}$ ) was plated onto QM5 cells in 6 well plates and rocked every 10 minutes at  $37^{\circ}\text{C}$  for 1 hour. At 1 hour post infection 2 ml of DMEM supplemented with 50U/ml of penicillin with 50  $\mu\text{g}/\text{ml}$  of streptomycin, 1% (w/v) carboxymethylcellulose (CMC) (Sigma-Aldrich), and 5% FBS was added to each well.

Formation of plaques on QM5 cells required incubation for 5-7 days at 37°C. The CMC overlay has a high viscosity and prevents the formation of secondary plaques due to prevention of progeny virus diffusion in the cell culture dish (254). Upon formation of plaques as determined through visualization under a light microscope, QM5 monolayers were stained with 2ml per well of a 0.13% crystal violet, 4.75% ethanol, and 11.1% formaldehyde solution, which was directly added to the CMC containing media. The plates were washed and air-dried. Plaques were counted on wells containing 10-150 plaques. The number of plaques was used to calculate the concentration of the virus stocks.

#### **2.4.4 Preparation of Virus Genomic DNA**

To extract and prepare viral genomic DNA for PCR reactions, SDS lysis and phenol:chloroform extraction was performed. QM5 cells ( $1 \times 10^6$ ) were infected with FWPV at an MOI of 5 for 16 hours. Cell lysis buffer (1.2% SDS, 50 mM Tris-HCl (pH 8.0), 4 mM EDTA, 4 mM CaCl<sub>2</sub>, 0.2 mg/mL proteinase K) was added to lyse the cells and incubated overnight (37°C and 5% CO<sub>2</sub>). The lysate was collected in a microfuge tube and DNA was extracted in half a volume of phenol:chloroform (1:1) by vigorous vortexing. After centrifugation, the aqueous layer was collected and 50 µl of 3 M NaCH<sub>3</sub>CO<sub>2</sub> and 2.5 volumes of 95% ethanol were added and incubated at -70°C for 10 minutes to precipitate the DNA. The DNA was pelleted by centrifugation (9000 x g, 10 minutes) and re-suspended in 50 µl ddH<sub>2</sub>O.

## **2.5 Protein Methodology**

### **2.5.1 Antibodies**

All antibodies used in this study are listed in **Table 2.4**, along with the source and working concentration for each assay. Antibodies used for western blots were diluted in 1% BSA (w/v), or 5% skim milk powder (w/v) in 1% Tris-buffered saline plus Tween-20 (TBST). Alternatively, antibodies were diluted in LI-COR blocking solution (Mandel Scientific Company Inc, Guelph, ON, Canada).

### **2.5.2 SDS Polyacrylamide Gel Electrophoresis**

Protein samples were resolved by sodium dodecyl sulfate polyacrylamide gel electrophoresis (SDS-PAGE). Protein samples were suspended in SDS sample loading buffer comprised of 6.26 mM Tris, pH 6.8, 2% SDS (Fisher Scientific), 32% glycerol (Anachemia, Norman Lachine, QC, Canada), 0.05M 2-mercaptoethanol (Bioshop, Burlington, ON, Canada), and 0.005% w/v Bromophenol blue. Prior to separation by gel electrophoresis, samples were boiled at 100°C for 15 minutes. In general, 10-30 µl of boiled protein samples were loaded on 8-12% acrylamide gels (1.5 mm) and run in a Mini-PROTEAN Cell system (BioRad) at 150-200V along with 7.5 µl of pre-stained low molecular weight protein markers (Fermentas, Burlington, ON, Canada). Gels were run in 1X SDS-PAGE running buffer (190 mM glycine, 25 mM Tris, and 3.5 mM SDS).

<b>Antibody(#Cat. No)</b>	<b>Dilution/Amount</b>	<b>Source</b>
<b>Immunoprecipitation</b>		
<b>Mouse anti-FLAG M2 (#F3165)</b>	2 µl	Sigma-Aldrich
<b>Mouse anti-HSP70 (#sc-66048)</b>	1:100	Santa Cruz
<b>Microscopy</b>		
<b>Mouse anti-FLAG M2 (#F3165)</b>	1:200	Sigma-Aldrich
<b>Rabbit anti-FLAG (#F7425)</b>	1:200	Sigma-Aldrich
<b>Rabbit anti-MSH2 (#D24B5)</b>	1:200	Cell Signaling
<b>Mouse anti-MSH6 (#610919)</b>	1:200	BD Transduction Laboratories
<b>Mouse anti-HSP70 (#sc-66048)</b>	1:200	Santa Cruz
<b>Rabbit anti- HSP90 (#ADI-SPA-836)</b>	1:200	Enzo
<b>Rabbit anti-ATM (#ab32420)</b>	1:200	Epitomics
<b>Mouse anti-Crm1 (# sc-74454)</b>	1:100	Santa Cruz
<b>Mouse anti-β-tubulin (TM1541)</b>	1:200	ECM Biosciences
<b>Mouse anti-HA (#12CA5)</b>	1:200	Roche
<b>Mouse anti-conjugated ubiquitin (FK2) (#BML- PW8810)</b>	1:200	Enzo Life Sciences
<b>Alexa Fluor 546 Goat anti- Rabbit (#A-11010)</b>	1:400	Life Technologies
<b>Alexa Fluor 488 Goat anti-Mouse (#A-1101)</b>	1:400	Life Technologies
<b>Western Blotting</b>		
<b>Mouse anti-FLAG M2 (#F3165)</b>	1:5,000	Sigma-Aldrich

<b>Rabbit anti-FLAG (#F7425)</b>	1:2000	Sigma-Aldrich
<b>Mouse anti-GFP (#MMS-118P)</b>	1:10,000	Covance
<b>Rabbit anti-MSH2 (#D24B5)</b>	1:1,000	Cell Signaling
<b>Mouse anti-MSH6 (#610919)</b>	1:1,000	BD Transduction Laboratories
<b>Mouse anti-HSP70 (#sc-66048)</b>	1:1,000	Santa Cruz
<b>Rabbit anti- HSP90 (#ADI-SPA-836)</b>	1:1,000	Enzo
<b>Rabbit anti-ATM (#ab32420)</b>	1:1,000	Epitomics
<b>Mouse anti-Crm1 (# sc-74454)</b>	1:1,000	Santa Cruz , Wozniak lab
<b>Mouse anti-HA (#12CA5)</b>	1:2000	Roche
<b>Rabbit anti-VCP (#2648)</b>	1:500	Cell Signaling
<b>Rabbit anti-PCNA (#ab2426)</b>	1:500	Abcam
<b>Mouse anti-<math>\beta</math>-tubulin (TM1541)</b>	1:1,000	ECM Biosciences
<b>Rabbit anti-A34</b>	1:1000	D. Evans
<b>Rabbit anti-A55</b>	1:5000	C. Upton
<b>Rabbit anti-G1</b>	1:800	SIGA Researchlabs
<b>Mouse anti-I3</b>	1:10,000	D. Evans
<b>Rabbit anti-E9</b>	1:2,000	D. Evans
<b>Donkey anti-mouse-HRP (#715-035-150)</b>	1:25,000	Jackson Immunoresearch
<b>Donkey anti-rabbit-HRP (#711-035-152)</b>	1:25,000	Jackson Immunoresearch
<b>Goat anti-mouse-Alexa Fluor 790 (# A11375)</b>	1:10,000	Life technologies

<b>Goat anti-rabbit-Alexa Fluor 680 (#A21109)</b>	1:10,000	Life technologies
---	----------	-------------------

**EGFP – enhanced green fluorescent protein, HRP – horseradish peroxidase**

**Table 2.4 Antibodies used in this study**

### **2.5.3 Semi-Dry Transfer**

Proteins resolved by SDS-PAGE were transferred to polyvinylidene difluoride (PVDF) membranes (GE Healthcare), or nitrocellulose membranes (Biorad) for 2 hours at 450 mA with a semi-dry transfer apparatus (Tyler Research, Edmonton, AB, Canada). Membranes were blocked in 1% (w/v) BSA, or 5% skim milk powder (w/v) in TBST, or Odyssey blocking buffer at room temperature for at least 1 hour at room temperature.

### **2.5.4 Western Blotting**

To detect proteins of interest, membranes were probed with primary antibodies according to the dilutions listed in **Table 2.4** overnight at 4°C. Three 15 minute washes with TBST removed any excess primary antibodies from membranes. Horseradish peroxidase conjugated secondary antibodies were added (**Table 2.4**) for 1 hour at room temperature, followed by four 15 minutes TBST washes. Proteins were visualized by enhanced chemiluminescence (ECL; GE Healthcare) according to the manufacturer's protocol. Alternatively, proteins were visualized with LI-COR. Membranes already probed with primary antibodies were probed with IR define dye-conjugated secondary antibodies for 1 hour, washed three times for 10 minutes in 1% TBST and once in 1x PBS, before bands were quantified on a LI-COR Odyssey Infrared Imager (LI-COR Biosciences, Lincoln, NE).

### **2.5.5 Image capture and processing**

Western Blots and Commassie gels were scanned on a CanoScan 5600F Scanner (Canon, Calgary, AB, Canada), using the accompanied Image Capture Version 6.2 software

package. Adobe Photoshop CC (Adobe, Ottawa, ON, Canada) was used to align and label images from scans and LI-COR Odyssey Infrared Imager to prepare Figures.

### **2.5.6 Immunoprecipitation to detect ubiquitination**

To detect ubiquitination of FWPV proteins, HeLa or QM5 cells ( $2 \times 10^6$ ) were infected/transfected with VACVCop or VACV $\Delta$ F1L-FLAG-FPV039 at an MOI of 5, and 2 $\mu$ g of the following plasmids; pSC66-FLAG-p28(IHDW), pSC66-FLAG-FWPV150 or pSC66-FLAG-FWPV157. Additionally, VACV-FLAG-FWPV039 was used as a positive control for ubiquitination. Cells were lysed in RIPA buffer containing 5mM NEM define (Sigma-Aldrich), 50mM Tris-HCl, 1% NP-40, 0.5% sodium deoxycholate, 0.1% SDS, 150mM NaCl and EDTA-free protease inhibitors (Roche Diagnostic, Montreal, QC, Canada). FLAG-tagged proteins were immunoprecipitated and pulled down with protein G beads (GE Health Care) with mouse anti-FLAG M2 (Sigma-Aldrich). Samples were analyzed by western blotting (see Section 2.5.4) with mouse anti-FLAG (Sigma-Aldrich), mouse anti-HA, or mouse anti-ubiquitin to detect ubiquitination (Enzo Life Science, Brockville, ON, Canada). To stabilize ubiquitination, cells were treated with MG132 (10 $\mu$ M) for 6 hrs prior to lysis.

To determine ubiquitination of p28 mutants, HeLa cells ( $2 \times 10^6$ ) were infected with VACV-HA-Ub define at an MOI of 5 and transfected with 2 $\mu$ g of the following plasmids; pSC66-FLAG-p28, pSC66-FLAG-p28(1-152), pSC66-FLAG-p28(153-242), pSC66-FLAG-p28( $\Delta$ 44-51), pSC66-FLAG-p28(C173S/C176S), pSC66-FLAG-p28(1-184), or pSC66-FLAG-p28(1-204). Cells were lysed in RIPA buffer and p28 was immunoprecipitated with mouse anti-FLAG M2 and western blotted with rabbit anti-

FLAG (Sigma-Aldrich), or mouse anti-HA (Enzo Life Science) to detect ubiquitination. To further detect ubiquitination, cells were treated in the absence or presence of MG132 (10  $\mu$ M) for 6 hours prior to lysis.

To determine, if HSP70 is a substrate of p28, HeLa cells ( $2 \times 10^7$ ) were infected with VACVCop, VACV-FLAG-p28, or VACV-FLAG-p28(C173S/C176S) and co-infected with VACV-HA-Ubiquitin at an MOI of 5. Infected cells were treated with MG132 (20  $\mu$ M) for the last 4 hours of the 16 hour infection. Cells were lysed in RIPA lysis buffer containing 5mM NEM (Sigma-Aldrich) and EDTA-free protease inhibitors (Roche Diagnostic). Endogenous HSP70 was immunoprecipitated with mouse anti-HSP70. Additionally, VACV-FLAG-p28 was immunoprecipitated with mouse anti-FLAG as a positive control for ubiquitination. We used isotype antibody mouse anti-GFP as a negative control for immunoprecipitation of VACV-FLAG-p28 infected cells. Samples were western blotted with rabbit anti-HSP70, mouse anti-FLAG, or mouse anti-HA to detect ubiquitination.

### **2.5.7 Acetone Precipitation of Cell Lysates**

Ten percent of cell lysates prior to immunoprecipitations were subjected to acetone precipitation to precipitate whole cell lysate proteins. Five volumes of ice-cold acetone (Fisher Scientific) were added to supernatants and protein precipitation was allowed to occur at -20°C for at least 1 hour. Proteins were isolated by centrifugation at 10,000 x g for 10 minutes, air-dried, and re-suspended in 100  $\mu$ l of SDS sample loading buffer.

### **2.5.8 *In vitro* ubiquitination assay**

QM5 cells ( $2.5 \times 10^6$ ) were infected with FWPV at a MOI of 5 and transfected with pSC66-FLAG-p28, pSC66-FLAG-p28(C173S/C176S), pSC66-FLAG-FWPV150, pSC66-FLAG-FWPV150(C196S/C199S), pSC66-FLAG-FWPV157, or pSC66-FLAG-FWPV157(C218S/C221S). Alternatively, HeLa cells ( $2.5 \times 10^6$ ) were infected with VACVCop at an MOI of 5 and transfected with pSC66-FLAG-p28, pSC66-FLAG-p28(1-152), pSC66-FLAG-p28(153-242), pSC66-FLAG-p28( $\Delta$ 44-51), pSC66-FLAG-p28(C173S/C176S), pSC66-FLAG-p28(1-184), or pSC66-FLAG-p28(1-204). Sixteen hours post-infection, immunoprecipitations were performed using anti-FLAG M2. The immunoprecipitates were washed with 1% NP-40 lysis buffer (described above) and then additionally washed with wash buffer (50 mM Tris-HCL pH7.5, 50 mM NaCl, 1 mM EDTA pH 8.0, 0.01% NP-40, 10% glycerol) (255). The *in vitro* ubiquitination protocol followed manufacturer's instructions (BIOMOL International, Kelayres, PA). The ubiquitination reaction was carried out in ubiquitination buffer (0.4 mM Tris-HCL, pH 7.5), 10 U/ml inorganic pyrophosphatase solution (Sigma-Aldrich), 1mM DTT, 5 mM MG-ATP) supplemented with 50 nM E1, 1.25  $\mu$ M E2 (UbcH3 or 5), and 1.25  $\mu$ M Biotinylated-Ub. This was directly added to the FLAG-tagged proteins immobilized at the protein G beads. The reaction was carried out at 37°C for 90 minutes and run on a SDS-PAGE gel (Biorad). The western blots were blocked in 1%BSA/TBST overnight and blotted with Streptavidin-HRP (Pierce, Rockford, IL) 1:10,000 dilution to detect ubiquitination.

### **2.5.9 Infection and immunoprecipitation for Mass Spectrometry**

HeLa cells ( $2 \times 10^6$ ) were infected with VACVCop, VACV-FLAG-p28, or VACV-FLAG-p28(C173S/C176S) at an MOI of 5. To stabilize ubiquitinated target proteins, cells were treated with MG132 (20 $\mu$ M) for the last 4 hours prior to lysis. Sixteen hours post-infection, cells were lysed in NP-40 lysis buffer and immunoprecipitations were performed using the anti-FLAG M2 mAb. Protein G beads were washed with 1% NP-40 lysis buffer. Immunoprecipitated proteins were then eluted from the beads by boiling in SDS-PAGE sample loading buffer.

For mass spectrometry follow up with immunoprecipitations and western blotting, we screened primary antibody staining, including rabbit anti-MSH2, mouse anti-MSH6, mouse anti-HSP70, rabbit anti-HSP90, rabbit anti-ATM, mouse anti-Crm1, rabbit anti-VCP, rabbit anti-PCNA, rabbit anti-A34, rabbit anti-A55, rabbit anti-G1, mouse anti-I3, rabbit anti-E9. Proteins were visualized after secondary antibody stain with donkey anti-mouse-HRP or donkey anti-rabbit-HRP by ECL, according to the manufacturer's protocol. Alternatively, proteins were visualized after IRDye-conjugated secondary antibodies for 1 hour using goat anti-mouse-Alexa Fluor, or goat anti-rabbit-Alexa Fluor 680 (see above).

### **2.5.10 Coomassie Staining**

To assess interacting partners, or substrates of FLAG-p28, anti-FLAG immunoprecipitates were subjected to SDS-PAGE on a Hoefer electrophoresis unit SE 600 series (GE Healthcare). Proteins were visualized using a high sensitivity Coomassie staining protocol (Dr. R. Fahlman, University of Alberta, Canada). The gel was first fixed

in a 50% methanol, 2% phosphoric acid solution for 1 hour. After two 20 minute washes in milli-Q water, a destaining solution comprised of 20% methanol, 10% phosphoric acid, 1.4 mM Coomassie Brilliant Blue G-250, and 0.8 M ammonium sulfate was added to the gel and incubated overnight at 4°C. The gel was washed and stored in milli-Q water.

### **2.5.11 Mass Spectrometry**

Whole lanes of gels from Section 2.5.9 were cut into smaller pieces and sent for identification by mass spectrometry in collaboration with Dr. Richard Fahlman and Dr. Jack Moore at the Institute for Biomolecular Design (IBD), University of Alberta. Proteins in p28 immunoprecipitates were identified with a liquid chromatography-tandem mass spectrometry (LC-MS/MS) using an LCQ Deca XP ion trap mass spectrometer (Thermo Fisher Scientific, Waltham, MA). We obtained a list of identified proteins via Thermo Proteome Discoverer software (Thermo Scientific) (**Appendix Table A1 and A2**) and considered mass spectrometry hits significant when the protein had at least two peptides identified at a medium confidence according to the common Molecular and Cellular Proteomics (MCP) guidelines. We excluded mass spectrometry hits, found in the negative control of immunoprecipitates from lysates of HeLa cells infected with VACVCop.

## **2.6 Bioinformatics**

### **2.6.1 Analysis of Functional Annotation Clustering**

To extract biological features and meaning associated with the identified mass spectrometry hits, we used DAVID Bioinformatics Resources 6.7 (DAVID; National Institute of Allergy and Infectious Diseases [NIAID, NIH], <http://david.abcc.ncifcrf.gov>) for the analysis of functional annotation clustering (256).

### **2.6.2 Protein sequence alignments**

Protein alignments for p28(IHDW), M143R, ECTV virus strain Moscow p28(ECTV), canarypox virus (CNPV197 and CNPV205), and fowlpox virus p28(FWPV150, FWPV157, FWPV075, FWPV124, FWPV155, FWPV159, FWPV161, FWPV163, FWPV236, and FWPV248) were performed via ClustalW (1.82) (<http://www.ebi.ac.uk/clustalW/#>) (257).

## **2.7 Assays**

### **2.7.1 Reverse Transcription PCR to Detect Virus Gene Expression**

RNA transcripts of FWPV150 and FWPV157 were analyzed by reverse transcription polymerase chain reaction (RT-PCR). QM5 cells ( $1 \times 10^6$ ) were infected with FWPV at an MOI 5 in the absence or presence of 80 $\mu$ g/ml of cytosine b-D-arabinofuranoside hydrochloride (AraC) (Sigma-Aldrich), a DNA replication inhibitor, which subsequently inhibits the expression of late genes. At 4, 12, and 24 hours post infection cells were collected, and RNA was extracted with TRIZOL according to the manufacturer's

protocol (Invitrogen). To prevent genomic DNA contamination, isolated RNA was treated with 1 U/ml DNase (Invitrogen) for 20 min at room temperature. The DNase treatment was inactivated by addition of 1µl 25mM EDTA for 10 min at 65 °C. To exclude DNA contamination an aliquot was set aside and used as a template for control PCR. Reverse transcription was performed using 1µg of DNase treated RNA, 200U of SuperScriptII reverse transcriptase (Invitrogen), 1µl 500 mg/ml Oligo-dT (Invitrogen), 0.2mM dNTPs (Invitrogen), and 2mM DTT (Invitrogen) and incubated at 42 °C for 50 min, followed by incubation at 70 °C for 15 minutes. This first strand RT reaction cDNA was used as a template for PCR using the following primers. FWPV primers for FWPV150, FWPV157, FWPV075, FWPV124, FWPV155, FWPV159, FWPV161, FWPV163, FWPV236, and FWPV248 are listed in **Table 2.2**. To show the inhibition of late gene expression in the presence of AraC, primers specific to FWPV085, ISL homologue, were used (**Table 2.2**). As a control for early gene expression, we used primers specific to the early gene FWPV037. As a positive control, GAPDH was amplified using GAPDH specific primers.

### **2.7.2 Confocal Microscopy**

HeLa or QM5 cells ( $5 \times 10^5$ ) were seeded on 18mm cover slips and infected/transfected as described in Section 2.3.2. Cells were fixed with 4% paraformaldehyde and permeabilized with 1% NP-40 (Sigma-Aldrich). Cells were stained with antibodies listed in **Table 2.4**. Coverslips were washed with PBS containing 1% FBS and mounted in 4mg/ml of N-propyl gallate (Sigma-Aldrich) in 50% glycerol containing 250 µg/ml 4', 6-diamidino-2-phenylindole (DAPI) (Invitrogen) to visualize nuclei and cytoplasmic viral

factories. Cells were examined using a Leica SP5 confocal microscope (Leica, Concord, ON, Canada) at 405 nm to detect DAPI.

In Chapter 3 and 4, we performed three independent experiments per Figure. We observed on average over 100 cells per sample, which were evaluated across the entire cover slip of the samples. We showed one representative single cells per sample in the Figures.

In Chapter 5, we performed three independent experiments and evaluated 60 cells per sample. Fiji software was used to measure the Region of interest (216) at the virus factories and whole cells. The obtained Raw Integrated Densities values were used to calculate the percentage of antibody-fluorescence labeled proteins at the virus factory in presence or absence of functional p28. The Department of Mathematical and Statistical Sciences, Training Consulting Centre (TCC) was consulted for the statistical analysis. Statistical analysis of data was performed using GraphPad Prism version 7. One-way Analysis of variance (ANOVA) tests with post-Tukey column comparison were used to compare calculate statistical significance. (GraphPad Software, La Jolla, CA)  $P < 0.05$  was considered significant and statistically significant results were reported as: \*  $p < 0.05$ , \*\* $p < 0.01$ , and \*\*\*  $p < 0.001$ . See also Section 2.7.5 Statistical analysis.

### **2.7.3 Flow cytometry**

HeLa cells were transfected with 0.5 $\mu$ g of pEGFP-C3 or 2 $\mu$ g of pEGFP-p28(IHDW), pEGFP-p28(ECTV), pEGFP-p28(1-152), pEGFP-p28(153-242), pEGFP-p28( $\Delta$ 44-51), pEGFP-p28(1-184), pEGFP-p28(1-204), pEGFP-p28(C173S/C176S) with Lipofectamine according to the manufacturers instructions (Invitrogen). Sixteen hours post-transfection

cells were treated with or without the proteasome inhibitor MG132 (10 $\mu$ M) (Sigma-Aldrich) for 6 hours. Cells were labelled with 0.2 $\mu$ M tetramethylrhodamine ethyl ester (TMRE) (Invitrogen) to label healthy cells, washed and resuspended in PBS containing 1% FBS and analyzed by two-color flow cytometry (Becton Dickinson, Franklin Lakes, NJ) (36). TMRE fluorescence was measured through the FL-2 channel equipped with a 585-nm filter (42nm band pass) and EGFP fluorescence was measured through the FL-1 channel equipped with a 489nm filter (42nm band pass). The fluorescence signals were acquired for 20,000 cells per sample at logarithmic gain and analysis was performed using CellQuest software (Becton Dickinson).

#### **2.7.4 Proteasome assay**

HeLa cells ( $1 \times 10^4$ ) were mock-infected or infected for 14 hours with VACV Cop, CPXV, or ECTV at an MOI of 10. QM5 cells ( $1 \times 10^4$ ) were mock-infected or infected for 14 hours with FWPV at an MOI of 10. Cells were left untreated or treated with 10 $\mu$ M MG132 at 12 hours post infection 6 hours prior to lysis (Sigma-Aldrich). The chymotrypsin-like activity of the proteasome was assessed using the cell-based Proteasome-Glo assay, according to the manufacturer's directions (Promega). Luminescence was recorded 10 min after the addition of the Proteasome-Glo reagent using an EnVision 2104 multilabel reader (Perkin-Elmer, Waltham, MA). The assay was performed in triplicate, and average relative light units (RLU) were presented. The measurements of relative light units from the proteasome assay were subjected to analysis using two-way ANOVA to explore statistical relationships between MG132 treatment

and between mock and virus infection. The level of statistical significance was set at  $p < 0.001$ . See also Section 2.7.5 Statistical analysis.

### **2.7.5 Statistical analysis**

Statistical analysis for confocal samples was performed as described in Section 2.7.2. In brief, a total of 60 cells per sample were collected from three independent experiments and the percentage of antibody-fluorescence labeled proteins at the virus factory in presence or absence of functional p28 was calculated. The Department of Mathematical and Statistical Sciences, Training Consulting Centre (TCC) was consulted for the statistical analysis. Statistical analysis of data was performed using GraphPad Prism version 6. One-way Analysis of variance (ANOVA) tests with post-Tukey column comparison were used, to test one dependent variable across different groups to calculate statistical significance.  $p < 0.05$  was considered significant and statistically significant results were reported as: \*  $p < 0.05$ , \*\* $p < 0.01$ , and \*\*\*  $p < 0.001$ .

Statistical analysis for the Proteasome assay was performed as described in Section 2.7.4. Statistical analysis of the results was computed using Prism-graph. The measurements of relative light units from the proteasome assay were subjected to analysis using two-way ANOVA with post-Tukey column comparison since statistical relationships were tested between two factors, MG132 treatment and between mock and virus infection. The level of statistical significance was reported as  $p < 0.001$ .

**CHAPTER 3: FOWLPOX VIRUS ENCODES TWO P28-LIKE UBIQUITIN  
LIGASES THAT ARE EXPRESSED EARLY AND LATE**

A version of the data presented in this chapter has been published:

Bareiss B. and Barry M. (2014) Fowlpox virus encodes two p28-like ubiquitin ligases that are expressed early and late during infection. *Virology*.462-463:60-70.

All of the experiments presented in this chapter were performed by myself. The original manuscript was written by myself with editorial contributions from Robyn-Lee Burton, Dr. Thibault, Dr. Noyce, and Dr. Barry.

### 3.1 Introduction

p28 is a poxvirus encoded ubiquitin ligase, which acts as a virulence factor during ECTV infection (37, 242, 243, 245). p28 is found in VACV-IHDW and ECTV, while p28-homologues are expressed in a wide range of poxviruses, including MYXV, VARV, Shope fibroma virus, and CPXV (**Table 1.3**). Interestingly, Avipoxviruses, such as CNPV and FWPV, contain two p28-like ubiquitin ligases, an observation not seen in other members of the poxvirus family (22, 23). Both p28 homologues in FWPV, FWPV150 and FWPV157 contain a putative Kila-N DNA binding domain, important for localization to the virus factory, and a putative RING domain, crucial for the ubiquitin ligase activity (22). Additionally, FWPV encodes eight Kila-N-only proteins, which are classified as p28-like genes, but are lacking the RING domain (22).

The work in this chapter focuses mainly on characterizing the two p28-like ubiquitin ligases, FWPV150 and FWPV157, encoded by FWPV. The data presented here shows that both FWPV150 and FWPV157 are functional ubiquitin ligases. Furthermore, both co-localize with conjugated ubiquitin at the virus factory and are ubiquitinated during poxvirus infection. Our data indicate that FWPV150 and FWPV157 are actively transcribed during FWPV infection. Intriguingly, FWPV150 was transcribed early on during infection, while FWPV157 was expressed late. Furthermore, all eight Kila-N only genes were actively transcribed early during infection. The presence of numerous Kila-N only proteins and FWPV-encoded ubiquitin ligases indicates their importance during FWPV infection.

## 3.2 Results

### 3.2.1 FWPV and CNPV encode p28-like ubiquitin ligases

Poxviruses promote infection by expressing a variety of effector proteins (20, 30). For example, ECTV encodes the virulence factor p28 that functions as a ubiquitin ligase (37, 245). Homologues of p28 are encoded by a wide range of poxviruses including ECTV, IHDW and CPXV, each encoding a single homologue. In contrast, members of the *Avipoxvirus* family, such as FWPV and CNPV, encode two homologues of p28-like ubiquitin ligases that have not been thoroughly investigated (22, 23). Compared to p28(IHDW) and p28(ECTV), the sequence identity/similarity of FWPV150, FWPV157, CNPV197, and CNPV205 demonstrate 23%, 43%, 43%, and 42% sequence identity, and 40%, 62%, 54%, and 56% sequence similarity, respectively. The sequence identity between FWPV150 and FWPV157 is 35%, whereas the sequence identity between CNPV197 and CNPV205 is 36%. Significantly, the cysteine and histidine residues within the RING domain, which were previously shown to be critical for ubiquitin ligase activity (242), are highly conserved among the four *Avipoxvirus* proteins and are similar to IHDW and ECTV (**Figure 3.1**). Additionally, residues 44 to 50 within the Kila-N domain, which are crucial for DNA binding, were similar among the proteins. Therefore we sought to investigate if both ubiquitin ligases, FWPV150 and FWPV157, functioned during infection.

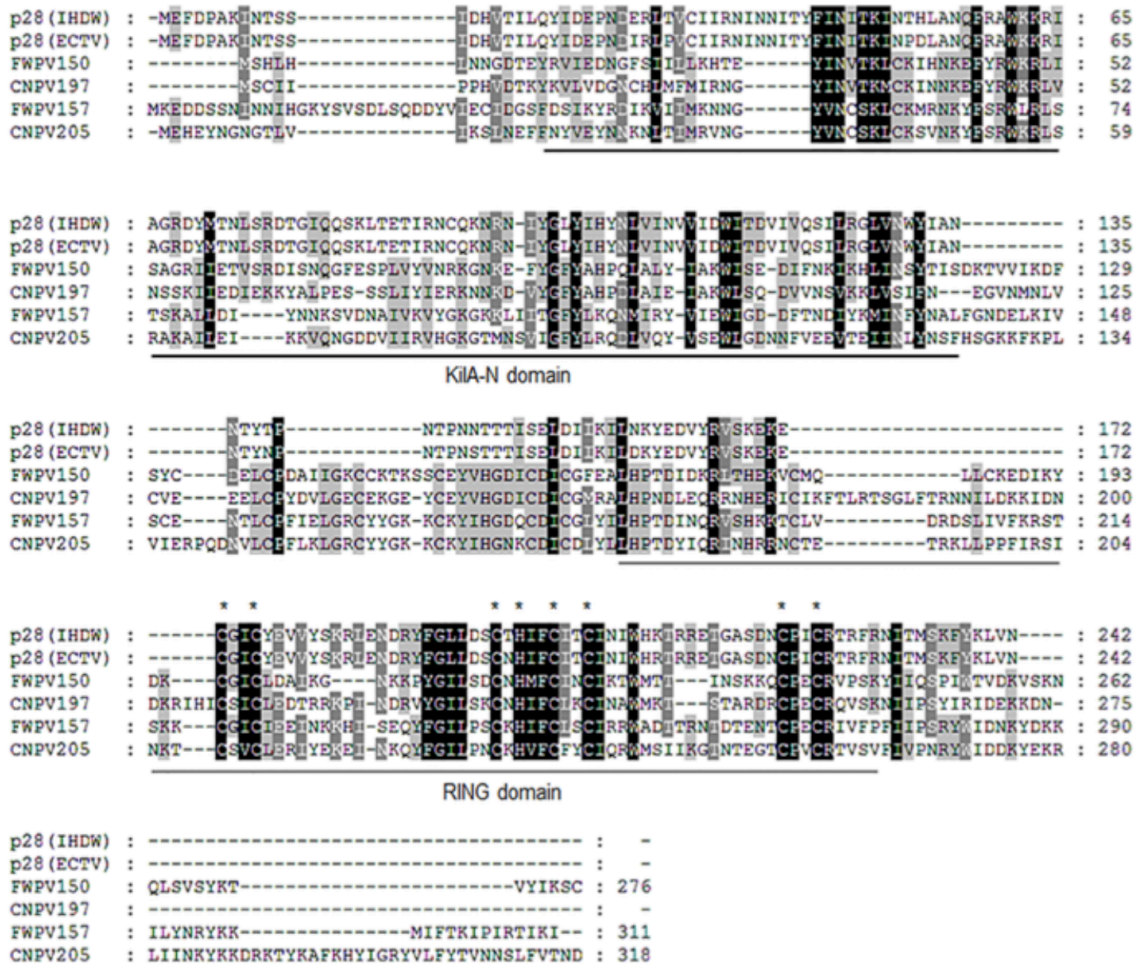


**Figure 3.1** Alignment of p28 homologues in FWPV and CNPV demonstrates conservation of the KilA-N and RING domains.

Protein alignments for p28(IHDW), p28(ECTV), FWPV150, FWPV157, CNPV197 and CNPV205 were performed via Clustal W (1.82) (<http://www.ebi.ac.uk/clustalW/#>) (8). The KilA-N domain is underlined in black and the RING domain is underlined in grey. Asterisks highlight the conserved cysteines and histidines within the RING domain. The thick black line marks the motif in p28, which is important for DNA binding (44-50). Conserved amino-acid residues were shaded using GeneDoc (258, 259). The Genedoc shading mode was set to conservation, with shading level 4 and the conserved percent was primary 100% (black), secondary 80% (dark grey), and tertiary 60% (light grey). The shade style was set to amino acid identity.

### 3.2.2 FWPV150 and FWPV157 localize to viral factories

Previous studies have demonstrated that p28(IHDW) localizes to viral factories (243). Given the conservation of key residues among p28(IHDW), FWPV150 and FWPV157, we sought to investigate whether FWPV150 and FWPV157 localize to virus factories as well. We used infection accompanied by transfection to investigate the cellular localization of proteins during infection. HeLa cells were mock-infected (**Figure 3.2; panel a-d**), infected with VACVCop (**Figure 3.2; panel e-h**), or infected with VACVCop and transfected with pSC66- FLAG-FWPV150 (**Figure 3.2; panel i-l**) or pSC66-FLAG-FWPV157 (**Figure 3.2; panel m-p**). DAPI was used to visualize both the nucleus and cytoplasmic virus factories and I3L, a ssDNA binding protein, which localizes to the virus factory, was used as a marker for virus factories. Staining for FLAG visualized FWPV150 and FWPV157. Using this approach, we observed that both FWPV150 and FWPV157 localized to virus factories during VACVCop infection. Given that p28(IHDW) co-localizes with conjugated ubiquitin (243), we determined if the same was true for FWPV150 and FWPV157. We included mutant versions of both FWPV150 and FWPV157 containing mutations of two cysteine residues in the RING domain, FWPV150(C196S/C199S) and FWPV157(C218S/C221S) (**Figure 3.3; panel q-t and panel y-bb**). Cells were stained with DAPI and co-stained with anti-FLAG to visualize FLAG-FWPV150, FLAG-FWPV157, FLAG-FWPV150(C196S/C199S), FLAG-FWPV157(C218S/C221S) and co-stained with an antibody specific for conjugated ubiquitin (122). As expected, infection with VACVCop resulted in a lack of conjugated ubiquitin accumulating at the virus factory (**Figure 3.3; panel f**). In contrast, conjugated ubiquitin was concentrated at the viral factory and co-localized in p28(IHDW),

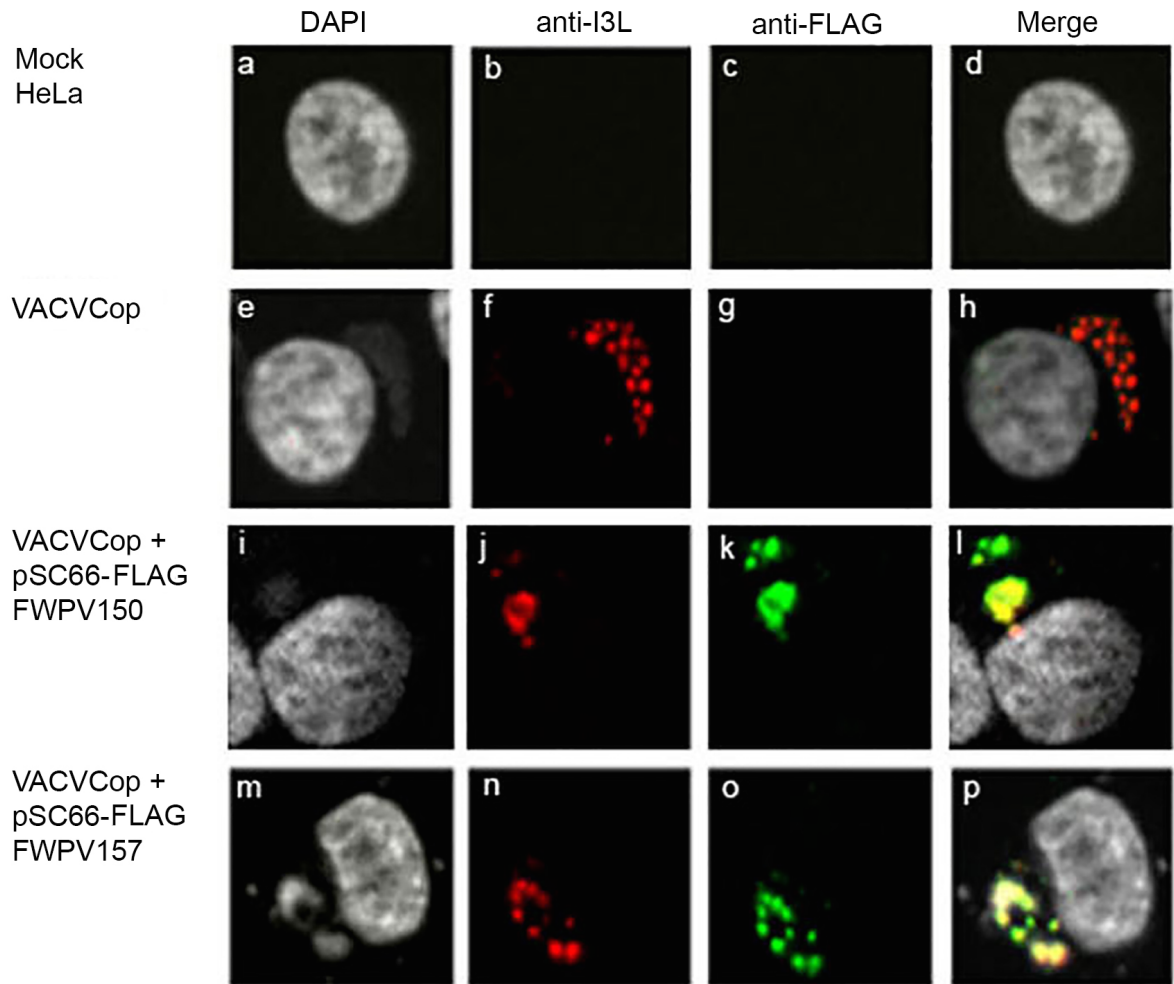


**Figure 3.2 FWPV150 and FWPV157 localize to viral factories.**

**(A)** HeLa cells were mock-infected or infected with VACVCop at an MOI of 5 and transfected with pSC66-FLAG-FWPV150 or pSC66-FLAG-FWPV157 for fourteen hours. Cells were fixed and stained for DAPI to visualize nuclei and virus factories. Anti-FLAG was used to visualize FWPV150 and FWPV157, and anti-I3L to visualize the virus factories. Co-localization of both FLAG-tagged proteins with I3L was visualized by confocal microscopy. This experiment was performed three independent times and we observed on average over 100 cells per sample, which were evaluated across the entire cover slips of the samples. We showed one representative cell per sample in this Figure.

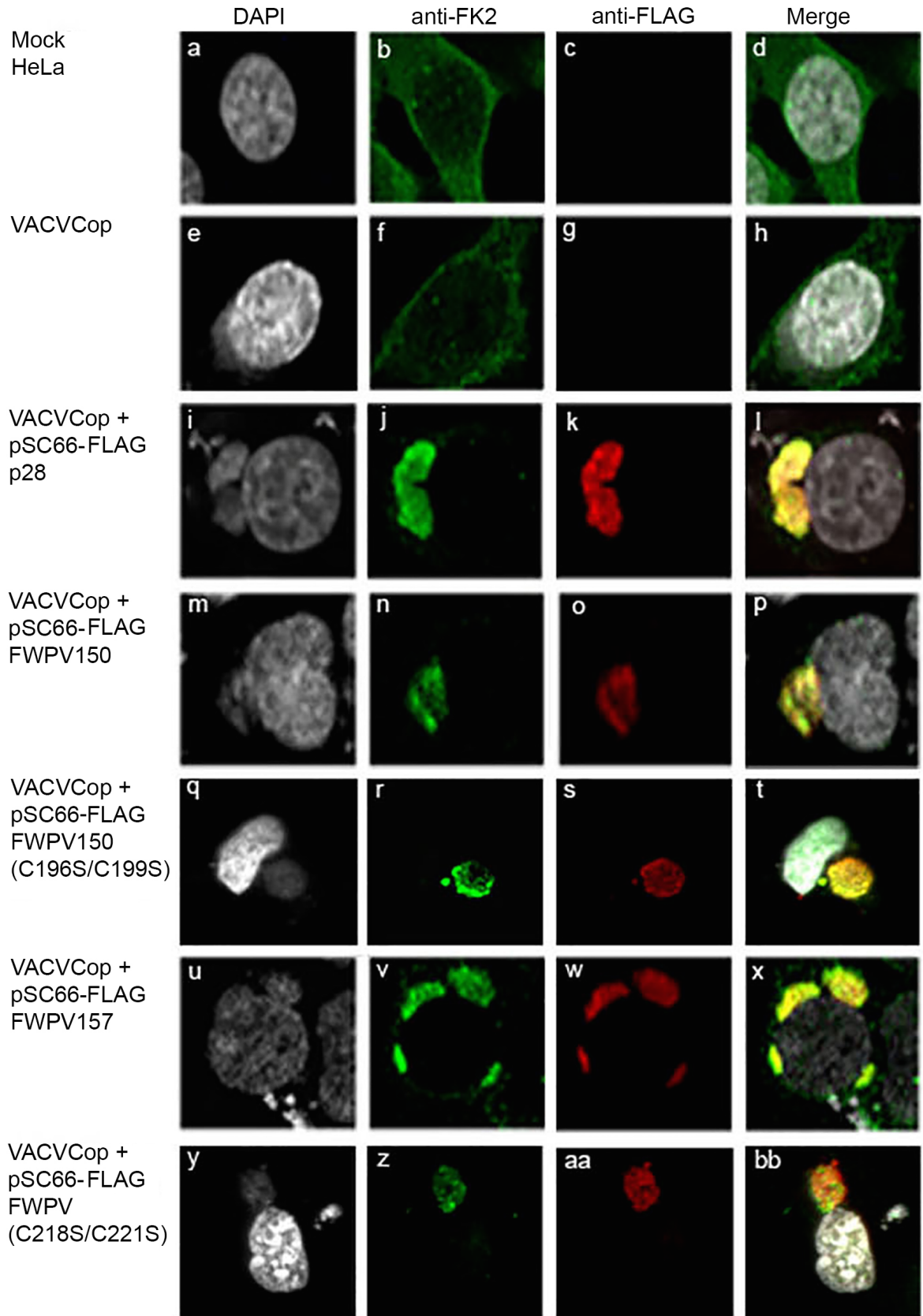


**Figure 3.3 FWPV150 and FWPV157 co-localize with conjugated ubiquitin to viral factories.**

HeLa cells were mock-infected or infected with VACV Cop at an MOI 5 and transfected with pSC66-FLAG-p28, pSC66-FLAG-FWPV150, pSC66-FLAG-FWPV150(C196S/C199S), pSC66-FLAG-FWPV157, or pSC66-FLAG-FWPV157(C218S/C221S). Cells were fixed and treated with DAPI, to visualize the nucleus and virus factories, and stained with anti-FLAG to visualize FLAG-tagged proteins and anti-FK2 to recognize conjugated ubiquitin. Co-localization was visualized by confocal microscopy. This experiment was performed three independent times and we observed on average over 100 cells per sample, which were evaluated across the entire cover slips of the samples. We showed one representative cells per sample in this Figure.

FWPV150 and FWPV157-expressing cells (**Figure 3.3; panel i-l**). In a similar manner, FWPV150(C196S/C199S), and FWPV157(C218S/C221S) also co-localized with conjugated ubiquitin at the virus factories upon disruption of the RING domain function (**Figure 3.3; panel t and bb**). Taken together, these data indicate that the accumulation of conjugated ubiquitin at the virus factory occurs in cells expressing 28(IHDW), FWPV150 and FWPV157 and that disruption of the RING domains of FWPV150 and FWPV157 does not prevent conjugated ubiquitin from accumulating at the factory.

Our previous experiments were conducted in HeLa cells during VACV Cop infection, we next wanted to determine if conjugated ubiquitin was also found at the virus factory during FWPV infection. We used QM5 quail cells as a source of a bird cell line, since FWPV cannot fully replicate in mammalian cells and failed to produce progeny viruses; FWPV only replicated in bird cells due to host tropism (260). QM5 cells were mock-infected (**Figure 3.4; panel a-d**), infected with FWPV (**Figure 3.4; panel e-h**), or infected with FWPV and transfected with pSC66-FLAG-FWPV150 (**Figure 3.4; panel i-l**), pSC66-FLAG-FWPV150(C196S/C199S) (**Figure 3.4; panel m-p**), pSC66-FLAG-FWPVFLAG157 (**Figure 3.4; panel q-t**) or pSC66-FWPV-FLAG-157(C218S/C221S) (**Figure 3.4; panel u-x**). Cells were co-stained with anti-FLAG to visualize FWPV150 (**Figure 3.4; panel k**), FWPV157 (**Figure 3.4; panel s**), FWPV150(C196S/C199S) (**Figure 3.4; panel o**) or FWPV(C218S/C221S) (**Figure 3.4; panel w**) and with FK2 to detect conjugated ubiquitin (**Figure 3.4; panel b, f, j, n, r, v**). Infection with wildtype FWPV resulted in a modest accumulation of conjugated ubiquitin at viral factories (**Figure 3.4; panel f**). FWPV150 and FWPV157 co-localized with conjugated ubiquitin

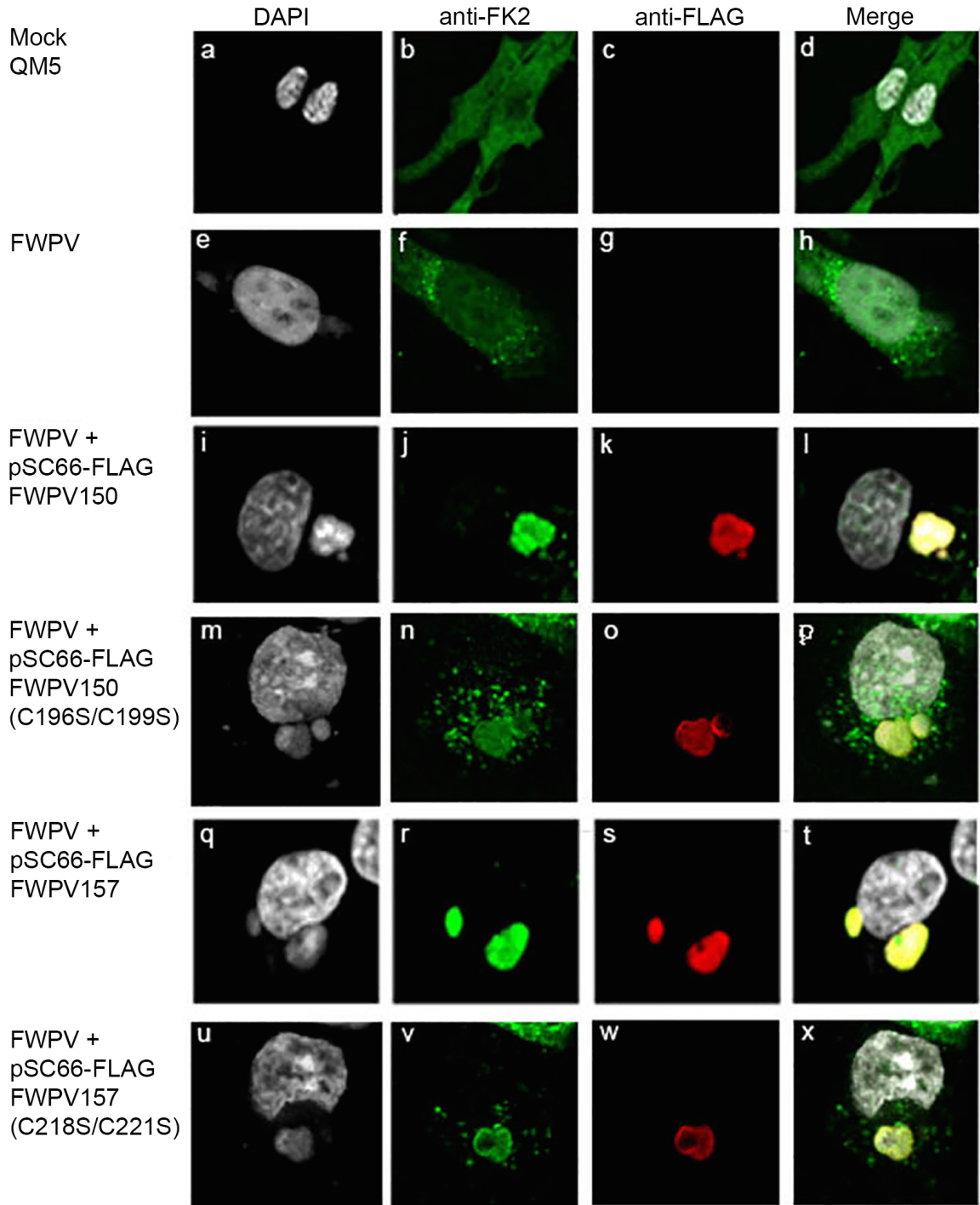


**Figure 3.4 FWPV150 and FWPV157 localize with conjugated ubiquitin at virus factories in quail cells.**

QM5 cells were mock-infected or infected with FWPV at an MOI of 5 and transfected with pSC66-FLAG-FWPV150, pSC66-FLAG150(C196S/C199S), pSC66-FLAG-FWPV157, or pSC66-FLAG-FWPV157(C218S/C221S). Cells were fixed and treated with DAPI, to visualize the nucleus and virus factories, and stained anti-FLAG to visualize FLAG-tagged proteins and anti-FK2 to recognize conjugated ubiquitin. Co-localization was visualized by confocal microscopy. This experiment was performed three independent times and we observed on average over 100 cells per sample, which were evaluated across the entire cover slips of the samples. We showed one representative cells per sample in this Figure.

at the viral factories (**Figure 3.4; panel l and t**). Despite the lack of key residues within the RING domain, both FWPV150(C196S/C199S) and FWPV157(C218S/C221S) still accumulated conjugated ubiquitin at the virus factory; however not to the same degree that FWPV150 or FWPV157 were able to (**Figure 3.4; panel l, p, t, and x**). Both RING domain mutants demonstrated some punctate staining of conjugated ubiquitin in the cytoplasm, which did not co-localize at the virus factories (**Figure 3.4; panel p and x**). We next investigated, whether FWPV150 or FWPV157 are regulated by ubiquitination, and if they indeed act as ubiquitin ligases.

### **3.2.3 FWPV150 and FWPV157 are ubiquitinated during infection and act as ubiquitin ligases**

Many cellular ubiquitin ligases are regulated by ubiquitination and subsequent proteasomal degradation (139). We next investigated whether FWPV150 and FWPV157 were regulated by the ubiquitin-proteasome pathway. HeLa cells were infected with VACV-HA-Ubiquitin at a MOI of 5 and transfected with pSC66-FLAG-p28, pSC66-FLAG-FWPV150 or pSC66-FLAG-FWPV157. As a further control for a ubiquitinated protein, cells were also infected with VACV-FLAG-FWPV039, an anti-apoptotic protein that is regulated by ubiquitination (84) (**Figure 3.5A**). Cells were lysed in the presence of NEM, thus preventing the removal of ubiquitin chains. FLAG-tagged proteins were immunoprecipitated with mouse anti-FLAG M2 and ubiquitination of the proteins was detected by western blot. Western blots showed high molecular bands for FLAG-p28, FLAG-FWPV150, FLAG-FWPV157 and FLAG-FWPV039, when stained with anti-

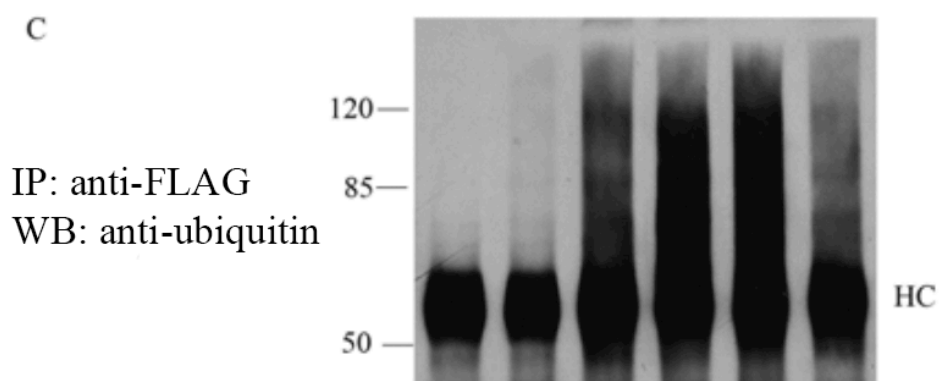
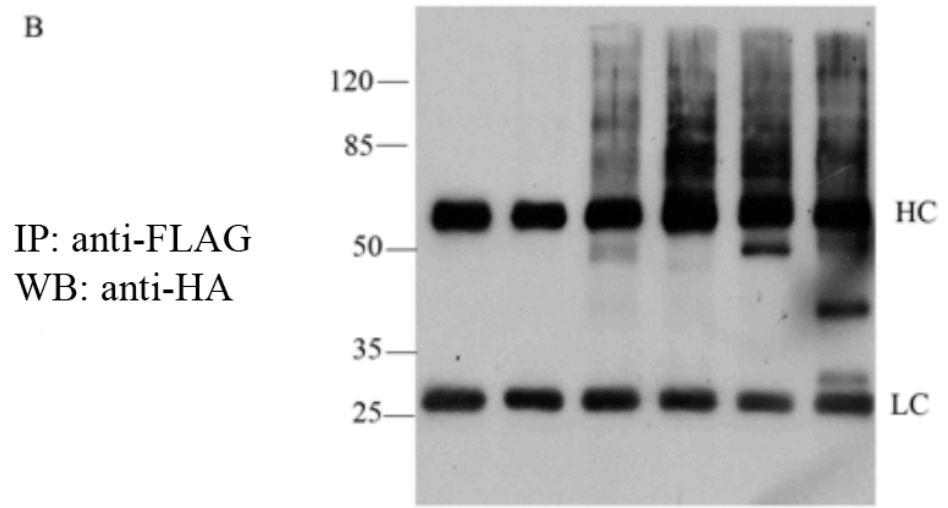
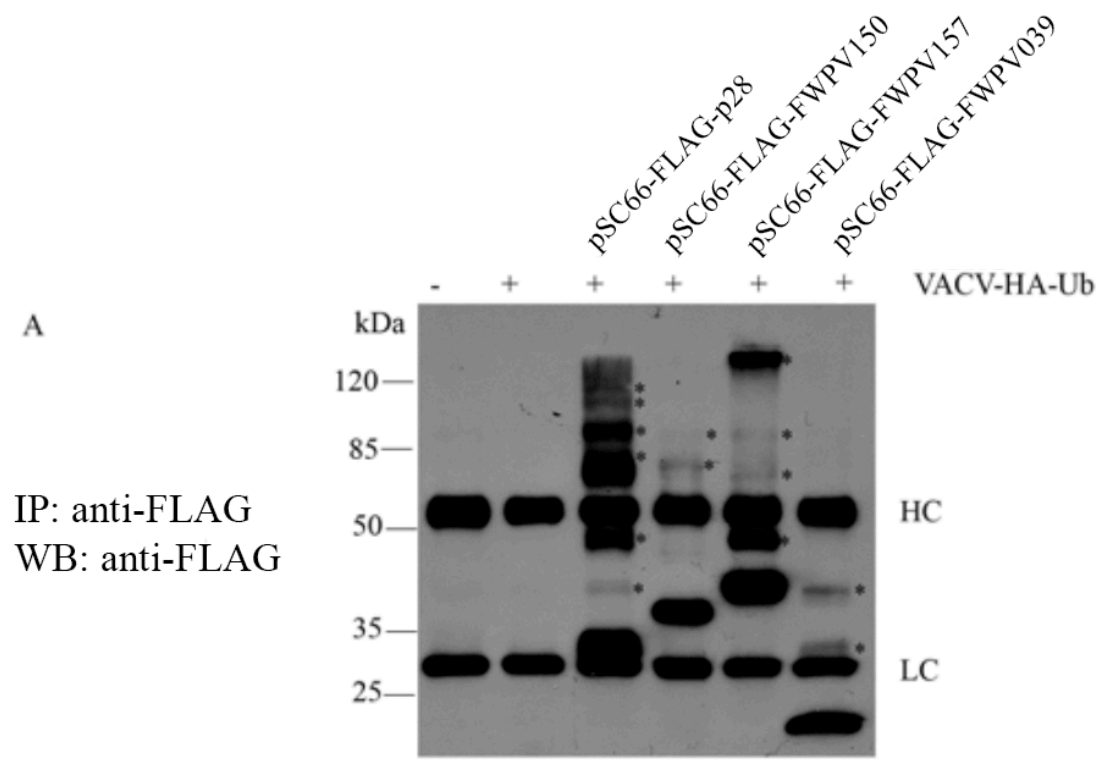


**Figure 3.5 FWPV150 and FWPV157 are regulated by ubiquitination.**

**(A)** To detect ubiquitination HeLa cells ( $2 \times 10^6$ ) were mock-infected or infected with recombinant virus VACV-HA-Ub, expressing HA-tagged ubiquitin, at an MOI of 5 and transfected with pSC66-FLAG-p28 (FLAG-p28 predicted molecular weight:  $\sim 30$  kDa), pSC66-FLAG-FWPV150 (FLAG-FWPV150 predicted molecular weight:  $\sim 35$  kDa), pSC66-FLAG-FWPV157 (FLAG-FWPV157 predicted molecular weight:  $\sim 39$  kDa), or infected with VV-FLAG-FWPV039 (FLAG-FWPV039 predicted molecular weight:  $\sim 22$  kDa), an anti-apoptotic protein that serves as a control ubiquitinated protein (195). To stabilize ubiquitination, cells were treated with MG132 ( $10\mu\text{M}$ ) for 6 hours. Cells were lysed in RIPA buffer, containing 5mM NEM, and FLAG-tagged proteins were immunoprecipitated with mouse anti-FLAG M2 and western blotting with mouse anti-FLAG to detect ubiquitination. To further visualize ubiquitination, the FLAG-tagged proteins were immunoprecipitated with mouse anti-FLAG M2 and **(B)** western blotted with mouse anti-HA, or **(C)** were western blotted with mouse anti-ubiquitin. \* indicates higher molecular weight proteins in **(A)**. HC stands for heavy chain and LC for light chain.

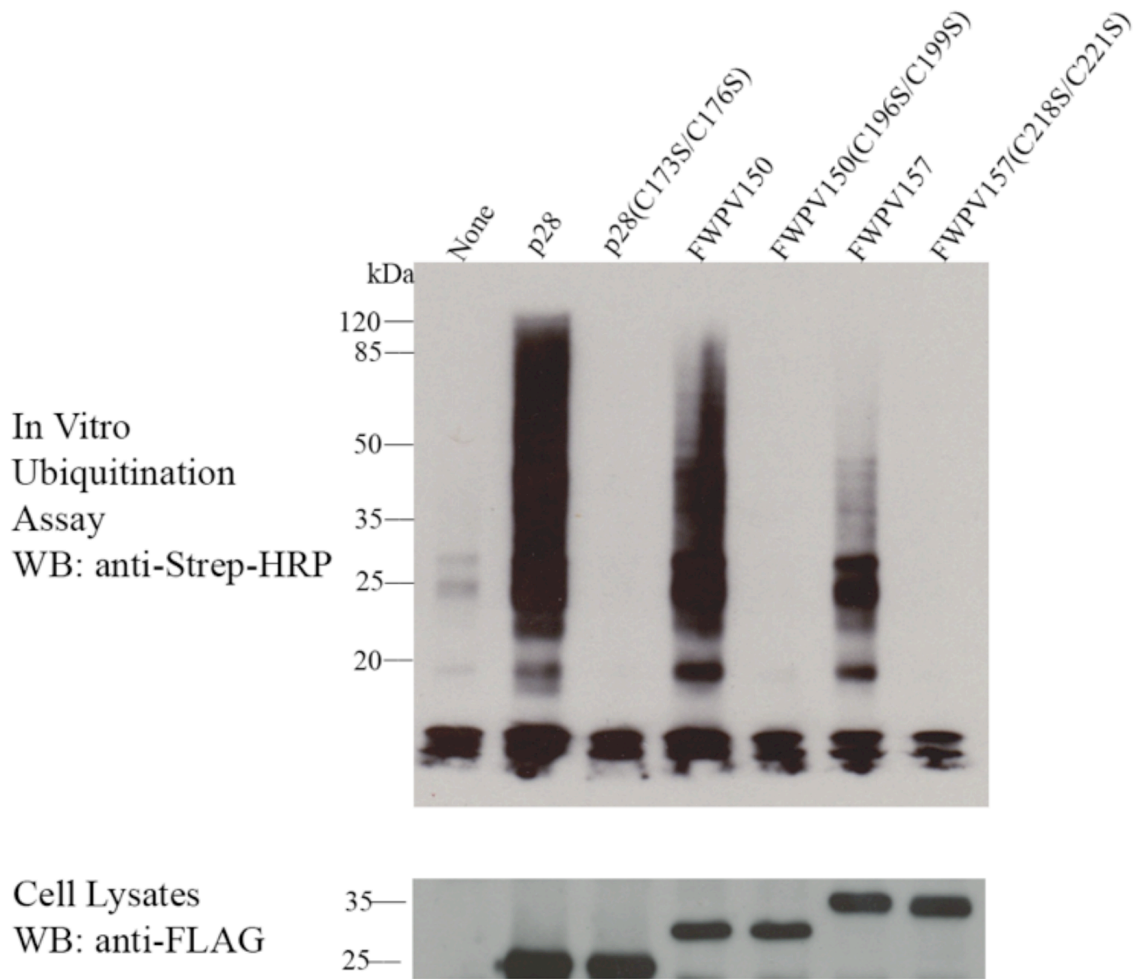


**Figure 3.6 Ubiquitin ligase activity of p28, FWPV150, and FWPV157.**

Protein G beads containing FLAG tagged proteins were combined in an *in vitro* ubiquitination reaction with E1, E2, ATP, and biotin-labeled ubiquitin. Reactions were separated by SDS-PAGE and were probed with streptavidin-tagged HRP. Western blotting shows the appearance of high-molecular mass ubiquitin adducts in reactions containing either p28, FWPV150, or FWPV157. Reactions with no input, or containing the double mutants of p28(C173S/C176S), FWPV150(C196S/C199S), or FWPV157(C218S/C221S) demonstrated no ubiquitination smear.

FLAG (**Figure 3.5A**), anti-HA (**Figure 3.5B**), or anti-ubiquitin (**Figure 3.5C**). Overall, these data indicate that FWPV150 and FWPV157 are ubiquitinated. We performed an *in vitro* ubiquitination assay to show that FWPV150 and FWPV157 act as functional ubiquitin ligases and to further demonstrate the catalytic loss of ubiquitin ligase activity in the double cysteine mutants FWPV150(C196S/C199S) and FWPV157(C218S/C221S) (**Figure 3.6**). Cells were infected with FWPV, transfected with pSC66-FLAG-p28, pSC66-FLAG-p28(C173S/C176S), pSC66-FLAG-FWPV150, pSC66-FLAG-FWPV150(C196S/C199S), pSC66-FLAG-FWPV157, or pSC66-FLAG-FWPV157(C218S/C221S), and were subjected to immunoprecipitation using an anti-FLAG antibody. The resulting immune complexes were immobilized on Protein G beads, and used as the source of ubiquitin ligase for an *in vitro* ubiquitination assay. The formation of ubiquitin conjugates was detected by western blotting for biotinylated ubiquitin adducts. Cell lysates stained with rabbit anti-FLAG showed the presence of all FLAG immunoprecipitated proteins (**Figure 3.6**). We previously demonstrated the ubiquitin ligase activity of p28 in an *in vitro* ubiquitination assay; at the same time we showed that the double cysteine mutant p28(C173S/C176S) lost its ubiquitin ligase activity (243). Therefore, we used p28 as a positive control and p28(C173S/C176S) as a negative control to investigate the ubiquitin ligase activity of FWPV150, FWPV150(C196S/C199S), FWPV157 and FWPV157(C218S/C221S) in the *in vitro* ubiquitination assay. Immune complexes precipitated from infected/transfected cells expressing FLAG-p28, FLAG-FWPV150 and FLAG-FWPV157 showed the presence of both free ubiquitin, as well as high molecular weight ubiquitin conjugates (**Figure 3.6**). These high molecular weight ubiquitin conjugates were absent in the double cysteine

mutants p28(C173S/C176S), FWPV150(C196S/C199S) and FWPV157(C218S/C221S). This confirms that FWPV150 and FWPV157 act as ubiquitin ligases and that the double cysteine mutation abolished their ubiquitin ligase activity.

### **3.2.4 K48-linked ubiquitin localizes to viral factories in association with FWPV150 and FWPV157**

Lysine-48 (K48) polyubiquitin chains are associated with targeting proteins for proteasomal degradation (261). Therefore, to determine if K48 ubiquitin linkages were present at the viral factories we used an HA-Ub-K48 construct under the control of a T7 promoter, lacking all six lysine residues except for lysine 48, allowing only K48-linked ubiquitin chains to be formed (121, 138). HeLa cells were infected with VACV-T7, which expresses the T7 polymerase under the control of an IPTG inducible promoter, and co-transfected with HA-Ub or HA-K48-Ub along with pSC66-FLAG-FWPV150, pSC66-FLAG-FWPV150(C196S/C199S), pSC66-FLAG-FWPV157, or pSC66-FLAG-FWPV157(C218S/C221S) (**Figure 3.7**). DAPI was used to stain the cells in order to visualize the viral factories, and anti-HA was used to detect ubiquitin. Upon infection and transfection, both HA-Ub and HA-K48-Ub were found diffuse throughout the cytoplasm in cells not expressing FWPV proteins (**Figure 3.7; panels b and f**). However, in the presence of the FWPV proteins, both HA-Ub and HA-K48-Ub co-localized at the virus factory (**Figure 3.7; panels l, p, t, x, bb, ff, jj, and nn**). These data indicate that FWPV150, FWPV157, and the double-mutants promote the enrichment of K48-ubiquitin at the virus factories.

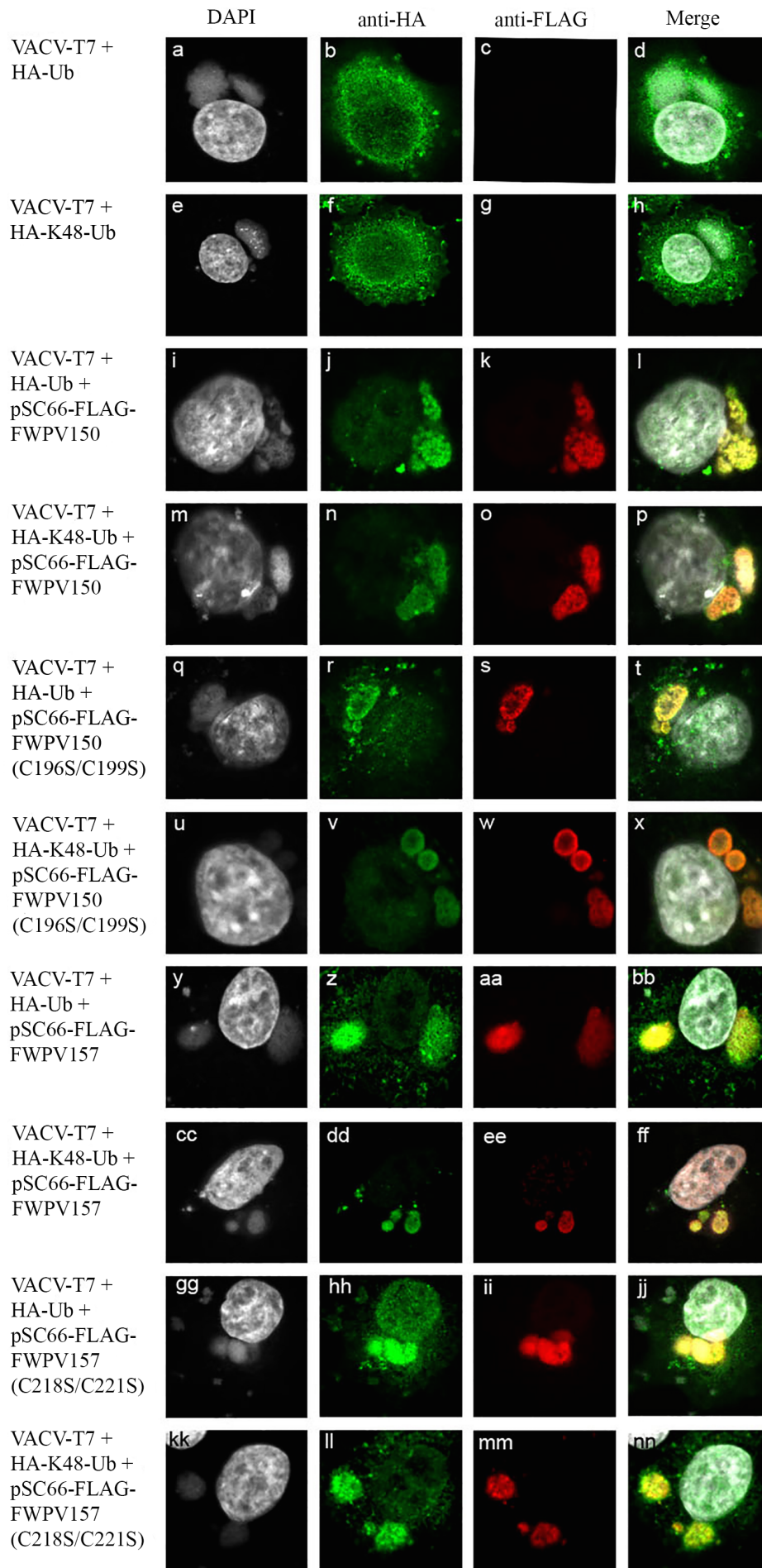


**Figure 3.7 FWPV150, FWPV157 and double-cysteine mutants co-localize with HA-Ub and HA-K48-Ub.**

HeLa cells were infected with VACV-T7 at an MOI of 5 and transfected with either pBluescript-HA-Ub, pBluescript-HA-K48-Ub, and either with pSC66-FLAG-FWPV150, pSC66-FLAG-FWPV150(C196S/C199S), pSC66-FLAG-FWPV157, or pSC66-FLAG-FWPV157(C218S/C221S). Cells were subsequently treated with 10 mM IPTG for 16 hours, fixed and stained with DAPI to visualize the nucleus and virus factories, anti-HA to visualize ubiquitin and K48-ubiquitin, and anti-FLAG to visualize FLAG-tagged proteins. This experiment was performed three independent times and we observed on average over 100 cells per sample, which were evaluated across the entire cover slips of the samples. We showed one representative cells per sample in this Figure.

K48-ubiquitin chains result in degradation of target proteins, suggesting that potential substrates for FWPV150 and FWPV157 could be located at the virus factories. However, the co-localization of conjugated ubiquitin with the double cysteine mutants of FWPV150 and FWPV157 rather indicate a possibility that the FWPV proteins were ubiquitinated by another ubiquitin ligase. These possibilities will be further argued in the discussion below.

### **2.3.5 FWPV150 and FWPV157 are expressed at different times during infection**

The genome of FWPV encodes two ubiquitin ligases, FWPV150 and FWPV157, therefore we sought to determine if both genes are actively transcribed during infection by examining mRNA levels using RT-PCR (**Figure 3.8**). QM5 cells were infected with FWPV at an MOI of 5, and RNA was extracted at 4, 12 and 24 hours post-infection and subjected to RT-PCR using primers specific for each FWPV gene. As a control, we used primers specific for an early gene, FWPV037, which encodes a protein that resides at the endoplasmic reticulum and nuclear membrane (Sing-Chi Lam and M. Barry, personal communication), and a late gene, FWPV085, the homologue of VACV I5L (235). FWPV037 transcripts were detected at 4, 12 and 24 hours post-infection. In the presence of AraC transcripts were still detected for early gene FWPV037 (**Figure 3.8; panel a**). Transcripts of FWPV085 were only detected at 12 and 24 hours post-infection, and treatment with AraC blocked transcription. FWPV150 transcripts were detected early

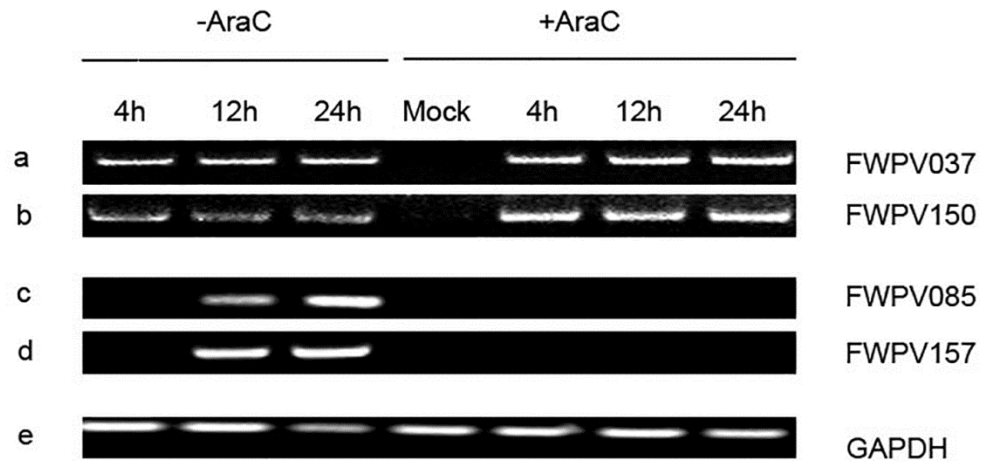


**Figure 3.8 FWPV150 is expressed early and FWPV157 is expressed late during FWPV infection.**

QM5 were infected with FWPV at an MOI of 5 in the absence or presence of 80 $\mu$ g/ml AraC. At 4, 12, and 24 hrs post infection, total RNA was isolated. Following DNase treatment, reverse transcription was performed to obtain cDNA, which was subsequently used as a template for PCR with specific primers for FWPV037, FWPV085, FWPV150, FWPV157, or GAPDH. PCR reactions were visualized using 1% agarose gel stained with ethidium bromide.

during infection and also in the presence of AraC (**Figure 3.8; panel b**), while FWPV157 transcripts were detected only at 12 and 24 hours post-infection and were blocked in the presence of AraC, identifying FWPV150 as an early gene and FWPV157 as a late gene (**Figure 3.8; panel d**). Levels of GAPDH transcripts were similar for all time points and treatments (**Figure 3.8; panel e**). Overall, the two p28-like ubiquitin ligases are expressed at different times during FWPV infection, FWPV150 was transcribed starting early during infection, whereas FWPV157 was transcribed only late. We next investigated, whether the eight Kila-N genes, which are also classified as p28-like genes, were actively transcribed during FWPV infection.

### **3.2.6 Avipoxviruses encode multiple Kila-N domains that are expressed early during FWPV infection:**

p28-like proteins are the only known ubiquitin ligases that combine a Kila-N domain with a RING domain (233). Avipoxviruses and Entomopoxvirinae are the only poxviruses that encode Kila-N-only ORFs lacking the RING domain. FWPV encodes six Kila-N-only ORFs, including FWPV075, FWPV159, FWPV161, FWPV163, FWPV236, and FWPV248 (22). FWPV also encodes two Kila-N ORFs, FWPV124 and FWPV155, which contain different C-terminal domain of unknown function (DUF) (22). Bioinformatics indicated that Kila-N only and Kila-N-DUF proteins lacked a RING domain that is crucial for ubiquitin ligase activity (**Figure 3.9**). Although, the Kila-N domains contain low sequence identity, a number of residues were conserved throughout the proteins. Residues 44-50, which were previously shown to be important for

```

                *      20      *      40      *
p28      : -----MEFDPAKINTSSIDHVTIIQYIIDEPNDIRLPVCIIRNI : 38
FWPV075 : -----MEFVPNTVKHID-ENFCFINYAN-----IEVIMLKY- : 30
FWPV124 : -----MDFSDLVTREID-DRFCYIKYDK-----FDLIMMKE- : 30
FWPV150 : -----MSHLHLNNGD-TEYRVIEDNG-----FSIILLKH- : 28
FWPV155 : -----MMFNSMITGYID-EEFCYIQYSG-----FHLVMMIS- : 30
FWPV157 : MKEDDSSNINNIHGKYSVSDLSQDDYVIECID-GSFDSIKYRD-----IKVIIMKN- : 50
FWPV159 : -----MSTITCYGN-DKFSYIIYDK-----IKIIMKS- : 27
FWPV161 : -----MDKRYISTRKLN-DGFLILYYDS-----IEIIVMSC- : 30
FWPV163 : -----MNTLPYIIQDID-SHFCYIKYDG-----ITLTMMKD- : 30
FWPV236 : -----MKFKEVRNTIKKMNITDIKICGIN-EYFMSMKLLD-----VEVIMRS- : 42
FWPV248 : -----MEIKVESIN-NNFCKLSYED-----IEIIMMKE- : 27

```

```

                60      *      80      *      100      *
p28      : NNITYFINITKINPDLANQFRAMKKRIAGRDMYTNISRD-----GIQQ : 82
FWPV075 : ---NGYINATKICDLGNKNFRQWCRIESSKKLIKTIYKN-----GIY--NKAV : 74
FWPV124 : ---NRFINATKLCCKLGGKDFHRWKRIDGSKEIMIKVNEMNEMW--KSAPPPP--DLGG : 81
FWPV150 : ---TEYINVTKCLKIHNKEFYRWKRLISAGRIIETVSRDI-----SNQG : 69
FWPV155 : ---NCYINASKLCDT--KDFKKWLRDSSLSLQLQEIENTFPS--EKKFSIK--NSKS : 79
FWPV157 : ---NGYVNC SKLCKMRNKYFSRWLRISTSKALLDIYNNKSV-----DNAI : 92
FWPV159 : ---NRYVNATRLCELGRKFTNWKKLSSESKILVDNVKKIN-----DKTNQLK--TDMI : 75
FWPV161 : ---NHFINISALLAKKNKDFNEWLKIESFREIDTLDKINYDLGQRYCEEYPYGASHSS : 85
FWPV163 : ---NGYINATQLOMLGNKDFKEWIKLDHSIELIKEIEKNI-----NKETTKY--VKAV : 78
FWPV236 : ---NGFVNITRLONLEGKDFENDWKQLESSRRLNLTIKDNN-----KLHD : 83
FWPV248 : ---NEYINATRLCSSRGRDILDWMSKESSELINELDRIN-----RSCNDYY--DYRG : 75

```

```

                120      *      140      *      160      *
p28      : SKLTETIRNCQKRNRIYGLYIHYNLVINVVIDWITDVIQSLIRGLVNWY---IAN-- : 135
FWPV075 : LEIGLA-SNSAYKYELVGTYYVHIDLVPH-IICQVFP SIALNFSK-IINSY---LSNSY : 126
FWPV124 : IIEVNGSNQYTEYDIAGSYVHQDLIPH-IASWISPLFALKVSK-IISCY---VSGKY : 134
FWPV150 : FESPLVYVNRKGNKEFYGFYAHPCIALY-IAKWISEDFNKIKH-IINSY---TISDK : 122
FWPV155 : VII---LEKYYHEEVEGYIHPDILPH-IVGWSPTFAISMSK-FINGY---ISNSF : 128
FWPV157 : VKV---YGKGGKLIITGFYIKQNMIRY-VIEWIGDDFTNDIYK-MINFY---NALFG : 141
FWPV159 : IYVK---DIDHKGRDTCGYVHQDLVSS-ISNWSISPLFAVKVSK-IINY---ICNEY : 125
FWPV161 : VIIIEVK-ASNLIDDRTAGFYVHKDLIPY-ILTCISIPFSLKVVR-VIDTY---IGEKL : 137
FWPV163 : ISVRSDYNNSETSNDIKGFYIHGNIMPH-ICAWISSKFAIKVSN-IVHNY---INDRY : 131
FWPV236 : PII---NIRHTRIKINGEYVSQLLLDY-VIPWISPYVATRVSI-LMRYRRCVALNI : 135
FWPV248 : IVL-----NVVSDSETSELYVHRDLILH-ISHWISPLFSLKVVK-FINSY---IQDSY : 123

```

```

                180      *      200      *      220      *
p28      : -----NTYNPNTPNSTTTTISELDIIKILDKYEDVY : 165
FWPV075 : CTRLKKG-----SDNEDQIRSGFFSEGISKILYDIHDNEILKLKKNTKKLE : 172
FWPV124 : EFKLKE-----KENKIEELDLLLHKFNKYDKDTLELKELYRQRKEAKS : 179
FWPV150 : TVVIKDFS YCDELCPD---AII GKCKTKSSCEYVHGDICDICGFEALHPTDIDKRLT : 177
FWPV155 : TITEKDDKKYNTLPPSSSYKQGDRNCFIDMLNEMTNKHLNDITELKTHYREQRELKY : 186
FWPV157 : NDELKIVSCENTLCP---FIELGRCYYGKCKYIHGDQCDICGLYILHPTDINQVRS : 195
FWPV159 : DIRLSE-----MESDMTEVIDVVDKLVGGYNDIEAIIYLFNKFIEKYIA : 170
FWPV161 : ENRIK-----LSQSMDLETNNSYNM----- : 157
FWPV163 : VQNDKE-----EIQEPDKDIKYIKKQCKLMREIRILFKKNYTRELD : 173
FWPV236 : ETEKDIDHSQE-----LQNQISKIDEVYDRSIKDISNRFKEIETSYSKSLSTYLL : 185
FWPV248 : QL-----EYELIHKKSL----- : 135

```

```

                240          *          260          *          280          *
p28      : RV-----SKEKECGICYEVVYSKRELENDRYFGL----- : 193
FWPV075 : EK----- : 174
FWPV124 : LR-----KINERIEEKYDKDTRELKQGLKELKDENKELKFELKKIEERLRDKVINP : 230
FWPV150 : HE--KVCM---QLLCKEDIKYDKCGICLDAIKG---NKKPYGI----- : 212
FWPV155 : QNTVLSSKITEKLVNDEFYRIKHFDSDSIKIKDENNTLKSNIKITEKHNLQORDN : 244
FWPV157 : HK--KTCLVDRDSLIVFKRSTSKKCGICIEEINKKHI-SEQYFGI----- : 237
FWPV159 : NI-----SLSTELSSILNNFINFNKKYNN----- : 195
FWPV161 : ----- : -
FWPV163 : EL-----KKVRELYYEKNGLEEYIDKLEYSYQRMKELTTLSE----- : 213
FWPV236 : TK-----AERVLEKDYSMEQDIDNNDIRTDemiaaIEAE----- : 220
FWPV248 : -----MDQLKEIIL----- : 144

```

```

                300          *          320          *          340
p28      : ----- : -
FWPV075 : ----- : -
FWPV124 : ----- : -
FWPV150 : ----- : -
FWPV155 : NRLKTLRELYEKNTSLQNNITELRETIARETKELHNQVIELSKDKGIEPIEYRVDR : 302
FWPV157 : ----- : -
FWPV159 : ----- : -
FWPV161 : ----- : -
FWPV163 : ----- : -
FWPV236 : ----- : -
FWPV248 : ----- : -

```

```

                *          360          *          380          *          400
p28      : -----LDSCNHIFCITCINIWHRTTRETGASDNCPICRTRFRNITMSKFKLVN-- : 242
FWPV075 : -----YEKTNLSI-----NQKISNLEVAVKGLSIK-- : 199
FWPV124 : -----FSPNKHRLVILQKKIDNNSFKTLRLQAERLNQEMNKYKTNILYFLMHTNL : 281
FWPV150 : -----LSDCNHMFICINIKTWMTT---INSKQCPECRVPSKYIIQSPIWTVDKVS : 260
FWPV155 : CFVRNRLHRSNKNYYIIIFQHKKDLFTFKYFKLHIRKVCIELFNRYRESHNLFLIYEP : 360
FWPV157 : -----LPSCKHIFCLSCIRRWADTTTRNTDENTCPECRIVFPFIIPSRYWIDNKYD : 288
FWPV159 : -----IKDIKSLI-LDLKNTSIKLDKCLFDKDNNESENDEKLETEVDKLIFFI---- : 241
FWPV161 : ----- : -
FWPV163 : -----LKNSNKQL---KNKLENIEKRIKCINPPTESSKNVIYDRFKKLYHILTFR : 260
FWPV236 : -----IEENRRYLSIISGIRKQHAEDRINISKIMLSGDSFNEIIVKIRDYIETTA : 271
FWPV248 : -----LNDDNM----- : 151

```

```

                *          420          *          440          *
p28      : ----- : -
FWPV075 : ----- : -
FWPV124 : TQYPVLIG----- : 289
FWPV150 : KNQLSVSYKTVYIKSC----- : 276
FWPV155 : TNKSIIRFKNMLENNEHIELKDNFNKITDTRYTVINILKDINKIFSDN : 408
FWPV157 : KKILYNRYKKMIFTKIPRTIKI----- : 311
FWPV159 : ----- : -
FWPV161 : ----- : -
FWPV163 : KSK----- : 263
FWPV236 : KPAVANNYE----- : 280
FWPV248 : ----- : -

```

**Figure 3.9 *Avipoxviruses* encode multiple Kila-N domains.**

Protein alignments for FWPV150, FWPV Kila-N only proteins FWPV075, FWPV159, FWPV161, FWPV163, FWPV236, and FWPV248, and Kila-N-DUF proteins FWPV124 and FWPV155 were performed via Clustal W (1.82) (<http://www.ebi.ac.uk/clustalW/#>). Black bar indicates Kila-N domain and grey bar indicates highly conserved residues within the Kila-N domains, which are important in p28 for localization to the virus factories. Conserved amino-acid residues were shaded using GeneDoc (258, 259). The Genedoc shading mode was set to conservation, with shading level 4 and the conserved percent was primary 100% (black), secondary 80% (dark grey), and tertiary 60% (light grey). The shade style was set to amino acid identity.

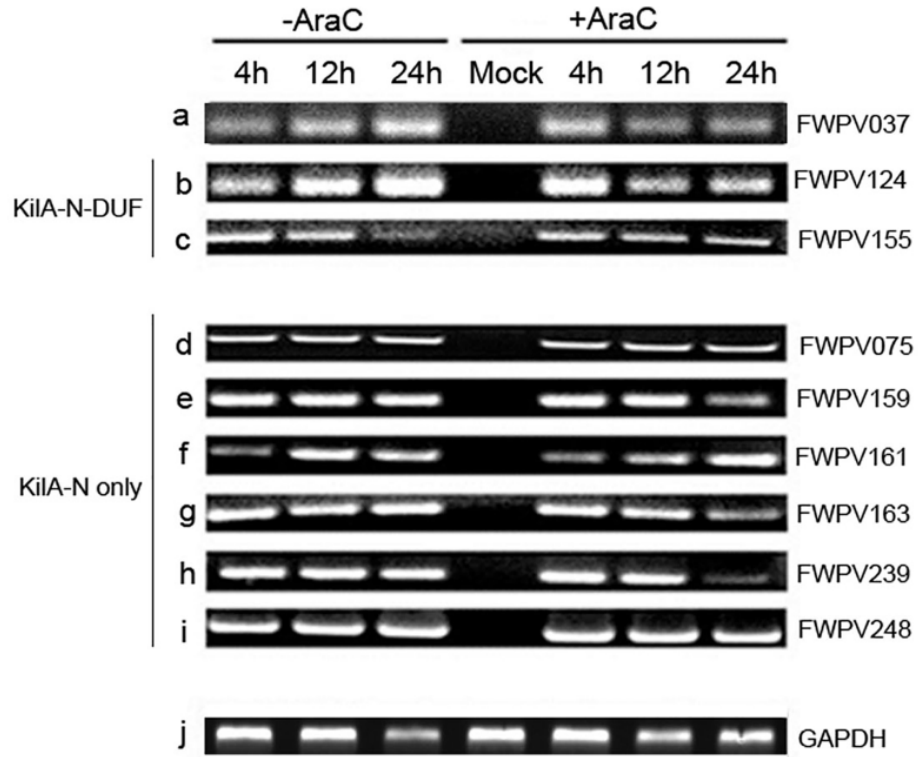
localization to the viral factories (247), were conserved throughout the Kila-N containing proteins (**Figure 3.9**). Therefore, we utilized RT-PCR with specific primers for Kila-N only proteins FWPV075, FWPV159, FWPV161, FWPV163, FWPV236, and FWPV248, and two Kila-N-DUF designated as FWPV124 and FWPV155 to investigate, if there was active transcription of Kila-N and Kila-N-DUF genes during FWPV infection. We used the same cDNA as a template as above in **Figure 3.8**; and the PCRs in 3.8 and 3.10 were done at the same time under the same conditions. Separate controls for GAPDH and early gene FWPV037 were done at the same time and shown in Figure 3.10. The AraC late gene control can be found in **Figure 3.8; panel c**. We again used primers for FWPV037 as a control for an early gene (**Figure 3.10A; panel a**), and GAPDH as a house-keeping gene (**Figure 3.10A; panel j**). Interestingly, all of the Kila-N only genes (**Figure 3.10A; panel d-i**) and the two Kila-N-DUF genes (**Figure 3.10A; panel b and c**) were transcribed at 4, 12, and 24 hours post infection, and genes were also transcribed in the presence of the late gene inhibitor AraC. Taken together, all of the Kila-N only and the two Kila-N-DUF genes were actively transcribed starting at early times during FWPV infection. We subsequently chose one representative from each group, FWPV075, containing only a Kila-N domain, and FWPV124, containing a Kila-N-DUF domain, to investigate the subcellular localization during FWPV infection and determine the effect on the localization of conjugated ubiquitin. QM5 cells were mock infected (**Figure 3.10B; panel a-d**), infected with FWPV (**Figure 3.10B; panel e-h**), and transfected with pSC66-FLAG-FWPV075 (**Figure 3.10B; panel i-l**), or pSC66-FLAG-FWPV124 (**Figure 3.10B; panel m-p**). Cells were co-stained with anti-FLAG to visualize FWPV075 (**Figure 3.10B; panel k**), FWPV124 (**Figure 3.10B; panel o**), and with FK2

(**Figure 3.10B; panel b, f, j, and n**). FWPV075 and FWPV124 localized at the viral factories without an effect on FK2 distribution within the cell (**Figure 3.10B; panel l and p**). To demonstrate the expression of FLAG-FWPV075 and FLAG-FWPV124, QM5 cells were infected with FWPV at an MOI of 5 and transfected with pSC66-FLAG-FWPV075 or pSC66-FLAG-FWPV124. Whole cell lysates were subjected to western blot analysis with anti-FLAG, or anti  $\beta$ -tubulin as a loading control (**Figure 3.10C**). Altogether, the Kila-N only protein FWPV075 and the Kila-N-DUF protein FWPV124 localized to the viral factories in QM5 cells during FWPV infection without any effect on accumulation of conjugated ubiquitin (**Figure 3.10B; panel l and p**). This underlines that a Kila-N domain alone is not sufficient to recruit conjugated ubiquitin and a RING domain is needed.

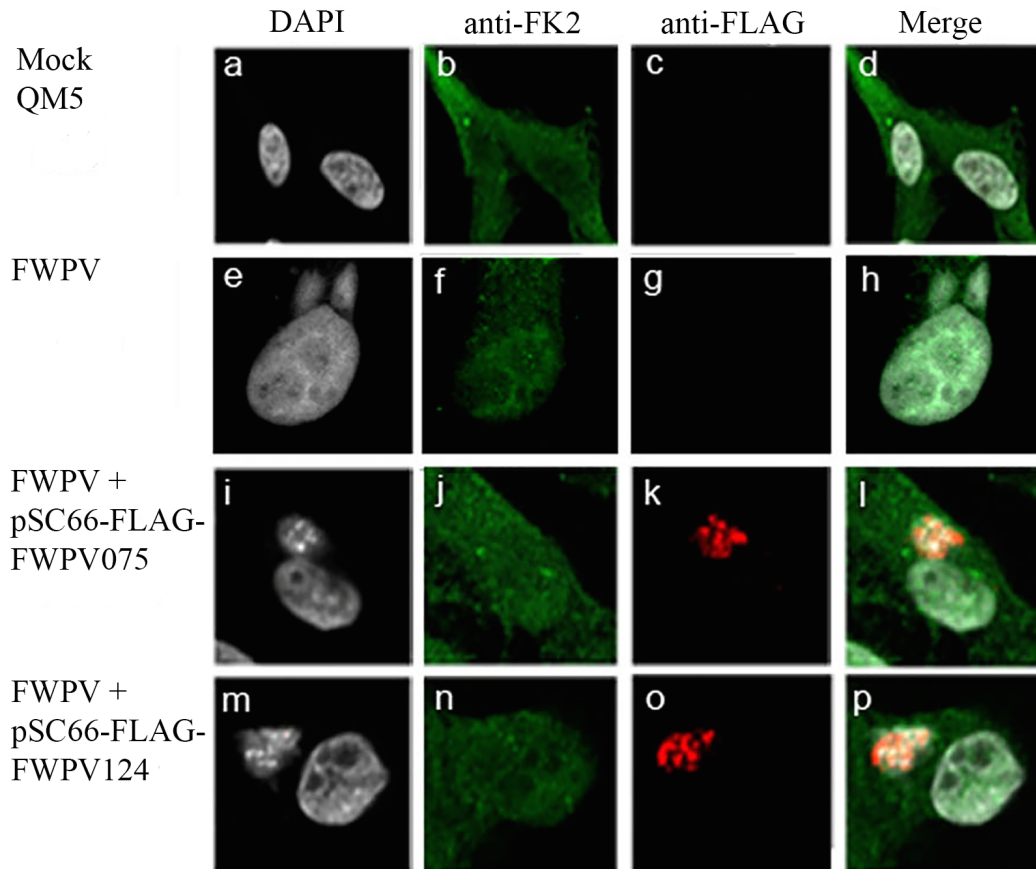
### **3.3 Summary and Brief Discussion**

Members of Avipoxviruses contain two p28-like ubiquitin ligases (22, 23). Here we demonstrate that FWPV150 is starting to be expressed early during infection, while FWPV157 is expressed late. Bioinformatics analysis also revealed that CNPV encodes two p28-like ubiquitin ligases, CNPV197 and CNPV205 (23). Investigation of the upstream sequences revealed an early promoter for FWPV150 and CNPV197 (early promoter: AAAAATGAAAAAAAAA), and a late promoter upstream of FWPV157 and CNPV205 (late promoter: TAAATG). These data suggest that members of the Avipoxviruses contain two distinct p28-like ubiquitin ligases that are expressed early and late during virus infection. In contrast, non-Avipoxviruses encode only one p28-like

A



B



C

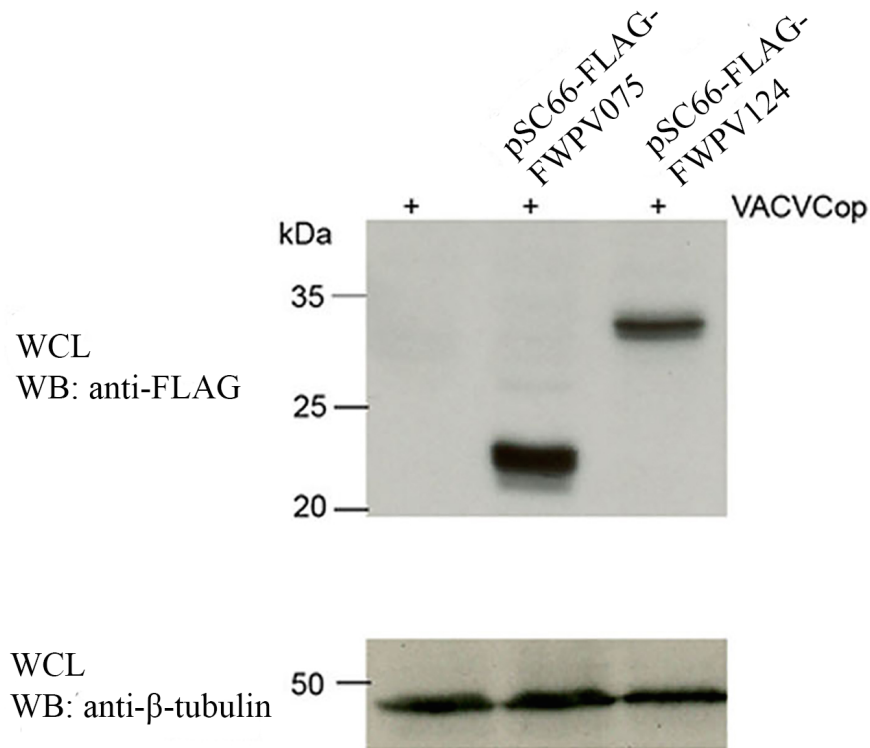


**Figure 3.10 Avipoxviruses encode multiple Kila-N domain proteins that are expressed early during FWPV infection.**

(A) QM5 cells were infected with FWPV at an MOI of 5 in the absence or presence of 80 $\mu$ g/ml AraC. At 4, 12, and 24 hrs post infection, total RNA was isolated. Following DNase treatment, reverse transcription was performed to obtain cDNA, which was subsequently used as a template for PCR with specific primers for FWPV037, the Kila-N only genes FWPV075, FWPV159, FWPV161, FWPV163, FWPV236, and FWPV248, or the Kila-N-DUF genes FWPV124 or FWPV155, or GAPDH. PCR reactions were visualized by electrophoresis on 1% agarose gels stained with ethidium bromide. (B) QM5 cells were mock infected, or infected with FWPV at an MOI of 5 and transfected with pSC66-FLAG-FWPV075 (Kila-N-only) and pSC66-FLAG-FWPV124 (Kila-N-DUF). Cells were fixed and treated with DAPI to visualize the nucleus and virus factories, and stained with anti-FLAG to visualize FLAG-tagged proteins and anti-FK2 to recognize conjugated ubiquitin, and analysed by confocal microscopy. This experiment was performed three independent times and we observed on average over 100 cells per sample, which were evaluated across the entire cover slips of the samples. We showed one representative cells per sample in this Figure. (C) QM5 cells were infected with FWPV at an MOI of 5 and transfected with pSC66-FLAG-FWPV075 or pSC66-FLAG-FWPV124. Whole cell lysates were subjected to western blot analysis with anti-FLAG, or anti  $\beta$ -tubulin as a loading control.

ubiquitin ligase that is expressed early during infection. The ubiquitin ligase activity of p28 lies in the C-terminal RING domain, while the N-terminal KIL-A-N domain is crucial for its localization to virus factories. Here we demonstrate, that the double cysteine mutants in the RING domain of FWPV150 and FWPV157 abolish the ubiquitin ligase activity. Moreover, we demonstrate that FWPV150 and FWPV157 co-localize with K48 at the virus factories, which typically leads to proteasomal degradation of target proteins. Surprisingly, the double cysteine mutants FWPV150(C196S/C199S) and FWPV157(C218S/C221S) still co-localize with K48 ubiquitin chains. It is possible, that other ubiquitin ligases or ubiquitinated proteins are enriched in the presence of the double cysteine mutants.

There was only a modest localization of conjugated ubiquitin at the virus factory during FWPV infection (**Figure 3.4**). We suspect that overexpression of the FWPV proteins FWPV150 and FWPV157 exaggerate the phenotype of complete co-localization of conjugated ubiquitin at the virus factories. We expected a modest co-localization of conjugated ubiquitin with endogenous FWPV150 or FWPV157 at the virus factory during wildtype FWPV infection. Furthermore, RING domain mutants FWPV150(C196S/C199S) and FWPV157(C218S/C221S) demonstrated co-localization with conjugated ubiquitin at the virus factory. However, there was a loss of complete localization at the virus factory and in addition punctate staining of ubiquitin was found in the cytoplasm. We speculate that this phenotype is due to the loss of ubiquitin ligase activity of the FWPV proteins.

The p28 ubiquitin ligase functions as a virulence factor during ECTV virus infection (37, 245). In order to test if FWPV150 and FWPV157 are virulence factors

during FWPV infection, an animal model will need to be established. FWPV cannot infect mammalian cells due to species tropism (262). FWPV can infect, amongst other birds, chickens and turkeys, and FWPV infection typically leads to proliferative lesions in the skin (cutaneous form) that progress to thick scabs (2, 24). In more severe cases, FWPV can lead to lesions in the upper GI and respiratory tracts (diphtheritic form) (24). Overall, future studies should investigate the importance of FWPV150 and FWPV157 *in vivo* to determine if the lack of one or both FWPV p28-homologues would alter the virulence of FWPV.

One distinguishing feature of the Avipoxviruses is the large genome compared to other poxviruses, as exemplified by FWPV (288 kbp) and CNPV (365 kbp) (22, 23). While FWPV and CNPV are the prototypical members of Avipoxviruses, they exhibit some interesting genomic differences. Out of the 328 open reading frames in CNPV, FWPV contains only 209 predicted homologues. Furthermore, Avipoxviruses encode a number of novel proteins, which might be important as host-range factors or immune evasion strategies in birds. In addition to the Kila-N domain containing ubiquitin ligases, FWPV150 and FWPV157, there are six Kila-N only and two Kila-N with C-terminal domains of unknown function (DUF) in the FWPV genome (22). CNPV contains twenty-five Kila-N only ORFs. We demonstrated here, that all eight Kila-N domains and Kila-N-DUF are actively transcribed early during FWPV infection (**Figure 3.9**). Future studies should investigate the role of these novel FWPV proteins during infection and interaction with host cells.

**CHAPTER 4: THE POXVIRUS ENCODED UBIQUITIN LIGASE P28 IS  
REGULATED BY PROTEASOMAL DEGRADATION AND  
AUTOUBIQUITINATION**

A version of the data presented in this chapter has been published:

Mottet K. <sup>Δ</sup>, Bareiss B. <sup>Δ</sup>, Milne C. D., Barry M. (2014) The poxvirus encoded ubiquitin ligase, p28, is regulated by proteasomal degradation and autoubiquitination. *Virology*. 468-470: 363-78.

<sup>Δ</sup> These authors contributed equally.

All experiments presented in this chapter were performed by myself, except for the flow cytometry assay in **Figure 4.6**, which was performed by Kelly Mottet. Parts of **Figure 4.3A**, **4.4** and **4.7** were initially performed by K. Mottet, but repeated by myself; the replications shown here were performed by myself. The original manuscript was written by myself with editorial contributions from Kelly Mottet, Robyn-Lee Burton, Dr. Thibault, Dr. Noyce, and Dr. Barry.

## 4.1 Introduction

This chapter focuses on the ubiquitin-proteasomal regulation of the poxvirus-encoded ubiquitin ligase p28 (139, 242). We suggest here that p28 is regulated by proteasomal degradation, initiated by both autoubiquitination and ubiquitination by another ubiquitin ligase. This feedback regulation has been seen in other ubiquitin ligases (171, 263-266). Our previous work demonstrated that p28 encoded by vaccinia virus strain IHDW is a functional ubiquitin ligase that localizes to cytoplasmic regions of virus replication, referred to as virus factories (243). In the presence of p28, conjugated ubiquitin localizes to virus factories during vaccinia infection (242, 243). Furthermore, *in vivo* studies indicate that p28 is a critical virulence factor during ectromelia virus infection (244, 245). Given that p28 is an important virulence factor, we investigated the regulation of p28 during virus infection. Here we show that p28 homologues localized with conjugated ubiquitin at the virus factories. We also demonstrate that p28 is regulated by proteasomal degradation. Upon treatment with proteasome inhibitors, p28 was dramatically stabilized and highly ubiquitinated, indicating that p28 is regulated by ubiquitination and proteasomal degradation. Furthermore, we suggest that p28 may regulate itself through autoubiquitination. Moreover, when p28 was disrupted by mutating the RING domain, conjugated ubiquitin still localized to the virus factories, indicating that an unknown ubiquitin ligase(s) was responsible. Taken together, we demonstrate that, like many cellular ubiquitin ligases, p28 is subjected to proteasomal degradation and highly regulated by ubiquitination.

## 4.2 Results

### 4.2.1 Mammalian poxviruses and *Avianpoxvirus* FWPV do not inhibit the proteasomal system

The ubiquitin-proteasome system has emerged as an important mechanism to control protein degradation (246, 267). Recently, it has become apparent that poxviruses use the UPS in order to manipulate host responses (30, 139, 233, 243, 268). Furthermore, it has been shown that a functioning proteasome is crucial for poxvirus replication (269, 270). Therefore, we sought to determine if the proteasome was fully functional during poxvirus infection. To perform these experiments, HeLa cells were mock-infected or infected with VACVCop, ECTV strain Moscow, CPXV strain Brighton red, or one *Avipoxvirus* member, FWPV (**Figure 4.1A and 4.1B**). The chymotrypsin-like activity of the proteasome was assessed using a cell-based luciferase Proteasome-Glo assay (Promega) (271). Mock-infected HeLa cells demonstrated high luminescence, corresponding to the amount of chymotrypsin-like activity of the proteasome and graphed as RLU (**Figure 4.1A**). Similarly, HeLa cells infected with VACVCop, CPXV, or ECTV demonstrated considerable proteasome activity with only a small difference between mock and infected cells (**Figure 4.1A**). However, infected cells treated with MG132 resulted in less than 1% proteasome activity compared to infected cells without MG132 treatment (**Figure 4.1A**). Although some decrease in proteasome function was evident late during VACV, CPXV and ECTV infection, the chymotrypsin-like activity of the proteasome remained largely functional (**Figure 4.1A**). To further investigate the proteasomal activity during poxvirus infection,

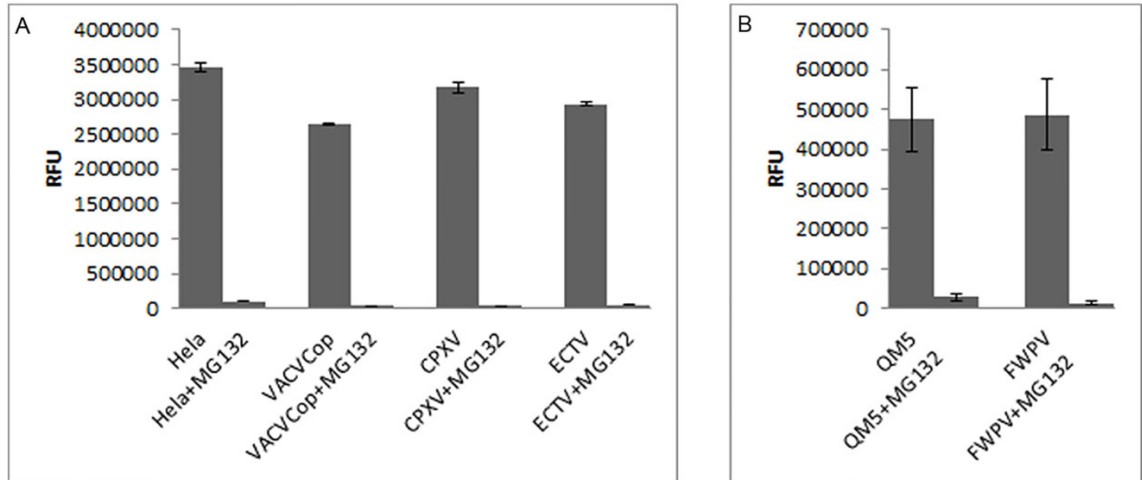


**Figure 4.1 Mammalian poxviruses and *Avianpoxvirus* FWPV do not inhibit the proteasomal system.**

**(A)** HeLa cells were mock-infected or infected with VACVcop, ECTV, or CPXV at an MOI of 10 for fourteen hours and at twelve hours post-infection treated with or without 10 $\mu$ M MG132. Proteasomal function was quantified by Proteasome-Glo assay (Promega), and standard deviations were calculated from three independent experiments. **(B)** QM5 cells were infected with FWPV at an MOI of 10 for fourteen hours and at twelve hours post-infection treated with or without 10 $\mu$ M MG132. Proteasomal function was quantified by Proteasome-Glo assay.

we focused on FWPV, a divergent member of the *Avipoxvirus* family (**Figure 4.1B**). Mock-infected QM5 quail cells demonstrated proteasomal activity that was significantly inhibited in the presence of MG132 ( $p < 0.0001$ ) (**Figure 4.1B**). FWPV infection demonstrated a non-significant loss of proteasomal function in QM5 cells compared to uninfected cells ( $p < 0.1$ ). Overall, these results demonstrate that the proteasome is functional during VACV, CPXV, ECTV and FWPV infection, which would allow poxviral encoded-ubiquitin ligases to make complete use of the cellular 26S proteasome system. Furthermore, the addition of MG132 inhibited the proteasome, as expected (**Figure 4.1**). We next investigated whether the poxviral encoded ubiquitin ligase p28 and its homologues effect on conjugated ubiquitin.

#### **4.2.2 p28 homologues co-localize with conjugated ubiquitin at the virus factory**

p28 homologues are encoded in a wide range of poxviruses including VACV(IHDW), ECTV, MYXV and FWPV, while VACVCop is missing endogenous p28. p28 encoded by VACV(IHDW) and ECTV share 95% sequence identity (**Figure 4.2**). In contrast, p28 encoded by VACV(IHDW) shared only 20% and 16% sequence identity and 48% and 40% sequence similarity with the MYXV homologue M143R, and the FWPV homologue, FWPV150, respectively (**Figure 4.2**) Notably, the cysteine and histidine residues critical for ubiquitin ligase function were highly conserved among the four proteins. Residues 44 to 51 within the KILAN domain that are crucial for DNA binding, are also conserved between the four proteins (**Figure 4.2**) (246). Given the conservation

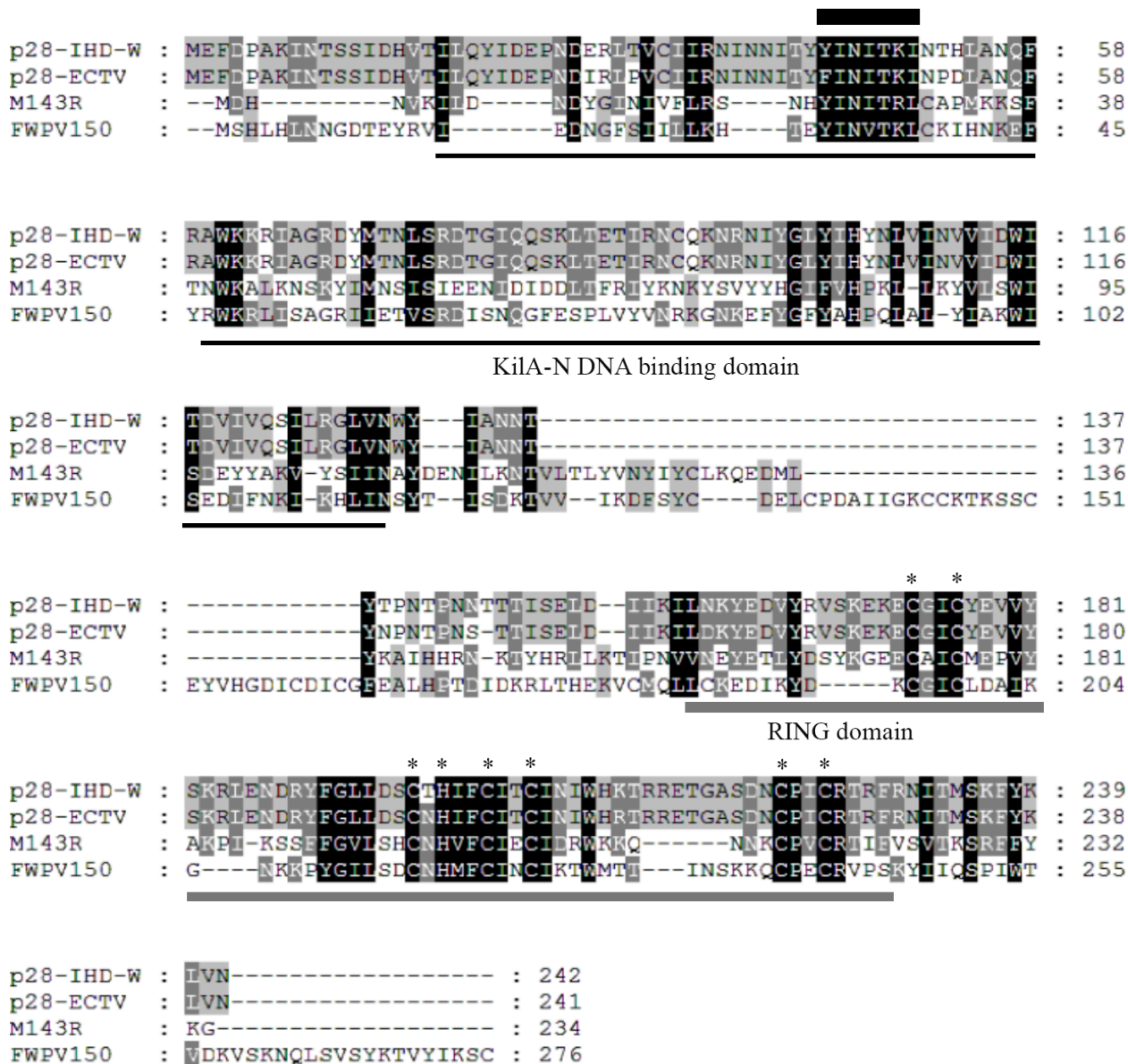


**Figure 4.2** Alignment of p28 homologues.

p28 protein alignments for VACV strain IHDW, ECTV strain Moscow, MYXV strain Lusanne, and FWPV were performed via ClustalW (1.82) (<http://www.ebi.ac.uk/clustalW/#>) (257). The KilA-N domain is underlined in black and the RING domain is underlined in grey. Asterisks highlight the conserved cysteines and histidine within the RING domain. The thick black line marks the motif in p28, which is important for DNA binding. Conserved amino-acid residues were shaded using GeneDoc (258, 259); The Genedoc shading mode was set to conservation, with shading level 4 and the conserved percent was primary 100% (black), secondary 80% (dark grey), and tertiary 60% (light grey). The shade style was set to amino acid identity.

of p28 throughout the poxvirus family, we sought to determine whether conjugated ubiquitin co-localized with other p28 homologues. HeLa cells were infected with VACVCop, VACV-FLAG-p28(IHDW), and VACV-FLAG- M143R that expresses the p28 homologue MYXV (**Figure 4.3; panel a-h and m-p**). We further included the p28 double cysteine mutant expressing virus VACV-FLAG-p28(C173S/C176S), which lost its ubiquitin ligase activity, to examine its effect on conjugated ubiquitin in HeLa cells (**Figure 4.3; panel i-l**). To express the p28 homologue FWPV150 encoded by FWPV, cells were infected with VACVCop and transfected with pSC66-FLAG-FWPV150 under the control of a poxvirus promoter (**Figure 4.3; panel q-t**). Cells were stained with DAPI to visualize both the nucleus and cytoplasmic viral factories, and co-stained with anti-FLAG to visualize FLAG-p28, FLAG-p28(C173S/C176S), FLAG-M143R, or FLAG-FWPV150. Using this approach, we could demonstrate that p28 homologues M143R and FWPV150, encoded by MYXV and FWPV, localized to viral factories (**Figure 4.3; panel g, k, o, s**). Furthermore, FK2 conjugated ubiquitin co-localized to viral factories upon expression of each p28 homologue (**Figure 4.3; panel h, l, p, t**). As expected, upon VACV infection only a minor accumulation of conjugated ubiquitin was observed at the virus factory, due to the lack of p28 (**Figure 4.3; panel d**), while the p28 mutant p28(C173S/C176S) still co-localized with conjugated ubiquitin at the virus factory (**Figure 4.3; panel l**) (245). Taken together, the data indicate that the accumulation of conjugated ubiquitin at the viral factories is conserved among close and distant relatives of the p28 family of poxvirus proteins. We further confirmed that the p28 mutant p28(C173S/C176S) still co-localized with FK2 at the virus factories in HeLa cells (243).

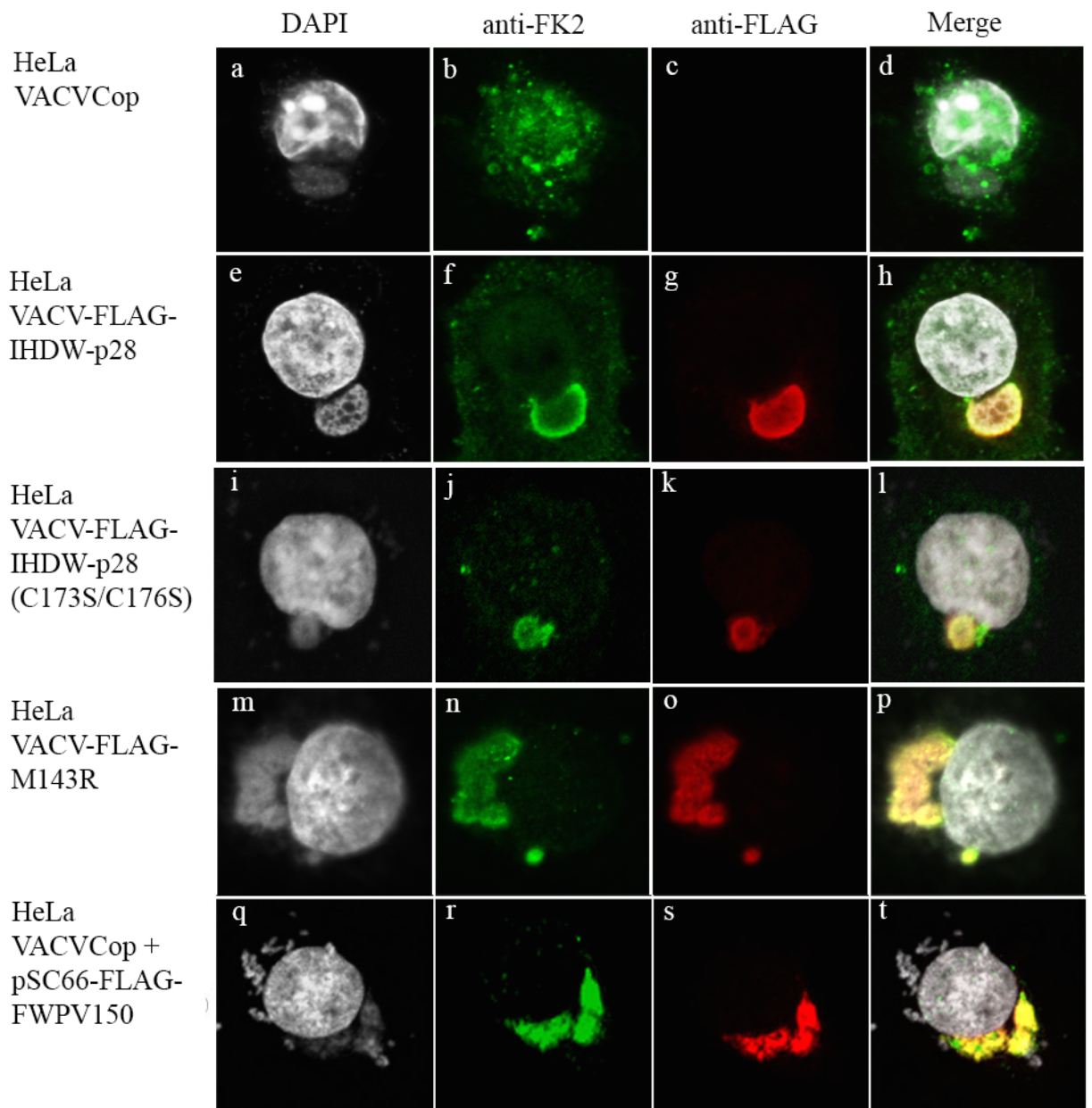


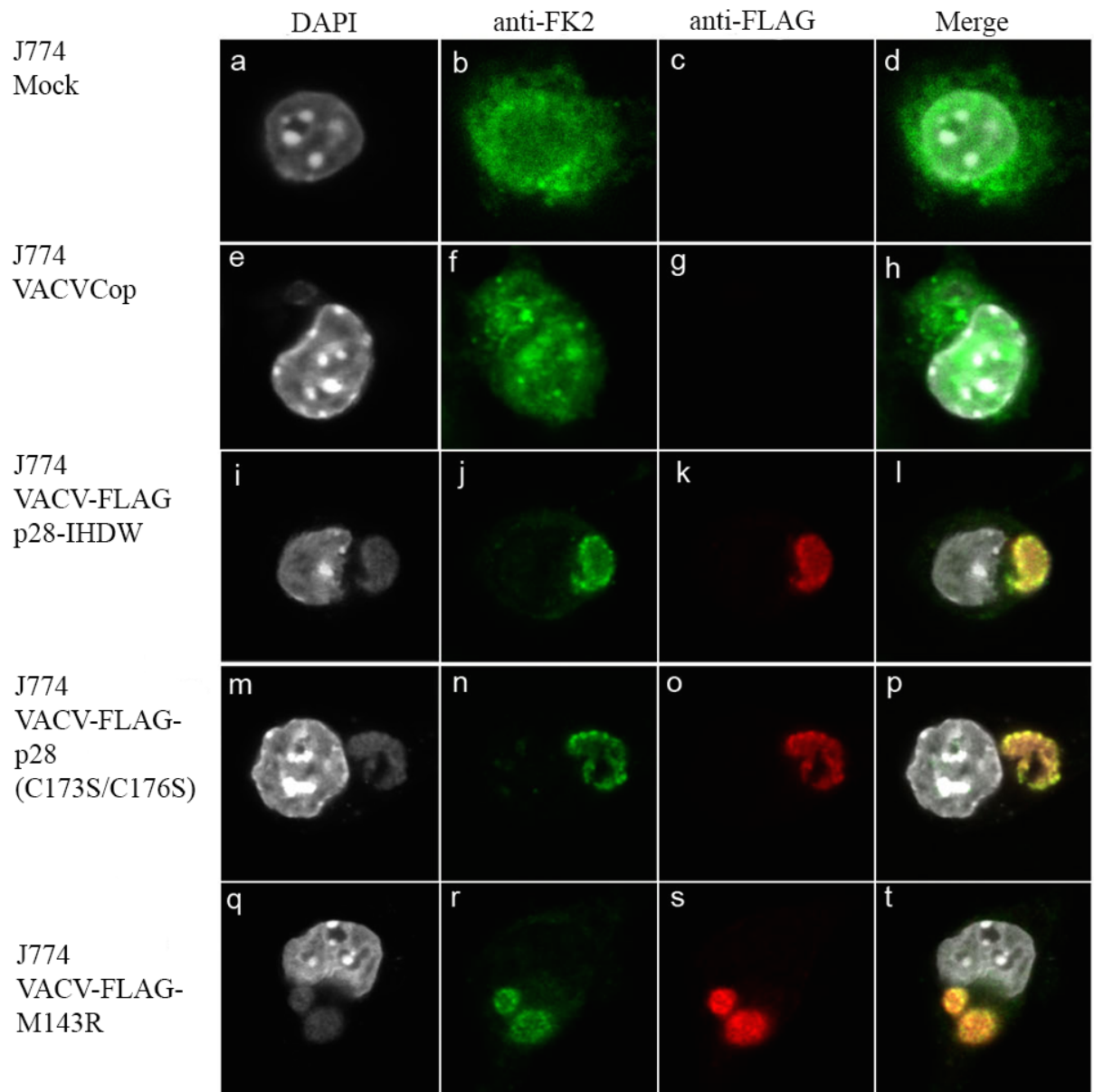
**Figure 4.3 p28 homologues co-localize to the virus factory with conjugated ubiquitin in HeLa cells.**

HeLa, were infected with VACVCop, VACV-FLAG-IHDW-p28, VACV-FLAG-p28(C173S/C176S), or VACV-FLAG-M143R, or infected with VACVCop and transfected with pSC66-FLAG-FWPV150 at an MOI of 5. Cells were fixed and treated with DAPI, to visualize the nucleus and virus factories, and stained anti-FLAG to detect FLAG-tagged proteins, and anti-FK2 to detect conjugated ubiquitin. This experiment was performed three independent times and we observed on average over 100 cells per sample, which were evaluated across the entire cover slips of the samples. We showed one representative cells per sample in this Figure.

Previous studies demonstrated that the p28 homologue in ECTV plays a crucial role for ECTV growth in macrophages (245). We started isolating bone marrow derived macrophages (BMDM) from mice and differentiated them into primary macrophages where ECTV lacking p28 fails to form virus factories in primary macrophages (245). The goal was to investigate, if a similar effect was seen to Senkevich *et.al.* Unfortunately, this project was terminated before we could conduct infection studies on primary macrophages, which is further discussed in Chapter 6. Instead, we characterized the co-localization of p28, and homologue M143R with FK2 in the readily available ATCC mouse macrophage cell lines J774 and Raw 264.7 (**Figure 4.4 A and B**). We further investigated, if co-localization of the double cysteine mutant p28(C173S/C176S) with FK2 at the virus factory is also observed in mouse macrophage cell lines (**Figure 4.4A and B; panel m-p**). p28, p28(C173S/C176S) and M143R co-localized with conjugated ubiquitin at the virus factories in mouse macrophage cell lines J774 and Raw 264.7, similar to the effect seen in HeLa cells (**Figure 4.4A and B; panel l, p, t**). Since we could not detect a different phenotype in mouse macrophage cell lines for p28 homologues and the p28 double cysteine mutant, we continued to use HeLa cells in the following experiments due to its superior transfection efficacy.

#### **4.2.3 The Kila-N DNA binding domain plays a critical role in localizing p28 to the virus factory, but does not affect the accumulation of conjugated ubiquitin at the virus factory**

A



B

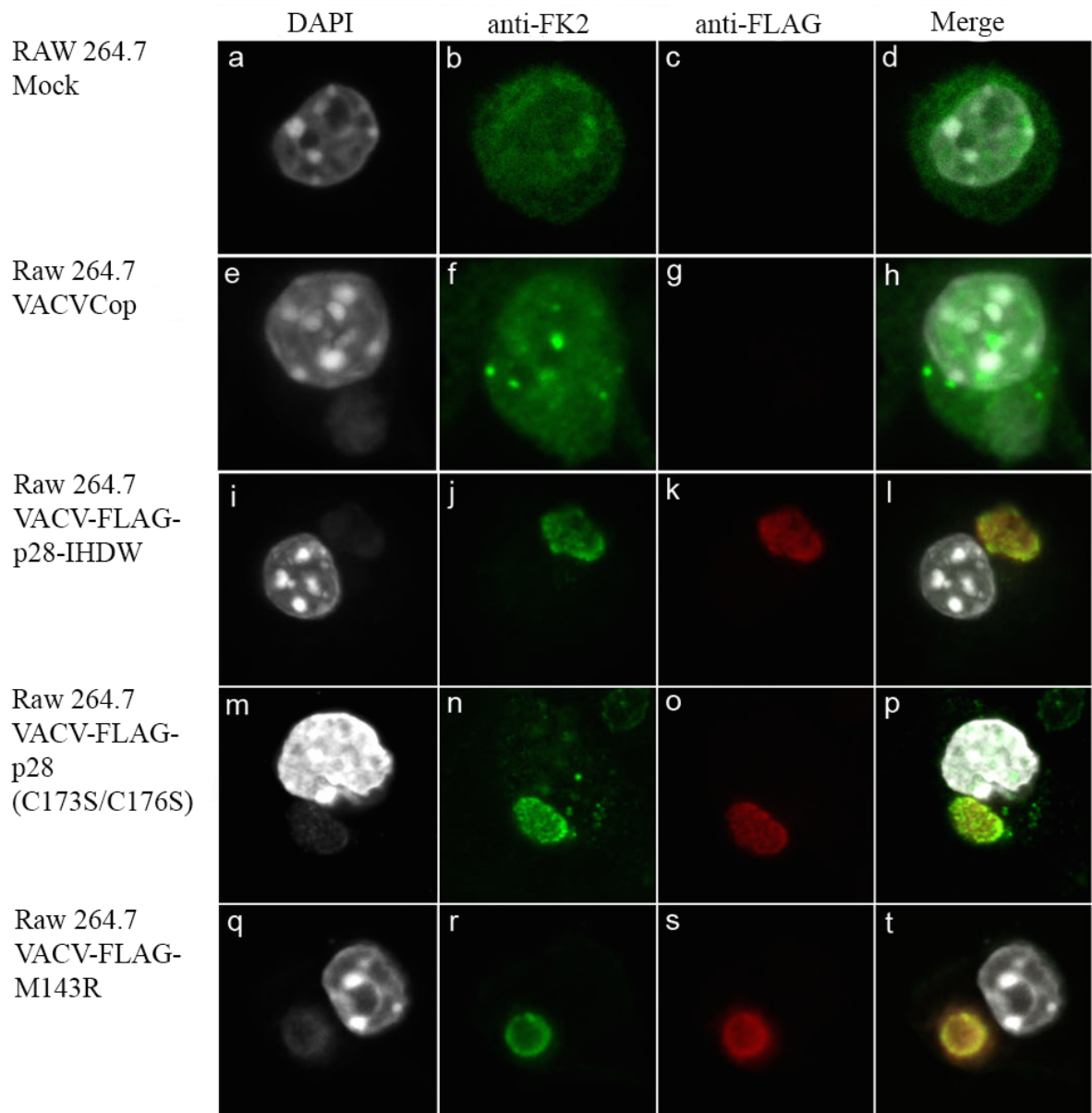
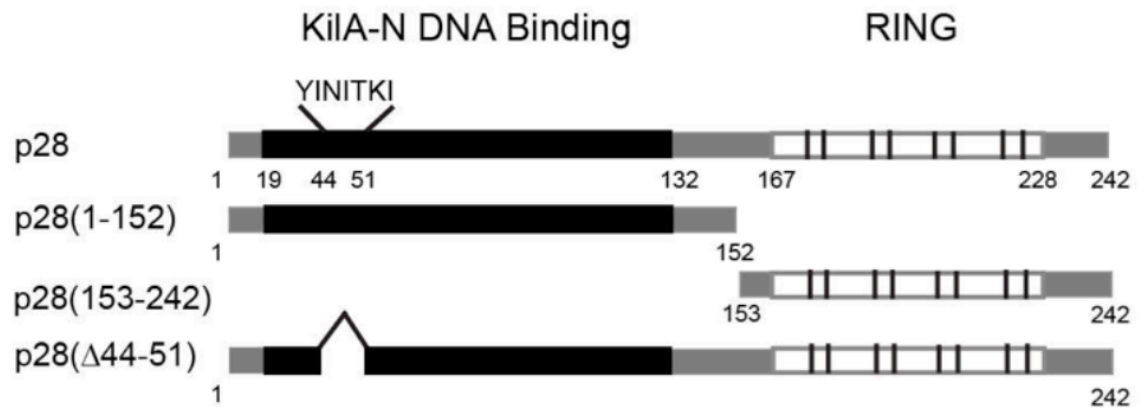


**Figure 4.4 p28 homologues co-localize to the virus factory with conjugated ubiquitin in macrophage cell lines.**

(A) J774, or (B) Raw264.7 were infected with VACVCop, VACV-FLAG-IHDW-p28, or VACV-FLAG-p28(C173S/C176S), or VACV-FLAG-M143R at an MOI of 5. Cells were fixed and treated with DAPI, to visualize the nucleus and virus factories, and stained anti-FLAG to detect FLAG-tagged proteins and anti-FK2 to detect conjugated ubiquitin. This experiment was performed three independent times and we observed on average over 100 cells per sample, which were evaluated across the entire cover slips of the samples. We showed one representative cells per sample in this Figure.

The N-terminus of p28 contains a Kila-N DNA binding domain (246), and deletions within this domain have previously been reported to prevent localization of p28 to viral factories (247). Therefore, we sought to determine if the Kila-N domain played a critical role in the co-localization of conjugated ubiquitin at the viral factory. To examine the co-localization of p28 with conjugated ubiquitin, HeLa cells were infected with VACVCop and transfected with pSC66-p28, pSC66-FLAG-p28(1-152), containing the Kila-N domain, pSC66-FLAG(153-242), containing the RING-only domain, or pSC66-FLAG( $\Delta$ 44-51), missing eight amino acids within the Kila-N domain (**Figure 4.5A and 4.5B**). Cells were stained with DAPI to visualize the virus factories and co-stained with anti-FK2 and anti-FLAG to visualize conjugated ubiquitin and p28, respectively. As expected, pSC66-FLAG-p28(IHDW) and pSC66-FLAG-p28(1-152), each containing a functional Kila-N domain, localized to the virus factory (**Figure 4.5B; panel g and k**). In contrast, pSC66-FLAG-p28(153-242), containing the RING-only domain, and pSC66-FLAG-p28( $\Delta$ 44-51), missing eight amino acids within the Kila-N domain, failed to accumulate at viral factories and instead were distributed throughout the cell and nucleus (**Figure 4.5B; panel o and s**). The data indicate that the Kila-N DNA binding domain was critical for localization to the viral factories, as previously demonstrated (247). Given the obvious differences in localization, we next determined whether conjugated ubiquitin was present at the factory. Conjugated ubiquitin was enriched at the virus factory upon expression of FLAG-p28 (**Figure 4.5B; panel f**). Significantly, pSC66-FLAG-p28(1-152), containing only the Kila-N domain, failed to accumulate significant amounts of conjugated ubiquitin at the virus factory, even though pSC66-FLAG-p28(1-152) localized predominantly to the virus factory (**Figure 4.5B; panel j**). Expression of the

A



B

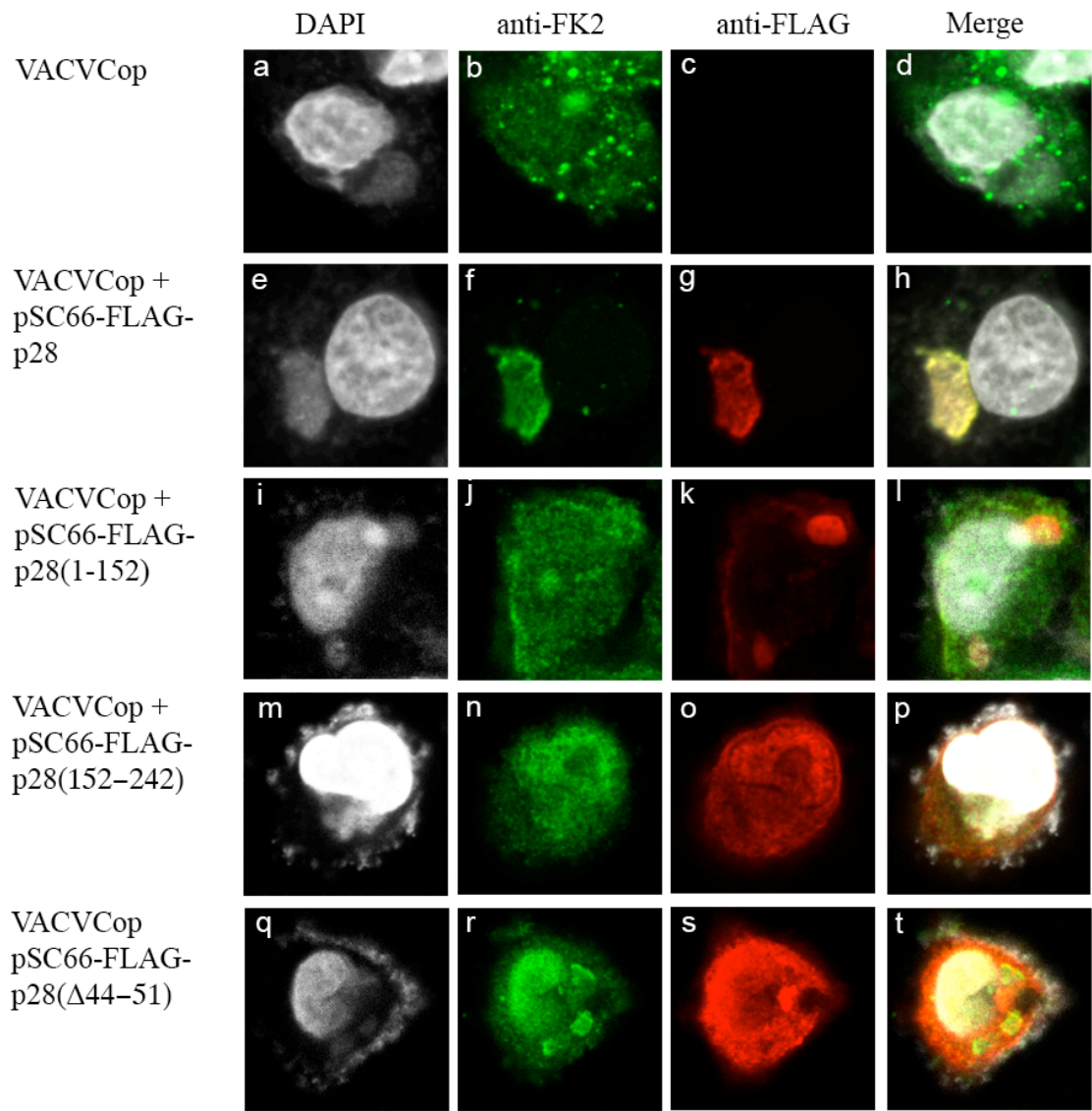


**Figure 4.5 The KilA-N DNA binding domain plays a critical role in p28 localization to the virus factory, but does not affect the accumulation of conjugated ubiquitin at the virus factory.**

**(A)** A schematic of wild type p28 and mutant versions of p28. The KilA-N DNA binding domain is highlighted in black and the RING domain is shown in white. **(B)** HeLa cells were infected with VACV Cop at an MOI of 5 and transfected with pSC66-FLAG-p28, pSC66-FLAG-p28(1-152), pSC66-FLAG-p28(153-242) and pSC66-FLAG-p28( $\Delta$ 44-51). Cells were fixed, stained with DAPI, and p28 was detected by anti-FLAG staining. Conjugated ubiquitin was detected by anti-FK2 staining. This experiment was performed three independent times and we observed on average over 100 cells per sample, which were evaluated across the entire cover slips of the samples. We showed one representative cells per sample in this Figure.

RING-only domain, pSC66-FLAG-p28(153-242), demonstrated only a minor enrichment of ubiquitin at the virus factory (**Figure 4.5B; panel n**). In cells expressing FLAG-p28( $\Delta$ 44-51), missing residues within the Kila-N domain, there was also only a minor accumulation of conjugated ubiquitin at the virus factory (**Figure 4.5B; panel r**). Overall, the data indicate that wild type p28 co-localized at the virus factory with conjugated ubiquitin, whereas the p28 mutants failed to accumulate conjugated ubiquitin at the virus factory (**Figure 4.5B**). This suggests that the localization of the RING domain at the virus factory, which is mediated by the Kila-N domain, is required for enrichment of conjugated ubiquitin at the virus factory. We next investigated the ubiquitin ligase activity of the p28 mutants to confirm their loss of catalytic activity.

#### **4.2.4 p28 RING mutants lost ubiquitin ligase activity**

We performed an *in vitro* ubiquitination assay to demonstrate the E3 ligase activity or catalytic loss of the p28 mutants and exclude residual ubiquitin ligase activity. Cells were infected with VACVCop, transfected with pSC66-FLAG-p28, pSC66-FLAG-p28(1-152), pSC66-FLAG-p28(153-242), pSC66-FLAG-p28( $\Delta$ 44-51), pSC66-FLAG-p28(C173S/C176S), pSC66-FLAG-p28(1-184), or pSC66-FLAG-p28(1-204) and were subjected to immunoprecipitation using an anti-FLAG antibody. We used the very stringent RIPA lysis buffer. The resulting immune complexes were immobilized on Protein G beads, and were used as the source of ubiquitin ligase and tested in an *in vitro* ubiquitination assay (255). The formation of ubiquitin conjugates was detected by western blotting for biotinylated ubiquitin adducts. Cell lysates stained with rabbit anti-

FLAG showed the presence of all FLAG immunoprecipitated proteins. We previously demonstrated the ubiquitin ligase activity of p28 in an *in vitro* ubiquitination assay; at the same time we showed that the double cysteine mutant p28(C173S/C176S) lost its ubiquitin ligase activity (243). Immune complexes generated from infected/transfected cells expressing FLAG-p28, and p28 mutants containing an intact RING domain FLAG-p28(153-242), and FLAG-p28( $\Delta$ 44-51) showed the presence of both free ubiquitin, as well as high molecular weight ubiquitin conjugates after being subjected to an *in vitro* ubiquitination assay (**Figure 4.6**). These high molecular weight ubiquitin conjugates were absent in the p28 double cysteine mutants and p28 mutants, which lack the RING domain (pSC66-FLAG-p28(1-152)), or have truncated versions of the RING domain (pSC66-FLAG-p28(1-184) and pSC66-FLAG-p28(1-204)) (**Figure 4.6**). This confirms that an intact RING domain is crucial for ubiquitin ligase activity in p28. We next investigated the ubiquitination pattern of the p28 mutants to see which domains are regulated by ubiquitination.

#### **4.2.5 Both the Kila-N and RING domains of p28 are ubiquitinated in the presence of MG132**

To further investigate which domains of p28 are ubiquitinated during infection, HeLa cells were infected with a VACV-HA-Ub strain, which expresses HA-tagged ubiquitin, and transfected with p28 mutants described in **Figure 4.5**. Ubiquitination was detected by blotting with anti-FLAG and anti-HA in the presence and absence of MG132 (**Figure 4.7A**). Significantly, FLAG-p28(IHDW), FLAG-p28(1-152), FLAG-p28(153-242) and

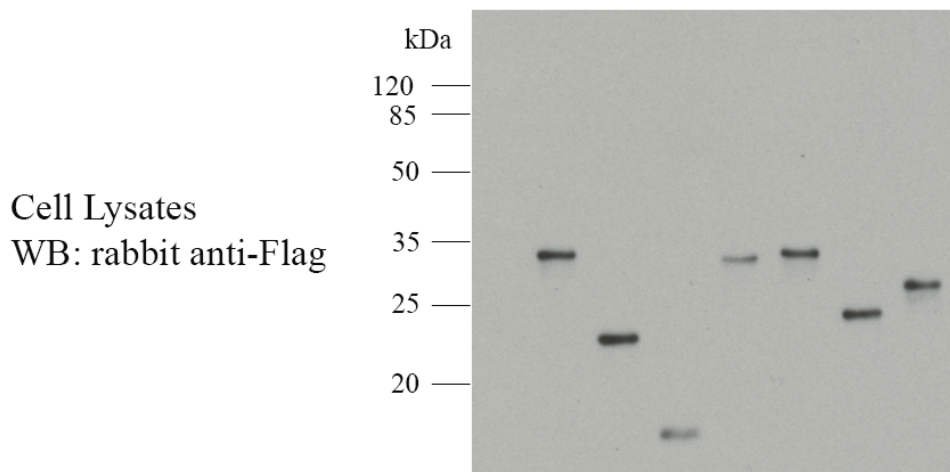
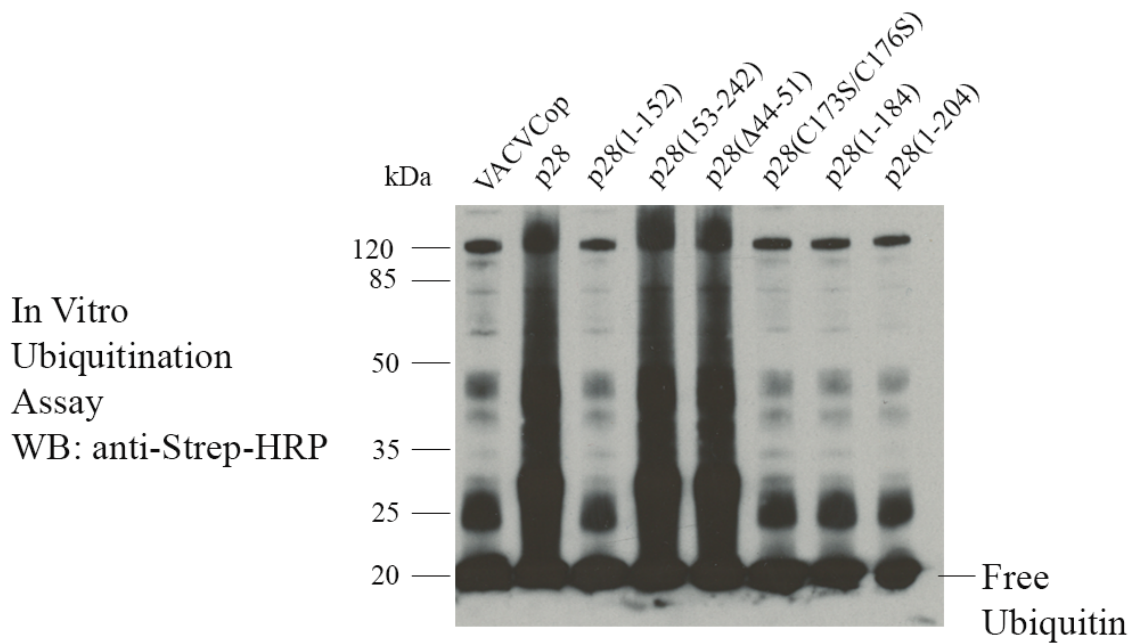
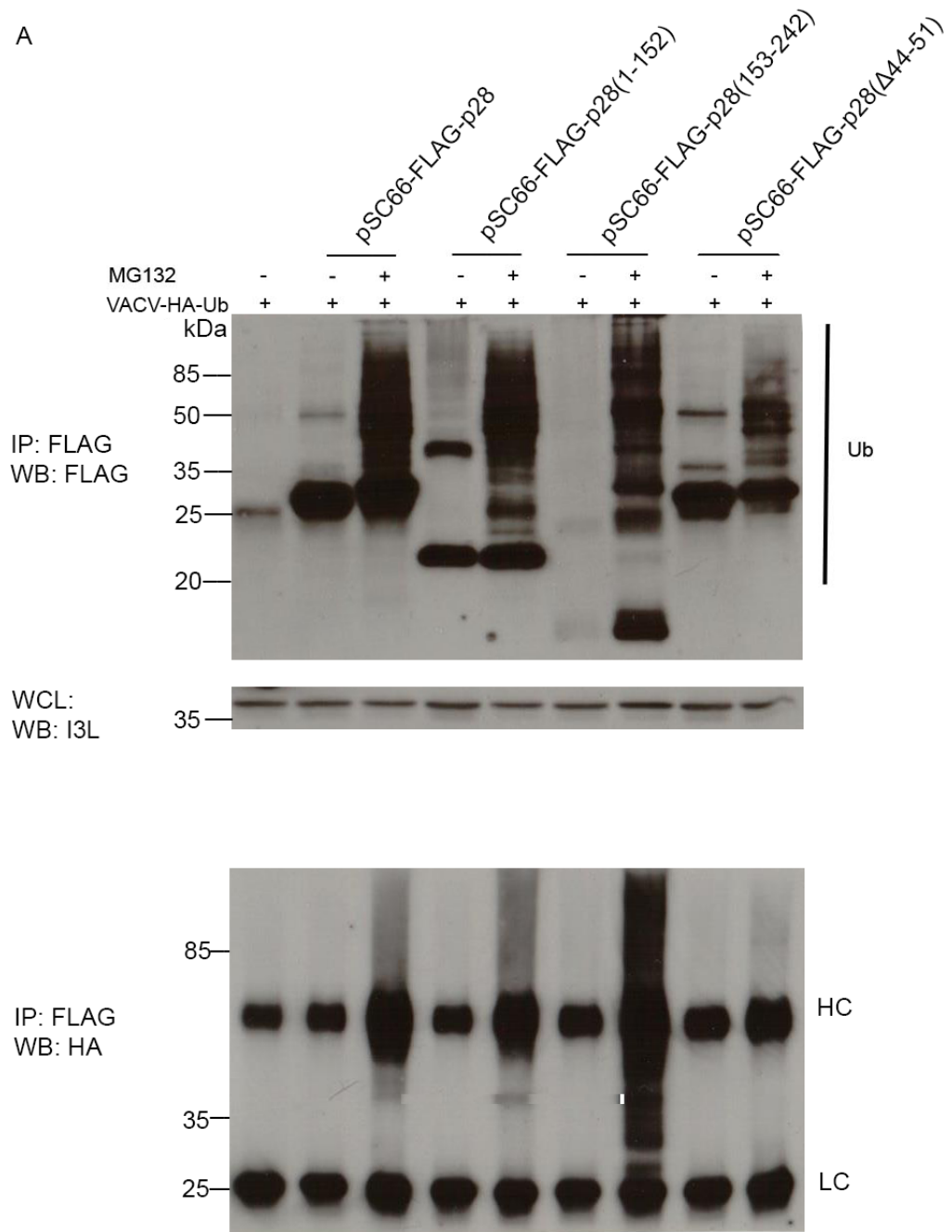


**Figure 4.6** *In vitro* ubiquitin ligase activity of p28 and p28 mutants.

Protein G beads containing FLAG tagged proteins were mixed in an *in vitro* ubiquitination reaction with E1, (E2), ATP, and biotin-labeled ubiquitin (BIOMOL International). Reactions were separated by SDS-PAGE and were probed with streptavidin-tagged HRP. Western blotting shows the appearance of high-molecular mass ubiquitin adducts in reactions containing either p28, or p28 mutants containing the RING domain.

A



B

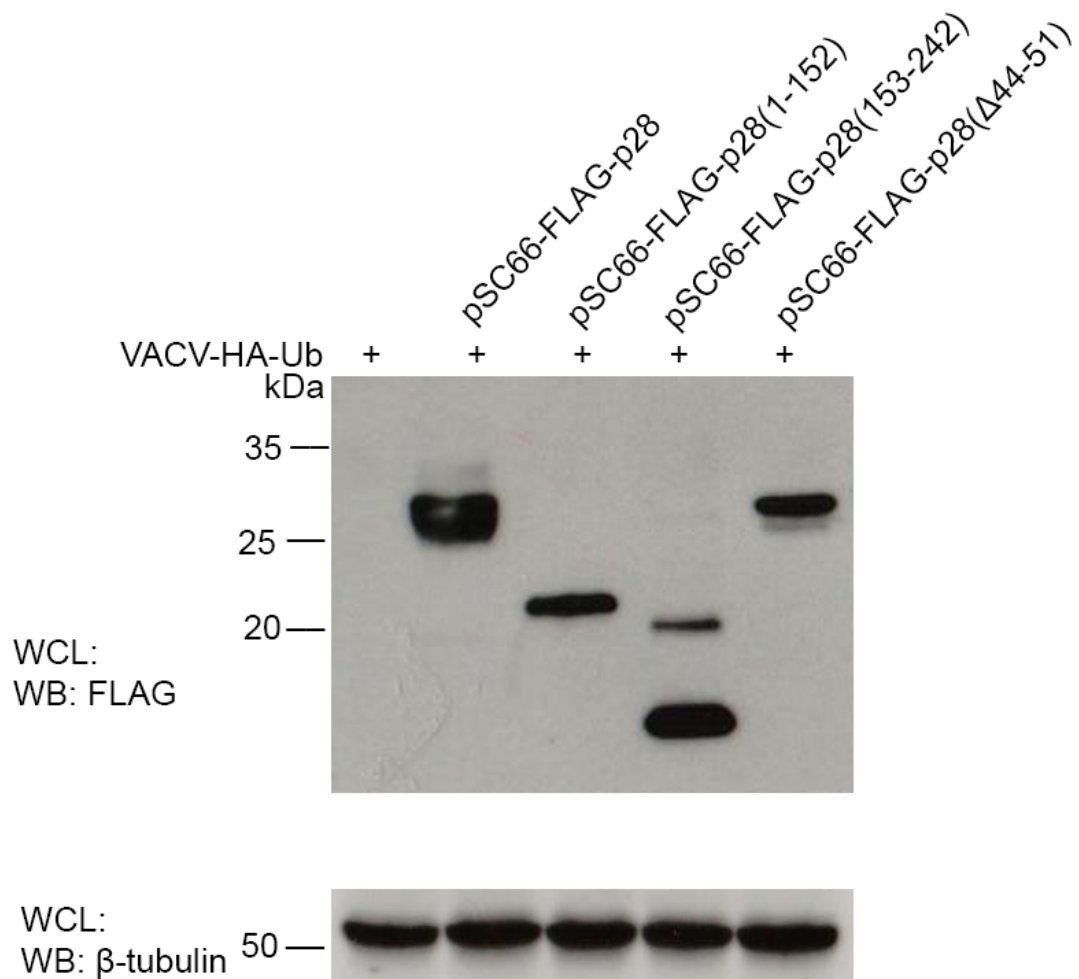


**Figure 4.7 p28 is regulated by ubiquitination.**

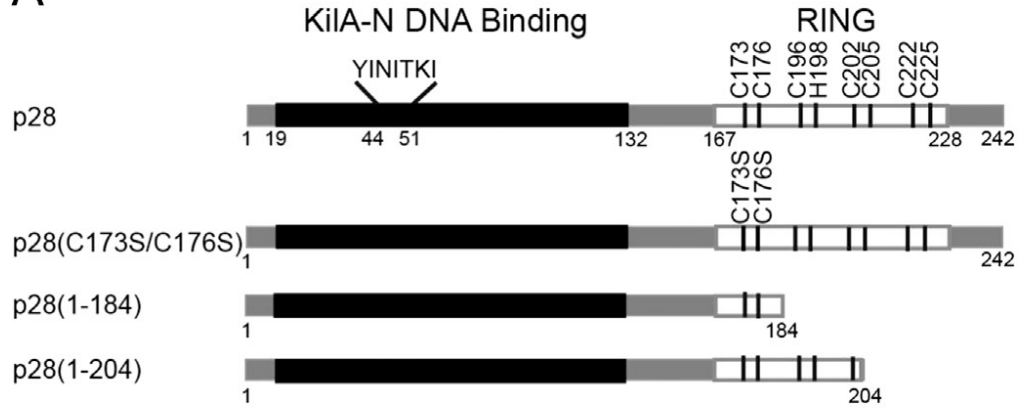
(A) To detect ubiquitination, HeLa cells ( $2 \times 10^6$ ) were infected with VACV-HA-Ub and transfected with pSC66-FLAG-p28, pSC66-FLAG-p28(1-152), pSC66-FLAG-p28(153-242) or pSC66-FLAG-p28(Δ44-51). Cells treated with or without MG132 (10mM) for six hours were lysed in RIPA buffer and p28 constructs were immunoprecipitated with mouse anti-FLAG M2 and western blotted with rabbit anti-FLAG and anti-HA to detect ubiquitination (B) Whole cell lysates were ubiquitinated in the presence of MG132 (Figure 4.7A). The next section evaluated the role of a functional RING domain for the ubiquitination-mediated regulation of p28. were harvested and western blotted with anti-FLAG and anti-β-tubulin as a loading control.

FLAG-p28( $\Delta$ 44-51) were all ubiquitinated upon treatment with MG132 (Figure 4.7A). Despite obvious differences in viral factory localization (Figure 4.5B), all four proteins were ubiquitinated in the presence of MG132 (Figure 4.7A). The next section evaluated the role of a functional RING domain for the ubiquitination-mediated regulation of p28.

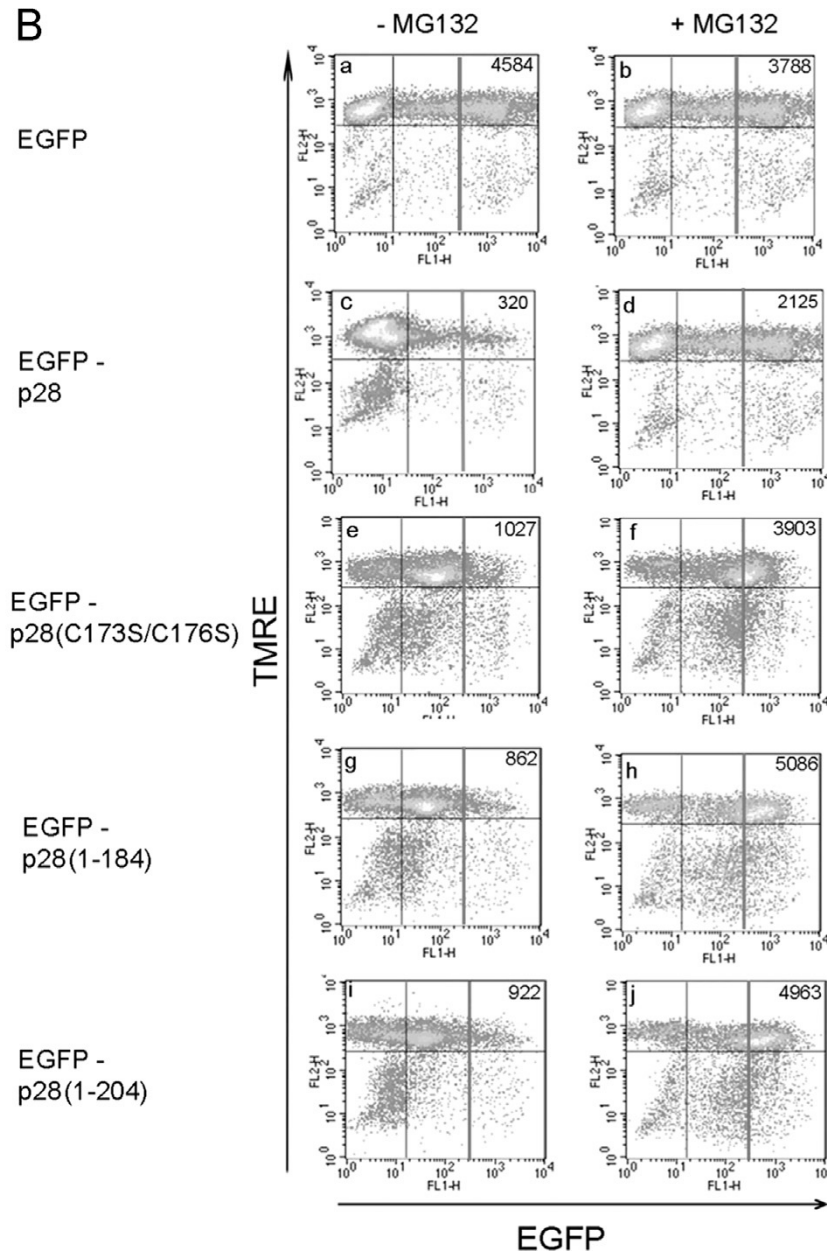
#### **4.2.6 p28 catalytic non-functional RING mutants are still stabilized in the presence of MG132**

p28 is controlled by proteosomal degradation and many ubiquitin ligases regulate themselves through autoubiquitination (139, 272, 273). Given this, we sought to determine the role of the RING domain in autoubiquitination. We generated three p28 RING mutants (243), pEGFP-p28(C173S/C176S), containing two point mutations critical for ubiquitin ligase function, pEGFP-p28(1-184), a truncated version lacking the majority of the RING domain, and pEGFP-p28(1-204), lacking amino acids 205-242 of the RING domain, thereby disrupting the ubiquitin ligase activity of p28 (**Figure 4.8A**) (243). Each of the three mutant proteins were analyzed for expression in the presence or absence of MG132 via flow cytometry (**Figure 4.8B**). Furthermore, cells were incubated in TMRE containing media. TMRE is a cell permeable dye, which is readily accumulated within healthy, respiring mitochondria (274). The loss of mitochondrial membrane potential in unhealthy cells is associated with a decrease in TMRE uptake (274). Here, we used TMRE as an indication for healthy cells. As shown previously, EGFP expression was unaltered upon MG132 treatment (**Figure 4.8B; panel a and b**), while EGFP-p28(IHDW) was stabilized upon the addition of MG132 suggesting it is regulated by proteasomal degradation (**Figure 4.8B; panels c and d**). In the absence of MG132,

A



B



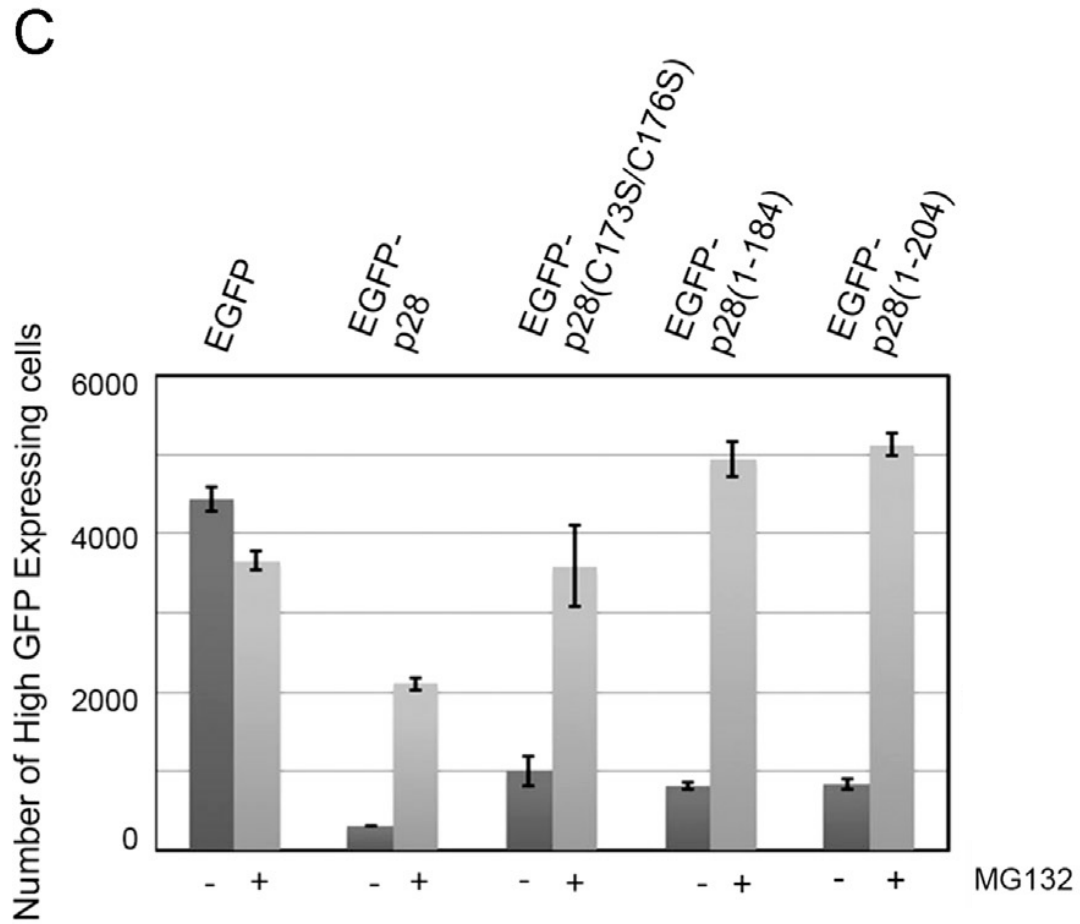


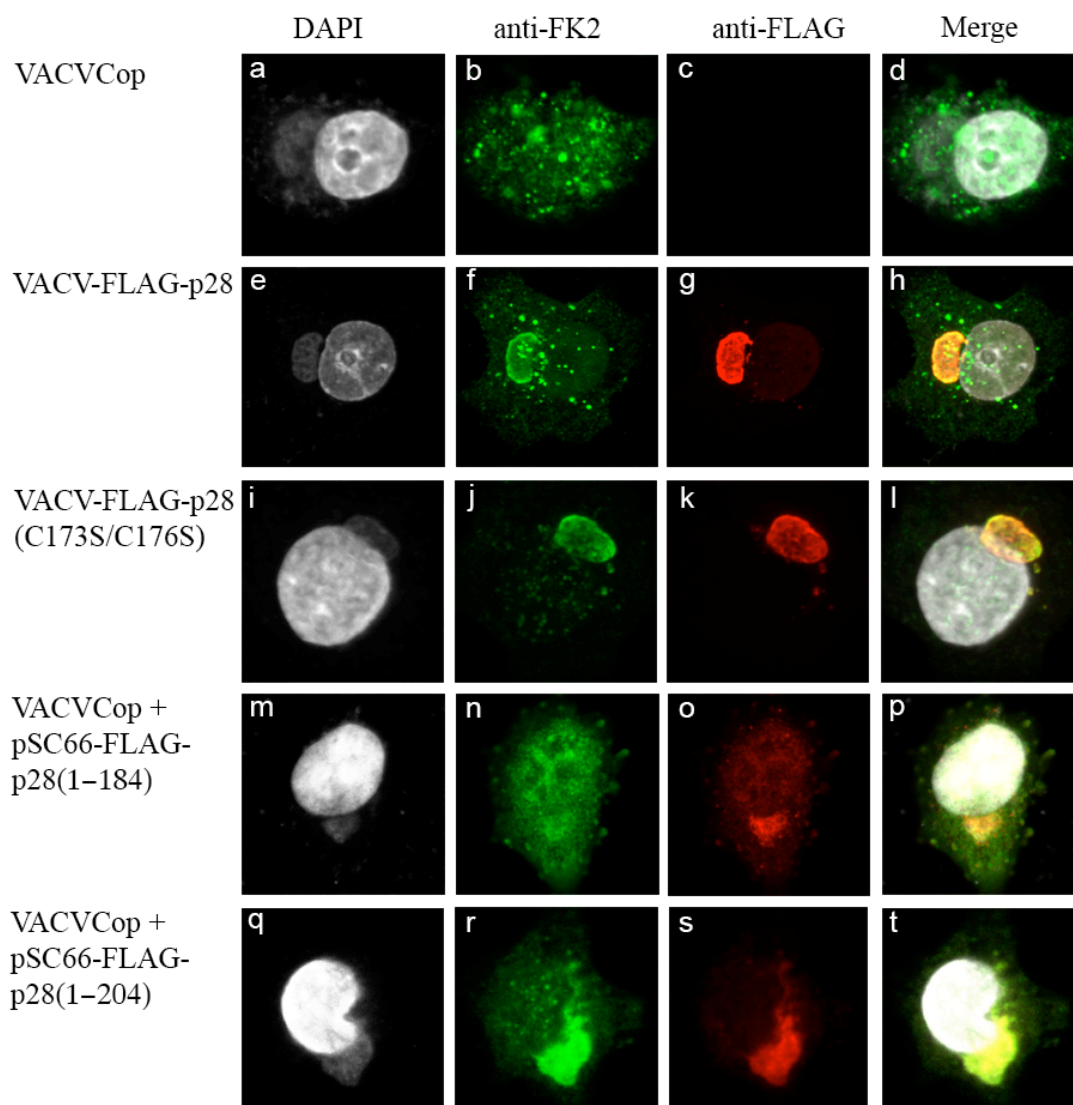
**Figure 4.8 Mutations in the RING domain stabilize p28 (Kelly Mottet).**

(A) Schematic representation of the p28 RING mutants. The data shown in (B) was collected by Kelly Mottet and repeated in triplicate and graphed as the number of high GFP-expressing cells in the upper right quadrant (C). (B) HeLa cells were transfected with pEGFP-p28(C173S/C176S), pEGFP-p28(1-184) or pEGFP-p28(1-204) for 16 hours and treated with or without 10 $\mu$ M MG132 for 6 hours. Cells were labeled with 0.2 $\mu$ M, washed and resuspended in PBS containing 1% FBS and analyzed by two-color flow cytometry (C) The number of EGFP cells were quantified in triplicate in the presence and absence of MG132.

EGFP-p28(C173S/C176S), EGFP-p28(1-184), and EGFP-p28(1-204) were stabilized due to inactivation or absence of the RING domain (**Figure 4.8B**), and were further stabilized upon MG132 treatment (**Figure 4.8B**), indicating that wild type p28 was regulated by proteasomal degradation (**Figure 4.8B**). The data indicated that mutation of the RING domain results in increased stabilization of the p28 mutant proteins, further suggesting that wild type p28(IHDW) uses its RING domain to regulate itself by autoubiquitination. However, since the RING mutants demonstrated an increase in stabilization this suggests that p28 is further regulated by another ubiquitin ligase.

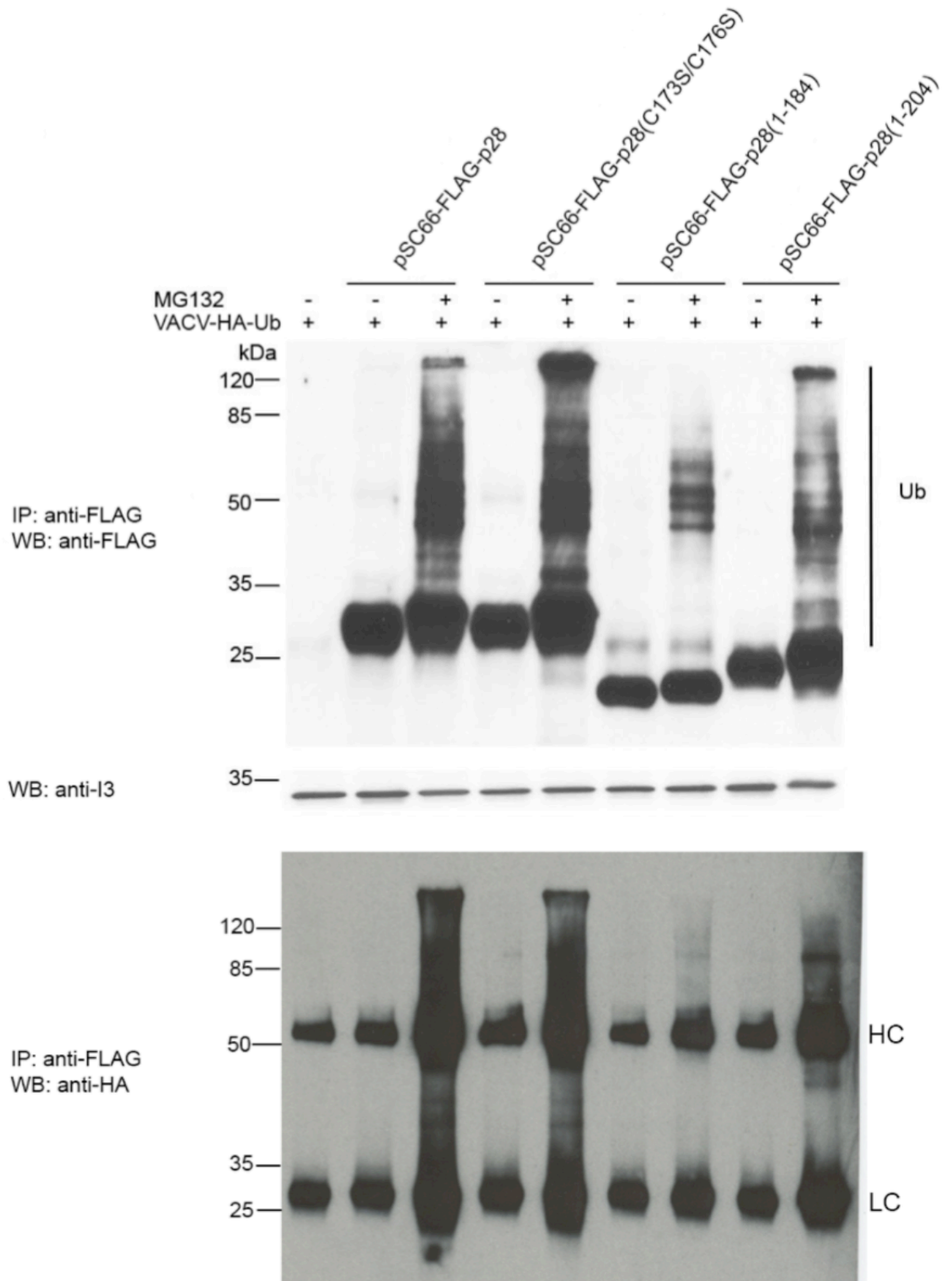
#### **4.2.7 An additional ubiquitin ligase promotes the accumulation of conjugated ubiquitin at the virus factory**

Since the p28(IHDW) RING mutants from the previous section were subjected to proteasomal degradation (**Figure 4.8**), we sought to determine if conjugated ubiquitin localized to viral factories in their presence (**Figure 4.9**). HeLa cells were mock-infected or infected with VACVCop and transfected with pSC66-FLAG-p28(IHDW), pSC66-FLAG-p28(C173S/C176S), pSC66-FLAG-p28(1-184) and pSC66-FLAG-p28(1-204). As expected, conjugated ubiquitin co-localized with FLAG-p28(IHDW) at the viral factory (**Figure 4.9**). Conjugated ubiquitin was still present at the virus factory when FLAG-p28(C173S/C176S) was expressed in cells (**Figure 4.9**), suggesting that an additional ubiquitin ligase was responsible since FLAG-p28(C173S/C176S) lacks intrinsic ubiquitin ligase activity (243). Similarly, conjugated ubiquitin was also present at the viral factory upon expression of FLAG-p28(1-204) (**Figure 4.9**). In contrast, little ubiquitin was



**(A)** HeLa cells were mock infected or infected with VACV at an MOI of 5 and transfected with pSC66-FLAG-p28, pSC66-FLAG-p28(C173S/C176S), pSC66-FLAG-p28(1-184), or pSC66-FLAG-p28(1-204). Cells were fixed, stained with DAPI, to visualize the nucleus and cytoplasmic virus factories, and stained with anti-FK2 and anti-FLAG to detect conjugated ubiquitin and p28 protein expression, respectively. This experiment was performed three independent times and we observed on average over 100 cells per sample, which were evaluated across the entire cover slips of the samples. We showed one representative cells per sample in this Figure.

A



B

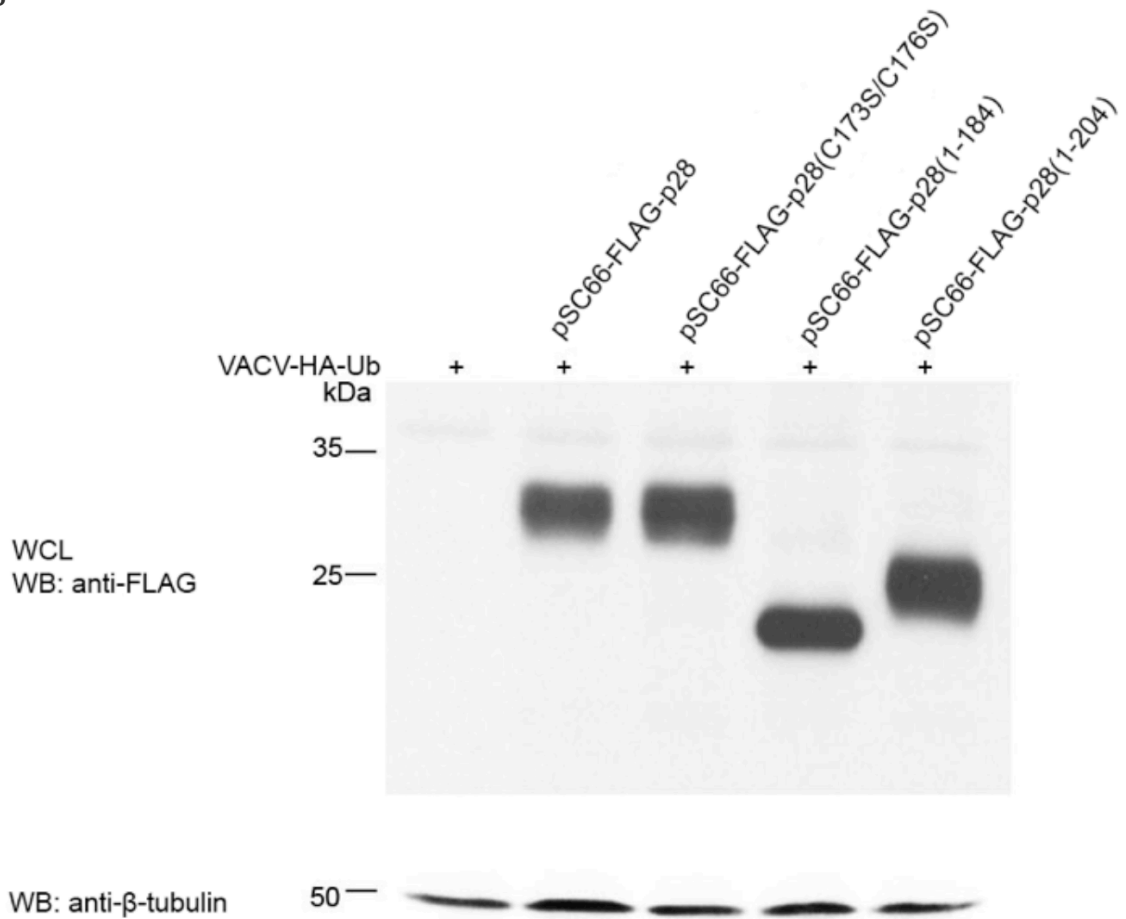


**Figure 4.10 p28 RING mutants demonstrate variable patterns of ubiquitination.**

**(A)** To detect ubiquitination, HeLa cells ( $2 \times 10^6$ ) were infected with VACV and transfected with pSC66-FLAG-p28, pSC66-FLAG-p28(C173S/C176S), pSC66-FLAG-p28(1-184), or pSC66-FLAG-p28(1-204). Cells treated with or without MG132 (10mM) for six hours were lysed in RIPA buffer and p28 constructs were immunoprecipitated with mouse anti-FLAG M2 and western blotted with rabbit anti-FLAG and anti-HA to detect ubiquitination. **(B)** Whole cell lysates were harvested and western blotted with anti-FLAG and anti-beta-tubulin as a loading control.

detected at the virus factories in FLAG-p28(1-184)-expressing cells (**Figure 4.9**), suggesting that the region between amino acids 184 and 204 may be critical for the ubiquitination of p28 by another ubiquitin ligase. The data indicate that at least one unknown additional ubiquitin ligase is responsible for the presence of conjugated ubiquitin at viral factories. To further investigate the ubiquitination of the p28 RING mutants we infected HeLa cells with VACVcop and transfected cells with p28 RING mutants in the absence and presence of MG132. Ubiquitination was detected by blotting with anti-FLAG and anti-HA (**Figure 4.10A and B**). pSC66-FLAG-p28(IHDW) and pSC66-FLAG-p28(C173/176S) demonstrated obvious ubiquitination upon treatment with MG132 (**Figure 4.10A**). In contrast, pSC66-FLAG-p28(1-184) and pSC66-FLAG-p28(1-204) showed less obvious ubiquitination upon treatment with MG132 (**Figure 4.10A**).

### **4.3 Summary and Brief Discussion**

Poxviruses survive and replicate within host cells through the manipulation of cellular pathways (20, 30). Recently, poxvirus manipulation of the host ubiquitin-proteasome system has become increasingly apparent (229). Since the ubiquitin-proteasome system plays an important role in cellular homeostasis, many viruses have evolved strategies to regulate the process of ubiquitination to their own advantage, and poxviruses are no exception (211, 212). Recent evidence indicates that poxviruses encode a family of BTB/kelch proteins and ankyrin/F-box proteins that likely function as substrate adaptors for cellular cullin-3 and cullin-1 based ubiquitin ligases (235, 240, 269, 270, 275-281). Additionally, poxviruses have also been shown to encode proteins with intrinsic ubiquitin ligase activity (242, 243). These include M153R, a membrane associated RING-CH

ubiquitin ligase encoded by MYXV, and p28, a RING encoded ubiquitin ligase (73, 242, 243). p28 is a highly conserved ubiquitin ligase that has been shown to be a critical virulence factor (242-245). Here we further investigate the regulation of p28.

Since many cellular and viral ubiquitin ligases are regulated through ubiquitination and autoubiquitination, we investigated the ubiquitin-proteasomal dependent regulation of p28. We first set out to determine if the ubiquitin-proteasome-system was functional during infection with a number of poxviruses, by measuring the chymotrypsin-like activity of the proteasome (**Figure 4.1**). These include VACV, CPXV, ECTV and FWPV in the presence and absence of MG132. Overall, we detected a functional proteasome during all types of poxvirus infections. This is in agreement with the literature, where an active proteasome was reported during VACV infection (282). The fact that the ubiquitin-proteasome system remains functional indicates a great advantage for poxviruses in using the cellular systems and encoding their own ubiquitin ligases. However, there is a potential disadvantage, since cellular ubiquitin ligases with anti-viral features can still function, as well.

In addition to p28(IHDW), other poxvirus encode p28-like ubiquitin ligases, as well. For example, p28 is conserved throughout the *Orthopoxviridae*; distantly related p28 proteins are found in other genera, including M143R encoded by MYXV, and FWPV150 encoded by FWPV (22, 283). Attenuated poxviruses, such as VACV strain Copenhagen and Western Reserve, contain deleted or truncated versions of p28, suggesting that p28 plays an important role in virulent viruses (284). Despite the lower sequence identity compared to p28-IHDW, both M143R and FWPV150 co-localized with conjugated ubiquitin at the virus factory indicating that p28 function is highly conserved

among members of the poxvirus family (**Figure 4.3**). Our data indicate that localization of p28 at the viral factories was dependent on the Kila-N DNA binding domain (**Figure 4.5**) that is found in bacteria, bacteriophage and large DNA viruses (246, 247). As suspected, the Kila-N domain alone was not sufficient to trigger the enrichment of conjugated ubiquitin at the virus factories (**Figure 4.5**). This is in accordance with our data in Chapter 3, where the Kila-N only protein FWPV075 in FWPV localized to the virus factory, without effect on accumulating conjugated ubiquitin at the virus factory (**Figure 3.9**).

We demonstrated the catalytic loss of ubiquitin ligase activity in p28 mutants lacking the RING domain, or containing mutations and truncations within the RING domain (**Figure 4.6**). Bearing this in mind, confocal imaging demonstrated conjugated ubiquitin at the virus factories in the presence of two of the RING mutants, FLAG-p28(C173S/C176S) and FLAG-p28(1-204) (**Figure 4.7**). In contrast, it appears that FLAG-p28(1-184) demonstrated only minor amounts of ubiquitination (**Figure 4.8**). Again, all three RING mutants lacked intrinsic ubiquitin ligase activity (**Figure 4.9**), indicating that the conjugated ubiquitin present at the factory was due to the activity of another ubiquitin ligase.

Since many cellular and viral ubiquitin ligases are regulated through ubiquitination and autoubiquitination, we investigated the regulation of p28 by the UPS (139). We used a flow cytometry assay to determine if p28 was regulated by the proteasome. In the absence of a proteasome inhibitor, EGFP-p28 was detected at low levels. However, upon MG132-mediated inhibition of the proteasome, p28 was significantly stabilized and detected at high levels (**Figure 4.6**), suggesting that p28 is

regulated by proteasomal degradation. This might be a mechanism to temporally control the activity of p28 during different stages of infection.

Given that our data indicates that p28 is tightly controlled by proteasomal degradation, we further examined the three p28 RING mutants p28(C173S/C176S), p28(1-184), and p28(1-204), which lost the ability of auto-ubiquitination (**Figure 4.6**). In the absence of MG132, all three of the RING mutants were detected at low levels, and were stabilized in presence of MG132. Interestingly, in the presence of MG132, the RING mutants were detected at even higher levels compared to wildtype p28 (**Figure 4.6B**). This suggests that the RING domain of p28 plays a role in ubiquitinating itself, and is further regulated by another ubiquitin ligase, leading to subsequent degradation via the proteasome. A large number of ubiquitin ligases are known to be autoubiquitinated in order to regulate themselves (139, 285). For example, Mdm2 is known to mediate its own degradation through autoubiquitination (286, 287). Similar to p28, mutating the RING domain of Mdm2 inhibits ubiquitin ligase activity stabilizing Mdm2 (139). Importantly, upon MG132 treatment, we found that all three p28 RING mutants were further stabilized (**Figure 4.5B**). Similar to p28, Mdm2 stability is also regulated by other ubiquitin ligases. This event appears to be common within the ubiquitin-proteasome pathway (288). Surprisingly, there was no significant difference between the stabilization of p28(1-184) and p28(1-204) in our transfection model. It is possible, that the ubiquitin ligase, which is ubiquitinating p28 is of poxviral origin and was missing in this model. Future experiments will investigate the MG132-mediated stabilization of p28(1-184) and p28(1-204) in presence of VACV Cop infection.

Our data suggests that p28 is a dually regulated ubiquitin ligase, which regulates itself through autoubiquitination in addition to being regulated by another ubiquitin ligase or ligases. Identification of this unknown ubiquitin ligase or ligases will provide further insight into the regulation of p28.

## **CHAPTER 5: IDENTIFICATION OF P28 INTERACTION PARTNERS**

This work represents a publication in progress. I performed all experiments presented here with input from Dr. Ingham, except for the Mass Spectrometry, which was performed by Jack Moore in a collaboration with the Dr. Richard Fahlman's group (Department of Biochemistry, University of Alberta). The first draft of this chapter was written by myself, while the final draft had editorial contributions from Dr. Ryan Noyce and Dr. Ingham.

## 5.1 Introduction

p28 is a E3 ubiquitin ligase, found in diverse members of the poxvirus family, including VACV, ECTV, MYXV, Shope fibroma virus, variola virus and avipoxviruses (22, 23, 289). The identification and characterization of both cellular and viral protein substrates targeted by p28 is important to understand its role as a virulence factor during infection and is the focus of this chapter.

Over the years a significant amount of effort has been devoted to identifying ubiquitinated target proteins as well as to understanding the role of ubiquitin ligases during cellular processes (290-295). Identification of ubiquitinated substrates, however, has generally been difficult due to the transient interaction of ubiquitin ligases with their substrates (296). Furthermore, substrates of ubiquitin ligases can also be of low abundance within cells, making their detection even more difficult (297).

In this study, we used the traditional interaction-based method of co-immunoprecipitating FLAG-tagged p28 during VACV infection to detect both cellular and viral protein substrates of the ubiquitin ligase p28. Cells were treated with MG132, a proteasomal inhibitor, to prevent the degradation of ubiquitinated substrates and allow for easier detection. A p28-FLAG expression construct lacking its ubiquitin ligase activity (C173S/C176S) was included as well since this protein should still likely interact with substrates without their subsequent ubiquitin-mediated degradation. Mass spectrometry identified over 100 cellular and viral proteins associated with the poxviral ubiquitin ligase p28 (**Appendix, Table A1 and A2**). 56% of the hits were identified in both the p28 and the p28 mutant immunoprecipitations, while 29% of the hits were only present in the p28

immunoprecipitations and 15% were only associated with the p28 mutant. Many of the co-immunoprecipitated cellular proteins associated with p28 and the p28 mutant are known members of (i) DNA mismatch repair proteins and DNA stress sensors, including MSH2, MSH6 and ATM; (222) components of the nuclear import and export machinery; (iii) the heat shock protein (HSP) family, including HSP70 and HSP90; as well as (iv) poxviral proteins (**Figure 5.2**). A number of these cellular and poxviral proteins accumulate at virus factories following infection, indicating that these proteins might play a role in viral replication, morphogenesis, or viral DNA sensing. A number of experiments were carried out to confirm the identity of these proteins and the authenticity of their association with p28 and p28(C173S/C176S). MSH2, ATM, exportin-1, HSP70 and HSP90 were detected in anti-FLAG immunoprecipitates from lysates of HeLa cells infected with VACVCop expressing FLAG-p28. Furthermore, the colocalization of these proteins with p28 at the viral factories was monitored by immunofluorescence microscopy. Only HSP70 was enriched at virus factories in the presence of FLAG-p28. Interestingly, HSP70 was not ubiquitinated in the presence of p28, suggesting that it did not act as a substrate for p28. Furthermore, confocal analysis showed that there was a trend within p28 homologues in MYXV and FWPV towards triggering enrichment of HSP70 at the virus factory.

## **5.2 Results**

### **5.2.1 Numerous cellular and viral proteins co-immunoprecipitate with FLAG-p28**

To identify interaction partners and potential substrates of p28, anti-FLAG immunoprecipitates were collected from lysates in HeLa cells infected with VACVCop,

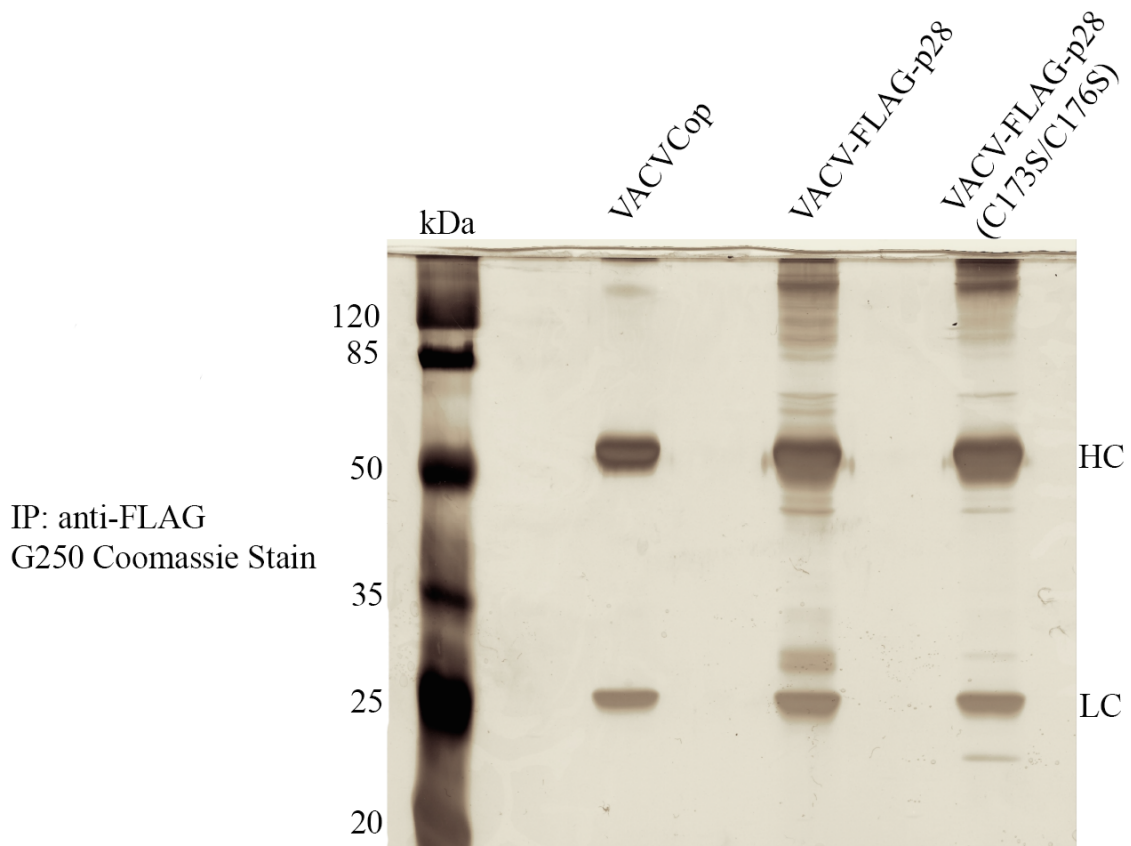


**Figure 5.1 FLAG-p28 and FLAG-p28(C173S/C176S) mutant-interacting proteins.**

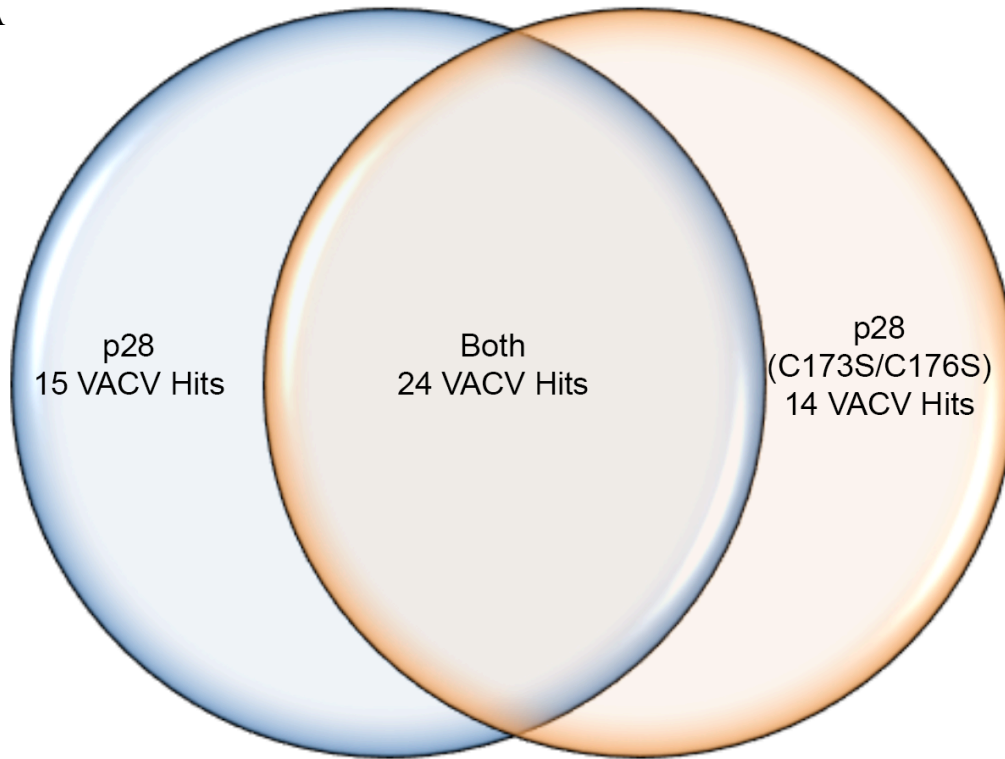
Coomassie blue stained SDS-PAGE gel of immunoprecipitates from lysates of VACVCop, VACVCop expressing FLAG-p28, or VACVCop expressing FLAG-p28(C173S/C176S). Gel slices of the entire lane for each sample were digested and analysed by Mass spectrometry in collaboration with the Fahlman group. Heavy chain (HC), Light chain (LC).

VACVCop expressing FLAG-p28, and VACVCop expressing a mutant of p28 that lacks the ubiquitin ligase activity, FLAG-p28(C173S/C176S). We included the FLAG-p28(C173S/C176S) in these experiments because we postulated that this mutant may bind substrates but not target them for degradation. Immunoprecipitates were run on an SDS-PAGE gel and stained with Coomassie Brilliant Blue G250 (**Figure 5.1**). In our negative control, immunoprecipitates from lysates of VACVCop-infected cells, the only bands observed were the heavy and light chain of the anti-FLAG antibody. In contrast, we detected multiple bands in the immunoprecipitates from the lysates of VACV-FLAG-p28-infected cells. The banding pattern observed in the immunoprecipitates from the VACV-FLAG-p28(C173S/C176S) infected cells were very similar to those observed in the immunoprecipitates of the VACV-FLAG-p28-infected cells. To identify the proteins present in the p28 immunoprecipitates, whole lanes were cut into smaller pieces and sent for identification using mass spectrometry in collaboration with Dr. Richard Fahlman's group (Department of Biochemistry, University of Alberta). The following subsection will cover bioinformatics analysis to group and highlight interesting p28 hits.

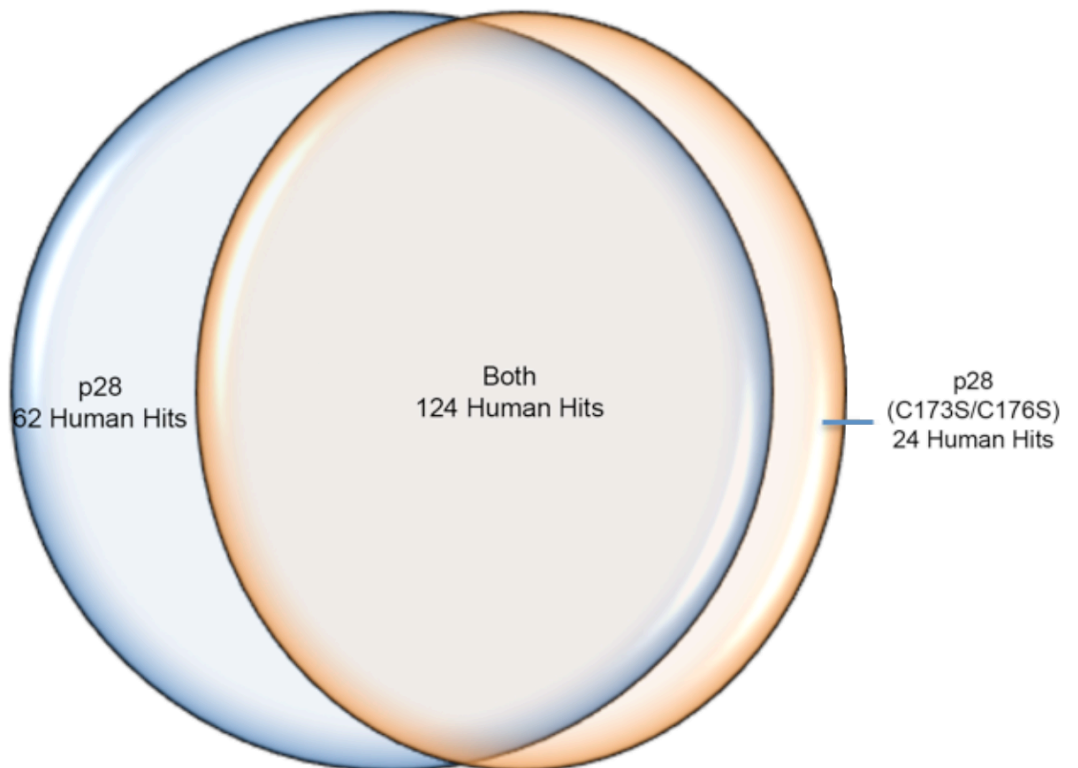
### **5.2.2 Identification and functional grouping of p28 mass spectrometry hits**

This subsection deals with the bioinformatics analysis and decision-making, which mass spectrometry hits to follow up with in the next subsections. The cellular and viral proteins that co-immunoprecipitated with FLAG-p28 were identified using a LC-MS/MS instrument and Thermo Proteome Discoverer software (**Appendix, Table A1 and A2**). Mass spectrometry hits were considered significant hits when the protein had at least two

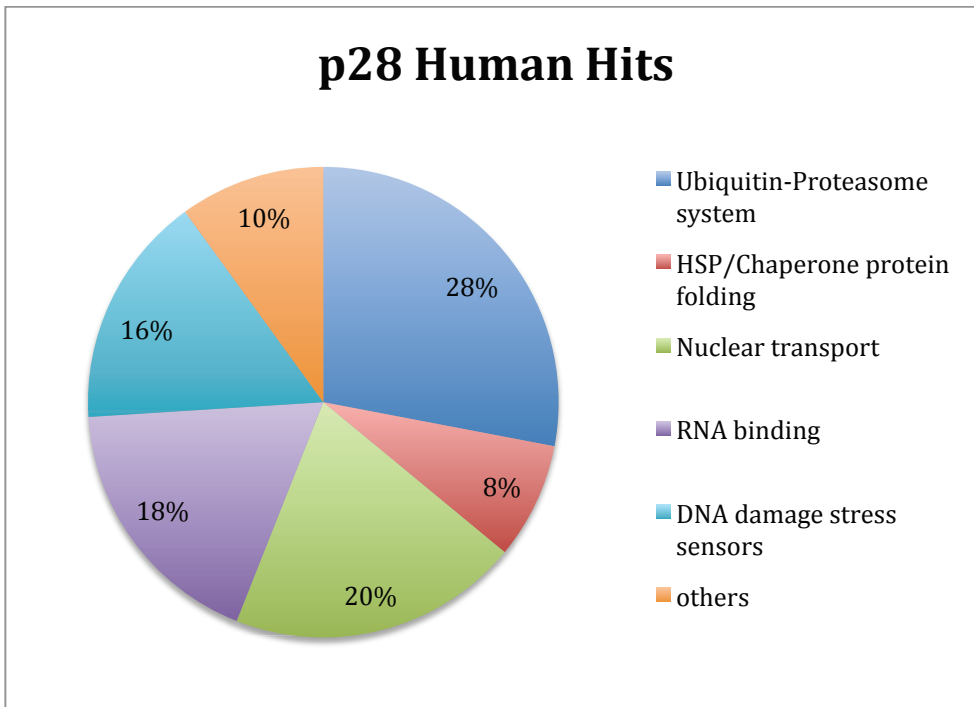
A



B



C



D

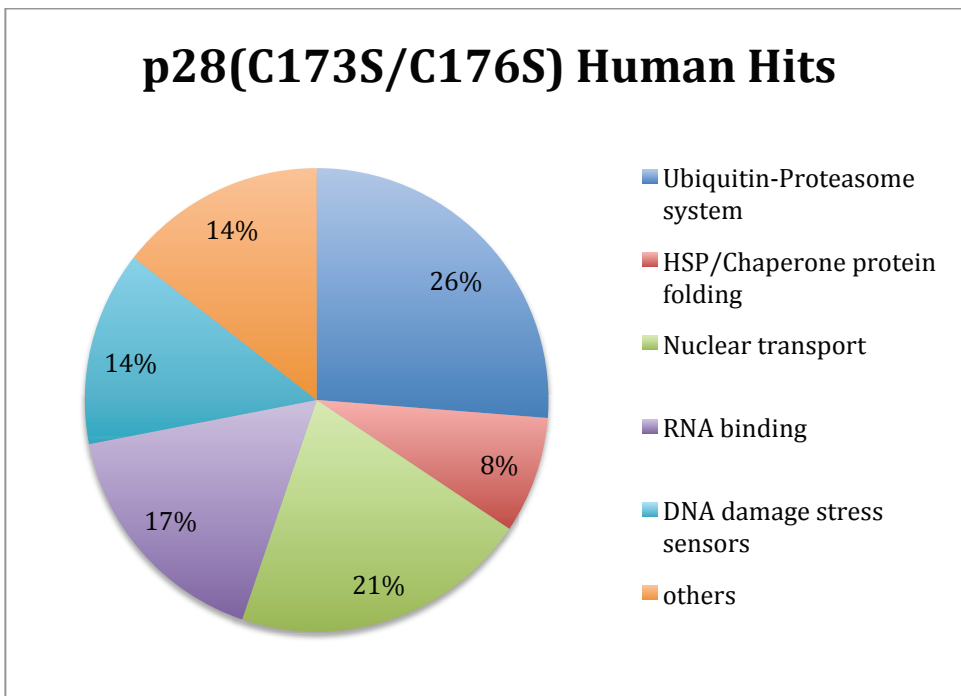


**Figure 5.2 Analysis of functional annotation clustering for p28 mass spectrometry hits.**

**(A)** Overlap of VACV Hits and **(B)** Human Hits in p28 and p28(C173S/C176S) samples. **(C)** DAVID Bioinformatics Resources 6.7 was used to analyze functional annotation clustering results from the mass spectrometry hits for p28 cellular interaction partners and **(D)** p28(C173S/C176S) cellular interaction partners. Amongst others, we found clustering of hits belonging to the ubiquitin-proteasome system, DNA damage and stress response pathways, HSP family, and components of the nuclear transport machinery.

peptides identified at a medium confidence according to the common Molecular and Cellular Proteomics (MCP) guidelines. We excluded mass spectrometry hits, found in the negative control of immunoprecipitates from lysates of HeLa cells infected with VACVCop. Interestingly, most of the proteins that were identified through co-immunoprecipitation with FLAG-p28 were also present in lysates co-immunoprecipitated with FLAG-p28(C173S/C176S) following poxvirus infection (**Figure 5.2**).

To extract biological features associated with the identified mass spectrometry protein hits, DAVID Bioinformatics Resources 6.7 (DAVID; National Institute of Allergy and Infectious Diseases [NIAID, NIH], <http://david.abcc.ncifcrf.gov>) was used for the analysis of functional annotation clustering (256). A number of the protein hits seemed to cluster into major cellular pathways, including the UPS, DNA damage and stress response pathways, the HSP family, as well as components of the nuclear transport machinery (**Figure 5.2**). Many of these proteins played an important role in the life cycles of other viruses, but have not been well documented during poxvirus infection (298-316). Several protein hits identified during the mass spectrometry screen were further characterized to confirm whether any interaction with p28 could be detected.

### **5.2.3 Verification of viral and cellular p28 mass spectrometry hits with co-immunoprecipitation studies**

To confirm mass spectrometry interaction partners and exclude false positive hits, we analyzed anti-FLAG immunoprecipitates from lysates of HeLa cells infected with VACVCop, VACVCop expressing FLAG-p28, or VACVCop expressing FLAG-

p28(C173S/C176S) by western blotting using antibodies specific for the identified p28 interaction partners. We included the VACVCop as a negative control and the FLAG-p28(C173S/C176S) control to keep samples consistent with the mass spectrometry experiment explained in section 5.2.1. WCL of HeLa cells infected with VACVCop expressing FLAG-p28 were also included to confirm that the interacting proteins were expressed in cells.

The viral proteins previously shown to interact with p28 in the mass spectrometry experiment were initially analyzed in these co-immunoprecipitation experiments using antibodies that recognize A34, A55, G1, I3, and E9 (**Figure 5.3.1; panel b-f**). A34 was detected in both, p28 and p28(C173S/C176S) VACV Hits; A55 was only detected in p28 VACV Hits; G1 was detected in both, p28 and p28(C173S/C176S) VACV Hits; I3 and E9 were detected in both, p28 and p28(C173S/C176S) VACV Hits. We were unable to detect A34, A55, G1, I3, or E9 in anti-FLAG-immunoprecipitates of cells expressing FLAG-p28 or FLAG-p28(C173S/C176S) even though FLAG-p28 was readily detected in these lysates (**Figure 5.3.1; panel a**). In addition, western blotting of WCL with anti-A34, anti-A55, anti-G1, anti-I3, and anti-E9 antibodies confirmed the expression and presence of these proteins in the lysates (**Figure 5.3.1 panel b-f**). These viral proteins, which failed to be detected in anti-FLAG immunoprecipitates, were excluded from our list of potential p28 hits for the next validation steps in the subsections below. The anti-FLAG western blot is representative of one immunoprecipitation and demonstrates that the anti-FLAG immunoprecipitations worked. This representative blot is also shown in Figure 5.3.2 and A.2.1.

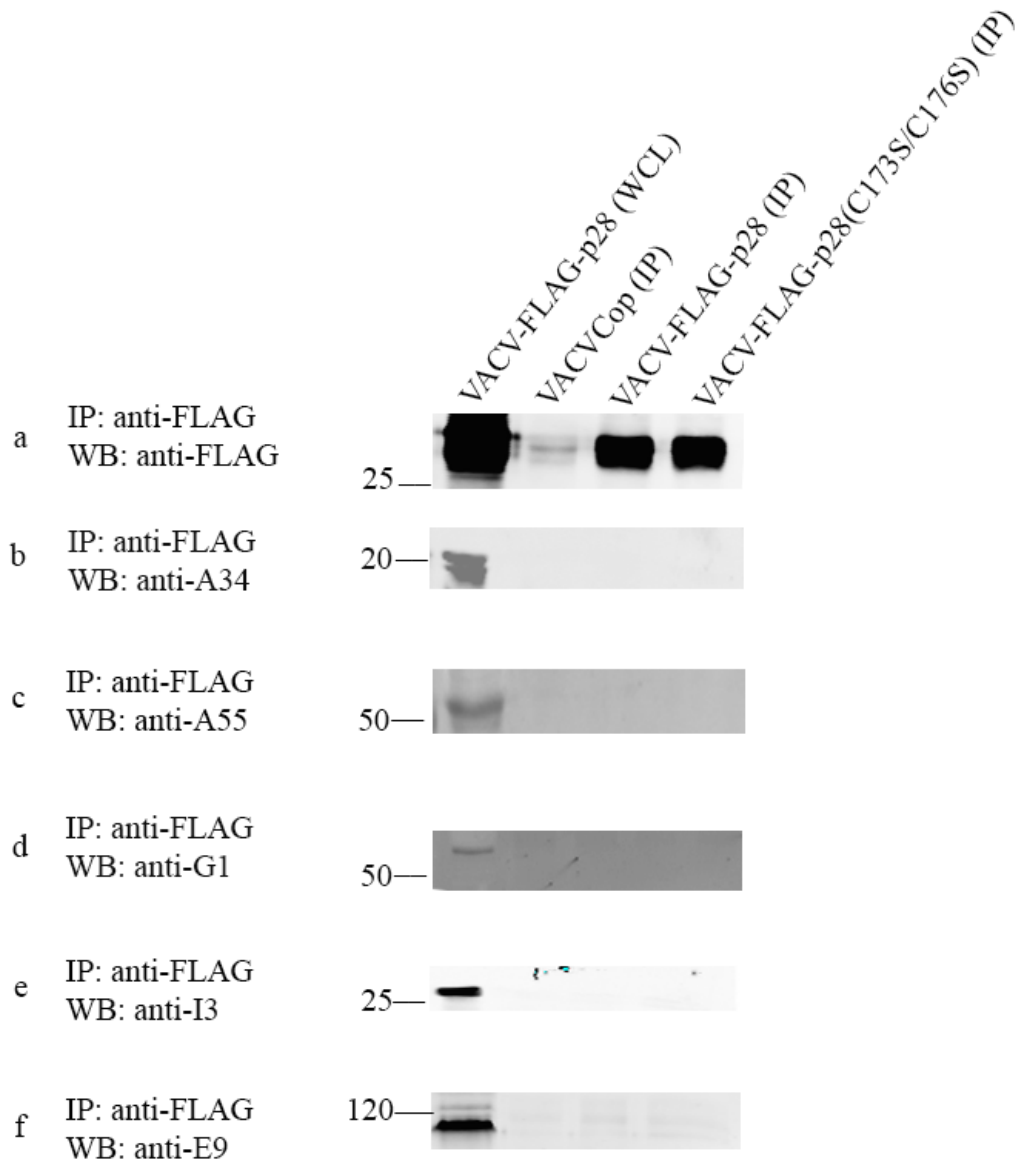


**Figure 5.3.1 Verification of viral and cellular p28 mass spectrometry hits with co-immunoprecipitation studies.**

HeLa cells were infected with VACVCop, VACV-FLAG-p28, or VACV-FLAG-p28(C173S/C176S) at an MOI of 5 and cells were treated with MG132 (20 $\mu$ M) for the last 4 hours of 16 hour infection. Cells were lysed in NP-40 lysis buffer and FLAG-p28, or FLAG-p28(C173S/C176S) were immunoprecipitated with mouse anti-FLAG M2 and western blotted with the indicated antibodies in panel a-f. Whole cell lysates (WCL). Note: All though some of these blots are from separate anti-FLAG IPs, we verified that the FLAG proteins were precipitated in all IPs. The anti-FLAG blot shown is representative from one IP. This representative blot is also shown in Figure 5.3.2 and A.2.1.

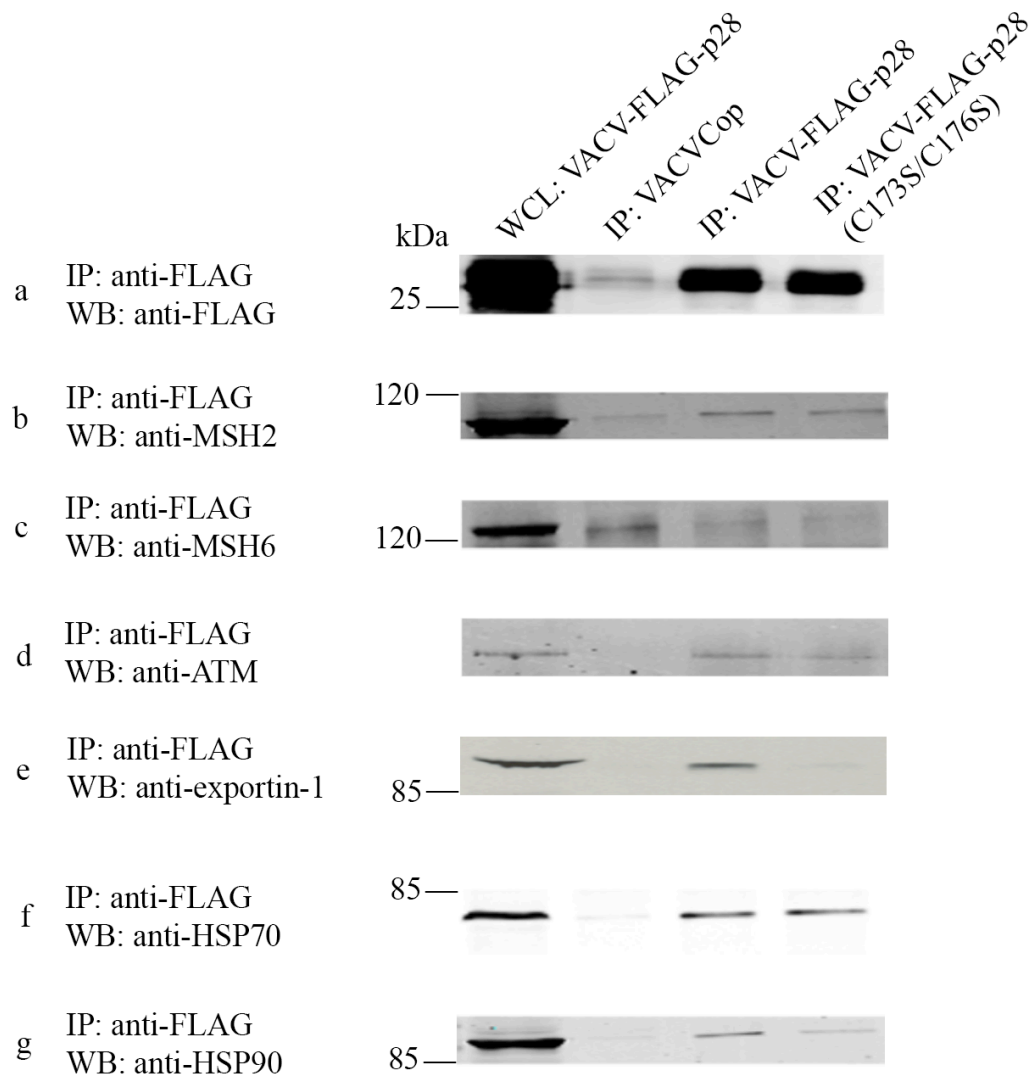


**Figure 5.3.2 Verification of cellular p28 mass spectrometry hits belonging to functional annotation clustering.**

HeLa cells were infected with VACVCop, VACV-FLAG-p28, or VACV-FLAG-p28(C173S/C176S) at an MOI of 5 and cells were treated with MG132 (20 $\mu$ M) for the last 4 hours of 16 hour infection. Cells were lysed in NP-40 lysis buffer and FLAG-p28, or FLAG-p28(C173S/C176S) were immunoprecipitated with mouse anti-FLAG M2 and immunoblotted with the indicated antibodies in panel a-g. Whole cell lysate (WCL). Note: All though some of these blots are from separate anti-FLAG IPs, we verified that the FLAG proteins were precipitated in all IPs. The anti-FLAG blot shown is representative from one IP. This representative blot is also shown in Figure 5.3.1 and A.2.1.

We further tested cellular hits from the functional cluster of DNA damage and stress sensor proteins (MSH2, MSH6, and ATM, which were all present in both, p28 and p28(C173S/C176S) immunoprecipitations) (**Figure 5.3.2; panel b-d**), components of the nuclear transport machinery (exportin-1, which was present in both, p28 and p28(C173S/C176S) immunoprecipitations) (**Figure 5.3.2; panel e**), and heat shock proteins (HSP70 and HSP90, which were both present in p28 and p28(C173S/C176S) Human Hits) (**Figure 5.3.2; panel f and g**) with specific antibodies. Western blotting with anti-MSH2, anti-MSH6, anti-ATM, anti-HSP70, and anti-HSP90 antibodies demonstrated that these proteins were present in anti-FLAG immunoprecipitates from lysates of both FLAG-p28 as well as FLAG-p28(C173S/C176S)-expressing cells (**Figure 5.3.2; panel b-d, f, and g**). We could consistently detect a background band in the anti-FLAG immunoprecipitates from lysates from HeLa cells infected with VACVCop, and VACVCop expressing FLAG-p28 and FLAG-p28(C173S/C176S) for MSH6 (**Figure 5.3.2; panel c**). We excluded MSH6 from further validation steps and focus on the hits, which were positive in our immunoprecipitation studies. Furthermore, we could detect an interaction between FLAG-p28 and exportin-1 in our western blots. However, we could only detect a weak interaction between the double cysteine mutant FLAG-p28(C173S/C176S) and exportin-1 (**Figure 5.3.2; panel e**). Our results were consistent in three independent experiments.

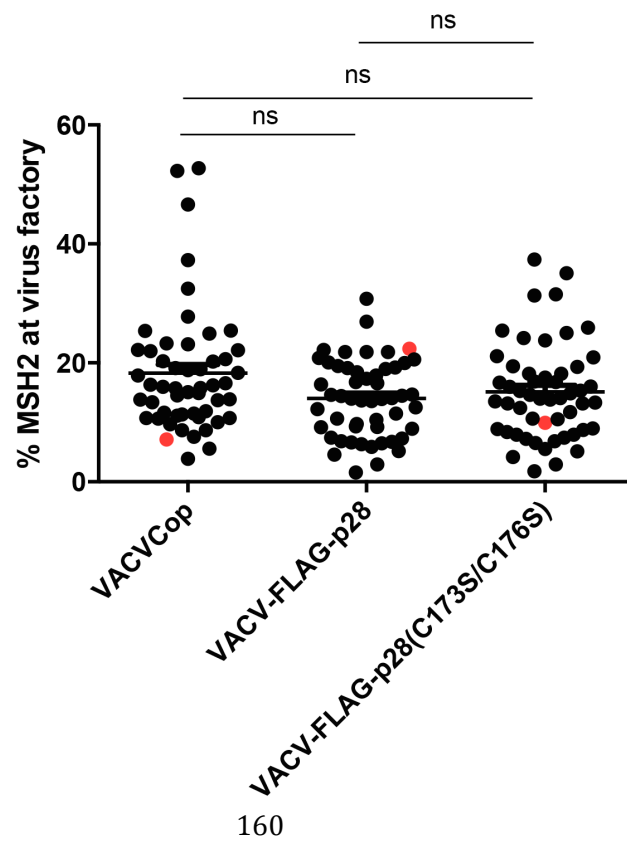
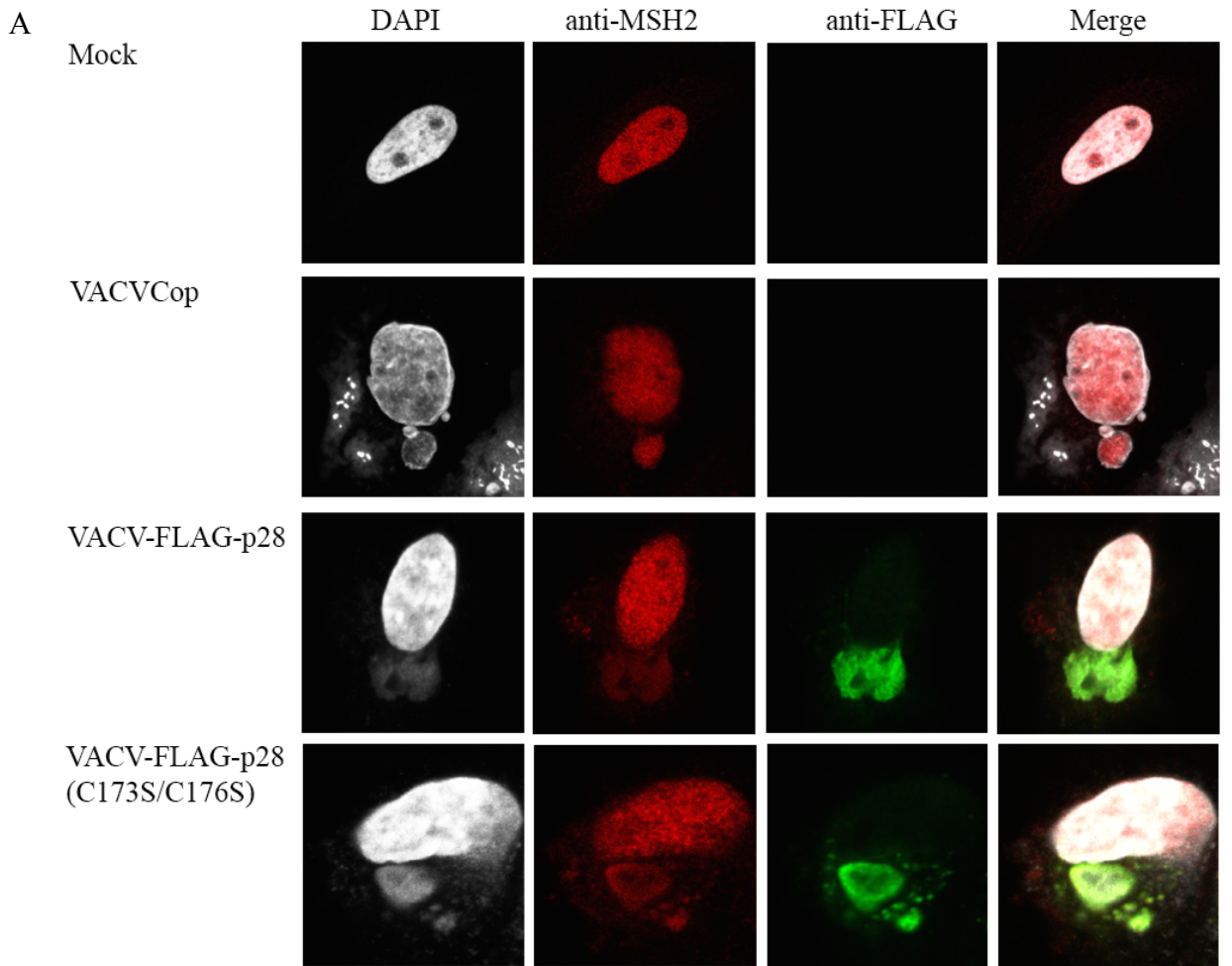
In summary, we selected poxviral proteins and prominent cellular hits from the functional annotation clustering of DNA mismatch repair proteins, nuclear transport and HSPs for further validation. Our co-immunoprecipitation data indicated a protein-protein interaction between the HSP70 and HSP90 chaperone proteins, the MSH2 and ATM

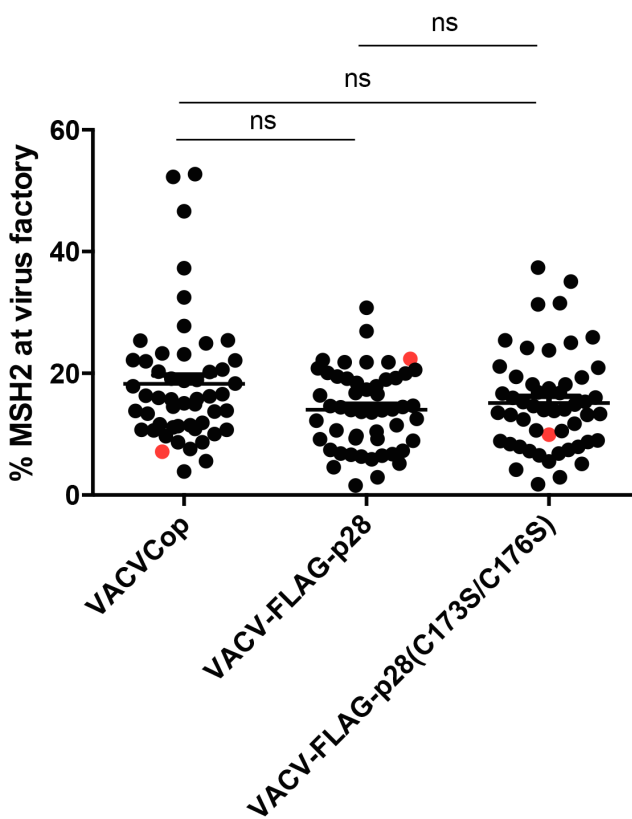
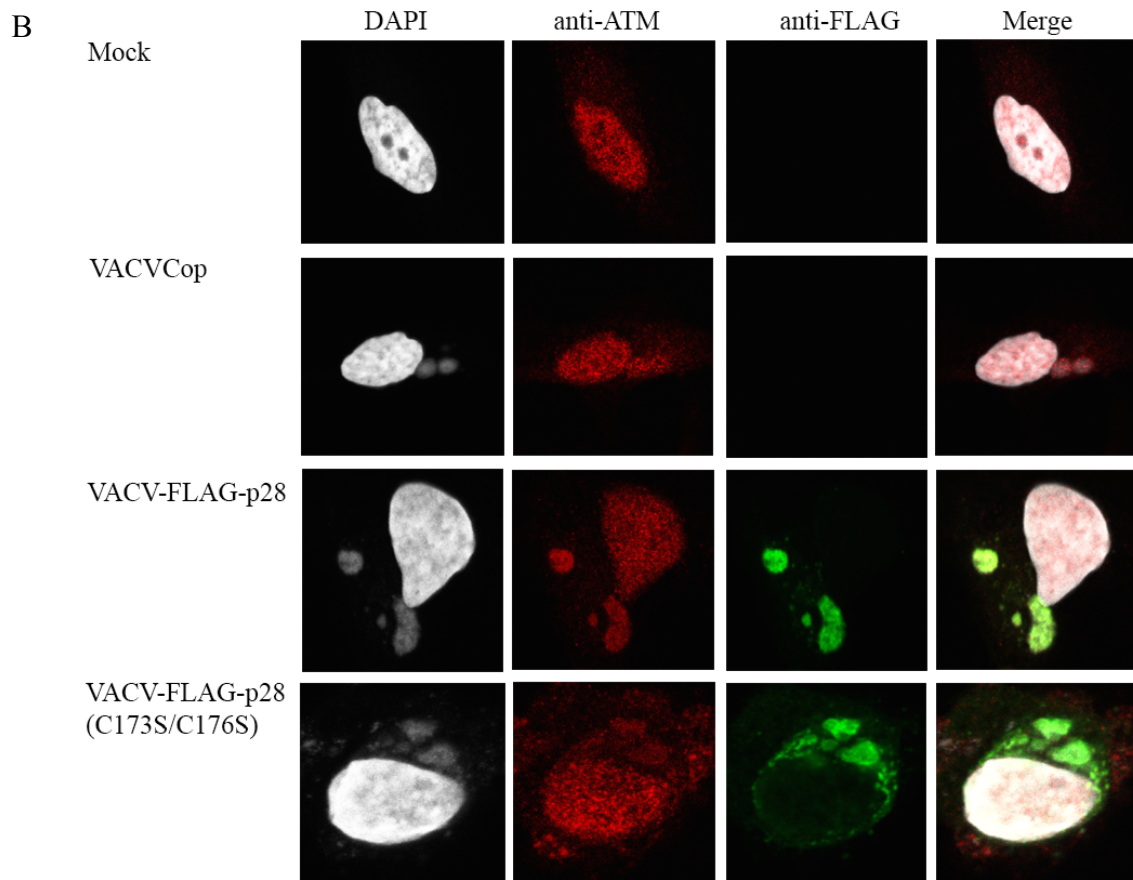
DNA repair proteins, and exportin-1 from the nuclear transport cluster with FLAG-p28. None of the tested poxviral proteins were detected in immunoprecipitates from the lysates of VACV-FLAG-p28-infected cells, suggesting that our mass spectrometry approach comes with a high false positive rate and that further validation steps are required.

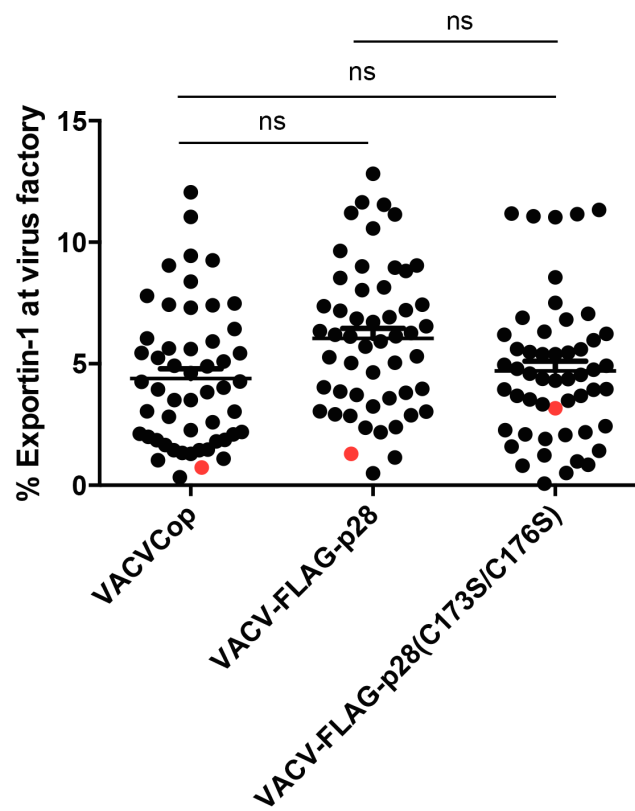
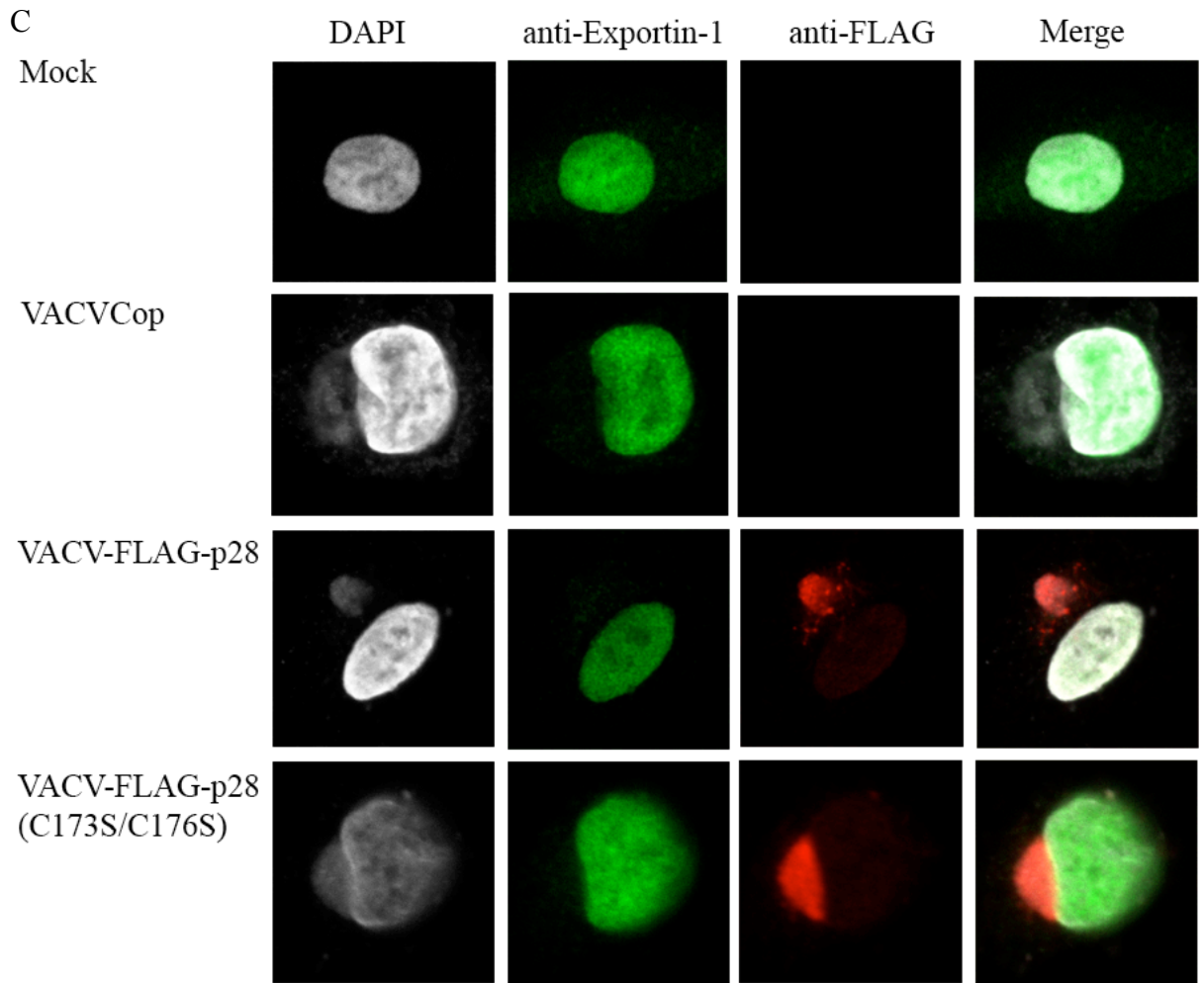
In the subsections below, I further investigated the subcellular localization of the confirmed co-immunoprecipitation hits during VACVCop infection and whether it is altered in the presence of VACVCop infected cells expressing FLAG-p28 or FLAG-p28(C173S/C176S).

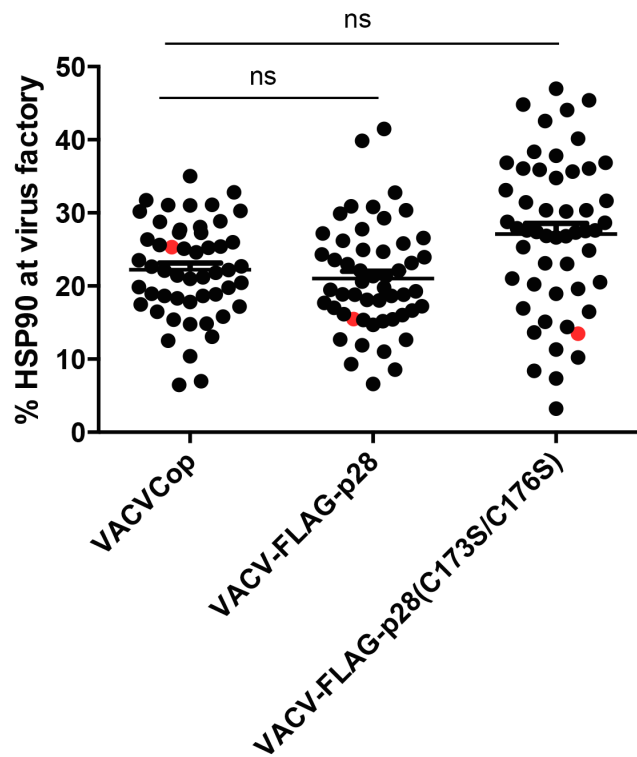
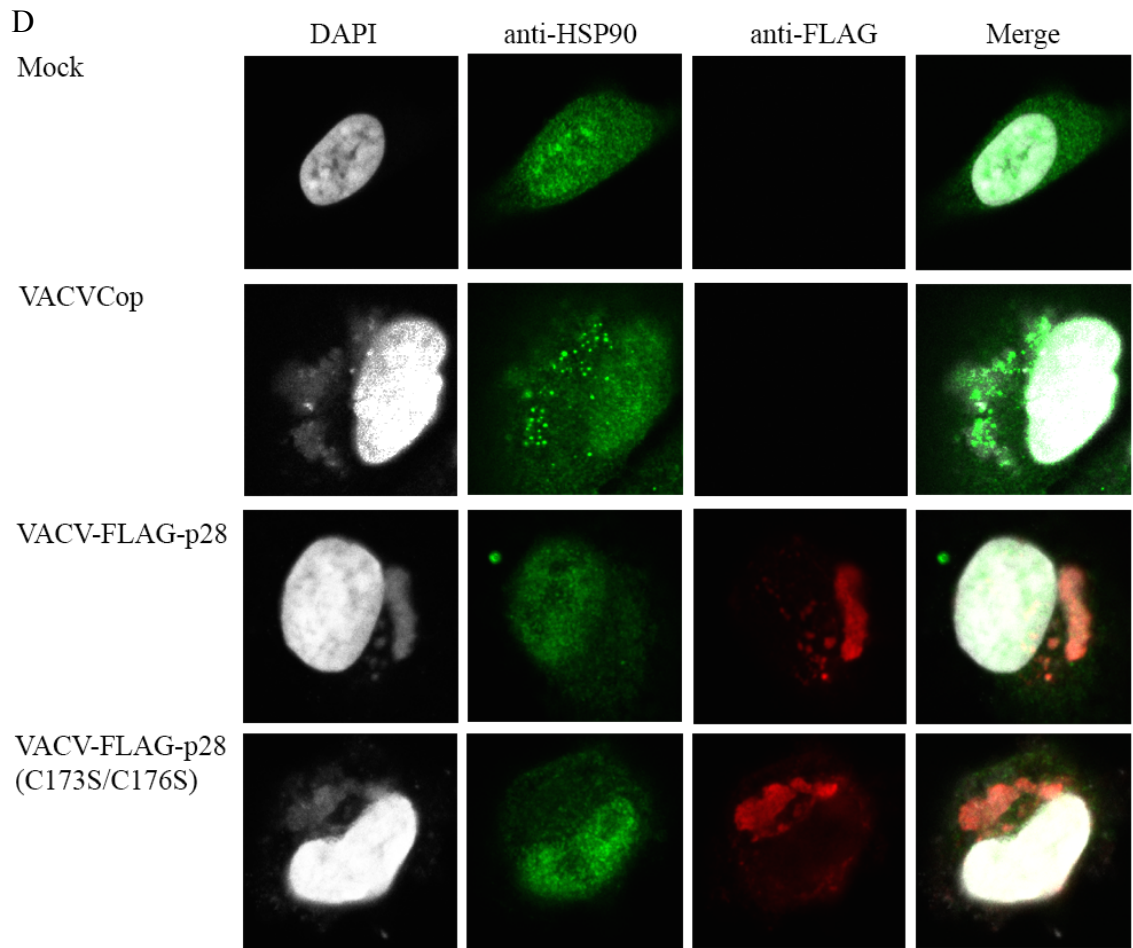
#### **5.2.4 Confocal studies reveal that p28 leads to the enrichment of HSP70 at virus factories**

This group of experiments was designed to investigate whether and how p28 affected the cellular localization of the mass spectrometry hits, which were positive in co-immunoprecipitation studies in **section 5.2.3.2**. We compared the localization and the amount of MSH2, ATM, exportin-1, HSP70, and HSP90 at the virus factory where p28 resides. HeLa cells were infected with VACVCop, VACV-FLAG-p28, or VACV-FLAG-p28(C173S/C176S) at an MOI of 5 for 14 hours. Cells were fixed in 4% PFA and stained for anti-FLAG, anti-MSH2, anti-ATM, anti-exportin-1, anti-HSP70, anti-HSP90, and DAPI and were evaluated with confocal analysis (**Figure 5.4.1**). We analyzed 60 cells from three independent experiments per sample and measured the raw fluorescence integrated densities of ROI at the virus factory and ROI of the entire cell. This allowed for calculation of the percentage of the substrate that is localized to the virus factory in









E

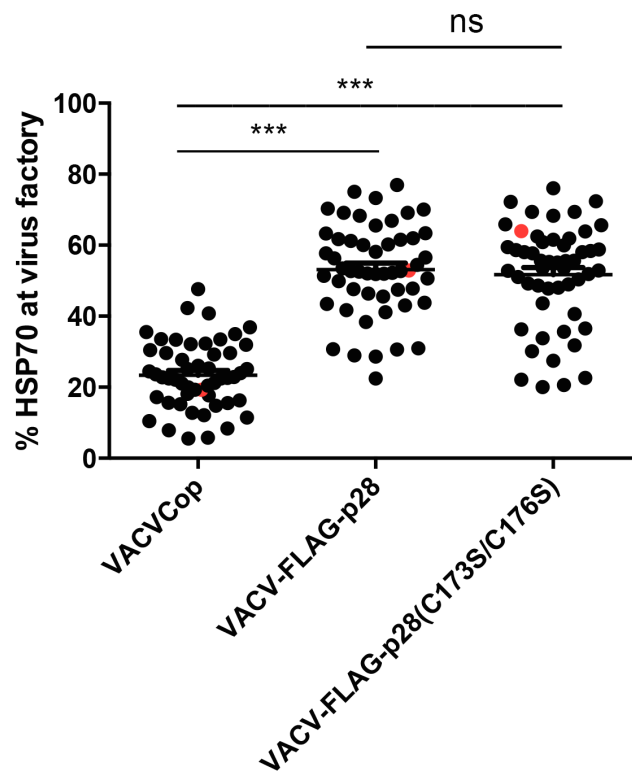
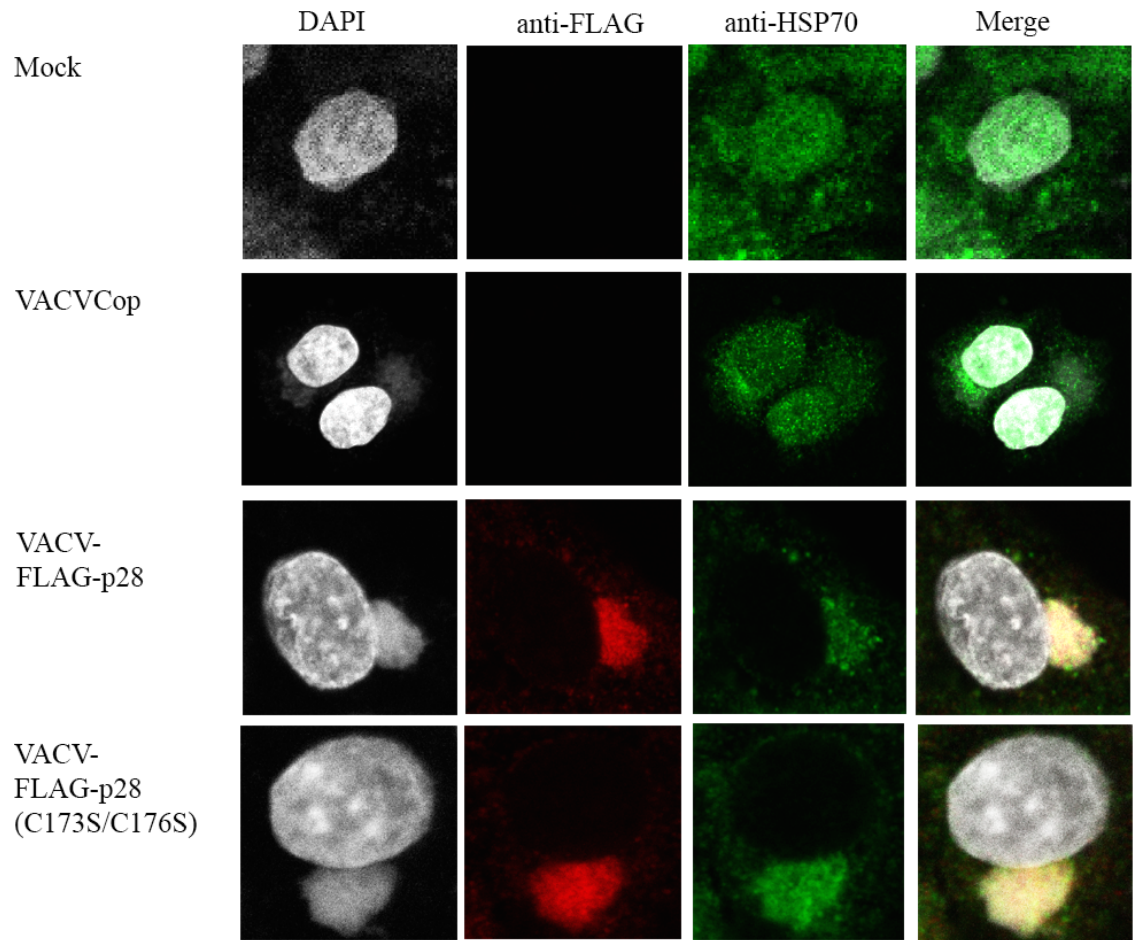


**Figure 5.4.1 p28 does not affect the cellular localization of MSH2, ATM, Exportin-1, and HSP90, but leads to enrichment of HSP70 at the virus factory.**

HeLa cells were infected with VACVCop, VACV-FLAG-p28, or VACV-FLAG-p28(C17S/C176S) at an MOI of 5 for 14 hours. Cells were fixed in 4% PFA stained for mouse anti-FLAG, DAPI, and (A) anti-MSH2, (B) anti-ATM, or (C) anti-Exportin-1, (D) anti-HSP90, and (E) anti-HSP70 and analyzed with confocal analysis and Fiji/Prism for statistical analysis. . One-way Analysis of variance (ANOVA) tests with Tukey post-hoc column comparison were used to compare calculate statistical significance. \*\*\*  $p < 0.001$  was considered statistically significant. Non significant (ns). The dots, which correspond to the cells in the panels, are marked in red. VACVCop dot corresponds to the right cell in the picture.

the presence or absence of functional p28. Both MSH2 and ATM, from the cluster of DNA damage sensors, and exportin-1, from the nuclear traffic cluster, were localized exclusively in the nucleus in mock infected cells (**Figure 5.4.1**). During VACVCop infection, an average of 17% of MSH2 and 22% of ATM, but only 4% of exportin-1 was localized to the virus factory. The presence of p28 or p28(C173S/C176S) did not significantly change this cellular distribution (**Figure 5.4.1**). HSP90 was enriched to an average of approximately 20% at the virus factory, which did not alter in the presence of p28. Therefore, this excludes the possibility that p28 recruits MSH2, ATM, exportin-1, or HSP70 to the virus factory. We further investigated the subcellular localization of HSP70. HSP70 was found speckled throughout the cytoplasm and in the nucleus in mock-infected cells (**Figure 5.4.1**). During VACVCop infection, roughly 20% of cellular HSP70 was localized to the virus factory. Intriguingly, in the presence of FLAG-p28, the amount of cellular HSP70 co-localizing to the virus factory increased significantly to 50% (p-value<0.001(\*\*\*)) (**Figure 5.4.1**). A similar localization was observed for FLAG-p28(C173S/C176S) (p-value<0.001(\*\*\*) and there was no significant difference between the presence of p28 and p28(C173S/C176S), indicating that HSP70 localization to the virus factory is independent of p28 ubiquitin ligase activity. To test if HSP70 enrichment at the virus factory is not merely an artifact during overexpression of a synthetic FLAG-tagged protein, we investigated the distribution of FLAG-A50, a poxviral DNA ligase (**Figure 5.4.2**). The presence of FLAG-A50 did not alter the amount of HSP70 at the virus factory, compared to VACVCop infection, suggesting that the effect is due to the presence of p28. In summary, while there was no effect on the

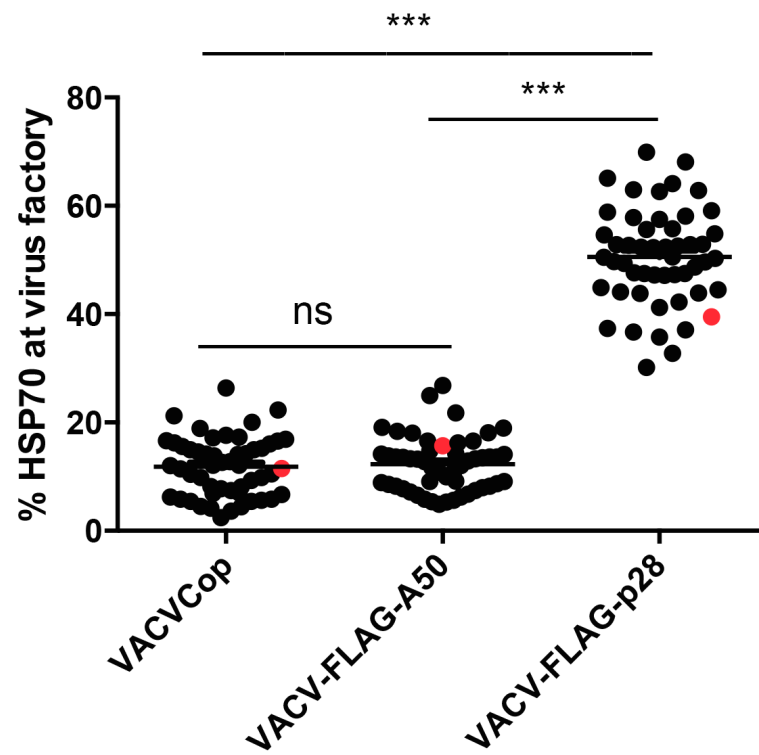
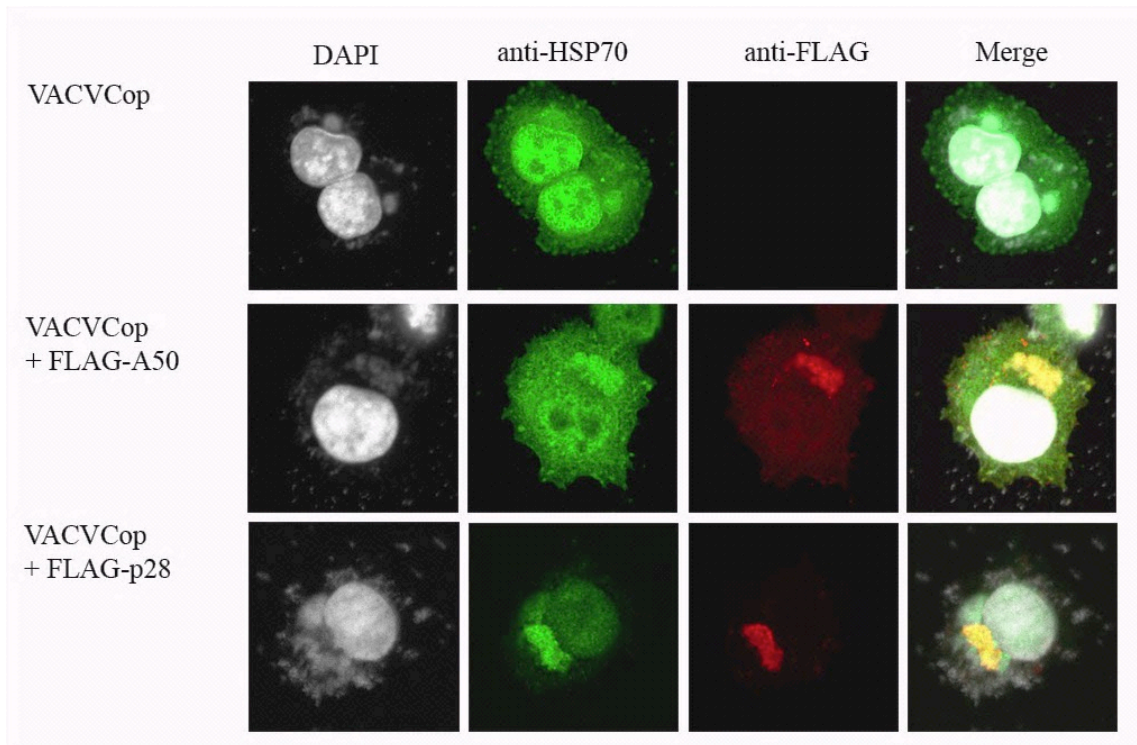


**Figure 5.4.2 HSP70 does not co-localize with FLAG control protein.**

HeLa cells were infected with VACVCop, VACVCop and transfected with pSC66-FLAG-A50 or VACVCop and transfected with pSC66-FLAG-p28 at an MOI of 5 for 14 hours. Cells were fixed in 4% PFA stained for mouse anti-FLAG, DAPI, and anti-HSP70 and analyzed with confocal analysis and Fiji/Prism for statistical analysis. One-way Analysis of variance (ANOVA) tests with Tukey post-hoc column comparison were used to compare calculate statistical significance. \*\*\*  $p < 0.001$  was considered statistically significant. The dots, which correspond to the cells in the panels, are marked in red. VACVCop dot corresponds to the right cell in the picture.

subcellular localization of MSH2, ATM, exportin-1 and HSP90, the presence of p28 did lead to the enrichment of HSP70 at the virus factory. For this reason, the following subsections focus on HSP70 only.

### **5.2.5 p28 does not promote the ubiquitination of HSP70**

This experiment followed up on the co-immunoprecipitation data from **section 5.2.3**. It investigated whether HSP70 was a substrate of p28, by determining its ubiquitination status in cells expressing p28. To do so, HeLa cells were infected with VACVCop or VACVCop expressing FLAG-p28 or FLAG-p28(C173S/C176S).

In addition, infected cells further expressed HA-tagged ubiquitin for the better detection of ubiquitination. Cells were also treated with proteasomal inhibitor MG132 to stabilize the ubiquitinated proteins (317). Cells were lysed in NP-40 lysis buffer containing 5mM NEM, an inhibitor of de-ubiquitinating enzymes (**Figure 5.5**). Immunoprecipitation was then performed with antibodies against endogenous HSP70 and western blotted with anti-HA to detect incorporation of HA-tagged ubiquitin. As a positive control for laddering, which is consistent with ubiquitin modification, we examined the ubiquitination laddering of FLAG-p28 (318). Western blotting of anti-FLAG immunoprecipitates from lysates of HeLa cells infected with VACVCop expressing FLAG-p28 demonstrated that we could immunoprecipitate p28 in our positive control and detect higher molecular weight laddering, which is typical for ubiquitination. We were also able to immunoprecipitate endogenous HSP70, but failed to detect higher molecular weight laddering in the presence of FLAG-p28 and MG132, which would have been an indication of substrate ubiquitination via p28. As a negative control, we

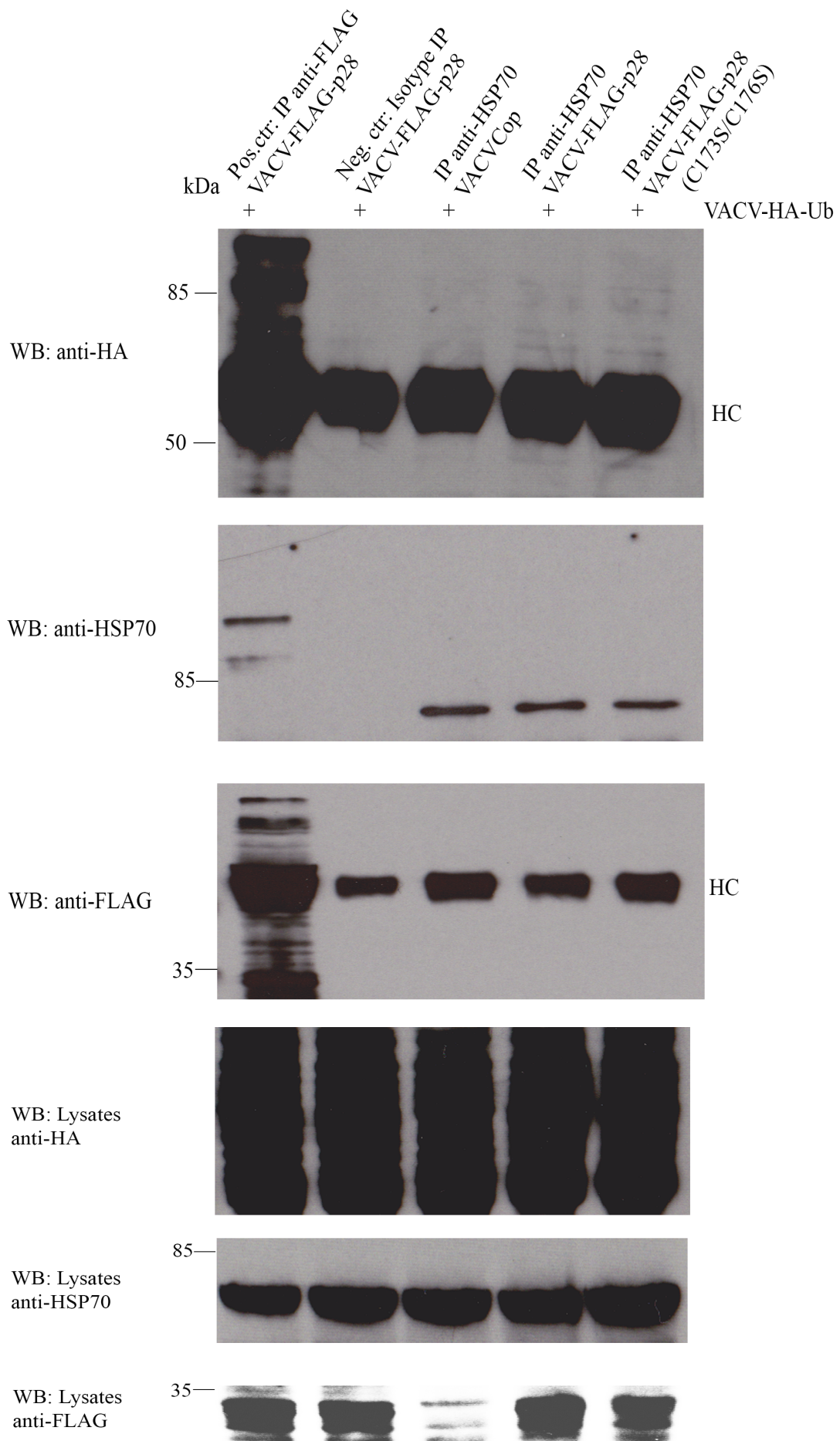


**Figure 5.5 p28 does not lead to the ubiquitination of HSP70.**

HeLa cells were infected with VACVcop, VACV-FLAG-p28, or VACV-FLAG-p28(C173S/C176S) and co-infected with VACV-HA-Ubiquitin at an MOI of 5 and cells were treated with MG132 for the last 4 hours of 16 hour infection. Cells were lysed in NP-40 lysis buffer containing 5mM NEM, an inhibitor of deubiquitinating enzymes. We performed immunoprecipitation for endogenous HSP70. As a positive control for laddering, we examined the ubiquitination associated laddering of FLAG-p28 and as a negative control we used isotype controls (anti-GFP). We stained western blots as stated above. Heavy chain (HC), light chain (LC), Whole cell lysates (WCL)

immunoprecipitated with an isotype control, where little to no ubiquitination smear or only background was expected. We saw a strong ubiquitination smear in our positive control staining anti-HA and little to none in both our negative control and HSP70 immunoprecipitated samples. Western blotting of WCL showed that HA-ubiquitin was expressed in all the samples. Furthermore, endogenous HSP70 was expressed in all the samples in a similar amount. Western blotting anti-FLAG in WCL also demonstrated the presence of FLAG-p28 and FLAG-p28(C173S/C176S) as indicated. We conducted these experiments three times with similar results. Taken together, we were not able to demonstrate that HSP70 is ubiquitinated in presence of p28 and that the enrichment of HSP70 is independent of the ubiquitin ligase activity of p28.

#### **5.2.6 p28 homologues in MYXV and FWPV show a trend to trigger enrichment of HSP70 at the virus factory**

In previous chapters, it was demonstrated that p28 homologues in MYXV (M143R) and in FWPV (FWPV150 and FWPV157) act as ubiquitin ligases and are localized to the virus factory. These homologues demonstrate a sequence identity to p28(IHDW) of 20% in MYXV homologues M143R, and 24% and 43% in the FWPV homologues, FWPV150 and FWPV157, respectively. This experiment was designed to investigate whether the effect of HSP70 enrichment at the virus factory is conserved in these homologues. We infected HeLa cells with VACVCop, VACV-FLAG-p28, VACV-FLAG-M143R, or transfected VACVCop infected cells with pSC66-FLAG-FWPV150, or pSC66-FLAG-FWPV157 at an MOI of 5 for 14 hours. Cells were fixed in 4% PFA and stained for anti-FLAG, anti-HSP70, and DAPI and were evaluated using confocal analysis (**Figure 5.6**).

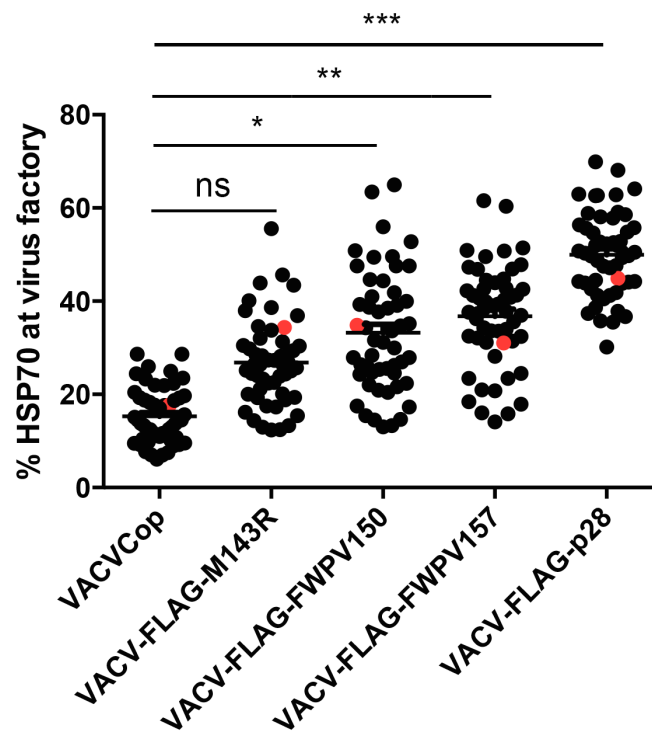
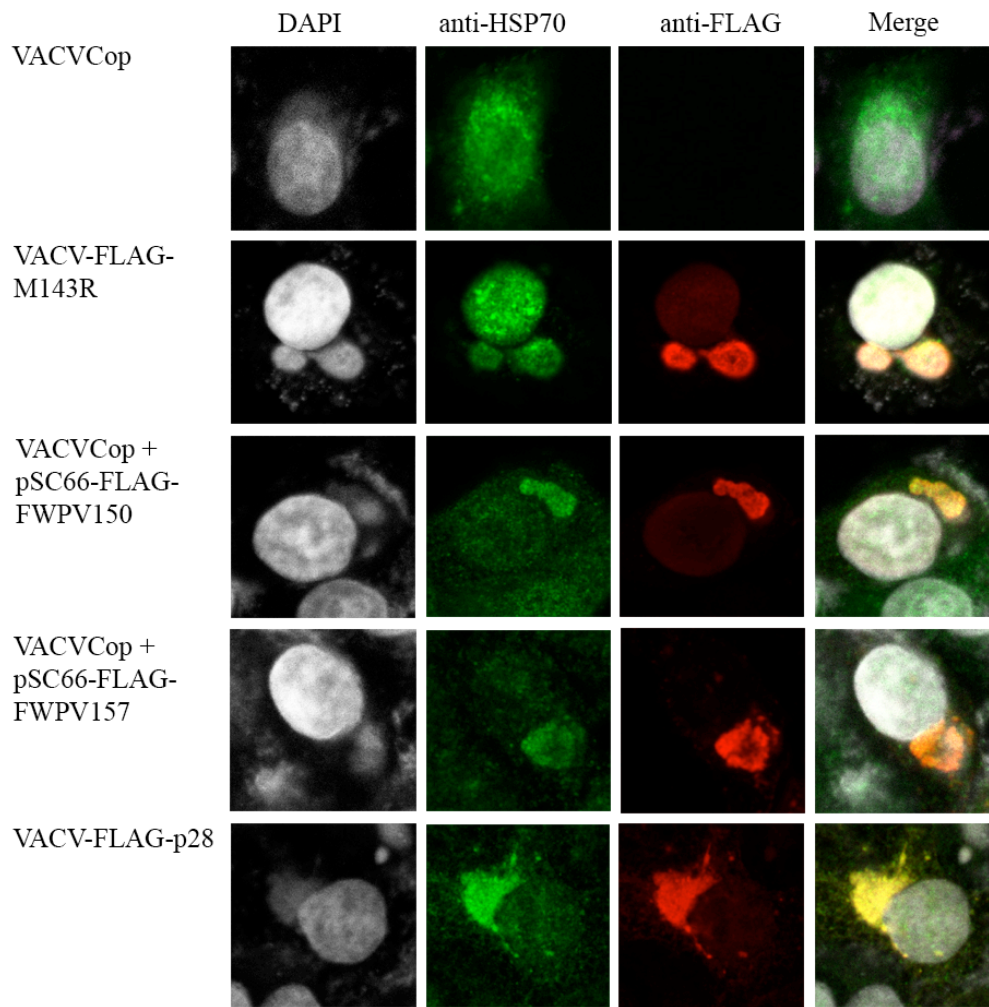


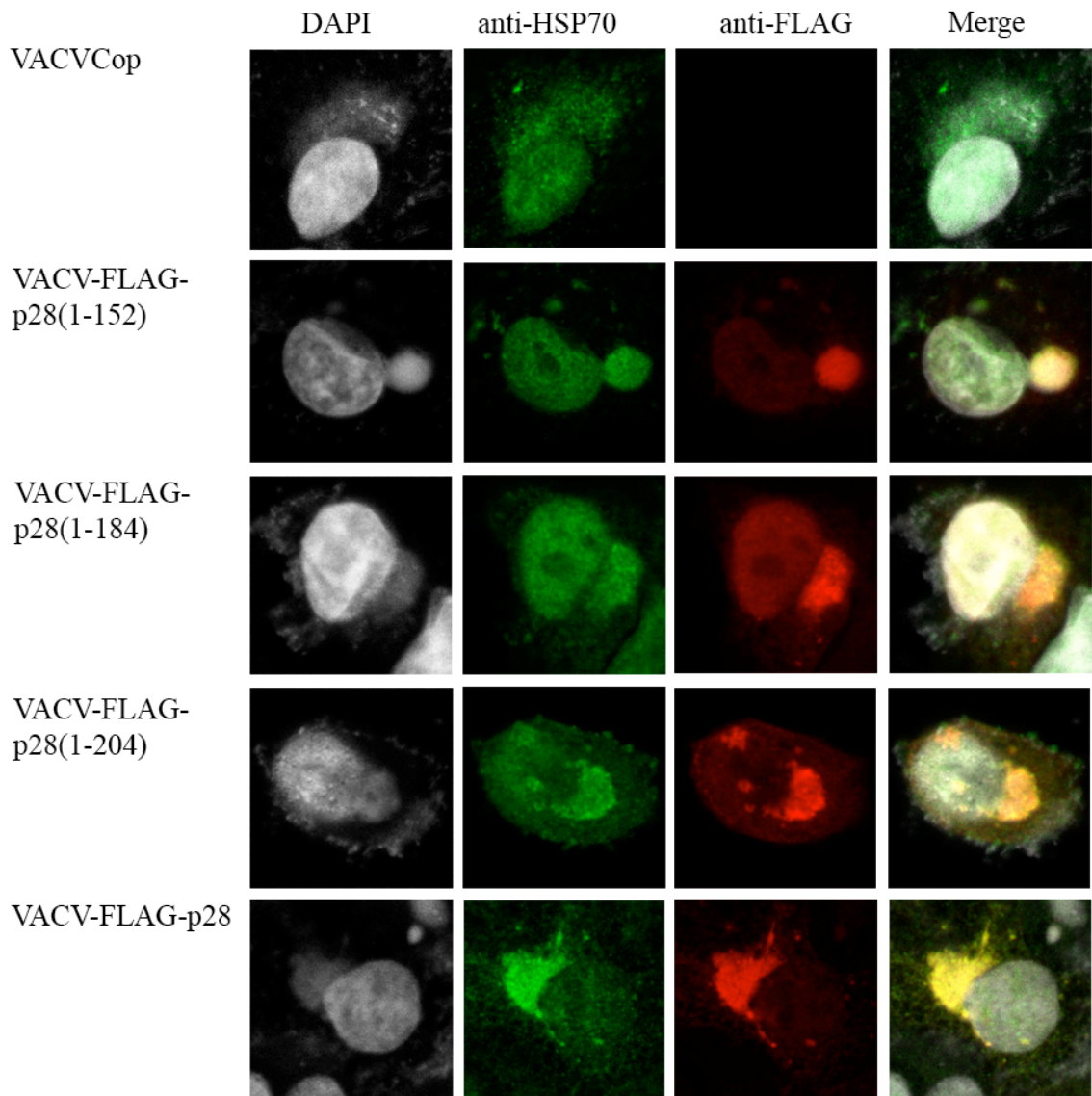
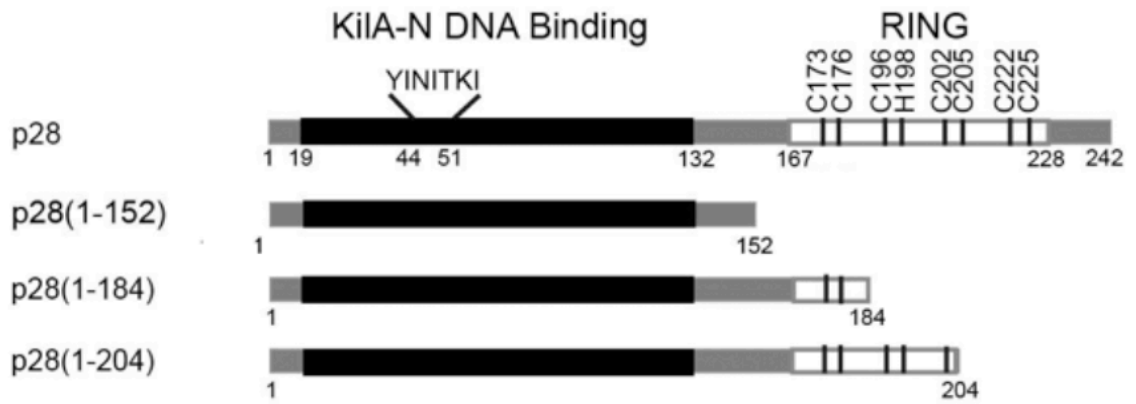
**Figure 5.6 p28 homologues in MYXV and FWPV show a trend to trigger enrichment of HSP70 at the virus factory.**

HeLa cells were infected with VACVCop, VACV-FLAG-M143R, VACV-FLAG-p28, or VACVCop infected cells were transfected with pSC66-FLAG-FWPV150, or pSC66-FLAG-FWPV157, at an MOI of 5 for 14 hours. Cells were fixed in 4% PFA stained for mouse anti-FLAG, DAPI, and anti-HSP70 and analyzed with confocal analysis and Fiji/Prism. One-way Analysis of variance (ANOVA) tests with Tukey post-hoc column comparison were used to compare calculate statistical significance.  $p < 0.05$  was considered significant and statistically significant results were reported as: \*  $p < 0.05$ , \*\* $p < 0.01$ , and \*\*\*  $p < 0.001$ . Actual p-values were: VACV vs M143:  $p < 0.1511$  (ns), VACV vs FWPV150:  $p < 0.0163$  (\*), VACV vs FWPV157:  $p < 0.0040$  (\*\*), and VACV vs p28:  $p < 0.0001$  (\*\*\*). The dots, which correspond to the cells in the panels, are marked in red. The experiments in Figure 5.6 and Figure 5.7 were conducted at the same time and the results were split into two Figures; therefore the same controls of VACVCop and VACV-FLAG-p28 appear in both Figures.

We observed a trend of HSP70 enrichment at the virus factory in all the homologues. Interestingly, the MYXV homologue seemed to trigger only enrichment of cytoplasmic HSP70 to the virus factory, while a strong nuclear staining of HSP70 was observed. In contrast, both FWPV homologues recruited both, nuclear and cytoplasmic HSP70 to the virus factory. From all tested homologues, FWPV157 demonstrated the highest HSP70 enrichment, though not to the same degree as p28. Overall, the effect of HSP70 enrichment at the virus factory was conserved across p28 homologues in both MYXV and FWPV. The experiments in Figure 5.6 and Figure 5.7 were conducted at the same time and the results were split into two Figures; therefore the same controls of VACVCop and VACV-FLAG-p28 appear in both Figures. In the next subsection, we will investigate, which part of p28 is important for the enrichment of HSP70 to the virus factories.

### **5.2.7 Residues 1-204 within p28 are necessary for recruiting HSP70 to the virus factory**

The previous subsection showed that the presence of p28 leads to the enrichment of HSP70 to the virus factory. Here, we investigated which part of p28 is crucial for the enrichment of HSP70 at the virus factories by utilizing p28 truncation mutants described in the previous chapter (318) including the KIL-A-N only p28(1-152), and truncations within the RING domain p28(1-184) and p28(1-204) (**Figure 5.7**). HeLa cells were infected with VACVCop, VACV-FLAG-p28(1-152), VACV-FLAG-p28(1-184), VACV-FLAG-p28(1-204), or VACV-FLAG-p28 (**Figure 5.7**) and the HSP70 localization was investigated as described above. p28(1-152) and p28(1-184) demonstrated only



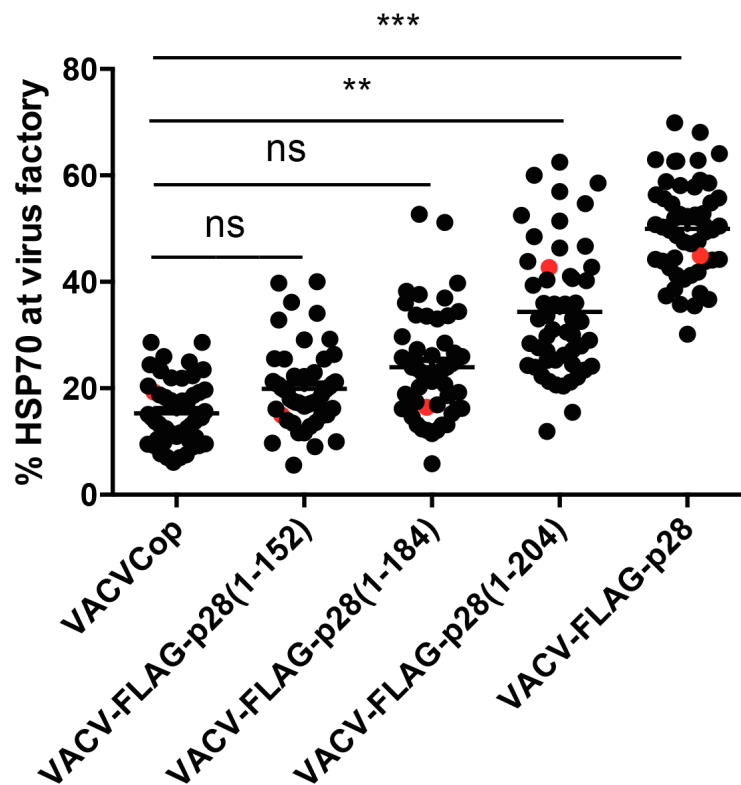


**Figure 5.7 Residues 1-204 within p28 are necessary for recruiting HSP70 to the virus factory.**

HeLa cells were infected with VACVCop, VACV-FLAG-p28(1-152), VACV-FLAG-p28(1-184), VACV-FLAG-p28(1-204), or VACV-FLAG-p28 at an MOI of 5 for 14 hours. Cells were fixed in 4% PFA stained for mouse anti-FLAG, DAPI, and anti-HSP70 and analyzed with confocal analysis and Fiji/Prism. One-way Analysis of variance (ANOVA) tests with Tukey post-hoc column comparison were used to compare calculate statistical significance.  $p < 0.05$  was considered significant and statistically significant results were reported as: \*  $p < 0.05$ , \*\*  $p < 0.01$ , and \*\*\*  $p < 0.001$ . Actual p-values were: VACV vs p28(1-152):  $p < 0.9986$  (ns); VACV vs p28(1-184):  $p < 0.8622$  (ns); VACV vs p28(1-204):  $p < 0.0052$  (\*\*); VACV vs p28:  $p < 0.0001$  (\*\*\*). The dots, which correspond to the cells in the panels, are marked in red. The experiments in Figure 5.6 and Figure 5.7 were conducted at the same time and the results were split into two Figures; therefore the same controls of VACVCop and VACV-FLAG-p28 appear in both Figures.

enrichment of cytoplasmic HSP70 to the virus factory, while there was still a strong nuclear HSP70 staining detected. In contrast, p28(1-204) showed a drastic enrichment of HSP70 at the virus factory, though not to the same degree as full length p28. Only p28(1-204) and full length p28 seem to have an effect of recruiting nuclear HSP70 to the virus factory. In summary, the residues 1-204 within p28 are necessary for recruiting HSP70 from the entire cellular pool to the virus factory.

### **5.3 Summary and Brief Discussion**

The goal of this study was to identify interaction partners or substrates of the poxviral encoded ubiquitin ligase p28. It was hypothesized that the host or viral proteins involved in VACV replication, viral morphogenesis, or viral sensing may be identified as potential interacting partners for p28. It is known that p28 is a virulence factor during ECTV infection, since ECTV( $\Delta$ p28) cannot replicate in macrophages, which are important for virus dissemination from skin lesions to lymph nodes and the liver (245). However, the substrates of p28, or how p28 is regulated is unknown. To this end, we applied FLAG-immunoprecipitation of FLAG-p28, and the FLAG-p28(C173S/C176S) mutant during VACV infection followed by Coomassie stain of SDS-PAGE gel and mass spectrometry analysis to identify potential substrates of p28 and attempt to shed light on how this viral protein may function as a virulence factor. As validation, we employed immunoprecipitation and western blotting with specific antibodies, which confirmed protein-protein interaction of potential hits with p28. Furthermore, we expected that potential interacting proteins would co-localize with p28 at the viral factories. We

demonstrated that co-immunoprecipitated proteins also accumulate within viral factories. However, only one hit, HSP70, demonstrated enrichment in the presence of p28 when compared with VACVCop infected cells alone. We followed up with ubiquitination studies and demonstrated that HSP70 is not a substrate of p28, but rather an interaction partner. The enrichment of HSP70 was conserved within p28 homologues and we pinpointed residues 184-204 within p28 as being important for recruiting HSP70 from the cellular nuclear and cytoplasmic pool to the virus factory.

There is an existing body of research, which highlights the important role of HSPs, including HSP70 and HSP90, during virus replication. For almost every step in viral replication, there is an example of how viruses hijack HSPs for their own purposes. HSP induction has been reported to propagate viral cell entry, uncoating, transcription and genome replication, virion morphogenesis, encapsidation, and virion release in numerous cases of viral infections (313-316, 319-331). In fact, it was recently reported that upregulation of HSPs enhances VACV replication and provides a mechanism for how VACV ensures sufficient levels of multiple chaperones (332). Further evidence that HSPs are beneficial for poxvirus infections is the fact that Crocodilepox virus and MCV encode their own version of HSP40 (333, 334). In addition, HSP70, HSP72 and HSP90 are packed into mature VACV virions to be readily available in the next round of infection (227, 335, 336). Interactions between HSPs and poxviral proteins were previously described: HSP90 interacts with A10L, while HSP27 binds to C2L and I4L (337, 338). However, the function of these interactions remains elusive. Our study contributes to this existing body of research by demonstrating that HSP70 is associated with p28 in co-immunoprecipitation studies. Furthermore, the presence of p28 enriches

HSP70 to the virus factory. This study demonstrates that HSP70 is not a substrate of p28, but rather an interacting partner. Future experiments will investigate if this p28 mediated HSP70 recruitment to the virus factory is crucial for VACV replication and if this is important for p28 to function as a virulence factor.

## **CHAPTER 6: DISCUSSION AND FUTURE DIRECTIONS**

## 6.1 Poxviruses modulate the UPS

Members of the poxvirus family encode a variety of proteins aimed at modulating the cellular UPS for their own advantage (233). These include p28, the membrane-bound ubiquitin ligase M153R, and adapter proteins that function in complexes with cellular ubiquitin ligases, such as BTB/kelch and F-box/ankyrin proteins (73, 74, 208, 235, 237). In addition, a functional UPS is essential for poxvirus infection at the level of uncoating and DNA replication (116, 117). The general shutdown of the UPS prevents VACV infection during early stages (116, 117). To date, the functions of most ubiquitin modulators remain unexplored. To this end, the present study sought to characterize the poxviral encoded ubiquitin ligase p28.

## 6.2 p28 homologues in FWPV

Many Chordopoxviruses described to date encode, or are predicted to encode, a p28 ubiquitin ligase homologue (**Table 1.2**). This is especially the case for “wildtype” strains, such as ECTV, CWPV, VARV, and MPXV. These strains cause severe disease for natural hosts (242). Within these strains, p28 homologues demonstrate a sequence conservation of up to 90%, with about 97% identity in the RING domain (242). In contrast, strains of VACV that have been repeatedly passaged in tissue culture (e.g. WR, Cop, Ankara, or MVA), have either inactivating mutations in, or lost their p28 gene (29, 238, 242). This suggests that while p28 may be important as a virulence factor *in vivo*, it is not necessary for efficient replication in tissue culture settings.

Only members of the *Avipoxvirus* family, encode two homologues to p28. In FWPV these are FWPV150 and FWPV157 (22). While these proteins show sequence divergence from other p28 homologs, they encode the critical KIL-A-N (YINITKI) and RING (C<sub>3</sub>HC<sub>4</sub>) domains found in functional ubiquitin ligases (Figure 3.2). These observations suggested that FWPV150 and FWPV157 may be functional ubiquitin ligases.

This study began by investigating whether both p28 homologues, FWPV150 and FWPV157, were produced during FWPV infection, if they were functional ubiquitin ligases, and how they interacted with ubiquitination. In Chapter 3 I demonstrated that FWPV150 and FWPV157 are indeed functional ubiquitin ligases, which are regulated by ubiquitination during infection. Interestingly, FWPV150 is expressed early on during infection and persists throughout infection, while FWPV157 is a late gene, as evident by AraC treatment and time course RT-PCR evaluation (**Figure 3.8**). The p28 homologue in ECTV is an early/intermediate gene, whereas the p28 protein is expressed as early as 2 hours post-infection and further accumulates throughout the infection cycle (245).

The biological relevance of FWPV expressing two p28 homologs, with different expression kinetics, is unknown. It would be interesting to examine if these proteins have different functions during infection or if a temporal switch occurs whereby FWPV157 takes over the function of FWPV150, or if both proteins can function late during infection. Unfortunately, no antibodies against FWPV150 or FWPV157 are available to examine their protein levels during infection. It is also possible that the single p28 version in the Chordopoxviruses have gathered and combined the substrate binding domains, which are present in FWPV150 and FWPV157, to act as a multifunctional

ubiquitin ligase. The evolutionary more divergent FWPV might still have two distinct proteins, FWPV150 and FWPV157, whose functions combine in the *Orthopoxvirus* versions of p28. Future experiments could include gene knockouts of p28 homologues in FWPV and will address if this affects FWPV replication *in vitro*. We should further investigate what happens when we switch the FWPV150 and FWPV157 promoters from early to late and vice versa in terms of virus replication and spread. This will show whether the temporal expression pattern is important, or if it is instead the case that FWPV150 and FWPV157 are interchangeable. Based on the effect of the p28 homologues in ECTV, it is possible that the absence of p28 homologues in FWPV will not affect viral growth *in vitro*. We will have to establish an animal model to evaluate the role of FWPV150 and FWPV157 *in vivo*. Infection models for FWPV have been rare and mostly focused on the evaluation of FWPV used as a vaccination vector (27, 260, 339). Less work has been published on models to evaluate virulence factors in FWPV during infection in a natural host, such as chicken and chicken embryos (chorioallantoic membrane (CAM)) (260, 340, 341).

An animal model has been established by the Buller group to evaluate ECTV infection lacking p28 (ECTV $\Delta$ p28), which produces an attenuated infection in mice compared to wildtype ECTV (244). Alternatively we could attempt to complement a p28-deficient strain of ECTV with combinations of FWPV150 and/or FWPV157. Recombinant ECTVs expressing these FWPV genes could then be tested for virulence in mice. This will indicate whether p28 in ECTV has combined the functions of FWPV150 and FWPV157. This is given, that the substrates of FWPV150 and FWPV157 in birds are similar enough to the homologues in mice to allow them to be recognized. Furthermore, it

is not to rule out, that FWPV150 and FWPV157 have functions, which dictate host tropism in birds. In this case, no rescue effect would be seen for ECTV $\Delta$ p28-FWPV150-FWPV157 infection in mice compared to ECTV infection. Another pitfall in this experimental setup is that the FWPV homologues might need another FWPV protein to function, which might be lacking in the ECTV infection in mice.

### **6.3 Speculations on the origin of the p28 gene**

It has been suggested that poxviruses may have gained some viral genes by incorporating cellular genes via recombination events (342-347). Nicholls and Gray found that p28 shares some homology to members of the cellular Makorin proteins (348). Makorin has been reported to induce degradation of West Nile Virus capsid proteins (349) and has been thought to regulate the functions of cellular RNA polymerase II-dependent transcription (350). Makorin and p28 show homology within the RING domain (351). However, the rest of the sequence varies considerably in amino acid composition. It is possible that p28 in poxviruses was derived by virus incorporation of Makorin cDNA during infection and recombination events.

Unlike other poxvirus p28 homologs, which show only similarity to Makorin RING domains, *Avipoxvirus* p28 homologues in FWPV and CNPV contain additional regions which show similarity to extra Makorin motifs, including a third zinc finger domain (348). This further suggests a connection between cellular Makorin and p28. Furthermore, Avipoxviruses FWPV and CNPV contain multiple copies of the Kila-N domain, but only two of these ORFs in each virus combine the Kila-N with a C-terminal RING domain. This could mean that p28 was acquired in the *Avipoxvirus* clade as a

fusion event between a KIL1-N domain and a RING domain, potentially from a Makorin-like protein.

#### **6.4 Regulation of p28**

While much is known about how ubiquitin ligases ubiquitinate other proteins leading to their degradation by the 26S proteasome (142, 144, 145), less is known about how ubiquitin ligases themselves are regulated. It is known that some ubiquitin ligases can be ubiquitinated by other ligases or can catalyze self-ubiquitination in a process known as autoubiquitination. (171). In Chapter 4, evidence was presented in form of flow cytometry data, where p28 and the p28 double cysteine mutant were both stabilized in presence of MG132 proteasomal inhibitor (**Figure 4.8**). These results indicated that mutation within the RING domain results in increased stabilization of the p28 mutant proteins, suggesting that wild type p28 uses its RING domain to regulate itself by autoubiquitination. However, since the RING mutants demonstrated an increase in stabilization that suggests that p28 may be potentially regulated by a combination of autoubiquitination via another ubiquitin ligase (**Figure 4.8**). The identity of the exogenous ubiquitin ligase is yet to be explored. Furthermore, it is not clear whether the autoubiquitination reaction is intermolecular or intramolecular.

Intermolecular self-ubiquitination requires the formation of dimers, which has been described for a number of ubiquitin ligases including E6-AP, seven in absentia 1 (SIAH1), and TRAF6 (352-354). Other ubiquitin ligases, including F-box protein Grr1p and HECT ligases Rsp5, WWP1, ITCH, SMURF2, NEDD4-1, and NEDD4-2 do not

form dimers and can autoubiquitinate themselves (355, 356). This process seems to be regulated by modifications, such as phosphorylation (357-359).

Autoubiquitination typically targets the ubiquitin ligase for degradation as a self-regulatory process within a negative feedback loop, which was demonstrated for CBL ligases (360), E6-AP (361), and Mdm2 (266, 362). Furthermore, autoubiquitination can happen in substrate dependent and independent ways, while the presence of the substrate can protect the ubiquitin ligase from autoubiquitination as part of the feedback loop (131, 171, 360, 363). In some instances, autoubiquitination does not lead to proteasomal degradation, but rather regulates the activity of the ubiquitin ligase or the recruitment of substrates (171).

Future studies should evaluate whether p28 autoubiquitination occurs intermolecularly or intramolecularly. By identifying whether p28 forms dimers one could gain information as to which method occurs. This could be done by a number of different methods including immunoprecipitation studies with two different tagged constructs of p28 (e.g. Myc and FLAG), solving the crystal structure of p28, which could also identify any potential interaction amino acids, or gel filtration analysis to identify any higher order molecular p28 complexes.

A scenario of dimerization would speak in favor of intermolecular autoubiquitination. In the case of monomeric p28, we will further evaluate the phosphorylation status and, in particular, whether conformational changes regulate p28 (357). This new knowledge will further contribute to our understanding of how the poxvirus encoded ubiquitin ligase and virulence factor is regulated.

## 6.5 Substrate identification of p28

### 6.5.1 Limitations of mass spectrometry approach in this thesis

Most substrates for poxviral proteins that manipulate the ubiquitin-proteasome system are unknown, with the exception of myxoma virus protein M153R (73, 74, 231). A preliminary 2D gel and mass spectrometry screen by a former graduate student in the Dr. Barry group identified a potential interaction of p28 with viral A6 protein, a virion core protein required for the formation of mature virion, but the group could not verify this interaction (253).

In Chapter 5, I report our efforts to identify interaction partners and substrates of p28. Following immunoprecipitation of p28 in virally-infected cells we performed mass-spectrometry on proteins that were co-immunoprecipitated. I am unable to comment on the false-negative rate of hits in this screen, since no previously known hits of p28 had been identified. It is noteworthy that A6 was also a hit in our screen, but we refrained from following up on this interaction due to a lack of easily obtainable reagents for A6. Our attempts to validate many of these putative hits were accompanied by a high false-positive rate.

We conducted our search for p28 substrates by identifying both viral and cellular proteins that co-immunoprecipitated with p28 using LC-MS/MS (**Figure 5.1**). This approach resulted in a high level of false positives. Given that p28 contains a DNA-binding domain, which localizes it to the virus factory, and many of these false hits also appear to localize to viral factories, it is possible that these false-positives were detected due to a DNA-mediated interaction. We tried a benzonase treatment step in the lysis buffer to remove the DNA in the virus factory. But despite this DNase treatment step, we

still co-immunoprecipitated the positive target proteins. Furthermore, we utilized the proteasomal inhibitor (MG132) for our experiments, since ubiquitinated proteins, including p28, are rapidly turned over by the 26S proteasome and this treatment stabilized p28 and the target proteins (**Chapter 4**). One downside of the MG132 treatment is the increase in the overall amount of ubiquitinated proteins in the cell. This could have increased the background of false positive hits.

A high level of 26S proteasomal subunits were found in the list of potential p28-interacting partners in our screen. Previous work by the Barry laboratory found that p28 expression results in the redistribution of the 26S proteasome to virus factories (364). It is possible that immunoprecipitation of p28 could pull down these proteasome subunits, which not only contain ubiquitinated p28, but also other cellular and viral proteins, contributing to the high false positive hits on our mass spectrometry screen. While leading to a high level of false positives this may have had the unintentional consequences of potentially identifying a list of viral proteins that are degraded by the 26S proteasome before the virion assembly occurs.

### **6.5.2 Alternative mass spectrometry approaches**

An alternative approach that could have been used to identify ubiquitinated substrates of p28 is stable isotope labeling of amino acids in cell culture (SILAC). SILAC was previously used to successfully identify substrates for cellular E3 ligases (365-367). In this approach two samples are prepared. In the first sample cells are grown in the presence of heavy amino acids ( $^{13}\text{C}$  labeling), while the second set is grown under normal conditions (unlabeled  $^{12}\text{C}$ ) (365-367). Samples are then mixed and compared using

quantitative mass spectrometry. In our future studies, heavily labelled cells could be infected with VACV-FLAG-p28(C173S/C176S) expressing only a non-functional p28, while the cells in normal media would be infected with VACV-FLAG-p28, expressing functional p28 ubiquitin ligase. Protein samples will be collected and compared using quantitative mass spectrometry, where the readout is expected contain higher amounts of <sup>13</sup>C labeled target proteins from the mutant sample and less of the unlabeled target protein from the wildtype p28 containing sample. This approach is well-suited for K48 ubiquitination, where substrates are degraded by the 26S proteasome.

Another method that could be used to identify p28 substrates makes use of a recent advance in the mass spectrometry field whereby antibodies specific for the remnants of ubiquitinated proteins (Lys-e-Gly-Gly (diGly)) are used (140, 292, 296, 368-371). In this approach cell lysates are trypsin digested and incubated with diGly-specific antibodies as affinity purification followed by mass spectrometry.

We could also combine SILAC and diGly affinity capture, which will further allow the comparison of enriched ubiquitinated proteins in the presence or absence of functional p28. This will not only allow identification of K48 ubiquitinated targets, which were degraded by the 26S proteasome, but also other non-proteolytic ubiquitination via K63 chains.

Another promising approach is to clone only the substrate-binding domain of a ubiquitin ligase to use as bait for immunoprecipitation and LC-MS/MS studies. This construct will still bind to the substrates, but without a ubiquitination reaction. This is a more stable interaction. Zhuang *et al.* developed an elegant method, the so-called Neddylator, where the substrate-binding domain is linked with a Neddylator reaction

(372). Since neddylation is more rare in cells compared to the overwhelming ubiquitination found throughout the cell, there would be less background when looking for neddylated substrates. Unfortunately, the substrate-binding domain of p28 is unknown to date and would be required for this approach to be successfully defined.

### **6.5.3 Choice of cell lines and virus**

A potential limitation of this study concerns the choice of cell line. This study mainly used HeLa cells. This was the cell line of choice at the time this project was initiated. For future experiments, we propose to investigate a cell type that is known to be more physiologically relevant. As mentioned above, the only recorded cell type, which demonstrated a different phenotype in the absence of p28 was murine resident peritoneal macrophages in the susceptible mouse strain A (though this was not the case for the resistant B6 mouse strain) (244, 245). In the future we could amend an animal protocol, and isolate primary peritoneal macrophages from susceptible (strain A), or resistant (strain B6) mouse strains, following the protocol established by the Buller group (245). Infection studies of these macrophages could allow us to draw a more relevant comparison between ECTV infections in the presence or absence of p28, for SILAC based mass spectrometry experiments. Follow up validation experiments would be more streamlined, since we would be able to evaluate which cellular factors and p28 interaction partners allow ECTV replication in susceptible macrophages.

#### 6.5.4 Validation of poxvirus proteins as substrates of p28

In our mass spectrometry validation experiments, we mostly focused on cellular substrates. For follow-up experiments on poxviral hits, we limited our validation to hits where antibodies were readily available (A55, A34, G1, I3, and E9). We initially speculated that p28 might be involved in poxvirus uncoating steps mediated by degradation of core proteins, transcription, replication or the production of early immunomodulatory proteins. This is based on the data from ECTV p28 knockout viruses and the sequence homology to Makorin (244, 245, 348). Senkevich *et al.* demonstrated the importance of the p28 homologue in ECTV for replication in murine resident peritoneal macrophages and dissemination to distant organs, such as the liver and the spleen (245). ECTV lacking a functional p28 gene (ECTV $\Delta$ p28) could not replicate in the aforementioned cells to the point where no virus factories were formed and no late genes were expressed (245). This phenotype was only observed in macrophages from the susceptible mouse A strain, but not in the resistant B6 mouse strain (244, 245). Furthermore, ECTV $\Delta$ p28 could successfully infect other cell lines isolated from the A strain. It is likely that in murine-resident peritoneal macrophages from strain A (which are a highly specialized non-dividing type of cell), p28 substitutes or activates an unknown cellular factor, which is required for virus replication. It is plausible that this factor is not readily available to the same levels in the susceptible A strain and the resistant B6 mouse strain.

Given the almost identical sequence identity to the p28 homologue in ECTV, we speculate that p28 in VACV has a similar function. VACV infection experiments in mouse resident peritoneal macrophages had different outcomes (373). It was mainly

reported that VACV-WR infection in mouse resident peritoneal macrophages led to the expression of early genes, partial uncoating and the activation of the virion-associated DNA-dependent RNA Polymerase (373). In the end, the virus did not fully uncoat, there was no virus replication and VACV-WR resulted in an aborted infection (373). VACV-WR infection in mouse macrophage J774 cells demonstrated virus replication, but not to the same degree as in other tested cell lines (373). We tested J774 and Raw264 mouse macrophage cell lines for VACVCop infection (Chapter 4), in the presence and absence of functional p28. In all cases, virus factories for virus replication were formed and p28 triggered the accumulation of conjugated ubiquitin to the virus factory. It is possible, that the function of p28 is required for the cell-type specific poxviral replication in primary peritoneal macrophages.

It would be interesting to investigate whether similar virus functions are impaired in VACVCop (which does not have p28) and ECTV( $\Delta$ p28) and whether the inability of these viruses to replicate in mouse resident peritoneal macrophages correlates with the absence of p28. Future studies will investigate the effect of VACV infection in the presence and absence of p28 in resident peritoneal mouse macrophages. We will investigate whether the presence of functional p28 can rescue the VACVCop replication. We will conduct growth curves in these macrophages to test for productive replication, investigate the formation of virus factories via microscopy, and test the expression levels of early and late genes.

Ubiquitin is incorporated into vaccinia virus virions and is readily accessible for the next round of infection (227). These data suggest that ubiquitination of specific proteins is important early during infection at a point prior to virion uncoating (227).

Furthermore, the expression of early genes is required for this uncoating step and a functional proteasome is required for a full poxvirus replication cycle (117, 374). We speculate that p28, which is expressed early during infection, might target viral core proteins for ubiquitination and degradation to promote viral uncoating. This is strengthened by observations that the cellular homologue of p28, Makorin-1, has been reported to ubiquitinate the West Nile virus capsid protein and target it for proteasome-mediated degradation (349). While Makorin-1 plays a protective role for the host cell in doing so, the function of p28 might be to ubiquitinate viral core proteins, uncoating and lead to productive virus infection.

Some of the major virion components are A10, A3, A4, L4, and F17, which collectively function to protect the dsDNA viral genome. (375, 376). Intriguingly, one major hit in our p28 mass spectrometry screen was the core protein A10. In future studies, we should evaluate the role of p28 on the ubiquitination and subsequent proteasomal degradation of A10. We will also explore whether p28 is involved in enhancing viral uncoating.

### **6.5.5 p28 interaction with HSP70**

Despite the above discussed high false-positive rate and limitation of our mass spectrometry approach, we verified HSP70 as an interaction partner of p28 during VACV infection. We could demonstrate that HSP70 and HSP90 are associated with p28 in co-immunoprecipitation studies (Chapter 5). Furthermore, the presence of p28 enriched HSP70 at the virus factory (**Figure 5.4.1 E**). In fact, HSP70 was the sole hit in our mass spectrometry validation, which demonstrated enrichment at the virus factory in the

presence of p28. While HSP70 interacted with p28 we found no evidence that this interaction resulted in the ubiquitination of HSP70, hence we could not verify HSP70 as a substrate of p28 (**Figure 5.5**). The p28-mediated accumulation of HSP70 at the virus factory was also seen in homologues of p28 (**Figure 5.6**). In the end, HSP70 proteins were validated as interaction partners of p28, but the biological significance of HSP70 enrichment at the virus factory remains elusive.

HSP families are named after their molecular mass, HSP40, HSP60, HSP70, HSP90, and HSP110 (377). The different families of HSP can facilitate protein trafficking, formation of complexes, and maintenance of protein conformation (377). Furthermore, some HSP families have the so-called HSP-mediated activity control, where HSPs can bind native proteins and alter their conformation and function (378). In general, HSPs are mostly known as stress response proteins, which include physiological stress, environmental stress, and infections by pathogens, including viruses (308, 379).

A number of DNA and RNA viruses have been reported to induce a HSP response. (308-312). Viruses hijack HSPs for their own purposes, including the propagation of viral cell entry, uncoating, transcription and genome replication, virion morphogenesis, encapsidation, and virion release in numerous cases of viral infections (313-316, 319, 320, 322-324, 326-328, 330, 331). HSP70 has previously been reported to associate with distinct viral proteins in the case of hepatitis C virus, porcine reproductive and respiratory syndrome virus, adenovirus and poliovirus (312, 331, 380-382).

It was recently shown that VACV-WR infection triggers heat shock factor 1 (HSF1) activation, the master transcriptional regulator of the HSP response. This may explain how VACV can ensure sufficient levels of multiple chaperones throughout

infection as the activation of HSF1 can lead to the induction of many HSP proteins (332). HSF1 appears to be important for VACV replication as siRNA-mediated silencing of HSF1 was reported to lower the rates of VACV-WR gene expression. In this context, VACV induces an increase in expression levels of HSP70 by 20-fold, while HSP90 and HSP60 levels were only increased by 3-fold (309, 383).

We observed an increase of HSP70 levels during VACVCop infection compared to uninfected cells; but the HSP70 levels did not differ between VACVCop, VACV-FLAG-p28, or VACV-FLAG-p28(C173S/C176S) infected cells. Interestingly, HSP70, HSP72 and HSP90 are also packed into mature poxvirus virions, which suggest the importance for chaperones in early stages of virus infection (227, 335, 336). Several poxviral proteins have been reported to interact or bind to HSPs during infection. Jindal *et al.* showed that HSP70 co-immunoprecipitated intracellular VACV proteins, which identities are still unknown (383). HSP90 interacts with A10, also known as VACV-WR core protein 4a, and co-localizes at the virus factory (337). Furthermore, several poxviral proteins are bound to HSP70/72 (383). HSP27 has been reported to bind to VACV proteins VACV-WR002, C2, and I4 in a yeast-two hybrid screen, but awaits confirmation (338). However, the function of these interactions remains elusive.

Our study contributes to this existing body of research by demonstrating that HSP70 and HSP90 are associated with p28 in co-immunoprecipitation studies and the presence of p28 homologues enrich HSP70 at the virus factory (**Figure 5.4.1 E, and 5.2.6**). It appeared that p28 and FWPV homologues were capable of triggering HSP70 from both the cytoplasm and the nucleus to the virus factory, whereas VACVCop infection alone and the M143R homologue in MYXV only seemed to have an effect on

cytoplasmic HSP70 enrichment at the virus factory (**Figure 5.6**). The effect of recruiting cytoplasmic and/or nuclear HSP70 remains elusive. Furthermore, the HSP70 family contains multiple homologues and isoforms. The most studied HSP70 members include the constitutively expressed cytosolic Hsc70 and the stress-induced HSP70 homologues (384-386). It is possible that we detected both Hsc70 and HSP70 due to their high sequence identity (>90%) and since many HSP70 antibodies are cross-reactive. The HSP70 isoform Hsc70 is constitutively expressed at elevated levels in the cytoplasm and is reported to be packed into mature virions during VACV-WR infection (227). We speculate that Hsc70 was also recruited to the virus factories during VACVCop infection. Interestingly, p28 mass spectrometry hits included both HSP70 members Hsc70 and HSPA1A. In contrast to Hsc70, which is readily available in the cytoplasm, HSPA1A is induced by HSF1 activation (387). Future studies should evaluate which HSP70 family members are packed into mature virions in the presence and absence of p28 and if there is a biological relevance to this.

While poxviruses appear to utilize different cellular chaperones at different stages throughout their lifecycle, some poxviruses encode their own HSF1-regulated genes which may lower their dependence on these host HSPs. MCV and Crocodilepox encode viral homologs of HSP40, which is lacking in all the other poxviruses (333, 334). Members of the HSP40 family typically regulate protein folding, assembly, and protein transport. HSP40 is a co-factor for HSP70, recognizing unfolded-proteins as well as chaperone proteins (388). It is possible that HSP70 works with HSP40 to help chaperone poxviral proteins at the virus factories. HSP40 was another hit in our p28 mass spectrometry screen, but we had no available antibody to follow up with HSP40. Since

VACVCop is lacking a HSP40 homologue, p28 might be also responsible for recruiting HSP40, together with HSP70 to the virus factories. Future studies will investigate the employment of HSP40 during VACV infection and interaction with p28. Other large DNA viruses also encode their own HSPs, including mimiviruses, which express HSP70 and HSP40 homologues (332, 389, 390). There seems to be a trend towards the large cytosolic DNA viruses utilizing large amounts of host cellular HSPs for chaperoning purposes.

It is unknown how poxviruses activate HSF1, resulting in the up-regulation of HSPs. HSF1 in its inactive form is kept in the cytoplasm by binding to HSP70 or HSP90 (391-393). VACV may activate HSF1 by recruiting HSPs to the virus factory, resulting in post-translational modification and nuclear translocation of free HSF1. So far, only HSP90 accumulation at the virus factories has been described (337). Here, we further showed HSP70 enrichment at the virus factory, which is significantly enhanced by the presence of p28. In future experiments we will investigate whether p28 affects HSP70 localization to the virus factory in order to permit HSF1 nuclear translocation and the subsequent upregulation of HSP gene transcription. Future experiments should also investigate if this p28 mediated HSP70 recruitment to the virus factory is crucial for VACV replication and if this is important for p28 to function as a virulence factor.

Interestingly, HSP70 can associate with the E3-ubiquitin ligase C-terminus of HSP70 Interacting Protein (CHIP) (394). CHIP assists in the decision-making, whether HSP70 is chaperoning the substrate proteins, or if it promotes the ubiquitination of HSP70 substrates leading to their proteasomal degradation (394, 395). In fact, CHIP interacts with the substrate-binding domain of HSP70 and negatively influences the

chaperone activity of HSP70. Furthermore, the ubiquitin ligase activity of CHIP can promote the degradation of proteins that were interaction partners of HSP70 (395-397). Future ubiquitination experiments could also explore whether CHIP is the unknown ubiquitin ligase, which mediates the ubiquitination of p28, and if this interaction is mediated through HSP70.

## **Conclusions**

This thesis characterized the poxviral encoded ubiquitin ligase p28 and homologues in FWPV. The large genomes of the prototypical members of *Avipoxvirus*, FWPV and CNPV, encode a number of yet uncharacterized proteins. We demonstrated that FWPV encodes two functional p28 homologues, which act as ubiquitin ligases. Interestingly, one is expressed early, while the other homologue is expressed only late during infection. An additional observation was that all Kila-N only and Kila-N-DUF genes were actively transcribed during FWPV infection. The function of the poxviral encoded Kila-N DNA binding domains seems to aid in the localization of the protein to the virus factories. The biological relevance of expressing two p28 homologs, which contain Kila-N a domain paired with a RING domain remains unknown. In contrast, non-Avipoxviruses encode only one p28-like ubiquitin ligase. FWPV further encodes two Kila-N domains paired with DUF (FWPV124 and FWPV155). We used BLAST analysis to speculate on the role of these DUFs, but we were unable to find similar proteins. It would be interesting to investigate what functions the DUF in FWPV124 and FWPV155 hold, in addition to the p28 homologues in FWPV.

The new knowledge gained from this thesis has increased our understanding into the regulation of p28 via ubiquitination and the UPS. Our data confirmed a role of the RING domain for the p28 ubiquitin ligase activity. The investigation of non-functional p28 RING mutants further revealed that p28 is regulated by both self-ubiquitination and ubiquitination by another unknown ubiquitin ligase(s). Continued work on the ubiquitination of p28 will allow us to better understand this regulatory mechanism. It will help us to clarify whether the ubiquitination events are a simple consequence of the E3 activity with no functional impact, or if ubiquitination is a feedback mechanism, where the presence of substrate shields the ubiquitin ligase from ubiquitination. This homeostatic feedback mechanism would result in accumulation of the ubiquitin ligase only in presence of abundant substrate (139, 155, 362, 398). In some cases, ubiquitination can have the opposite effect exemplified by the ubiquitin ligases Bmi1-Ring1b and Bard1-Brcal, where ubiquitination leads to an increase in their E3 ligase activity (399, 400). We could also distinguish, if the ubiquitination of p28 is solely required for the proteasomal degradation of p28 at a certain stage during infection, or if the ubiquitination is nonproteolytic and activate signaling, as in the case of TRAF6 (139).

Finally, we conducted a mass spectrometry screen for p28 interaction partners in an attempt to understand the function of this ubiquitin ligase. We identified HSP70 as an interaction partner of p28 during VACV infection. HSP70 was enriched at the virus factory in the presence of p28 compared with VACVCop infection alone. Many viruses use HSP70 for their own purposes, including viral cell entry, uncoating, transcription and genome replication, virion morphogenesis, encapsidation, virion release, and co-chaperoning purposes in general (313-316, 319, 320, 322-324, 326-328, 330, 331). It

remains elusive which purpose the p28 mediated HSP70 recruitment to the virus factory holds. This study of how viruses exploit cellular signaling pathways provides a stepping-stone to further understand virus host interactions with the ultimate goal of developing therapeutic anti-viral drugs for the treatment of virus infection.

## References

1. Damon IK. Poxviruses. D.M. HPMK, editor. Philadelphia: Lippincott Williams & Wilkins; 2007. 2947-75 p.
2. B. M. Poxviridae: The Viruses and their replication. Howley DMKaPM, editor. Philadelphia: Lippincott Williams & Wilkins; 2007. p. 2906-45 p.
3. McFadden G. Poxvirus tropism. *Nat Rev Microbiol.* 2005 Mar;3(3):201-13. PubMed PMID: 15738948. Epub 2005/03/02. eng.
4. Virus Taxonomy. al. MQKAe, editor: Elsevir; 2012.
5. Emerson GL, Li Y, Frace MA, Olsen-Rasmussen MA, Khristova ML, Govil D, Sammons SA, Regnery RL, Karem KL, Damon IK, Carroll DS. The phylogenetics and ecology of the orthopoxviruses endemic to North America. *PloS one.* 2009;4(10):e7666. PubMed PMID: 19865479. Pubmed Central PMCID: PMC2764843. Epub 2009/10/30. eng.
6. Frank Fenner RW, Keith R. Dumbell. *The Orthopoxviruses.* San Diego: Academic Press; 1989.
7. Esteban DJ, Buller RM. Ectromelia virus: the causative agent of mousepox. *The Journal of general virology.* 2005 Oct;86(Pt 10):2645-59. PubMed PMID: 16186218. Epub 2005/09/28. eng.
8. Multistate outbreak of monkeypox--Illinois, Indiana, and Wisconsin, 2003. *MMWR Morbidity and mortality weekly report.* 2003 Jun 13;52(23):537-40. PubMed PMID: 12803191. Epub 2003/06/14. eng.
9. Hutin YJ, Williams RJ, Malfait P, Pebody R, Loparev VN, Ropp SL, Rodriguez M, Knight JC, Tshioko FK, Khan AS, Szczeniowski MV, Esposito JJ. Outbreak of human monkeypox, Democratic Republic of Congo, 1996 to 1997. *Emerging infectious diseases.* 2001 May-Jun;7(3):434-8. PubMed PMID: 11384521. Pubmed Central PMCID: PMC2631782. Epub 2001/06/01. eng.
10. Meyer H, Perrichot M, Stemmler M, Emmerich P, Schmitz H, Varaine F, Shungu R, Tshioko F, Formenty P. Outbreaks of disease suspected of being due to human monkeypox virus infection in the Democratic Republic of Congo in 2001. *Journal of clinical microbiology.* 2002 Aug;40(8):2919-21. PubMed PMID: 12149352. Pubmed Central PMCID: PMC120683. Epub 2002/08/01. eng.
11. Reed KD, Melski JW, Graham MB, Regnery RL, Sotir MJ, Wegner MV, Kazmierczak JJ, Stratman EJ, Li Y, Fairley JA, Swain GR, Olson VA, Sargent EK, Kehl SC, Frace MA, Kline R, Foldy SL, Davis JP, Damon IK. The detection of monkeypox in humans in the Western Hemisphere. *The New England journal of medicine.* 2004 Jan 22;350(4):342-50. PubMed PMID: 14736926. Epub 2004/01/23. eng.

12. Hughes AL, Irausquin S, Friedman R. The evolutionary biology of poxviruses. Infection, genetics and evolution : journal of molecular epidemiology and evolutionary genetics in infectious diseases. 2010 Jan;10(1):50-9. PubMed PMID: 19833230. Pubmed Central PMCID: PMC2818276. Epub 2009/10/17. eng.
13. Fenner F. The eradication of smallpox. Progress in medical virology Fortschritte der medizinischen Virusforschung Progres en virologie medicale. 1977;23:1-21. PubMed PMID: 201963. Epub 1977/01/01. eng.
14. Shchelkunov SN. How long ago did smallpox virus emerge? Archives of virology. 2009;154(12):1865-71. PubMed PMID: 19882103. Epub 2009/11/03. eng.
15. Byrd D, Shepherd N, Lan J, Hu N, Amet T, Yang K, Desai M, Yu Q. Primary human macrophages serve as vehicles for vaccinia virus replication and dissemination. Journal of virology. 2014 Jun;88(12):6819-31. PubMed PMID: 24696488. Pubmed Central PMCID: PMC4054380. Epub 2014/04/04. eng.
16. Wehrle PF. A reality in our time--certification of the global eradication of smallpox. The Journal of infectious diseases. 1980 Oct;142(4):636-8. PubMed PMID: 7003037. Epub 1980/10/01. eng.
17. Turner GS. Jenner's smallpox vaccine-the riddle of vaccinia, virus and its origin by Derrick Baxby, Heineman Educational Books Ltd, 1981. pound8.50 (xiii + 214 pages) ISBN 0 435 54047 2. Immunology today. 1982 Jan;3(1):26. PubMed PMID: 25290879. Epub 1982/01/01. eng.
18. Alcami A, Smith GL. Vaccinia, cowpox, and camelpox viruses encode soluble gamma interferon receptors with novel broad species specificity. Journal of virology. 1995 Aug;69(8):4633-9. PubMed PMID: 7609027. Pubmed Central PMCID: PMC189264. Epub 1995/08/01. eng.
19. Johnston JB, McFadden G. Technical knockout: understanding poxvirus pathogenesis by selectively deleting viral immunomodulatory genes. Cellular microbiology. 2004 Aug;6(8):695-705. PubMed PMID: 15236637. Epub 2004/07/09. eng.
20. Seet BT, Johnston JB, Brunetti CR, Barrett JW, Everett H, Cameron C, Sypula J, Nazarian SH, Lucas A, McFadden G. Poxviruses and immune evasion. Annual review of immunology. 2003;21:377-423. PubMed PMID: 12543935. Epub 2003/01/25. eng.
21. Moss B, Flexner C. Vaccinia virus expression vectors. Annual review of immunology. 1987;5:305-24. PubMed PMID: 2439103. Epub 1987/01/01. eng.
22. Afonso CL, Tulman ER, Lu Z, Zsak L, Kutish GF, Rock DL. The genome of fowlpox virus. Journal of virology. 2000 Apr;74(8):3815-31. PubMed PMID: 10729156. Pubmed Central PMCID: PMC111890. Epub 2000/03/23. eng.

23. Tulman ER, Afonso CL, Lu Z, Zsak L, Kutish GF, Rock DL. The genome of canarypox virus. *Journal of virology*. 2004 Jan;78(1):353-66. PubMed PMID: 14671117. Pubmed Central PMCID: PMC303417. Epub 2003/12/13. eng.
24. Tripathy DN, Hanson LE. Pathogenesis of fowlpox in laying hens. *Avian diseases*. 1978 Apr-Jun;22(2):259-65. PubMed PMID: 209778. Epub 1978/04/01. eng.
25. Beukema EL, Brown MP, Hayball JD. The potential role of fowlpox virus in rational vaccine design. *Expert review of vaccines*. 2006 Aug;5(4):565-77. PubMed PMID: 16989636. Epub 2006/09/23. eng.
26. Skinner MA, Laidlaw SM, Eldaghayes I, Kaiser P, Cottingham MG. Fowlpox virus as a recombinant vaccine vector for use in mammals and poultry. *Expert review of vaccines*. 2005 Feb;4(1):63-76. PubMed PMID: 15757474. Epub 2005/03/11. eng.
27. Odunsi K, Matsuzaki J, Karbach J, Neumann A, Mhawech-Fauceglia P, Miller A, Beck A, Morrison CD, Ritter G, Godoy H, Lele S, duPont N, Edwards R, Shrikant P, Old LJ, Gnjjatic S, Jager E. Efficacy of vaccination with recombinant vaccinia and fowlpox vectors expressing NY-ESO-1 antigen in ovarian cancer and melanoma patients. *Proceedings of the National Academy of Sciences of the United States of America*. 2012 Apr 10;109(15):5797-802. PubMed PMID: 22454499. Pubmed Central PMCID: PMC3326498. Epub 2012/03/29. eng.
28. Lefkowitz EJ, Wang C, Upton C. Poxviruses: past, present and future. *Virus research*. 2006 Apr;117(1):105-18. PubMed PMID: 16503070. Epub 2006/03/01. eng.
29. Gubser C, Hue S, Kellam P, Smith GL. Poxvirus genomes: a phylogenetic analysis. *The Journal of general virology*. 2004 Jan;85(Pt 1):105-17. PubMed PMID: 14718625. Epub 2004/01/14. eng.
30. Johnston JB, McFadden G. Poxvirus immunomodulatory strategies: current perspectives. *Journal of virology*. 2003 Jun;77(11):6093-100. PubMed PMID: 12743266. Pubmed Central PMCID: PMC155018. Epub 2003/05/14. eng.
31. Mohamed MR, McFadden G. NFkB inhibitors: strategies from poxviruses. *Cell cycle (Georgetown, Tex)*. 2009 Oct 1;8(19):3125-32. PubMed PMID: 19738427. Epub 2009/09/10. eng.
32. Bengali Z, Townsley AC, Moss B. Vaccinia virus strain differences in cell attachment and entry. *Virology*. 2009 Jun 20;389(1-2):132-40. PubMed PMID: 19428041. Pubmed Central PMCID: PMC2700833. Epub 2009/05/12. eng.
33. Roberts KL, Smith GL. Vaccinia virus morphogenesis and dissemination. *Trends in microbiology*. 2008 Oct;16(10):472-9. PubMed PMID: 18789694. Epub 2008/09/16. eng.
34. Schmidt FI, Bleck CK, Mercer J. Poxvirus host cell entry. *Current opinion in virology*. 2012 Feb;2(1):20-7. PubMed PMID: 22440962. Epub 2012/03/24. eng.

35. Whitbeck JC, Foo CH, Ponce de Leon M, Eisenberg RJ, Cohen GH. Vaccinia virus exhibits cell-type-dependent entry characteristics. *Virology*. 2009 Mar 15;385(2):383-91. PubMed PMID: 19162290. Pubmed Central PMCID: PMC4041486. Epub 2009/01/24. eng.
36. Moss B. Poxvirus entry and membrane fusion. *Virology*. 2006 Jan 5;344(1):48-54. PubMed PMID: 16364735. Epub 2005/12/21. eng.
37. Senkevich TG, Ojeda S, Townsley A, Nelson GE, Moss B. Poxvirus multiprotein entry-fusion complex. *Proceedings of the National Academy of Sciences of the United States of America*. 2005 Dec 20;102(51):18572-7. PubMed PMID: 16339313. Pubmed Central PMCID: PMC1309049. Epub 2005/12/13. eng.
38. Earp LJ, Delos SE, Park HE, White JM. The many mechanisms of viral membrane fusion proteins. *Current topics in microbiology and immunology*. 2005;285:25-66. PubMed PMID: 15609500. Epub 2004/12/22. eng.
39. Sieczkarski SB, Whittaker GR. Viral entry. *Current topics in microbiology and immunology*. 2005;285:1-23. PubMed PMID: 15609499. Epub 2004/12/22. eng.
40. Mercer J, Knebel S, Schmidt FI, Crouse J, Burkard C, Helenius A. Vaccinia virus strains use distinct forms of macropinocytosis for host-cell entry. *Proceedings of the National Academy of Sciences of the United States of America*. 2010 May 18;107(20):9346-51. PubMed PMID: 20439710. Pubmed Central PMCID: PMC2889119. Epub 2010/05/05. eng.
41. Sandgren KJ, Wilkinson J, Miranda-Saksena M, McInerney GM, Byth-Wilson K, Robinson PJ, Cunningham AL. A differential role for macropinocytosis in mediating entry of the two forms of vaccinia virus into dendritic cells. *PLoS pathogens*. 2010 Apr;6(4):e1000866. PubMed PMID: 20421949. Pubmed Central PMCID: PMC2858709. Epub 2010/04/28. eng.
42. Carter GC, Rodger G, Murphy BJ, Law M, Krauss O, Hollinshead M, Smith GL. Vaccinia virus cores are transported on microtubules. *The Journal of general virology*. 2003 Sep;84(Pt 9):2443-58. PubMed PMID: 12917466. Epub 2003/08/15. eng.
43. Mallardo M, Schleich S, Krijnse Locker J. Microtubule-dependent organization of vaccinia virus core-derived early mRNAs into distinct cytoplasmic structures. *Molecular biology of the cell*. 2001 Dec;12(12):3875-91. PubMed PMID: 11739787. Pubmed Central PMCID: PMC60762. Epub 2001/12/12. eng.
44. Dales S, Siminovitch L. The development of vaccinia virus in Earle's L strain cells as examined by electron microscopy. *The Journal of biophysical and biochemical cytology*. 1961 Aug;10:475-503. PubMed PMID: 13719413. Pubmed Central PMCID: PMC2225098. Epub 1961/08/01. eng.
45. Katsafanas GC, Moss B. Colocalization of transcription and translation within cytoplasmic poxvirus factories coordinates viral expression and subjugates host

functions. *Cell host & microbe*. 2007 Oct 11;2(4):221-8. PubMed PMID: 18005740. Pubmed Central PMCID: PMC2084088. Epub 2007/11/17. eng.

46. Cairns J. The initiation of vaccinia infection. *Virology*. 1960 Jul;11:603-23. PubMed PMID: 13806834. Epub 1960/07/01. eng.

47. Tolonen N, Doglio L, Schleich S, Krijnse Locker J. Vaccinia virus DNA replication occurs in endoplasmic reticulum-enclosed cytoplasmic mini-nuclei. *Molecular biology of the cell*. 2001 Jul;12(7):2031-46. PubMed PMID: 11452001. Pubmed Central PMCID: PMC55651. Epub 2001/07/14. eng.

48. DeFilippes FM. Restriction enzyme mapping of vaccinia virus DNA. *Journal of virology*. 1982 Jul;43(1):136-49. PubMed PMID: 6286993. Pubmed Central PMCID: PMC256104. Epub 1982/07/01. eng.

49. Assarsson E, Greenbaum JA, Sundstrom M, Schaffer L, Hammond JA, Pasquetto V, Oseroff C, Hendrickson RC, Lefkowitz EJ, Tschärke DC, Sidney J, Grey HM, Head SR, Peters B, Sette A. Kinetic analysis of a complete poxvirus transcriptome reveals an immediate-early class of genes. *Proceedings of the National Academy of Sciences of the United States of America*. 2008 Feb 12;105(6):2140-5. PubMed PMID: 18245380. Pubmed Central PMCID: PMC2542872. Epub 2008/02/05. eng.

50. Broyles SS. Vaccinia virus transcription. *The Journal of general virology*. 2003 Sep;84(Pt 9):2293-303. PubMed PMID: 12917449. Epub 2003/08/15. eng.

51. Smith GL, Murphy BJ, Law M. Vaccinia virus motility. *Annual review of microbiology*. 2003;57:323-42. PubMed PMID: 14527282. Epub 2003/10/07. eng.

52. Joklik WK. THE INTRACELLULAR UNCOATING OF POXVIRUS DNA. II. THE MOLECULAR BASIS OF THE UNCOATING PROCESS. *Journal of molecular biology*. 1964 Feb;8:277-88. PubMed PMID: 14126296. Epub 1964/02/01. eng.

53. Yang Z, Reynolds SE, Martens CA, Bruno DP, Porcella SF, Moss B. Expression profiling of the intermediate and late stages of poxvirus replication. *Journal of virology*. 2011 Oct;85(19):9899-908. PubMed PMID: 21795349. Pubmed Central PMCID: PMC3196450. Epub 2011/07/29. eng.

54. Chakrabarti S, Sisler JR, Moss B. Compact, synthetic, vaccinia virus early/late promoter for protein expression. *BioTechniques*. 1997 Dec;23(6):1094-7. PubMed PMID: 9421642. Epub 1998/01/09. eng.

55. Sodeik B, Doms RW, Ericsson M, Hiller G, Machamer CE, van 't Hof W, van Meer G, Moss B, Griffiths G. Assembly of vaccinia virus: role of the intermediate compartment between the endoplasmic reticulum and the Golgi stacks. *The Journal of cell biology*. 1993 May;121(3):521-41. PubMed PMID: 8486734. Pubmed Central PMCID: PMC2119557. Epub 1993/05/01. eng.

56. Schmelz M, Sodeik B, Ericsson M, Wolffe EJ, Shida H, Hiller G, Griffiths G. Assembly of vaccinia virus: the second wrapping cisterna is derived from the trans Golgi network. *Journal of virology*. 1994 Jan;68(1):130-47. PubMed PMID: 8254722. Pubmed Central PMCID: PMC236272. Epub 1994/01/01. eng.
57. Hiller G, Weber K. Golgi-derived membranes that contain an acylated viral polypeptide are used for vaccinia virus envelopment. *Journal of virology*. 1985 Sep;55(3):651-9. PubMed PMID: 4020961. Pubmed Central PMCID: PMC255032. Epub 1985/09/01. eng.
58. Tooze J, Hollinshead M, Reis B, Radsak K, Kern H. Progeny vaccinia and human cytomegalovirus particles utilize early endosomal cisternae for their envelopes. *European journal of cell biology*. 1993 Feb;60(1):163-78. PubMed PMID: 8385018. Epub 1993/02/01. eng.
59. Ward BM. Visualization and characterization of the intracellular movement of vaccinia virus intracellular mature virions. *Journal of virology*. 2005 Apr;79(8):4755-63. PubMed PMID: 15795261. Pubmed Central PMCID: PMC1069544. Epub 2005/03/30. eng.
60. Geada MM, Galindo I, Lorenzo MM, Perdiguero B, Blasco R. Movements of vaccinia virus intracellular enveloped virions with GFP tagged to the F13L envelope protein. *The Journal of general virology*. 2001 Nov;82(Pt 11):2747-60. PubMed PMID: 11602786. Epub 2001/10/17. eng.
61. Sanderson CM, Hollinshead M, Smith GL. The vaccinia virus A27L protein is needed for the microtubule-dependent transport of intracellular mature virus particles. *The Journal of general virology*. 2000 Jan;81(Pt 1):47-58. PubMed PMID: 10640541. Epub 2000/01/21. eng.
62. Sakala IG, Chaudhri G, Buller RM, Nuara AA, Bai H, Chen N, Karupiah G. Poxvirus-encoded gamma interferon binding protein dampens the host immune response to infection. *Journal of virology*. 2007 Apr;81(7):3346-53. PubMed PMID: 17229697. Pubmed Central PMCID: PMC1866021. Epub 2007/01/19. eng.
63. Alcami A. Viral mimicry of cytokines, chemokines and their receptors. *Nature reviews Immunology*. 2003 Jan;3(1):36-50. PubMed PMID: 12511874. Epub 2003/01/04. eng.
64. Fenner F. Mousepox (infectious ectromelia): past, present, and future. *Laboratory animal science*. 1981 Oct;31(5 Pt 2):553-9. PubMed PMID: 6281556. Epub 1981/10/01. eng.
65. Chaudhri G, Panchanathan V, Buller RM, van den Eertwegh AJ, Claassen E, Zhou J, de Chazal R, Laman JD, Karupiah G. Polarized type 1 cytokine response and cell-mediated immunity determine genetic resistance to mousepox. *Proceedings of the National Academy of Sciences of the United States of America*. 2004 Jun

15;101(24):9057-62. PubMed PMID: 15184649. Pubmed Central PMCID: PMC428472. Epub 2004/06/09. eng.

66. Jackson RJ, Ramsay AJ, Christensen CD, Beaton S, Hall DF, Ramshaw IA. Expression of mouse interleukin-4 by a recombinant ectromelia virus suppresses cytolytic lymphocyte responses and overcomes genetic resistance to mousepox. *Journal of virology*. 2001 Feb;75(3):1205-10. PubMed PMID: 11152493. Pubmed Central PMCID: PMC114026. Epub 2001/01/11. eng.

67. Roberts JA. GROWTH OF VIRULENT AND ATTENUATED ECTROMELIA VIRUS IN CULTURED MACROPHAGES FROM NORMAL AND ECTROMELIAIMMUNE MICE. *Journal of immunology (Baltimore, Md : 1950)*. 1964 Jun;92:837-42. PubMed PMID: 14210788. Epub 1964/06/01. eng.

68. Kochneva GV, Urmanov IH, Ryabchikova EI, Streltsov VV, Serpinsky OI. Fine mechanisms of ectromelia virus thymidine kinase-negative mutants avirulence. *Virus research*. 1994 Oct;34(1):49-61. PubMed PMID: 7831964. Epub 1994/10/01. eng.

69. Mims CA. THE PERITONEAL MACROPHAGES OF MICE. *British journal of experimental pathology*. 1964 Feb;45:37-43. PubMed PMID: 14119272. Pubmed Central PMCID: PMC2094654. Epub 1964/02/01. eng.

70. Mims CA. The response of mice to large intravenous injections of ectromelia virus. I. The fate of injected virus. *British journal of experimental pathology*. 1959 Dec;40:533-42. PubMed PMID: 14422711. Pubmed Central PMCID: PMC2082326. Epub 1959/12/01. eng.

71. Mims CA. The response of mice to large intravenous injections of ectromelia virus. II. The growth of virus in the liver. *British journal of experimental pathology*. 1959 Dec;40:543-50. PubMed PMID: 14422712. Pubmed Central PMCID: PMC2082325. Epub 1959/12/01. eng.

72. Van Blerkom LM. Role of viruses in human evolution. *American journal of physical anthropology*. 2003;Suppl 37:14-46. PubMed PMID: 14666532. Epub 2003/12/11. eng.

73. Mansouri M, Bartee E, Gouveia K, Hovey Nerenberg BT, Barrett J, Thomas L, Thomas G, McFadden G, Fruh K. The PHD/LAP-domain protein M153R of myxomavirus is a ubiquitin ligase that induces the rapid internalization and lysosomal destruction of CD4. *Journal of virology*. 2003 Jan;77(2):1427-40. PubMed PMID: 12502858. Pubmed Central PMCID: PMC140772. Epub 2002/12/28. eng.

74. Guerin JL, Gelfi J, Boullier S, Delverdier M, Bellanger FA, Bertagnoli S, Drexler I, Sutter G, Messud-Petit F. Myxoma virus leukemia-associated protein is responsible for major histocompatibility complex class I and Fas-CD95 down-regulation and defines scrapins, a new group of surface cellular receptor abductor proteins. *Journal of virology*. 2002 Mar;76(6):2912-23. PubMed PMID: 11861858. Pubmed Central PMCID: PMC135958. Epub 2002/02/28. eng.

75. McCormack SJ, Thomis DC, Samuel CE. Mechanism of interferon action: identification of a RNA binding domain within the N-terminal region of the human RNA-dependent P1/eIF-2 alpha protein kinase. *Virology*. 1992 May;188(1):47-56. PubMed PMID: 1373554. Epub 1992/05/01. eng.
76. Chang HW, Watson JC, Jacobs BL. The E3L gene of vaccinia virus encodes an inhibitor of the interferon-induced, double-stranded RNA-dependent protein kinase. *Proceedings of the National Academy of Sciences of the United States of America*. 1992 Jun 1;89(11):4825-9. PubMed PMID: 1350676. Pubmed Central PMCID: PMC49180. Epub 1992/06/01. eng.
77. Najarro P, Traktman P, Lewis JA. Vaccinia virus blocks gamma interferon signal transduction: viral VH1 phosphatase reverses Stat1 activation. *Journal of virology*. 2001 Apr;75(7):3185-96. PubMed PMID: 11238845. Pubmed Central PMCID: PMC114112. Epub 2001/03/10. eng.
78. Davies MV, Elroy-Stein O, Jagus R, Moss B, Kaufman RJ. The vaccinia virus K3L gene product potentiates translation by inhibiting double-stranded-RNA-activated protein kinase and phosphorylation of the alpha subunit of eukaryotic initiation factor 2. *Journal of virology*. 1992 Apr;66(4):1943-50. PubMed PMID: 1347793. Pubmed Central PMCID: PMC288982. Epub 1992/04/01. eng.
79. Schroder M, Baran M, Bowie AG. Viral targeting of DEAD box protein 3 reveals its role in TBK1/IKKepsilon-mediated IRF activation. *The EMBO journal*. 2008 Aug 6;27(15):2147-57. PubMed PMID: 18636090. Pubmed Central PMCID: PMC2516890. Epub 2008/07/19. eng.
80. Quan LT, Caputo A, Bleackley RC, Pickup DJ, Salvesen GS. Granzyme B is inhibited by the cowpox virus serpin cytokine response modifier A. *The Journal of biological chemistry*. 1995 May 5;270(18):10377-9. PubMed PMID: 7737968. Epub 1995/05/05. eng.
81. Kettle S, Alcami A, Khanna A, Ehret R, Jassoy C, Smith GL. Vaccinia virus serpin B13R (SPI-2) inhibits interleukin-1beta-converting enzyme and protects virus-infected cells from TNF- and Fas-mediated apoptosis, but does not prevent IL-1beta-induced fever. *The Journal of general virology*. 1997 Mar;78 ( Pt 3):677-85. PubMed PMID: 9049422. Epub 1997/03/01. eng.
82. Ray CA, Black RA, Kronheim SR, Greenstreet TA, Sleath PR, Salvesen GS, Pickup DJ. Viral inhibition of inflammation: cowpox virus encodes an inhibitor of the interleukin-1 beta converting enzyme. *Cell*. 1992 May 15;69(4):597-604. PubMed PMID: 1339309. Epub 1992/05/15. eng.
83. Pickup DJ, Ink BS, Hu W, Ray CA, Joklik WK. Hemorrhage in lesions caused by cowpox virus is induced by a viral protein that is related to plasma protein inhibitors of serine proteases. *Proceedings of the National Academy of Sciences of the United States of America*. 1986 Oct;83(20):7698-702. PubMed PMID: 3532120. Pubmed Central PMCID: PMC386788. Epub 1986/10/01. eng.

84. Banadyga L, Gerig J, Stewart T, Barry M. Fowlpox virus encodes a Bcl-2 homologue that protects cells from apoptotic death through interaction with the proapoptotic protein Bak. *Journal of virology*. 2007 Oct;81(20):11032-45. PubMed PMID: 17686864. Pubmed Central PMCID: PMC2045560. Epub 2007/08/10. eng.
85. Wasilenko ST, Stewart TL, Meyers AF, Barry M. Vaccinia virus encodes a previously uncharacterized mitochondrial-associated inhibitor of apoptosis. *Proceedings of the National Academy of Sciences of the United States of America*. 2003 Nov 25;100(24):14345-50. PubMed PMID: 14610284. Pubmed Central PMCID: PMC283594. Epub 2003/11/12. eng.
86. Banadyga L, Lam SC, Okamoto T, Kvensakul M, Huang DC, Barry M. Deerpox virus encodes an inhibitor of apoptosis that regulates Bak and Bax. *Journal of virology*. 2011 Mar;85(5):1922-34. PubMed PMID: 21159883. Pubmed Central PMCID: PMC3067780. Epub 2010/12/17. eng.
87. Shisler JL, Moss B. Molluscum contagiosum virus inhibitors of apoptosis: The MC159 v-FLIP protein blocks Fas-induced activation of procaspases and degradation of the related MC160 protein. *Virology*. 2001 Mar 30;282(1):14-25. PubMed PMID: 11259186. Epub 2001/03/22. eng.
88. Upton C, Macen JL, Wishart DS, McFadden G. Myxoma virus and malignant rabbit fibroma virus encode a serpin-like protein important for virus virulence. *Virology*. 1990 Dec;179(2):618-31. PubMed PMID: 2173255. Epub 1990/12/01. eng.
89. Turner PC, Moyer RW. Orthopoxvirus fusion inhibitor glycoprotein SPI-3 (open reading frame K2L) contains motifs characteristic of serine proteinase inhibitors that are not required for control of cell fusion. *Journal of virology*. 1995 Oct;69(10):5978-87. PubMed PMID: 7666502. Pubmed Central PMCID: PMC189493. Epub 1995/10/01. eng.
90. Smith VP, Alcami A. Expression of secreted cytokine and chemokine inhibitors by ectromelia virus. *Journal of virology*. 2000 Sep;74(18):8460-71. PubMed PMID: 10954546. Pubmed Central PMCID: PMC116357. Epub 2000/08/23. eng.
91. Born TL, Morrison LA, Esteban DJ, VandenBos T, Thebeau LG, Chen N, Spriggs MK, Sims JE, Buller RM. A poxvirus protein that binds to and inactivates IL-18, and inhibits NK cell response. *Journal of immunology (Baltimore, Md : 1950)*. 2000 Mar 15;164(6):3246-54. PubMed PMID: 10706717. Epub 2000/03/08. eng.
92. Mossman K, Nation P, Macen J, Garbutt M, Lucas A, McFadden G. Myxoma virus M-T7, a secreted homolog of the interferon-gamma receptor, is a critical virulence factor for the development of myxomatosis in European rabbits. *Virology*. 1996 Jan 1;215(1):17-30. PubMed PMID: 8553583. Epub 1996/01/01. eng.
93. Vinitsky A, Michaud C, Powers JC, Orlowski M. Inhibition of the chymotrypsin-like activity of the pituitary multicatalytic proteinase complex. *Biochemistry*. 1992 Oct 6;31(39):9421-8. PubMed PMID: 1356435. Epub 1992/10/06. eng.

94. Lalani AS, Graham K, Mossman K, Rajarathnam K, Clark-Lewis I, Kelvin D, McFadden G. The purified myxoma virus gamma interferon receptor homolog M-T7 interacts with the heparin-binding domains of chemokines. *Journal of virology*. 1997 Jun;71(6):4356-63. PubMed PMID: 9151824. Pubmed Central PMCID: PMC191652. Epub 1997/06/01. eng.
95. Kotwal GJ, Hugin AW, Moss B. Mapping and insertional mutagenesis of a vaccinia virus gene encoding a 13,800-Da secreted protein. *Virology*. 1989 Aug;171(2):579-87. PubMed PMID: 2763467. Epub 1989/08/01. eng.
96. Kotwal GJ, Moss B. Vaccinia virus encodes a secretory polypeptide structurally related to complement control proteins. *Nature*. 1988 Sep 8;335(6186):176-8. PubMed PMID: 3412473. Epub 1988/09/08. eng.
97. Rosengard AM, Liu Y, Nie Z, Jimenez R. Variola virus immune evasion design: expression of a highly efficient inhibitor of human complement. *Proceedings of the National Academy of Sciences of the United States of America*. 2002 Jun 25;99(13):8808-13. PubMed PMID: 12034872. Pubmed Central PMCID: PMC124380. Epub 2002/05/30. eng.
98. Spriggs MK, Hruby DE, Maliszewski CR, Pickup DJ, Sims JE, Buller RM, VanSlyke J. Vaccinia and cowpox viruses encode a novel secreted interleukin-1-binding protein. *Cell*. 1992 Oct 2;71(1):145-52. PubMed PMID: 1339315. Epub 1992/10/02. eng.
99. Symons JA, Alcami A, Smith GL. Vaccinia virus encodes a soluble type I interferon receptor of novel structure and broad species specificity. *Cell*. 1995 May 19;81(4):551-60. PubMed PMID: 7758109. Epub 1995/05/19. eng.
100. Hu FQ, Smith CA, Pickup DJ. Cowpox virus contains two copies of an early gene encoding a soluble secreted form of the type II TNF receptor. *Virology*. 1994 Oct;204(1):343-56. PubMed PMID: 8091665. Epub 1994/10/01. eng.
101. Loparev VN, Parsons JM, Knight JC, Panus JF, Ray CA, Buller RM, Pickup DJ, Esposito JJ. A third distinct tumor necrosis factor receptor of orthopoxviruses. *Proceedings of the National Academy of Sciences of the United States of America*. 1998 Mar 31;95(7):3786-91. PubMed PMID: 9520445. Pubmed Central PMCID: PMC19915. Epub 1998/05/09. eng.
102. Panus JF, Smith CA, Ray CA, Smith TD, Patel DD, Pickup DJ. Cowpox virus encodes a fifth member of the tumor necrosis factor receptor family: a soluble, secreted CD30 homologue. *Proceedings of the National Academy of Sciences of the United States of America*. 2002 Jun 11;99(12):8348-53. PubMed PMID: 12034885. Pubmed Central PMCID: PMC123070. Epub 2002/05/30. eng.
103. Saraiva M, Alcami A. CrmE, a novel soluble tumor necrosis factor receptor encoded by poxviruses. *Journal of virology*. 2001 Jan;75(1):226-33. PubMed PMID: 11119592. Pubmed Central PMCID: PMC113916. Epub 2000/12/19. eng.

104. Kadi Z, Bouguermouh A, Djenaoui T, Allouache A, Dali S, Hadji N. Chlamydial genital infection in Algiers: a sero-epidemiological survey. *Transactions of the Royal Society of Tropical Medicine and Hygiene*. 1990 Nov-Dec;84(6):863-5. PubMed PMID: 2096526. Epub 1990/11/01. eng.
105. Alcami A, Smith GL. A soluble receptor for interleukin-1 beta encoded by vaccinia virus: a novel mechanism of virus modulation of the host response to infection. *Cell*. 1992 Oct 2;71(1):153-67. PubMed PMID: 1394428. Epub 1992/10/02. eng.
106. Bowie A, Kiss-Toth E, Symons JA, Smith GL, Dower SK, O'Neill LA. A46R and A52R from vaccinia virus are antagonists of host IL-1 and toll-like receptor signaling. *Proceedings of the National Academy of Sciences of the United States of America*. 2000 Aug 29;97(18):10162-7. PubMed PMID: 10920188. Pubmed Central PMCID: PMC27775. Epub 2000/08/02. eng.
107. Chen RA, Jacobs N, Smith GL. Vaccinia virus strain Western Reserve protein B14 is an intracellular virulence factor. *The Journal of general virology*. 2006 Jun;87(Pt 6):1451-8. PubMed PMID: 16690909. Epub 2006/05/13. eng.
108. Chen RA, Ryzhakov G, Cooray S, Randow F, Smith GL. Inhibition of IkappaB kinase by vaccinia virus virulence factor B14. *PLoS pathogens*. 2008 Feb 8;4(2):e22. PubMed PMID: 18266467. Pubmed Central PMCID: PMC2233672. Epub 2008/02/13. eng.
109. DiPerna G, Stack J, Bowie AG, Boyd A, Kotwal G, Zhang Z, Arvikar S, Latz E, Fitzgerald KA, Marshall WL. Poxvirus protein N1L targets the I-kappaB kinase complex, inhibits signaling to NF-kappaB by the tumor necrosis factor superfamily of receptors, and inhibits NF-kappaB and IRF3 signaling by toll-like receptors. *The Journal of biological chemistry*. 2004 Aug 27;279(35):36570-8. PubMed PMID: 15215253. Epub 2004/06/25. eng.
110. Gedey R, Jin XL, Hinthong O, Shisler JL. Poxviral regulation of the host NF-kappaB response: the vaccinia virus M2L protein inhibits induction of NF-kappaB activation via an ERK2 pathway in virus-infected human embryonic kidney cells. *Journal of virology*. 2006 Sep;80(17):8676-85. PubMed PMID: 16912315. Pubmed Central PMCID: PMC1563854. Epub 2006/08/17. eng.
111. Graham SC, Bahar MW, Cooray S, Chen RA, Whalen DM, Abrescia NG, Alderton D, Owens RJ, Stuart DI, Smith GL, Grimes JM. Vaccinia virus proteins A52 and B14 Share a Bcl-2-like fold but have evolved to inhibit NF-kappaB rather than apoptosis. *PLoS pathogens*. 2008;4(8):e1000128. PubMed PMID: 18704168. Pubmed Central PMCID: PMC2494871. Epub 2008/08/16. eng.
112. Harte MT, Haga IR, Maloney G, Gray P, Reading PC, Bartlett NW, Smith GL, Bowie A, O'Neill LA. The poxvirus protein A52R targets Toll-like receptor signaling complexes to suppress host defense. *The Journal of experimental medicine*. 2003 Feb 3;197(3):343-51. PubMed PMID: 12566418. Pubmed Central PMCID: PMC2193841. Epub 2003/02/05. eng.

113. Hinthong O, Jin XL, Shisler JL. Characterization of wild-type and mutant vaccinia virus M2L proteins' abilities to localize to the endoplasmic reticulum and to inhibit NF-kappaB activation during infection. *Virology*. 2008 Apr 10;373(2):248-62. PubMed PMID: 18190944. Pubmed Central PMCID: PMC2679263. Epub 2008/01/15. eng.
114. Myskiw C, Arsenio J, van Bruggen R, Deschambault Y, Cao J. Vaccinia virus E3 suppresses expression of diverse cytokines through inhibition of the PKR, NF-kappaB, and IRF3 pathways. *Journal of virology*. 2009 Jul;83(13):6757-68. PubMed PMID: 19369349. Pubmed Central PMCID: PMC2698532. Epub 2009/04/17. eng.
115. Shisler JL, Jin XL. The vaccinia virus K1L gene product inhibits host NF-kappaB activation by preventing IkappaBalpha degradation. *Journal of virology*. 2004 Apr;78(7):3553-60. PubMed PMID: 15016878. Pubmed Central PMCID: PMC371086. Epub 2004/03/16. eng.
116. Satheshkumar PS, Anton LC, Sanz P, Moss B. Inhibition of the ubiquitin-proteasome system prevents vaccinia virus DNA replication and expression of intermediate and late genes. *Journal of virology*. 2009 Mar;83(6):2469-79. PubMed PMID: 19129442. Pubmed Central PMCID: PMC2648259. Epub 2009/01/09. eng.
117. Teale A, Campbell S, Van Buuren N, Magee WC, Watmough K, Couturier B, Shipclark R, Barry M. Orthopoxviruses require a functional ubiquitin-proteasome system for productive replication. *Journal of virology*. 2009 Mar;83(5):2099-108. PubMed PMID: 19109393. Pubmed Central PMCID: PMC2643736. Epub 2008/12/26. eng.
118. Hershko A, Ciechanover A. The ubiquitin system. *Annual review of biochemistry*. 1998;67:425-79. PubMed PMID: 9759494. Epub 1998/10/06. eng.
119. Wang C, Xi J, Begley TP, Nicholson LK. Solution structure of ThiS and implications for the evolutionary roots of ubiquitin. *Nature structural biology*. 2001 Jan;8(1):47-51. PubMed PMID: 11135670. Epub 2001/01/03. eng.
120. Hicke L. Protein regulation by monoubiquitin. *Nature reviews Molecular cell biology*. 2001 Mar;2(3):195-201. PubMed PMID: 11265249. Epub 2001/03/27. eng.
121. Pickart CM, Fushman D. Polyubiquitin chains: polymeric protein signals. *Current opinion in chemical biology*. 2004 Dec;8(6):610-6. PubMed PMID: 15556404. Epub 2004/11/24. eng.
122. Weissman AM. Themes and variations on ubiquitylation. *Nature reviews Molecular cell biology*. 2001 Mar;2(3):169-78. PubMed PMID: 11265246. Epub 2001/03/27. eng.
123. Meierhofer D, Wang X, Huang L, Kaiser P. Quantitative analysis of global ubiquitination in HeLa cells by mass spectrometry. *Journal of proteome research*. 2008 Oct;7(10):4566-76. PubMed PMID: 18781797. Pubmed Central PMCID: PMC2758155. Epub 2008/09/11. eng.

124. Ravid T, Hochstrasser M. NF-kappaB signaling: flipping the switch with polyubiquitin chains. *Current biology : CB*. 2004 Oct 26;14(20):R898-900. PubMed PMID: 15498483. Epub 2004/10/23. eng.
125. Park Y, Jin HS, Aki D, Lee J, Liu YC. The ubiquitin system in immune regulation. *Advances in immunology*. 2014;124:17-66. PubMed PMID: 25175772. Epub 2014/09/02. eng.
126. Handley-Gearhart PM, Stephen AG, Trausch-Azar JS, Ciechanover A, Schwartz AL. Human ubiquitin-activating enzyme, E1. Indication of potential nuclear and cytoplasmic subpopulations using epitope-tagged cDNA constructs. *The Journal of biological chemistry*. 1994 Dec 30;269(52):33171-8. PubMed PMID: 7528747. Epub 1994/12/30. eng.
127. Finley D, Ciechanover A, Varshavsky A. Thermolability of ubiquitin-activating enzyme from the mammalian cell cycle mutant ts85. *Cell*. 1984 May;37(1):43-55. PubMed PMID: 6327059. Epub 1984/05/01. eng.
128. Hofmann RM, Pickart CM. Noncanonical MMS2-encoded ubiquitin-conjugating enzyme functions in assembly of novel polyubiquitin chains for DNA repair. *Cell*. 1999 Mar 5;96(5):645-53. PubMed PMID: 10089880. Epub 1999/03/25. eng.
129. Ardley HC, Robinson PA. E3 ubiquitin ligases. *Essays in biochemistry*. 2005;41:15-30. PubMed PMID: 16250895. Epub 2005/10/28. eng.
130. Scheffner M, Huibregtse JM, Vierstra RD, Howley PM. The HPV-16 E6 and E6-AP complex functions as a ubiquitin-protein ligase in the ubiquitination of p53. *Cell*. 1993 Nov 5;75(3):495-505. PubMed PMID: 8221889. Epub 1993/11/05. eng.
131. Petroski MD, Deshaies RJ. Function and regulation of cullin-RING ubiquitin ligases. *Nature reviews Molecular cell biology*. 2005 Jan;6(1):9-20. PubMed PMID: 15688063. Epub 2005/02/03. eng.
132. Willems AR, Schwab M, Tyers M. A hitchhiker's guide to the cullin ubiquitin ligases: SCF and its kin. *Biochimica et biophysica acta*. 2004 Nov 29;1695(1-3):133-70. PubMed PMID: 15571813. Epub 2004/12/02. eng.
133. Borden KL, Freemont PS. The RING finger domain: a recent example of a sequence-structure family. *Current opinion in structural biology*. 1996 Jun;6(3):395-401. PubMed PMID: 8804826. Epub 1996/06/01. eng.
134. Aravind L, Koonin EV. The U box is a modified RING finger - a common domain in ubiquitination. *Current biology : CB*. 2000 Feb 24;10(4):R132-4. PubMed PMID: 10704423. Epub 2000/03/08. eng.
135. Nathan JA, Lehner PJ. The trafficking and regulation of membrane receptors by the RING-CH ubiquitin E3 ligases. *Experimental cell research*. 2009 May 15;315(9):1593-600. PubMed PMID: 19013150. Epub 2008/11/18. eng.

136. Ohi MD, Vander Kooi CW, Rosenberg JA, Chazin WJ, Gould KL. Structural insights into the U-box, a domain associated with multi-ubiquitination. *Nature structural biology*. 2003 Apr;10(4):250-5. PubMed PMID: 12627222. Epub 2003/03/11. eng.
137. Ohmura-Hoshino M, Goto E, Matsuki Y, Aoki M, Mito M, Uematsu M, Hotta H, Ishido S. A novel family of membrane-bound E3 ubiquitin ligases. *Journal of biochemistry*. 2006 Aug;140(2):147-54. PubMed PMID: 16954532. Epub 2006/09/07. eng.
138. Komander D. The emerging complexity of protein ubiquitination. *Biochemical Society transactions*. 2009 Oct;37(Pt 5):937-53. PubMed PMID: 19754430. Epub 2009/09/17. eng.
139. Deshaies RJ, Joazeiro CA. RING domain E3 ubiquitin ligases. *Annual review of biochemistry*. 2009;78:399-434. PubMed PMID: 19489725. Epub 2009/06/06. eng.
140. Peng J, Schwartz D, Elias JE, Thoreen CC, Cheng D, Marsischky G, Roelofs J, Finley D, Gygi SP. A proteomics approach to understanding protein ubiquitination. *Nature biotechnology*. 2003 Aug;21(8):921-6. PubMed PMID: 12872131. Epub 2003/07/23. eng.
141. Sakamoto H, Egashira S, Saito N, Kirisako T, Miller S, Sasaki Y, Matsumoto T, Shimonishi M, Komatsu T, Terai T, Ueno T, Hanaoka K, Kojima H, Okabe T, Wakatsuki S, Iwai K, Nagano T. Gliotoxin Suppresses NF-kappaB Activation by Selectively Inhibiting Linear Ubiquitin Chain Assembly Complex (LUBAC). *ACS chemical biology*. 2015 Mar 20;10(3):675-81. PubMed PMID: 25494483. Epub 2014/12/11. eng.
142. Eddins MJ, Varadan R, Fushman D, Pickart CM, Wolberger C. Crystal structure and solution NMR studies of Lys48-linked tetraubiquitin at neutral pH. *Journal of molecular biology*. 2007 Mar 16;367(1):204-11. PubMed PMID: 17240395. Epub 2007/01/24. eng.
143. Komander D, Reyes-Turcu F, Licchesi JD, Odenwaelder P, Wilkinson KD, Barford D. Molecular discrimination of structurally equivalent Lys 63-linked and linear polyubiquitin chains. *EMBO reports*. 2009 May;10(5):466-73. PubMed PMID: 19373254. Pubmed Central PMCID: PMC2680876. Epub 2009/04/18. eng.
144. Newton K, Matsumoto ML, Wertz IE, Kirkpatrick DS, Lill JR, Tan J, Dugger D, Gordon N, Sidhu SS, Fellouse FA, Komuves L, French DM, Ferrando RE, Lam C, Compaan D, Yu C, Bosanac I, Hymowitz SG, Kelley RF, Dixit VM. Ubiquitin chain editing revealed by polyubiquitin linkage-specific antibodies. *Cell*. 2008 Aug 22;134(4):668-78. PubMed PMID: 18724939. Epub 2008/08/30. eng.
145. Thrower JS, Hoffman L, Rechsteiner M, Pickart CM. Recognition of the polyubiquitin proteolytic signal. *The EMBO journal*. 2000 Jan 4;19(1):94-102. PubMed PMID: 10619848. Pubmed Central PMCID: PMC1171781. Epub 2000/01/05. eng.

146. Matsumoto ML, Wickliffe KE, Dong KC, Yu C, Bosanac I, Bustos D, Phu L, Kirkpatrick DS, Hymowitz SG, Rape M, Kelley RF, Dixit VM. K11-linked polyubiquitination in cell cycle control revealed by a K11 linkage-specific antibody. *Molecular cell*. 2010 Aug 13;39(3):477-84. PubMed PMID: 20655260. Epub 2010/07/27. eng.
147. Xu P, Duong DM, Seyfried NT, Cheng D, Xie Y, Robert J, Rush J, Hochstrasser M, Finley D, Peng J. Quantitative proteomics reveals the function of unconventional ubiquitin chains in proteasomal degradation. *Cell*. 2009 Apr 3;137(1):133-45. PubMed PMID: 19345192. Pubmed Central PMCID: PMC2668214. Epub 2009/04/07. eng.
148. Chastagner P, Israel A, Brou C. Itch/AIP4 mediates Deltex degradation through the formation of K29-linked polyubiquitin chains. *EMBO reports*. 2006 Nov;7(11):1147-53. PubMed PMID: 17028573. Pubmed Central PMCID: PMC1679774. Epub 2006/10/10. eng.
149. Deng L, Wang C, Spencer E, Yang L, Braun A, You J, Slaughter C, Pickart C, Chen ZJ. Activation of the IkappaB kinase complex by TRAF6 requires a dimeric ubiquitin-conjugating enzyme complex and a unique polyubiquitin chain. *Cell*. 2000 Oct 13;103(2):351-61. PubMed PMID: 11057907. Epub 2000/11/01. eng.
150. Duncan LM, Piper S, Dodd RB, Saville MK, Sanderson CM, Luzio JP, Lehner PJ. Lysine-63-linked ubiquitination is required for endolysosomal degradation of class I molecules. *The EMBO journal*. 2006 Apr 19;25(8):1635-45. PubMed PMID: 16601694. Pubmed Central PMCID: PMC1440841. Epub 2006/04/08. eng.
151. Morris JR, Solomon E. BRCA1 : BARD1 induces the formation of conjugated ubiquitin structures, dependent on K6 of ubiquitin, in cells during DNA replication and repair. *Human molecular genetics*. 2004 Apr 15;13(8):807-17. PubMed PMID: 14976165. Epub 2004/02/21. eng.
152. Tokunaga F, Iwai K. Linear ubiquitination: a novel NF-kappaB regulatory mechanism for inflammatory and immune responses by the LUBAC ubiquitin ligase complex. *Endocrine journal*. 2012;59(8):641-52. PubMed PMID: 22673407. Epub 2012/06/08. eng.
153. Rudner AD, Murray AW. Phosphorylation by Cdc28 activates the Cdc20-dependent activity of the anaphase-promoting complex. *The Journal of cell biology*. 2000 Jun 26;149(7):1377-90. PubMed PMID: 10871279. Pubmed Central PMCID: PMC2175139. Epub 2000/06/28. eng.
154. Lamothe B, Besse A, Campos AD, Webster WK, Wu H, Darnay BG. Site-specific Lys-63-linked tumor necrosis factor receptor-associated factor 6 auto-ubiquitination is a critical determinant of I kappa B kinase activation. *The Journal of biological chemistry*. 2007 Feb 9;282(6):4102-12. PubMed PMID: 17135271. Pubmed Central PMCID: PMC3221607. Epub 2006/12/01. eng.

155. Deshaies RJ. SCF and Cullin/Ring H2-based ubiquitin ligases. *Annual review of cell and developmental biology*. 1999;15:435-67. PubMed PMID: 10611969. Epub 1999/12/28. eng.
156. Lecker SH, Goldberg AL, Mitch WE. Protein degradation by the ubiquitin-proteasome pathway in normal and disease states. *Journal of the American Society of Nephrology : JASN*. 2006 Jul;17(7):1807-19. PubMed PMID: 16738015. Epub 2006/06/02. eng.
157. Mitch WE, Goldberg AL. Mechanisms of muscle wasting. The role of the ubiquitin-proteasome pathway. *The New England journal of medicine*. 1996 Dec 19;335(25):1897-905. PubMed PMID: 8948566. Epub 1996/12/19. eng.
158. Bignell GR, Warren W, Seal S, Takahashi M, Rapley E, Barfoot R, Green H, Brown C, Biggs PJ, Lakhani SR, Jones C, Hansen J, Blair E, Hofmann B, Siebert R, Turner G, Evans DG, Schrandt-Stumpel C, Beemer FA, van Den Ouweland A, Halley D, Delpech B, Cleveland MG, Leigh I, Leisti J, Rasmussen S. Identification of the familial cylindromatosis tumour-suppressor gene. *Nature genetics*. 2000 Jun;25(2):160-5. PubMed PMID: 10835629. Epub 2000/06/03. eng.
159. Hymowitz SG, Wertz IE. A20: from ubiquitin editing to tumour suppression. *Nature reviews Cancer*. 2010 May;10(5):332-41. PubMed PMID: 20383180. Epub 2010/04/13. eng.
160. Popovic D, Vucic D, Dikic I. Ubiquitination in disease pathogenesis and treatment. *Nature medicine*. 2014 Nov;20(11):1242-53. PubMed PMID: 25375928. Epub 2014/11/07. Eng.
161. Schwartz AL, Ciechanover A. Targeting proteins for destruction by the ubiquitin system: implications for human pathobiology. *Annual review of pharmacology and toxicology*. 2009;49:73-96. PubMed PMID: 18834306. Epub 2008/10/07. eng.
162. Muratani M, Tansey WP. How the ubiquitin-proteasome system controls transcription. *Nature reviews Molecular cell biology*. 2003 Mar;4(3):192-201. PubMed PMID: 12612638. Epub 2003/03/04. eng.
163. Lipford JR, Smith GT, Chi Y, Deshaies RJ. A putative stimulatory role for activator turnover in gene expression. *Nature*. 2005 Nov 3;438(7064):113-6. PubMed PMID: 16267558. Epub 2005/11/04. eng.
164. Karin M, Ben-Neriah Y. Phosphorylation meets ubiquitination: the control of NF-[kappa]B activity. *Annual review of immunology*. 2000;18:621-63. PubMed PMID: 10837071. Epub 2000/06/03. eng.
165. Hicke L, Dunn R. Regulation of membrane protein transport by ubiquitin and ubiquitin-binding proteins. *Annual review of cell and developmental biology*. 2003;19:141-72. PubMed PMID: 14570567. Epub 2003/10/23. eng.

166. Sigismund S, Polo S, Di Fiore PP. Signaling through monoubiquitination. *Current topics in microbiology and immunology*. 2004;286:149-85. PubMed PMID: 15645713. Epub 2005/01/14. eng.
167. Nijman SM, Luna-Vargas MP, Velds A, Brummelkamp TR, Dirac AM, Sixma TK, Bernards R. A genomic and functional inventory of deubiquitinating enzymes. *Cell*. 2005 Dec 2;123(5):773-86. PubMed PMID: 16325574. Epub 2005/12/06. eng.
168. Sulea T, Lindner HA, Menard R. Structural aspects of recently discovered viral deubiquitinating activities. *Biological chemistry*. 2006 Jul;387(7):853-62. PubMed PMID: 16913834. Epub 2006/08/18. eng.
169. Lindner HA. Deubiquitination in virus infection. *Virology*. 2007 Jun 5;362(2):245-56. PubMed PMID: 17291557. Epub 2007/02/13. eng.
170. Rawlings ND, Tolle DP, Barrett AJ. MEROPS: the peptidase database. *Nucleic acids research*. 2004 Jan 1;32(Database issue):D160-4. PubMed PMID: 14681384. Pubmed Central PMCID: PMC308805. Epub 2003/12/19. eng.
171. de Bie P, Ciechanover A. Ubiquitination of E3 ligases: self-regulation of the ubiquitin system via proteolytic and non-proteolytic mechanisms. *Cell death and differentiation*. 2011 Sep;18(9):1393-402. PubMed PMID: 21372847. Pubmed Central PMCID: PMC3178436. Epub 2011/03/05. eng.
172. Sun SC. CYLD: a tumor suppressor deubiquitinase regulating NF-kappaB activation and diverse biological processes. *Cell death and differentiation*. 2010 Jan;17(1):25-34. PubMed PMID: 19373246. Epub 2009/04/18. eng.
173. Boone DL, Turer EE, Lee EG, Ahmad RC, Wheeler MT, Tsui C, Hurley P, Chien M, Chai S, Hitotsumatsu O, McNally E, Pickart C, Ma A. The ubiquitin-modifying enzyme A20 is required for termination of Toll-like receptor responses. *Nature immunology*. 2004 Oct;5(10):1052-60. PubMed PMID: 15334086. Epub 2004/08/31. eng.
174. Wertz IE, O'Rourke KM, Zhou H, Eby M, Aravind L, Seshagiri S, Wu P, Wiesmann C, Baker R, Boone DL, Ma A, Koonin EV, Dixit VM. De-ubiquitination and ubiquitin ligase domains of A20 downregulate NF-kappaB signalling. *Nature*. 2004 Aug 5;430(7000):694-9. PubMed PMID: 15258597. Epub 2004/07/20. eng.
175. Dey A, Seshasayee D, Noubade R, French DM, Liu J, Chaurushiya MS, Kirkpatrick DS, Pham VC, Lill JR, Bakalarski CE, Wu J, Phu L, Katavolos P, LaFave LM, Abdel-Wahab O, Modrusan Z, Seshagiri S, Dong K, Lin Z, Balazs M, Suriben R, Newton K, Hymowitz S, Garcia-Manero G, Martin F, Levine RL, Dixit VM. Loss of the tumor suppressor BAP1 causes myeloid transformation. *Science (New York, NY)*. 2012 Sep 21;337(6101):1541-6. PubMed PMID: 22878500. Epub 2012/08/11. eng.

176. Schrader EK, Harstad KG, Matouschek A. Targeting proteins for degradation. *Nature chemical biology*. 2009 Nov;5(11):815-22. PubMed PMID: 19841631. Pubmed Central PMCID: PMC4228941. Epub 2009/10/21. eng.
177. Finley D. Recognition and processing of ubiquitin-protein conjugates by the proteasome. *Annual review of biochemistry*. 2009;78:477-513. PubMed PMID: 19489727. Pubmed Central PMCID: PMC3431160. Epub 2009/06/06. eng.
178. Groll M, Ditzel L, Lowe J, Stock D, Bochtler M, Bartunik HD, Huber R. Structure of 20S proteasome from yeast at 2.4 Å resolution. *Nature*. 1997 Apr 3;386(6624):463-71. PubMed PMID: 9087403. Epub 1997/04/03. eng.
179. Whitby FG, Masters EI, Kramer L, Knowlton JR, Yao Y, Wang CC, Hill CP. Structural basis for the activation of 20S proteasomes by 11S regulators. *Nature*. 2000 Nov 2;408(6808):115-20. PubMed PMID: 11081519. Epub 2000/11/18. eng.
180. Glickman MH, Ciechanover A. The ubiquitin-proteasome proteolytic pathway: destruction for the sake of construction. *Physiological reviews*. 2002 Apr;82(2):373-428. PubMed PMID: 11917093. Epub 2002/03/28. eng.
181. Kisselev AF, Akopian TN, Woo KM, Goldberg AL. The sizes of peptides generated from protein by mammalian 26 and 20 S proteasomes. Implications for understanding the degradative mechanism and antigen presentation. *The Journal of biological chemistry*. 1999 Feb 5;274(6):3363-71. PubMed PMID: 9920878. Epub 1999/01/28. eng.
182. Dahlmann B. Proteasomes. *Essays in biochemistry*. 2005;41:31-48. PubMed PMID: 16250896. Epub 2005/10/28. eng.
183. de Bettignies G, Coux O. Proteasome inhibitors: Dozens of molecules and still counting. *Biochimie*. 2010 Nov;92(11):1530-45. PubMed PMID: 20615448. Epub 2010/07/10. eng.
184. Tsukamoto S, Yokosawa H. Targeting the proteasome pathway. *Expert opinion on therapeutic targets*. 2009 May;13(5):605-21. PubMed PMID: 19397479. Epub 2009/04/29. eng.
185. Rock KL, Gramm C, Rothstein L, Clark K, Stein R, Dick L, Hwang D, Goldberg AL. Inhibitors of the proteasome block the degradation of most cell proteins and the generation of peptides presented on MHC class I molecules. *Cell*. 1994 Sep 9;78(5):761-71. PubMed PMID: 8087844. Epub 1994/09/09. eng.
186. Merin NM, Kelly KR. Clinical use of proteasome inhibitors in the treatment of multiple myeloma. *Pharmaceuticals (Basel, Switzerland)*. 2014;8(1):1-20. PubMed PMID: 25545164. Epub 2014/12/30. eng.

187. Niewerth D, Dingjan I, Cloos J, Jansen G, Kaspers G. Proteasome inhibitors in acute leukemia. Expert review of anticancer therapy. 2013 Mar;13(3):327-37. PubMed PMID: 23477519. Epub 2013/03/13. eng.
188. Delboy MG, Roller DG, Nicola AV. Cellular proteasome activity facilitates herpes simplex virus entry at a postpenetration step. Journal of virology. 2008 Apr;82(7):3381-90. PubMed PMID: 18234803. Pubmed Central PMCID: PMC2268500. Epub 2008/02/01. eng.
189. Tran K, Mahr JA, Spector DH. Proteasome subunits relocalize during human cytomegalovirus infection, and proteasome activity is necessary for efficient viral gene transcription. Journal of virology. 2010 Mar;84(6):3079-93. PubMed PMID: 20042513. Pubmed Central PMCID: PMC2826056. Epub 2010/01/01. eng.
190. Bandi P, Garcia ML, Booth CJ, Chisari FV, Robek MD. Bortezomib inhibits hepatitis B virus replication in transgenic mice. Antimicrobial agents and chemotherapy. 2010 Feb;54(2):749-56. PubMed PMID: 19949053. Pubmed Central PMCID: PMC2812171. Epub 2009/12/02. eng.
191. Gupta A, Jha S, Engel DA, Ornelles DA, Dutta A. Tip60 degradation by adenovirus relieves transcriptional repression of viral transcriptional activator E1A. Oncogene. 2013 Oct 17;32(42):5017-25. PubMed PMID: 23178490. Pubmed Central PMCID: PMC3955737. Epub 2012/11/28. eng.
192. Widjaja I, de Vries E, Tscherne DM, Garcia-Sastre A, Rottier PJ, de Haan CA. Inhibition of the ubiquitin-proteasome system affects influenza A virus infection at a postfusion step. Journal of virology. 2010 Sep;84(18):9625-31. PubMed PMID: 20631148. Pubmed Central PMCID: PMC2937638. Epub 2010/07/16. eng.
193. Schubert U, Ott DE, Chertova EN, Welker R, Tessmer U, Princiotta MF, Bennink JR, Krausslich HG, Yewdell JW. Proteasome inhibition interferes with gag polyprotein processing, release, and maturation of HIV-1 and HIV-2. Proceedings of the National Academy of Sciences of the United States of America. 2000 Nov 21;97(24):13057-62. PubMed PMID: 11087859. Pubmed Central PMCID: PMC27177. Epub 2000/11/23. eng.
194. Strack B, Calistri A, Accola MA, Palu G, Gottlinger HG. A role for ubiquitin ligase recruitment in retrovirus release. Proceedings of the National Academy of Sciences of the United States of America. 2000 Nov 21;97(24):13063-8. PubMed PMID: 11087860. Pubmed Central PMCID: PMC27178. Epub 2000/11/23. eng.
195. Ott DE, Coren LV, Sowder RC, 2nd, Adams J, Schubert U. Retroviruses have differing requirements for proteasome function in the budding process. Journal of virology. 2003 Mar;77(6):3384-93. PubMed PMID: 12610113. Pubmed Central PMCID: PMC149504. Epub 2003/03/01. eng.
196. Yu GY, Lai MM. The ubiquitin-proteasome system facilitates the transfer of murine coronavirus from endosome to cytoplasm during virus entry. Journal of virology.

2005 Jan;79(1):644-8. PubMed PMID: 15596861. Pubmed Central PMCID: PMC538694. Epub 2004/12/15. eng.

197. Lupfer C, Pastey MK. Decreased replication of human respiratory syncytial virus treated with the proteasome inhibitor MG-132. *Virus research*. 2010 Apr;149(1):36-41. PubMed PMID: 20080137. Epub 2010/01/19. eng.

198. Si X, Gao G, Wong J, Wang Y, Zhang J, Luo H. Ubiquitination is required for effective replication of coxsackievirus B3. *PloS one*. 2008;3(7):e2585. PubMed PMID: 18612413. Pubmed Central PMCID: PMC2440516. Epub 2008/07/10. eng.

199. Lopez T, Silva-Ayala D, Lopez S, Arias CF. Replication of the rotavirus genome requires an active ubiquitin-proteasome system. *Journal of virology*. 2011 Nov;85(22):11964-71. PubMed PMID: 21900156. Pubmed Central PMCID: PMC3209302. Epub 2011/09/09. eng.

200. Sarkari F, Sanchez-Alcaraz T, Wang S, Holowaty MN, Sheng Y, Frappier L. EBNA1-mediated recruitment of a histone H2B deubiquitylating complex to the Epstein-Barr virus latent origin of DNA replication. *PLoS pathogens*. 2009 Oct;5(10):e1000624. PubMed PMID: 19834552. Pubmed Central PMCID: PMC2757719. Epub 2009/10/17. eng.

201. Bres V, Kiernan RE, Linares LK, Chable-Bessia C, Plechakova O, Treand C, Emiliani S, Peloponese JM, Jeang KT, Coux O, Scheffner M, Benkirane M. A non-proteolytic role for ubiquitin in Tat-mediated transactivation of the HIV-1 promoter. *Nature cell biology*. 2003 Aug;5(8):754-61. PubMed PMID: 12883554. Epub 2003/07/29. eng.

202. Peloponese JM, Jr., Iha H, Yedavalli VR, Miyazato A, Li Y, Haller K, Benkirane M, Jeang KT. Ubiquitination of human T-cell leukemia virus type 1 tax modulates its activity. *Journal of virology*. 2004 Nov;78(21):11686-95. PubMed PMID: 15479810. Pubmed Central PMCID: PMC523283. Epub 2004/10/14. eng.

203. Ikeda M, Ikeda A, Longan LC, Longnecker R. The Epstein-Barr virus latent membrane protein 2A PY motif recruits WW domain-containing ubiquitin-protein ligases. *Virology*. 2000 Mar 1;268(1):178-91. PubMed PMID: 10683340. Epub 2000/02/23. eng.

204. Ning S, Pagano JS. The A20 deubiquitinase activity negatively regulates LMP1 activation of IRF7. *Journal of virology*. 2010 Jun;84(12):6130-8. PubMed PMID: 20392859. Pubmed Central PMCID: PMC2876664. Epub 2010/04/16. eng.

205. Oudshoorn D, Versteeg GA, Kikkert M. Regulation of the innate immune system by ubiquitin and ubiquitin-like modifiers. *Cytokine & growth factor reviews*. 2012 Dec;23(6):273-82. PubMed PMID: 22964110. Epub 2012/09/12. eng.

206. Bhoj VG, Chen ZJ. Ubiquitylation in innate and adaptive immunity. *Nature*. 2009 Mar 26;458(7237):430-7. PubMed PMID: 19325622. Epub 2009/03/28. eng.

207. Banks L, Pim D, Thomas M. Viruses and the 26S proteasome: hacking into destruction. *Trends in biochemical sciences*. 2003 Aug;28(8):452-9. PubMed PMID: 12932734. Epub 2003/08/23. eng.
208. Barry M, Fruh K. Viral modulators of cullin RING ubiquitin ligases: culling the host defense. *Science's STKE : signal transduction knowledge environment*. 2006 May 16;2006(335):pe21. PubMed PMID: 16705129. Epub 2006/05/18. eng.
209. Blanchette P, Branton PE. Manipulation of the ubiquitin-proteasome pathway by small DNA tumor viruses. *Virology*. 2009 Feb 20;384(2):317-23. PubMed PMID: 19013629. Epub 2008/11/18. eng.
210. Chen M, Gerlier D. Viral hijacking of cellular ubiquitination pathways as an anti-innate immunity strategy. *Viral immunology*. 2006 Summer;19(3):349-62. PubMed PMID: 16987055. Epub 2006/09/22. eng.
211. Isaacson MK, Ploegh HL. Ubiquitination, ubiquitin-like modifiers, and deubiquitination in viral infection. *Cell host & microbe*. 2009 Jun 18;5(6):559-70. PubMed PMID: 19527883. Epub 2009/06/17. eng.
212. Randow F, Lehner PJ. Viral avoidance and exploitation of the ubiquitin system. *Nature cell biology*. 2009 May;11(5):527-34. PubMed PMID: 19404332. Epub 2009/05/01. eng.
213. Boname JM, Lehner PJ. What has the study of the K3 and K5 viral ubiquitin E3 ligases taught us about ubiquitin-mediated receptor regulation? *Viruses*. 2011 Feb;3(2):118-31. PubMed PMID: 22049306. Pubmed Central PMCID: PMC3206601. Epub 2011/11/04. eng.
214. Coscoy L, Ganem D. A viral protein that selectively downregulates ICAM-1 and B7-2 and modulates T cell costimulation. *The Journal of clinical investigation*. 2001 Jun;107(12):1599-606. PubMed PMID: 11413168. Pubmed Central PMCID: PMC200195. Epub 2001/06/20. eng.
215. Boutell C, Sadis S, Everett RD. Herpes simplex virus type 1 immediate-early protein ICP0 and its isolated RING finger domain act as ubiquitin E3 ligases in vitro. *Journal of virology*. 2002 Jan;76(2):841-50. PubMed PMID: 11752173. Pubmed Central PMCID: PMC136846. Epub 2001/12/26. eng.
216. Gu H, Roizman B. The two functions of herpes simplex virus 1 ICP0, inhibition of silencing by the CoREST/REST/HDAC complex and degradation of PML, are executed in tandem. *Journal of virology*. 2009 Jan;83(1):181-7. PubMed PMID: 18945770. Pubmed Central PMCID: PMC2612314. Epub 2008/10/24. eng.
217. Everett RD, Meredith M, Orr A, Cross A, Kathoria M, Parkinson J. A novel ubiquitin-specific protease is dynamically associated with the PML nuclear domain and binds to a herpesvirus regulatory protein. *The EMBO journal*. 1997 Apr 1;16(7):1519-30.

PubMed PMID: 9130697. Pubmed Central PMCID: PMC1169756. Epub 1997/04/01. eng.

218. Holowaty MN, Frappier L. HAUSP/USP7 as an Epstein-Barr virus target. *Biochemical Society transactions*. 2004 Nov;32(Pt 5):731-2. PubMed PMID: 15494000. Epub 2004/10/21. eng.

219. Li M, Chen D, Shiloh A, Luo J, Nikolaev AY, Qin J, Gu W. Deubiquitination of p53 by HAUSP is an important pathway for p53 stabilization. *Nature*. 2002 Apr 11;416(6881):648-53. PubMed PMID: 11923872. Epub 2002/03/30. eng.

220. Canning M, Boutell C, Parkinson J, Everett RD. A RING finger ubiquitin ligase is protected from autocatalyzed ubiquitination and degradation by binding to ubiquitin-specific protease USP7. *The Journal of biological chemistry*. 2004 Sep 10;279(37):38160-8. PubMed PMID: 15247261. Epub 2004/07/13. eng.

221. Ovaa H, Kessler BM, Rolen U, Galardy PJ, Ploegh HL, Masucci MG. Activity-based ubiquitin-specific protease (USP) profiling of virus-infected and malignant human cells. *Proceedings of the National Academy of Sciences of the United States of America*. 2004 Feb 24;101(8):2253-8. PubMed PMID: 14982996. Pubmed Central PMCID: PMC356937. Epub 2004/02/26. eng.

222. Yokota S, Okabayashi T, Yokosawa N, Fujii N. Measles virus P protein suppresses Toll-like receptor signal through up-regulation of ubiquitin-modifying enzyme A20. *FASEB journal : official publication of the Federation of American Societies for Experimental Biology*. 2008 Jan;22(1):74-83. PubMed PMID: 17720800. Epub 2007/08/28. eng.

223. Kattenhorn LM, Korbel GA, Kessler BM, Spooner E, Ploegh HL. A deubiquitinating enzyme encoded by HSV-1 belongs to a family of cysteine proteases that is conserved across the family Herpesviridae. *Molecular cell*. 2005 Aug 19;19(4):547-57. PubMed PMID: 16109378. Epub 2005/08/20. eng.

224. Schlieker C, Weihofen WA, Frijns E, Kattenhorn LM, Gaudet R, Ploegh HL. Structure of a herpesvirus-encoded cysteine protease reveals a unique class of deubiquitinating enzymes. *Molecular cell*. 2007 Mar 9;25(5):677-87. PubMed PMID: 17349955. Epub 2007/03/14. eng.

225. Schlieker C, Korbel GA, Kattenhorn LM, Ploegh HL. A deubiquitinating activity is conserved in the large tegument protein of the herpesviridae. *Journal of virology*. 2005 Dec;79(24):15582-5. PubMed PMID: 16306630. Pubmed Central PMCID: PMC1316044. Epub 2005/11/25. eng.

226. Wang J, Loveland AN, Kattenhorn LM, Ploegh HL, Gibson W. High-molecular-weight protein (pUL48) of human cytomegalovirus is a competent deubiquitinating protease: mutant viruses altered in its active-site cysteine or histidine are viable. *Journal of virology*. 2006 Jun;80(12):6003-12. PubMed PMID: 16731939. Pubmed Central PMCID: PMC1472576. Epub 2006/05/30. eng.

227. Chung CS, Chen CH, Ho MY, Huang CY, Liao CL, Chang W. Vaccinia virus proteome: identification of proteins in vaccinia virus intracellular mature virion particles. *Journal of virology*. 2006 Mar;80(5):2127-40. PubMed PMID: 16474121. Pubmed Central PMCID: PMC1395410. Epub 2006/02/14. eng.
228. Webb JH, Mayer RJ, Dixon LK. A lipid modified ubiquitin is packaged into particles of several enveloped viruses. *FEBS letters*. 1999 Feb 5;444(1):136-9. PubMed PMID: 10037162. Epub 1999/02/26. eng.
229. Zhang L, Villa NY, McFadden G. Interplay between poxviruses and the cellular ubiquitin/ubiquitin-like pathways. *FEBS letters*. 2009 Feb 18;583(4):607-14. PubMed PMID: 19174161. Epub 2009/01/29. eng.
230. Barry M, Lee SF, Boshkov L, McFadden G. Myxoma virus induces extensive CD4 downregulation and dissociation of p56lck in infected rabbit CD4+ T lymphocytes. *Journal of virology*. 1995 Sep;69(9):5243-51. PubMed PMID: 7636966. Pubmed Central PMCID: PMC189357. Epub 1995/09/01. eng.
231. Bartee E, McCormack A, Fruh K. Quantitative membrane proteomics reveals new cellular targets of viral immune modulators. *PLoS pathogens*. 2006 Oct;2(10):e107. PubMed PMID: 17238276. Pubmed Central PMCID: PMC1626102. Epub 2007/01/24. eng.
232. Zuniga MC, Wang H, Barry M, McFadden G. Endosomal/lysosomal retention and degradation of major histocompatibility complex class I molecules is induced by myxoma virus. *Virology*. 1999 Sep 1;261(2):180-92. PubMed PMID: 10497104. Epub 1999/09/25. eng.
233. Barry M, van Buuren N, Burles K, Mottet K, Wang Q, Teale A. Poxvirus exploitation of the ubiquitin-proteasome system. *Viruses*. 2010 Oct;2(10):2356-80. PubMed PMID: 21994622. Pubmed Central PMCID: PMC3185573. Epub 2011/10/14. eng.
234. Mo M, Fleming SB, Mercer AA. Cell cycle deregulation by a poxvirus partial mimic of anaphase-promoting complex subunit 11. *Proceedings of the National Academy of Sciences of the United States of America*. 2009 Nov 17;106(46):19527-32. PubMed PMID: 19887645. Pubmed Central PMCID: PMC2780751. Epub 2009/11/06. eng.
235. van Buuren N, Couturier B, Xiong Y, Barry M. Ectromelia virus encodes a novel family of F-box proteins that interact with the SCF complex. *Journal of virology*. 2008 Oct;82(20):9917-27. PubMed PMID: 18684824. Pubmed Central PMCID: PMC2566254. Epub 2008/08/08. eng.
236. Burles K, van Buuren N, Barry M. Ectromelia virus encodes a family of Ankyrin/F-box proteins that regulate NFkappaB. *Virology*. 2014 Nov;468-470:351-62. PubMed PMID: 25240225. Epub 2014/09/23. eng.

237. van Buuren N, Burles K, Schriewer J, Mehta N, Parker S, Buller RM, Barry M. EVM005: an ectromelia-encoded protein with dual roles in NF-kappaB inhibition and virulence. *PLoS pathogens*. 2014 Aug;10(8):e1004326. PubMed PMID: 25122471. Pubmed Central PMCID: PMC4133408. Epub 2014/08/15. eng.
238. Chen N, Danila MI, Feng Z, Buller RM, Wang C, Han X, Lefkowitz EJ, Upton C. The genomic sequence of ectromelia virus, the causative agent of mousepox. *Virology*. 2003 Dec 5;317(1):165-86. PubMed PMID: 14675635. Epub 2003/12/17. eng.
239. Shchelkunov S, Totmenin A, Kolosova I. Species-specific differences in organization of orthopoxvirus kelch-like proteins. *Virus genes*. 2002 Mar;24(2):157-62. PubMed PMID: 12018707. Epub 2002/05/23. eng.
240. Wilton BA, Campbell S, Van Buuren N, Garneau R, Furukawa M, Xiong Y, Barry M. Ectromelia virus BTB/kelch proteins, EVM150 and EVM167, interact with cullin-3-based ubiquitin ligases. *Virology*. 2008 Apr 25;374(1):82-99. PubMed PMID: 18221766. Pubmed Central PMCID: PMC2441824. Epub 2008/01/29. eng.
241. Wang Q, Burles K, Couturier B, Randall CM, Shisler J, Barry M. Ectromelia virus encodes a BTB/kelch protein, EVM150, that inhibits NF-kappaB signaling. *Journal of virology*. 2014 May;88(9):4853-65. PubMed PMID: 24522926. Pubmed Central PMCID: PMC3993801. Epub 2014/02/14. eng.
242. Huang J, Huang Q, Zhou X, Shen MM, Yen A, Yu SX, Dong G, Qu K, Huang P, Anderson EM, Daniel-Issakani S, Buller RM, Payan DG, Lu HH. The poxvirus p28 virulence factor is an E3 ubiquitin ligase. *The Journal of biological chemistry*. 2004 Dec 24;279(52):54110-6. PubMed PMID: 15496420. Epub 2004/10/22. eng.
243. Nerenberg BT, Taylor J, Bartee E, Gouveia K, Barry M, Fruh K. The poxviral RING protein p28 is a ubiquitin ligase that targets ubiquitin to viral replication factories. *Journal of virology*. 2005 Jan;79(1):597-601. PubMed PMID: 15596852. Pubmed Central PMCID: PMC538746. Epub 2004/12/15. eng.
244. Senkevich TG, Koonin EV, Buller RM. A poxvirus protein with a RING zinc finger motif is of crucial importance for virulence. *Virology*. 1994 Jan;198(1):118-28. PubMed PMID: 8259647. Epub 1994/01/01. eng.
245. Senkevich TG, Wolffe EJ, Buller RM. Ectromelia virus RING finger protein is localized in virus factories and is required for virus replication in macrophages. *Journal of virology*. 1995 Jul;69(7):4103-11. PubMed PMID: 7769668. Pubmed Central PMCID: PMC189145. Epub 1995/07/01. eng.
246. Iyer LM, Koonin EV, Aravind L. Extensive domain shuffling in transcription regulators of DNA viruses and implications for the origin of fungal APSES transcription factors. *Genome biology*. 2002;3(3):RESEARCH0012. PubMed PMID: 11897024. Pubmed Central PMCID: PMC88810. Epub 2002/03/19. eng.

247. Brick DJ, Burke RD, Schiff L, Upton C. Shope fibroma virus RING finger protein N1R binds DNA and inhibits apoptosis. *Virology*. 1998 Sep 15;249(1):42-51. PubMed PMID: 9740775. Epub 1998/09/19. eng.
248. Brick DJ, Burke RD, Minkley AA, Upton C. Ectromelia virus virulence factor p28 acts upstream of caspase-3 in response to UV light-induced apoptosis. *The Journal of general virology*. 2000 Apr;81(Pt 4):1087-97. PubMed PMID: 10725436. Epub 2000/03/22. eng.
249. Upton C, Schiff L, Rice SA, Dowdeswell T, Yang X, McFadden G. A poxvirus protein with a RING finger motif binds zinc and localizes in virus factories. *Journal of virology*. 1994 Jul;68(7):4186-95. PubMed PMID: 8207794. Pubmed Central PMCID: PMC236341. Epub 1994/07/01. eng.
250. Fuerst TR, Niles EG, Studier FW, Moss B. Eukaryotic transient-expression system based on recombinant vaccinia virus that synthesizes bacteriophage T7 RNA polymerase. *Proceedings of the National Academy of Sciences of the United States of America*. 1986 Nov;83(21):8122-6. PubMed PMID: 3095828. Pubmed Central PMCID: PMC386879. Epub 1986/11/01. eng.
251. Fuerst TR, Earl PL, Moss B. Use of a hybrid vaccinia virus-T7 RNA polymerase system for expression of target genes. *Molecular and cellular biology*. 1987 Jul;7(7):2538-44. PubMed PMID: 3112559. Pubmed Central PMCID: PMC365388. Epub 1987/07/01. eng.
252. Stuart D, Graham K, Schreiber M, Macaulay C, McFadden G. The target DNA sequence for resolution of poxvirus replicative intermediates is an active late promoter. *Journal of virology*. 1991 Jan;65(1):61-70. PubMed PMID: 1845909. Pubmed Central PMCID: PMC240489. Epub 1991/01/01. eng.
253. Meng X, Embry A, Sochia D, Xiang Y. Vaccinia virus A6L encodes a virion core protein required for formation of mature virion. *Journal of virology*. 2007 Feb;81(3):1433-43. PubMed PMID: 17108027. Pubmed Central PMCID: PMC1797496. Epub 2006/11/17. eng.
254. Sabara MI, Larence JE. Plaque assay for avian metapneumovirus using a Japanese quail fibrosarcoma cell line (QT-35). *Journal of virological methods*. 2003 Jan;107(1):9-14. PubMed PMID: 12445932. Epub 2002/11/26. eng.
255. Furukawa M, Ohta T, Xiong Y. Activation of UBC5 ubiquitin-conjugating enzyme by the RING finger of ROC1 and assembly of active ubiquitin ligases by all cullins. *The Journal of biological chemistry*. 2002 May 3;277(18):15758-65. PubMed PMID: 11861641. Epub 2002/02/28. eng.
256. Huang DW, Sherman BT, Tan Q, Kir J, Liu D, Bryant D, Guo Y, Stephens R, Baseler MW, Lane HC, Lempicki RA. DAVID Bioinformatics Resources: expanded annotation database and novel algorithms to better extract biology from large gene lists.

Nucleic acids research. 2007 Jul;35(Web Server issue):W169-75. PubMed PMID: 17576678. Pubmed Central PMCID: PMC1933169. Epub 2007/06/20. eng.

257. Chenna R, Sugawara H, Koike T, Lopez R, Gibson TJ, Higgins DG, Thompson JD. Multiple sequence alignment with the Clustal series of programs. Nucleic acids research. 2003 Jul 1;31(13):3497-500. PubMed PMID: 12824352. Pubmed Central PMCID: PMC168907. Epub 2003/06/26. eng.

258. Nicholas HB, Jr., Graves SB. Clustering of transfer RNAs by cell type and amino acid specificity. Journal of molecular biology. 1983 Dec 5;171(2):111-8. PubMed PMID: 6655689. Epub 1983/12/05. eng.

259. Nicholas HB, Jr., McClain WH. Searching tRNA sequences for relatedness to aminoacyl-tRNA synthetase families. Journal of molecular evolution. 1995 May;40(5):482-6. PubMed PMID: 7783223. Epub 1995/05/01. eng.

260. Weli SC, Tryland M. Avipoxviruses: infection biology and their use as vaccine vectors. Virology journal. 2011;8:49. PubMed PMID: 21291547. Pubmed Central PMCID: PMC3042955. Epub 2011/02/05. eng.

261. Petroski MD, Deshaies RJ. Mechanism of lysine 48-linked ubiquitin-chain synthesis by the cullin-RING ubiquitin-ligase complex SCF-Cdc34. Cell. 2005 Dec 16;123(6):1107-20. PubMed PMID: 16360039. Epub 2005/12/20. eng.

262. Somogyi P, Frazier J, Skinner MA. Fowlpox virus host range restriction: gene expression, DNA replication, and morphogenesis in nonpermissive mammalian cells. Virology. 1993 Nov;197(1):439-44. PubMed PMID: 8212580. Epub 1993/11/01. eng.

263. Yang Y, Yu X. Regulation of apoptosis: the ubiquitous way. FASEB journal : official publication of the Federation of American Societies for Experimental Biology. 2003 May;17(8):790-9. PubMed PMID: 12724336. Epub 2003/05/02. eng.

264. Wu H, Tschopp J, Lin SC. Smac mimetics and TNFalpha: a dangerous liaison? Cell. 2007 Nov 16;131(4):655-8. PubMed PMID: 18022360. Pubmed Central PMCID: PMC3184251. Epub 2007/11/21. eng.

265. Meek DW, Knippschild U. Posttranslational modification of MDM2. Molecular cancer research : MCR. 2003 Dec;1(14):1017-26. PubMed PMID: 14707285. Epub 2004/01/07. eng.

266. Lorick KL, Jensen JP, Fang S, Ong AM, Hatakeyama S, Weissman AM. RING fingers mediate ubiquitin-conjugating enzyme (E2)-dependent ubiquitination. Proceedings of the National Academy of Sciences of the United States of America. 1999 Sep 28;96(20):11364-9. PubMed PMID: 10500182. Pubmed Central PMCID: PMC18039. Epub 1999/09/29. eng.

267. Morita E, Sandrin V, McCullough J, Katsuyama A, Baci Hamilton I, Sundquist WI. ESCRT-III protein requirements for HIV-1 budding. Cell host & microbe. 2011 Mar

17;9(3):235-42. PubMed PMID: 21396898. Pubmed Central PMCID: PMC3070458. Epub 2011/03/15. eng.

268. Everett RD. ICP0, a regulator of herpes simplex virus during lytic and latent infection. *BioEssays : news and reviews in molecular, cellular and developmental biology*. 2000 Aug;22(8):761-70. PubMed PMID: 10918307. Epub 2000/08/05. eng.

269. Mercer AA, Fleming SB, Ueda N. F-box-like domains are present in most poxvirus ankyrin repeat proteins. *Virus Genes*. 2005 Oct;31(2):127-33. PubMed PMID: 16025237. Epub 2005/07/19. eng.

270. Johnston JB, Wang G, Barrett JW, Nazarian SH, Colwill K, Moran M, McFadden G. Myxoma virus M-T5 protects infected cells from the stress of cell cycle arrest through its interaction with host cell cullin-1. *J Virol*. 2005 Aug;79(16):10750-63. PubMed PMID: 16051867. Pubmed Central PMCID: 1182661. Epub 2005/07/30. eng.

271. Dettmer S, Theile D, Seckinger A, Burhenne J, Weiss J. Fetal calf sera can distort cell-based luminescent proteasome assays through heat-resistant chymotrypsin-like activity. *Analytical biochemistry*. 2014 Nov 4;471C:23-5. PubMed PMID: 25447494. Epub 2014/12/03. Eng.

272. Chaugule VK, Burchell L, Barber KR, Sidhu A, Leslie SJ, Shaw GS, Walden H. Autoregulation of Parkin activity through its ubiquitin-like domain. *EMBO J*. 2011 Jul 20;30(14):2853-67. PubMed PMID: 21694720. Pubmed Central PMCID: 3160258. Epub 2011/06/23. eng.

273. Dueber EC, Schoeffler AJ, Lingel A, Elliott JM, Fedorova AV, Giannetti AM, Zobel K, Maurer B, Varfolomeev E, Wu P, Wallweber HJ, Hymowitz SG, Deshayes K, Vucic D, Fairbrother WJ. Antagonists induce a conformational change in cIAP1 that promotes autoubiquitination. *Science*. 2011 Oct 21;334(6054):376-80. PubMed PMID: 22021857. Epub 2011/10/25. eng.

274. Scaduto RC, Jr., Grotyohann LW. Measurement of mitochondrial membrane potential using fluorescent rhodamine derivatives. *Biophysical journal*. 1999 Jan;76(1 Pt 1):469-77. PubMed PMID: 9876159. Pubmed Central PMCID: PMC1302536. Epub 1999/01/06. eng.

275. Chang SJ, Hsiao JC, Sonnberg S, Chiang CT, Yang MH, Tzou DL, Mercer AA, Chang W. Poxvirus host range protein CP77 contains an F-box-like domain that is necessary to suppress NF-kappaB activation by tumor necrosis factor alpha but is independent of its host range function. *J Virol*. 2009 May;83(9):4140-52. PubMed PMID: 19211746. Pubmed Central PMCID: 2668469. Epub 2009/02/13. eng.

276. Meng X, Xiang Y. Vaccinia virus K1L protein supports viral replication in human and rabbit cells through a cell-type-specific set of its ankyrin repeat residues that are distinct from its binding site for ACAP2. *Virology*. 2006 Sep 15;353(1):220-33. PubMed PMID: 16806385. Epub 2006/06/30. eng.

277. Mohamed MR, Rahman MM, Lanchbury JS, Shattuck D, Neff C, Dufford M, van Buuren N, Fagan K, Barry M, Smith S, Damon I, McFadden G. Proteomic screening of variola virus reveals a unique NF-kappaB inhibitor that is highly conserved among pathogenic orthopoxviruses. *Proc Natl Acad Sci U S A*. 2009 Jun 2;106(22):9045-50. PubMed PMID: 19451633. Pubmed Central PMCID: 2683884. Epub 2009/05/20. eng.
278. Mohamed MR, Rahman MM, Rice A, Moyer RW, Werden SJ, McFadden G. Cowpox virus expresses a novel ankyrin repeat NF-kappaB inhibitor that controls inflammatory cell influx into virus-infected tissues and is critical for virus pathogenesis. *J Virol*. 2009 Sep;83(18):9223-36. PubMed PMID: 19570875. Pubmed Central PMCID: 2738262. Epub 2009/07/03. eng.
279. Sonnberg S, Seet BT, Pawson T, Fleming SB, Mercer AA. Poxvirus ankyrin repeat proteins are a unique class of F-box proteins that associate with cellular SCF1 ubiquitin ligase complexes. *Proc Natl Acad Sci U S A*. 2008 Aug 5;105(31):10955-60. PubMed PMID: 18667692. Pubmed Central PMCID: 2504846. Epub 2008/08/01. eng.
280. Sperling KM, Schwantes A, Schnierle BS, Sutter G. The highly conserved orthopoxvirus 68k ankyrin-like protein is part of a cellular SCF ubiquitin ligase complex. *Virology*. 2008 May 10;374(2):234-9. PubMed PMID: 18353424. Epub 2008/03/21. eng.
281. Werden SJ, Lanchbury J, Shattuck D, Neff C, Dufford M, McFadden G. The myxoma virus m-t5 ankyrin repeat host range protein is a novel adaptor that coordinately links the cellular signaling pathways mediated by Akt and Skp1 in virus-infected cells. *J Virol*. 2009 Dec;83(23):12068-83. PubMed PMID: 19776120. Pubmed Central PMCID: 2786711. Epub 2009/09/25. eng.
282. Fagan-Garcia K, Barry M. A vaccinia virus deletion mutant reveals the presence of additional inhibitors of NF-kappaB. *Journal of virology*. 2011 Jan;85(2):883-94. PubMed PMID: 20980497. Pubmed Central PMCID: PMC3020013. Epub 2010/10/29. eng.
283. Cameron C, Hota-Mitchell S, Chen L, Barrett J, Cao JX, Macaulay C, Willer D, Evans D, McFadden G. The complete DNA sequence of myxoma virus. *Virology*. 1999 Nov 25;264(2):298-318. PubMed PMID: 10562494. Epub 1999/11/24. eng.
284. Goebel SJ, Johnson GP, Perkus ME, Davis SW, Winslow JP, Paoletti E. The complete DNA sequence of vaccinia virus. *Virology*. 1990 Nov;179(1):247-66, 517-63. PubMed PMID: 2219722. Epub 1990/11/01. eng.
285. Weissman AM, Shabek N, Ciechanover A. The predator becomes the prey: regulating the ubiquitin system by ubiquitylation and degradation. *Nat Rev Mol Cell Biol*. 2011 Sep;12(9):605-20. PubMed PMID: 21860393. Epub 2011/08/24. eng.
286. Magnifico A, Ettenberg S, Yang C, Mariano J, Tiwari S, Fang S, Lipkowitz S, Weissman AM. WW domain HECT E3s target Cbl RING finger E3s for proteasomal degradation. *J Biol Chem*. 2003 Oct 31;278(44):43169-77. PubMed PMID: 12907674. Epub 2003/08/09. eng.

287. Tang J, Qu LK, Zhang J, Wang W, Michaelson JS, Degenhardt YY, El-Deiry WS, Yang X. Critical role for Daxx in regulating Mdm2. *Nat Cell Biol.* 2006 Aug;8(8):855-62. PubMed PMID: 16845383. Epub 2006/07/18. eng.
288. Itahana K, Mao H, Jin A, Itahana Y, Clegg HV, Lindstrom MS, Bhat KP, Godfrey VL, Evan GI, Zhang Y. Targeted inactivation of Mdm2 RING finger E3 ubiquitin ligase activity in the mouse reveals mechanistic insights into p53 regulation. *Cancer Cell.* 2007 Oct;12(4):355-66. PubMed PMID: 17936560. Epub 2007/10/16. eng.
289. Bratke KA, McLysaght A, Rothenburg S. A survey of host range genes in poxvirus genomes. *Infection, genetics and evolution : journal of molecular epidemiology and evolutionary genetics in infectious diseases.* 2013 Mar;14:406-25. PubMed PMID: 23268114. Pubmed Central PMCID: PMC4080715. Epub 2012/12/27. eng.
290. Rubel CE, Schisler JC, Hamlett ED, DeKroon RM, Gautel M, Alzate O, Patterson C. Diggin' on u(biquitin): a novel method for the identification of physiological E3 ubiquitin ligase substrates. *Cell biochemistry and biophysics.* 2013 Sep;67(1):127-38. PubMed PMID: 23695782. Pubmed Central PMCID: PMC3758785. Epub 2013/05/23. eng.
291. Ruan HH, Li Y, Zhang XX, Liu Q, Ren H, Zhang KS, Zhao H. Identification of TRAF6 as a ubiquitin ligase engaged in the ubiquitination of SopB, a virulence effector protein secreted by *Salmonella typhimurium*. *Biochemical and biophysical research communications.* 2014 Apr 25;447(1):172-7. PubMed PMID: 24704445. Epub 2014/04/08. eng.
292. Lee KA, Hammerle LP, Andrews PS, Stokes MP, Mustelin T, Silva JC, Black RA, Doedens JR. Ubiquitin ligase substrate identification through quantitative proteomics at both the protein and peptide levels. *The Journal of biological chemistry.* 2011 Dec 2;286(48):41530-8. PubMed PMID: 21987572. Pubmed Central PMCID: PMC3308864. Epub 2011/10/12. eng.
293. Ungermannova D, Lee J, Zhang G, Dallmann HG, McHenry CS, Liu X. High-throughput screening AlphaScreen assay for identification of small-molecule inhibitors of ubiquitin E3 ligase SCFSkp2-Cks1. *Journal of biomolecular screening.* 2013 Sep;18(8):910-20. PubMed PMID: 23589337. Pubmed Central PMCID: PMC4168015. Epub 2013/04/17. eng.
294. Harper JW, Tan MK. Understanding cullin-RING E3 biology through proteomics-based substrate identification. *Molecular & cellular proteomics : MCP.* 2012 Dec;11(12):1541-50. PubMed PMID: 22962057. Pubmed Central PMCID: PMC3518111. Epub 2012/09/11. eng.
295. Andrews PS, Schneider S, Yang E, Michaels M, Chen H, Tang J, Emkey R. Identification of substrates of SMURF1 ubiquitin ligase activity utilizing protein microarrays. *Assay and drug development technologies.* 2010 Aug;8(4):471-87. PubMed PMID: 20804422. Epub 2010/09/02. eng.

296. Kim W, Bennett EJ, Huttlin EL, Guo A, Li J, Possemato A, Sowa ME, Rad R, Rush J, Comb MJ, Harper JW, Gygi SP. Systematic and quantitative assessment of the ubiquitin-modified proteome. *Molecular cell*. 2011 Oct 21;44(2):325-40. PubMed PMID: 21906983. Pubmed Central PMCID: PMC3200427. Epub 2011/09/13. eng.
297. Kirkpatrick DS, Denison C, Gygi SP. Weighing in on ubiquitin: the expanding role of mass-spectrometry-based proteomics. *Nature cell biology*. 2005 Aug;7(8):750-7. PubMed PMID: 16056266. Pubmed Central PMCID: PMC1224607. Epub 2005/08/02. eng.
298. Lilley CE, Carson CT, Muotri AR, Gage FH, Weitzman MD. DNA repair proteins affect the lifecycle of herpes simplex virus 1. *Proceedings of the National Academy of Sciences of the United States of America*. 2005 Apr 19;102(16):5844-9. PubMed PMID: 15824307. Pubmed Central PMCID: PMC556126. Epub 2005/04/13. eng.
299. Wilkinson DE, Weller SK. Recruitment of cellular recombination and repair proteins to sites of herpes simplex virus type 1 DNA replication is dependent on the composition of viral proteins within prereplicative sites and correlates with the induction of the DNA damage response. *Journal of virology*. 2004 May;78(9):4783-96. PubMed PMID: 15078960. Pubmed Central PMCID: PMC387708. Epub 2004/04/14. eng.
300. Weitzman MD, Carson CT, Schwartz RA, Lilley CE. Interactions of viruses with the cellular DNA repair machinery. *DNA repair*. 2004 Aug-Sep;3(8-9):1165-73. PubMed PMID: 15279805. Epub 2004/07/29. eng.
301. Shi Y, Dodson GE, Shaikh S, Rundell K, Tibbetts RS. Ataxia-telangiectasia-mutated (ATM) is a T-antigen kinase that controls SV40 viral replication in vivo. *The Journal of biological chemistry*. 2005 Dec 2;280(48):40195-200. PubMed PMID: 16221684. Epub 2005/10/14. eng.
302. Shirata N, Kudoh A, Daikoku T, Tatsumi Y, Fujita M, Kiyono T, Sugaya Y, Isomura H, Ishizaki K, Tsurumi T. Activation of ataxia telangiectasia-mutated DNA damage checkpoint signal transduction elicited by herpes simplex virus infection. *The Journal of biological chemistry*. 2005 Aug 26;280(34):30336-41. PubMed PMID: 15964848. Epub 2005/06/21. eng.
303. Dahl J, You J, Benjamin TL. Induction and utilization of an ATM signaling pathway by polyomavirus. *Journal of virology*. 2005 Oct;79(20):13007-17. PubMed PMID: 16189003. Pubmed Central PMCID: PMC1235815. Epub 2005/09/29. eng.
304. Daikoku T, Kudoh A, Sugaya Y, Iwahori S, Shirata N, Isomura H, Tsurumi T. Postreplicative mismatch repair factors are recruited to Epstein-Barr virus replication compartments. *The Journal of biological chemistry*. 2006 Apr 21;281(16):11422-30. PubMed PMID: 16510450. Epub 2006/03/03. eng.
305. Taylor TJ, Knipe DM. Proteomics of herpes simplex virus replication compartments: association of cellular DNA replication, repair, recombination, and

chromatin remodeling proteins with ICP8. *Journal of virology*. 2004 Jun;78(11):5856-66. PubMed PMID: 15140983. Pubmed Central PMCID: PMC415816. Epub 2004/05/14. eng.

306. Wilcock D, Lane DP. Localization of p53, retinoblastoma and host replication proteins at sites of viral replication in herpes-infected cells. *Nature*. 1991 Jan 31;349(6308):429-31. PubMed PMID: 1671528. Epub 1991/01/31. eng.

307. Yarbrough ML, Mata MA, Sakthivel R, Fontoura BM. Viral subversion of nucleocytoplasmic trafficking. *Traffic (Copenhagen, Denmark)*. 2014 Feb;15(2):127-40. PubMed PMID: 24289861. Pubmed Central PMCID: PMC3910510. Epub 2013/12/03. eng.

308. Sedger L, Ruby J. Heat shock response to vaccinia virus infection. *Journal of virology*. 1994 Jul;68(7):4685-9. PubMed PMID: 8207845. Pubmed Central PMCID: PMC236399. Epub 1994/07/01. eng.

309. Phillips B, Abravaya K, Morimoto RI. Analysis of the specificity and mechanism of transcriptional activation of the human hsp70 gene during infection by DNA viruses. *Journal of virology*. 1991 Nov;65(11):5680-92. PubMed PMID: 1656064. Pubmed Central PMCID: PMC250228. Epub 1991/11/01. eng.

310. Collins PL, Hightower LE. Newcastle disease virus stimulates the cellular accumulation of stress (heat shock) mRNAs and proteins. *Journal of virology*. 1982 Nov;44(2):703-7. PubMed PMID: 7143579. Pubmed Central PMCID: PMC256315. Epub 1982/11/01. eng.

311. Peluso RW, Lamb RA, Choppin PW. Infection with paramyxoviruses stimulates synthesis of cellular polypeptides that are also stimulated in cells transformed by Rous sarcoma virus or deprived of glucose. *Proceedings of the National Academy of Sciences of the United States of America*. 1978 Dec;75(12):6120-4. PubMed PMID: 216013. Pubmed Central PMCID: PMC393130. Epub 1978/12/01. eng.

312. Kim MY, Oglesbee M. Virus-heat shock protein interaction and a novel axis for innate antiviral immunity. *Cells*. 2012;1(3):646-66. PubMed PMID: 24710494. Pubmed Central PMCID: PMC3901102. Epub 2012/01/01. eng.

313. Fang D, Haraguchi Y, Jinno A, Soda Y, Shimizu N, Hoshino H. Heat shock cognate protein 70 is a cell fusion-enhancing factor but not an entry factor for human T-cell lymphotropic virus type I. *Biochemical and biophysical research communications*. 1999 Aug 2;261(2):357-63. PubMed PMID: 10425190. Epub 1999/07/30. eng.

314. Guerrero CA, Bouyssounade D, Zarate S, Isa P, Lopez T, Espinosa R, Romero P, Mendez E, Lopez S, Arias CF. Heat shock cognate protein 70 is involved in rotavirus cell entry. *Journal of virology*. 2002 Apr;76(8):4096-102. PubMed PMID: 11907249. Pubmed Central PMCID: PMC136078. Epub 2002/03/22. eng.

315. Vasconcelos DY, Cai XH, Oglesbee MJ. Constitutive overexpression of the major inducible 70 kDa heat shock protein mediates large plaque formation by measles virus. *The Journal of general virology*. 1998 Sep;79 ( Pt 9):2239-47. PubMed PMID: 9747734. Epub 1998/09/25. eng.
316. Breitenbach JE, Popham HJ. Baculovirus replication induces the expression of heat shock proteins in vivo and in vitro. *Archives of virology*. 2013 Jul;158(7):1517-22. PubMed PMID: 23443933. Epub 2013/02/28. eng.
317. Lee DH, Goldberg AL. Proteasome inhibitors: valuable new tools for cell biologists. *Trends in cell biology*. 1998 Oct;8(10):397-403. PubMed PMID: 9789328. Epub 1998/10/28. eng.
318. Mottet K, Bareiss B, Milne CD, Barry M. The poxvirus encoded ubiquitin ligase, p28, is regulated by proteasomal degradation and autoubiquitination. *Virology*. 2014 Nov;468-470:363-78. PubMed PMID: 25240226. Epub 2014/09/23. eng.
319. Xiao A, Wong J, Luo H. Viral interaction with molecular chaperones: role in regulating viral infection. *Archives of virology*. 2010 Jul;155(7):1021-31. PubMed PMID: 20461534. Epub 2010/05/13. eng.
320. Niewiarowska J, D'Halluin JC, Belin MT. Adenovirus capsid proteins interact with HSP70 proteins after penetration in human or rodent cells. *Experimental cell research*. 1992 Aug;201(2):408-16. PubMed PMID: 1639138. Epub 1992/08/01. eng.
321. Kampmueller KM, Miller DJ. The cellular chaperone heat shock protein 90 facilitates Flock House virus RNA replication in *Drosophila* cells. *Journal of virology*. 2005 Jun;79(11):6827-37. PubMed PMID: 15890922. Pubmed Central PMCID: PMC1112161. Epub 2005/05/14. eng.
322. Liu JS, Kuo SR, Makhov AM, Cyr DM, Griffith JD, Broker TR, Chow LT. Human Hsp70 and Hsp40 chaperone proteins facilitate human papillomavirus-11 E1 protein binding to the origin and stimulate cell-free DNA replication. *The Journal of biological chemistry*. 1998 Nov 13;273(46):30704-12. PubMed PMID: 9804845. Epub 1998/11/07. eng.
323. Park SG, Lee SM, Jung G. Antisense oligodeoxynucleotides targeted against molecular chaperonin Hsp60 block human hepatitis B virus replication. *The Journal of biological chemistry*. 2003 Oct 10;278(41):39851-7. PubMed PMID: 12869561. Epub 2003/07/19. eng.
324. Lopez T, Lopez S, Arias CF. Heat shock enhances the susceptibility of BHK cells to rotavirus infection through the facilitation of entry and post-entry virus replication steps. *Virus research*. 2006 Oct;121(1):74-83. PubMed PMID: 16737757. Epub 2006/06/02. eng.

325. Guerrero CA, Moreno LP. Rotavirus receptor proteins Hsc70 and integrin alphavbeta3 are located in the lipid microdomains of animal intestinal cells. *Acta virologica*. 2012;56(1):63-70. PubMed PMID: 22404611. Epub 2012/03/13. eng.
326. Santoro MG. Heat shock proteins and virus replication: hsp70s as mediators of the antiviral effects of prostaglandins. *Experientia*. 1994 Nov 30;50(11-12):1039-47. PubMed PMID: 7988663. Epub 1994/11/30. eng.
327. Liu J, Bai J, Zhang L, Jiang Z, Wang X, Li Y, Jiang P. Hsp70 positively regulates porcine circovirus type 2 replication in vitro. *Virology*. 2013 Dec;447(1-2):52-62. PubMed PMID: 24210099. Epub 2013/11/12. eng.
328. Ye J, Chen Z, Zhang B, Miao H, Zohaib A, Xu Q, Chen H, Cao S. Heat shock protein 70 is associated with replicase complex of Japanese encephalitis virus and positively regulates viral genome replication. *PloS one*. 2013;8(9):e75188. PubMed PMID: 24086464. Pubmed Central PMCID: PMC3781048. Epub 2013/10/03. eng.
329. Florin L, Becker KA, Sapp C, Lambert C, Sirma H, Muller M, Streeck RE, Sapp M. Nuclear translocation of papillomavirus minor capsid protein L2 requires Hsc70. *Journal of virology*. 2004 Jun;78(11):5546-53. PubMed PMID: 15140951. Pubmed Central PMCID: PMC415841. Epub 2004/05/14. eng.
330. Prange R, Werr M, Loffler-Mary H. Chaperones involved in hepatitis B virus morphogenesis. *Biological chemistry*. 1999 Mar;380(3):305-14. PubMed PMID: 10223333. Epub 1999/05/01. eng.
331. Macejak DG, Sarnow P. Association of heat shock protein 70 with enterovirus capsid precursor P1 in infected human cells. *Journal of virology*. 1992 Mar;66(3):1520-7. PubMed PMID: 1310763. Pubmed Central PMCID: PMC240877. Epub 1992/03/01. eng.
332. Filone CM, Caballero IS, Dower K, Mendillo ML, Cowley GS, Santagata S, Rozelle DK, Yen J, Rubins KH, Hachohen N, Root DE, Hensley LE, Connor J. The master regulator of the cellular stress response (HSF1) is critical for orthopoxvirus infection. *PLoS pathogens*. 2014 Feb;10(2):e1003904. PubMed PMID: 24516381. Pubmed Central PMCID: PMC3916389. Epub 2014/02/12. eng.
333. Afonso CL, Tulman ER, Delhon G, Lu Z, Viljoen GJ, Wallace DB, Kutish GF, Rock DL. Genome of crocodilepox virus. *Journal of virology*. 2006 May;80(10):4978-91. PubMed PMID: 16641289. Pubmed Central PMCID: PMC1472061. Epub 2006/04/28. eng.
334. Chen N, Baudino T, MacDonald PN, Green M, Kelley WL, Burnett JW, Buller RM. Selective inhibition of nuclear steroid receptor function by a protein from a human tumorigenic poxvirus. *Virology*. 2000 Aug 15;274(1):17-25. PubMed PMID: 10936084. Epub 2000/08/11. eng.
335. Manes NP, Estep RD, Mottaz HM, Moore RJ, Clauss TR, Monroe ME, Du X, Adkins JN, Wong SW, Smith RD. Comparative proteomics of human monkeypox and

vaccinia intracellular mature and extracellular enveloped virions. *Journal of proteome research*. 2008 Mar;7(3):960-8. PubMed PMID: 18205298. Pubmed Central PMCID: PMC2517256. Epub 2008/01/22. eng.

336. Resch W, Hixson KK, Moore RJ, Lipton MS, Moss B. Protein composition of the vaccinia virus mature virion. *Virology*. 2007 Feb 5;358(1):233-47. PubMed PMID: 17005230. Epub 2006/09/29. eng.

337. Hung JJ, Chung CS, Chang W. Molecular chaperone Hsp90 is important for vaccinia virus growth in cells. *Journal of virology*. 2002 Feb;76(3):1379-90. PubMed PMID: 11773412. Pubmed Central PMCID: PMC135870. Epub 2002/01/05. eng.

338. Van Vliet K, Mohamed MR, Zhang L, Villa NY, Werden SJ, Liu J, McFadden G. Poxvirus proteomics and virus-host protein interactions. *Microbiology and molecular biology reviews : MMBR*. 2009 Dec;73(4):730-49. PubMed PMID: 19946139. Pubmed Central PMCID: PMC2786582. Epub 2009/12/01. eng.

339. Bhanuprakash V, Hosamani M, Venkatesan G, Balamurugan V, Yogisharadhya R, Singh RK. Animal poxvirus vaccines: a comprehensive review. *Expert review of vaccines*. 2012 Nov;11(11):1355-74. PubMed PMID: 23249235. Epub 2012/12/20. eng.

340. Jordan FT. DIAGNOSIS OF INFECTIOUS LARYNGOTRACHEITIS BY CHICK EMBRYO INOCULATION. *Journal of comparative pathology*. 1964 Apr;74:119-28. PubMed PMID: 14155351. Epub 1964/04/01. eng.

341. Zhao K, He W, Xie S, Song D, Lu H, Pan W, Zhou P, Liu W, Lu R, Zhou J, Gao F. Highly pathogenic fowlpox virus in cutaneously infected chickens, China. *Emerging infectious diseases*. 2014 Jul;20(7):1208-10. PubMed PMID: 24963887. Pubmed Central PMCID: PMC4073872. Epub 2014/06/26. eng.

342. Odom MR, Hendrickson RC, Lefkowitz EJ. Poxvirus protein evolution: family wide assessment of possible horizontal gene transfer events. *Virus research*. 2009 Sep;144(1-2):233-49. PubMed PMID: 19464330. Pubmed Central PMCID: PMC2779260. Epub 2009/05/26. eng.

343. Hughes AL, Friedman R. Poxvirus genome evolution by gene gain and loss. *Molecular phylogenetics and evolution*. 2005 Apr;35(1):186-95. PubMed PMID: 15737590. Epub 2005/03/02. eng.

344. Barry M, McFadden G. Virus encoded cytokines and cytokine receptors. *Parasitology*. 1997;115 Suppl:S89-100. PubMed PMID: 9571694. Epub 1997/01/01. eng.

345. Hughes AL. Origin and evolution of viral interleukin-10 and other DNA virus genes with vertebrate homologues. *Journal of molecular evolution*. 2002 Jan;54(1):90-101. PubMed PMID: 11734902. Epub 2001/12/06. eng.

346. Lalani AS, McFadden G. Evasion and exploitation of chemokines by viruses. *Cytokine & growth factor reviews*. 1999 Sep-Dec;10(3-4):219-33. PubMed PMID: 10647778. Epub 2000/01/27. eng.
347. Wall EM, Cao JX, Upton C. Subversion of cytokine networks by viruses. *International reviews of immunology*. 1998;17(1-4):121-55. PubMed PMID: 9914946. Epub 1999/01/23. eng.
348. Nicholls RD, Gray TA. Cellular source of the poxviral N1R/p28 gene family. *Virus genes*. 2004 Dec;29(3):359-64. PubMed PMID: 15550777. Epub 2004/11/20. eng.
349. Ko A, Lee EW, Yeh JY, Yang MR, Oh W, Moon JS, Song J. MKRN1 induces degradation of West Nile virus capsid protein by functioning as an E3 ligase. *Journal of virology*. 2010 Jan;84(1):426-36. PubMed PMID: 19846531. Pubmed Central PMCID: PMC2798448. Epub 2009/10/23. eng.
350. Omwancha J, Zhou XF, Chen SY, Baslan T, Fisher CJ, Zheng Z, Cai C, Shemshedini L. Makorin RING finger protein 1 (MKRN1) has negative and positive effects on RNA polymerase II-dependent transcription. *Endocrine*. 2006 Apr;29(2):363-73. PubMed PMID: 16785614. Epub 2006/06/21. eng.
351. Freemont PS. The RING finger. A novel protein sequence motif related to the zinc finger. *Annals of the New York Academy of Sciences*. 1993 Jun 11;684:174-92. PubMed PMID: 8317827. Epub 1993/06/11. eng.
352. Nuber U, Schwarz SE, Scheffner M. The ubiquitin-protein ligase E6-associated protein (E6-AP) serves as its own substrate. *European journal of biochemistry / FEBS*. 1998 Jun 15;254(3):643-9. PubMed PMID: 9688277. Epub 1998/08/04. eng.
353. Hu G, Fearon ER. Siah-1 N-terminal RING domain is required for proteolysis function, and C-terminal sequences regulate oligomerization and binding to target proteins. *Molecular and cellular biology*. 1999 Jan;19(1):724-32. PubMed PMID: 9858595. Pubmed Central PMCID: PMC83929. Epub 1998/12/22. eng.
354. Yin Q, Lin SC, Lamothe B, Lu M, Lo YC, Hura G, Zheng L, Rich RL, Campos AD, Myszka DG, Lenardo MJ, Darnay BG, Wu H. E2 interaction and dimerization in the crystal structure of TRAF6. *Nature structural & molecular biology*. 2009 Jun;16(6):658-66. PubMed PMID: 19465916. Pubmed Central PMCID: PMC2834951. Epub 2009/05/26. eng.
355. Galan JM, Peter M. Ubiquitin-dependent degradation of multiple F-box proteins by an autocatalytic mechanism. *Proceedings of the National Academy of Sciences of the United States of America*. 1999 Aug 3;96(16):9124-9. PubMed PMID: 10430906. Pubmed Central PMCID: PMC17743. Epub 1999/08/04. eng.
356. Huibregtse JM, Scheffner M, Beaudenon S, Howley PM. A family of proteins structurally and functionally related to the E6-AP ubiquitin-protein ligase. *Proceedings of the National Academy of Sciences of the United States of America*. 1995 Mar

28;92(7):2563-7. PubMed PMID: 7708685. Pubmed Central PMCID: PMC42258. Epub 1995/03/28. eng.

357. Gallagher E, Gao M, Liu YC, Karin M. Activation of the E3 ubiquitin ligase Itch through a phosphorylation-induced conformational change. *Proceedings of the National Academy of Sciences of the United States of America*. 2006 Feb 7;103(6):1717-22. PubMed PMID: 16446428. Pubmed Central PMCID: PMC1413664. Epub 2006/02/01. eng.

358. Bruce MC, Kanelis V, Fouladkou F, Debonneville A, Staub O, Rotin D. Regulation of Nedd4-2 self-ubiquitination and stability by a PY motif located within its HECT-domain. *The Biochemical journal*. 2008 Oct 1;415(1):155-63. PubMed PMID: 18498246. Epub 2008/05/24. eng.

359. Wiesner S, Ogunjimi AA, Wang HR, Rotin D, Sicheri F, Wrana JL, Forman-Kay JD. Autoinhibition of the HECT-type ubiquitin ligase Smurf2 through its C2 domain. *Cell*. 2007 Aug 24;130(4):651-62. PubMed PMID: 17719543. Epub 2007/08/28. eng.

360. Ryan PE, Davies GC, Nau MM, Lipkowitz S. Regulating the regulator: negative regulation of Cbl ubiquitin ligases. *Trends in biochemical sciences*. 2006 Feb;31(2):79-88. PubMed PMID: 16406635. Epub 2006/01/13. eng.

361. Kao WH, Beaudenon SL, Talis AL, Huibregtse JM, Howley PM. Human papillomavirus type 16 E6 induces self-ubiquitination of the E6AP ubiquitin-protein ligase. *Journal of virology*. 2000 Jul;74(14):6408-17. PubMed PMID: 10864652. Pubmed Central PMCID: PMC112148. Epub 2000/06/23. eng.

362. Fang S, Jensen JP, Ludwig RL, Vousden KH, Weissman AM. Mdm2 is a RING finger-dependent ubiquitin protein ligase for itself and p53. *The Journal of biological chemistry*. 2000 Mar 24;275(12):8945-51. PubMed PMID: 10722742. Epub 2000/03/18. eng.

363. Okamoto K, Taya Y, Nakagama H. Mdmx enhances p53 ubiquitination by altering the substrate preference of the Mdm2 ubiquitin ligase. *FEBS letters*. 2009 Sep 3;583(17):2710-4. PubMed PMID: 19619542. Epub 2009/07/22. eng.

364. Mottet K. *The poxvirus ubiquitin ligase p28 manipulates the ubiquitin proteasome system*. Edmonton, Alberta: University of Alberta; 2010.

365. Anania VG, Bustos DJ, Lill JR, Kirkpatrick DS, Coscoy L. A Novel Peptide-Based SILAC Method to Identify the Posttranslational Modifications Provides Evidence for Unconventional Ubiquitination in the ER-Associated Degradation Pathway. *International journal of proteomics*. 2013;2013:857918. PubMed PMID: 23431445. Pubmed Central PMCID: PMC3574754. Epub 2013/02/23. eng.

366. Ota K, Kito K, Okada S, Ito T. A proteomic screen reveals the mitochondrial outer membrane protein Mdm34p as an essential target of the F-box protein Mdm30p.

Genes to cells : devoted to molecular & cellular mechanisms. 2008 Oct;13(10):1075-85. PubMed PMID: 18775025. Epub 2008/09/09. eng.

367. Hor S, Ziv T, Admon A, Lehner PJ. Stable isotope labeling by amino acids in cell culture and differential plasma membrane proteome quantitation identify new substrates for the MARCH9 transmembrane E3 ligase. *Molecular & cellular proteomics : MCP*. 2009 Aug;8(8):1959-71. PubMed PMID: 19457934. Pubmed Central PMCID: PMC2722766. Epub 2009/05/22. eng.

368. Xu G, Paige JS, Jaffrey SR. Global analysis of lysine ubiquitination by ubiquitin remnant immunoaffinity profiling. *Nature biotechnology*. 2010 Aug;28(8):868-73. PubMed PMID: 20639865. Pubmed Central PMCID: PMC2946519. Epub 2010/07/20. eng.

369. Udeshi ND, Mani DR, Eisenhaure T, Mertins P, Jaffe JD, Clauser KR, Hacohen N, Carr SA. Methods for quantification of in vivo changes in protein ubiquitination following proteasome and deubiquitinase inhibition. *Molecular & cellular proteomics : MCP*. 2012 May;11(5):148-59. PubMed PMID: 22505724. Pubmed Central PMCID: PMC3418844. Epub 2012/04/17. eng.

370. Kronke J, Udeshi ND, Narla A, Grauman P, Hurst SN, McConkey M, Svinkina T, Heckl D, Comer E, Li X, Ciarlo C, Hartman E, Munshi N, Schenone M, Schreiber SL, Carr SA, Ebert BL. Lenalidomide causes selective degradation of IKZF1 and IKZF3 in multiple myeloma cells. *Science (New York, NY)*. 2014 Jan 17;343(6168):301-5. PubMed PMID: 24292625. Pubmed Central PMCID: PMC4077049. Epub 2013/12/03. eng.

371. Sarraf SA, Raman M, Guarani-Pereira V, Sowa ME, Huttlin EL, Gygi SP, Harper JW. Landscape of the PARKIN-dependent ubiquitylome in response to mitochondrial depolarization. *Nature*. 2013 Apr 18;496(7445):372-6. PubMed PMID: 23503661. Pubmed Central PMCID: PMC3641819. Epub 2013/03/19. eng.

372. Zhuang M, Guan S, Wang H, Burlingame AL, Wells JA. Substrates of IAP ubiquitin ligases identified with a designed orthogonal E3 ligase, the NEDDylator. *Molecular cell*. 2013 Jan 24;49(2):273-82. PubMed PMID: 23201124. Pubmed Central PMCID: PMC3557559. Epub 2012/12/04. eng.

373. Natuk RJ, Holowczak JA. Vaccinia virus proteins on the plasma membrane of infected cells. III. Infection of peritoneal macrophages. *Virology*. 1985 Dec;147(2):354-72. PubMed PMID: 3878029. Epub 1985/12/01. eng.

374. Mercer J, Snijder B, Sacher R, Burkard C, Bleck CK, Stahlberg H, Pelkmans L, Helenius A. RNAi screening reveals proteasome- and Cullin3-dependent stages in vaccinia virus infection. *Cell reports*. 2012 Oct 25;2(4):1036-47. PubMed PMID: 23084750. Epub 2012/10/23. eng.

375. Jensen ON, Houthaeve T, Shevchenko A, Cudmore S, Ashford T, Mann M, Griffiths G, Krijnse Locker J. Identification of the major membrane and core proteins of

vaccinia virus by two-dimensional electrophoresis. *Journal of virology*. 1996 Nov;70(11):7485-97. PubMed PMID: 8892867. Pubmed Central PMCID: PMC190816. Epub 1996/11/01. eng.

376. Pedersen K, Snijder EJ, Schleich S, Roos N, Griffiths G, Locker JK. Characterization of vaccinia virus intracellular cores: implications for viral uncoating and core structure. *Journal of virology*. 2000 Apr;74(8):3525-36. PubMed PMID: 10729126. Pubmed Central PMCID: PMC111860. Epub 2000/03/23. eng.

377. Velichko AK, Markova EN, Petrova NV, Razin SV, Kantidze OL. Mechanisms of heat shock response in mammals. *Cellular and molecular life sciences : CMLS*. 2013 Nov;70(22):4229-41. PubMed PMID: 23633190. Epub 2013/05/02. eng.

378. Zhang X, Oglesbee M. Use of surface plasmon resonance for the measurement of low affinity binding interactions between HSP72 and measles virus nucleocapsid protein. *Biological procedures online*. 2003;5:170-81. PubMed PMID: 14615813. Pubmed Central PMCID: PMC248471. Epub 2003/11/15. Eng.

379. Morimoto RI, and Kim L. Milarski. . *Expression and Function of Vertebrate hsp70 Genes*: Cold Spring Harbor 1990.

380. Gao J, Xiao S, Liu X, Wang L, Ji Q, Mo D, Chen Y. Inhibition of HSP70 reduces porcine reproductive and respiratory syndrome virus replication in vitro. *BMC microbiology*. 2014;14:64. PubMed PMID: 24625230. Pubmed Central PMCID: PMC3984673. Epub 2014/03/15. eng.

381. Khachatoorian R, Ganapathy E, Ahmadiéh Y, Wheatley N, Sundberg C, Jung CL, Arumugaswami V, Raychaudhuri S, Dasgupta A, French SW. The NS5A-binding heat shock proteins HSC70 and HSP70 play distinct roles in the hepatitis C viral life cycle. *Virology*. 2014 Apr;454-455:118-27. PubMed PMID: 24725938. Pubmed Central PMCID: PMC4011396. Epub 2014/04/15. eng.

382. Macejak DG, Luftig RB. Association of HSP70 with the adenovirus type 5 fiber protein in infected HEp-2 cells. *Virology*. 1991 Jan;180(1):120-5. PubMed PMID: 1984643. Epub 1991/01/01. eng.

383. Jindal S, Young RA. Vaccinia virus infection induces a stress response that leads to association of Hsp70 with viral proteins. *Journal of virology*. 1992 Sep;66(9):5357-62. PubMed PMID: 1501279. Pubmed Central PMCID: PMC289091. Epub 1992/09/01. eng.

384. Arispe N, Doh M, De Maio A. Lipid interaction differentiates the constitutive and stress-induced heat shock proteins Hsc70 and Hsp70. *Cell stress & chaperones*. 2002 Oct;7(4):330-8. PubMed PMID: 12653477. Pubmed Central PMCID: PMC514832. Epub 2003/03/26. eng.

385. Young JC. The role of the cytosolic HSP70 chaperone system in diseases caused by misfolding and aberrant trafficking of ion channels. *Disease models & mechanisms*.

2014 Mar;7(3):319-29. PubMed PMID: 24609033. Pubmed Central PMCID: PMC3944492. Epub 2014/03/13. eng.

386. Callahan MK, Chaillot D, Jacquin C, Clark PR, Menoret A. Differential acquisition of antigenic peptides by Hsp70 and Hsc70 under oxidative conditions. *The Journal of biological chemistry*. 2002 Sep 13;277(37):33604-9. PubMed PMID: 12114509. Epub 2002/07/13. eng.

387. Anckar J, Sistonen L. Heat shock factor 1 as a coordinator of stress and developmental pathways. *Advances in experimental medicine and biology*. 2007;594:78-88. PubMed PMID: 17205677. Epub 2007/01/09. eng.

388. Fan CY, Lee S, Cyr DM. Mechanisms for regulation of Hsp70 function by Hsp40. *Cell stress & chaperones*. 2003 Winter;8(4):309-16. PubMed PMID: 15115283. Pubmed Central PMCID: PMC514902. Epub 2004/04/30. eng.

389. Raoult D, Audic S, Robert C, Abergel C, Renesto P, Ogata H, La Scola B, Suzan M, Claverie JM. The 1.2-megabase genome sequence of Mimivirus. *Science (New York, NY)*. 2004 Nov 19;306(5700):1344-50. PubMed PMID: 15486256. Epub 2004/10/16. eng.

390. Legendre M, Santini S, Rico A, Abergel C, Claverie JM. Breaking the 1000-gene barrier for Mimivirus using ultra-deep genome and transcriptome sequencing. *Virology journal*. 2011;8:99. PubMed PMID: 21375749. Pubmed Central PMCID: PMC3058096. Epub 2011/03/08. eng.

391. Santoro MG. Heat shock factors and the control of the stress response. *Biochemical pharmacology*. 2000 Jan 1;59(1):55-63. PubMed PMID: 10605935. Epub 1999/12/22. eng.

392. Jolly C, Usson Y, Morimoto RI. Rapid and reversible relocalization of heat shock factor 1 within seconds to nuclear stress granules. *Proceedings of the National Academy of Sciences of the United States of America*. 1999 Jun 8;96(12):6769-74. PubMed PMID: 10359787. Pubmed Central PMCID: PMC21990. Epub 1999/06/09. eng.

393. Holmberg CI, Tran SE, Eriksson JE, Sistonen L. Multisite phosphorylation provides sophisticated regulation of transcription factors. *Trends in biochemical sciences*. 2002 Dec;27(12):619-27. PubMed PMID: 12468231. Epub 2002/12/07. eng.

394. Connell P, Ballinger CA, Jiang J, Wu Y, Thompson LJ, Hohfeld J, Patterson C. The co-chaperone CHIP regulates protein triage decisions mediated by heat-shock proteins. *Nature cell biology*. 2001 Jan;3(1):93-6. PubMed PMID: 11146632. Epub 2001/01/09. eng.

395. Ballinger CA, Connell P, Wu Y, Hu Z, Thompson LJ, Yin LY, Patterson C. Identification of CHIP, a novel tetratricopeptide repeat-containing protein that interacts with heat shock proteins and negatively regulates chaperone functions. *Molecular and*

cellular biology. 1999 Jun;19(6):4535-45. PubMed PMID: 10330192. Pubmed Central PMCID: PMC104411. Epub 1999/05/18. eng.

396. Jiang J, Ballinger CA, Wu Y, Dai Q, Cyr DM, Hohfeld J, Patterson C. CHIP is a U-box-dependent E3 ubiquitin ligase: identification of Hsc70 as a target for ubiquitylation. *The Journal of biological chemistry*. 2001 Nov 16;276(46):42938-44. PubMed PMID: 11557750. Epub 2001/09/15. eng.

397. Hatakeyama S, Yada M, Matsumoto M, Ishida N, Nakayama KI. U box proteins as a new family of ubiquitin-protein ligases. *The Journal of biological chemistry*. 2001 Aug 31;276(35):33111-20. PubMed PMID: 11435423. Epub 2001/07/04. eng.

398. Li Y, Gazdoui S, Pan ZQ, Fuchs SY. Stability of homologue of Slimb F-box protein is regulated by availability of its substrate. *The Journal of biological chemistry*. 2004 Mar 19;279(12):11074-80. PubMed PMID: 14707120. Epub 2004/01/07. eng.

399. Ben-Saadon R, Zaaroor D, Ziv T, Ciechanover A. The polycomb protein Ring1B generates self atypical mixed ubiquitin chains required for its in vitro histone H2A ligase activity. *Molecular cell*. 2006 Dec 8;24(5):701-11. PubMed PMID: 17157253. Epub 2006/12/13. eng.

400. Mallery DL, Vandenberg CJ, Hiom K. Activation of the E3 ligase function of the BRCA1/BARD1 complex by polyubiquitin chains. *The EMBO journal*. 2002 Dec 16;21(24):6755-62. PubMed PMID: 12485996. Pubmed Central PMCID: PMC139111. Epub 2002/12/18. eng.

## **Appendix: Supporting methodology and data**

### **A.1 Generation of recombinant VACVCop expressing FLAG-p28 mutants**

Many experiments presented in this thesis were conducted with poxviral infection and simultaneously transfection of pSC66 plasmids expressing FLAG-tagged p28 mutant proteins, following the general infection/transfection protocol (**Section 2.3.2**). We list the generation of recombinant viruses in the Appendix, since we did not use any of these viruses in the main thesis. However, the recombinant viruses could be used in future experiments to avoid a low transfection rate and allow protein expression in macrophages during VACV infection.

Recombinant VACVCop viruses that express FLAG-tagged versions of p28 mutants were generated by homologous recombination into the TK locus. CV-1 cells were infected with VACVCop and simultaneously transfected with pSC66-FLAG-p28(1-152), pSC66-FLAG-p28(153-242), pSC66-FLAG-p28( $\Delta$ 44-51), pSC66-FLAG-p28(1-184), or pSC66-FLAG-p28(1-204). The pSC66 plasmid contains both a *LacZ* gene and FLAG tagged p28 mutant under control of poxviral promoters flanked by regions of homology to the VACV TK locus (**Figure A.1.A**). Cells that become both infected and transfected may undergo a double-crossover event between the VACV TK locus and flanking regions of homology in pSC66, resulting in a TK negative virus that expresses both FLAG-tagged protein and  $\beta$ -galactosidase. Briefly, CV-1 cells (ATCC) ( $8 \times 10^5$ ) were infected with VACV at an MOI of 0.05 in 500  $\mu$ l of OptiMEM for 1 hour. During this time, 10  $\mu$ g of pSC66-FLAG-p28(1-152), pSC66-FLAG-p28(153-242), pSC66-FLAG-p28( $\Delta$ 44-51), pSC66-FLAG-p28(1-184), or pSC66-FLAG-p28(1-204) (**Figure A.1.A**) was mixed with 10  $\mu$ l of Lipofectamine 2000 in 200  $\mu$ l of OptiMEM as described

in 2.3.1. After one hour, the infection media was removed and replaced with 800  $\mu$ l of OptiMEM along with the 200  $\mu$ l DNA-Lipid mixture, then allowed to incubate at 37°C and 5% CO<sub>2</sub> for 5 hours. The cells were then supplemented with 1 mL of recovery media and incubated for another 24 hours. Cells were harvested in SSC, centrifuged at 1000 x g, and re-suspended in 100  $\mu$ l of ice-cold swelling buffer. For selection of recombinant VACV-FLAG-p28(1-152), VACV-FLAG-p28(153-242), VACV-FLAG-p28( $\Delta$ 44-51), VACV-FLAG-p28(1-184), or VACV-FLAG-p28(1-204), cell monolayers ( $1 \times 10^6$ ) infected with serial dilutions of virus were overlaid with 1.5 mL of a low melting point (LMP) agarose (Invitrogen) mixture containing 2.5 mL of 3% LMP agarose in water (w/v), 2.5 mL DMEM, 1 mL NCS, and 100  $\mu$ l of 100 mg/mL X-gal. The overlay was allowed to solidify at room temperature for 15 minutes, followed by incubation at 37°C and 5% CO<sub>2</sub>. Recombinant viruses will express  $\beta$ -galactosidase, the product of the *LacZ* gene, which will hydrolyze X-gal in the overlay and result in a bright blue product. Blue plaques were picked the following day using a pasteur pipette and suspended in 100  $\mu$ l of ice cold swelling buffer. Plaque picks containing virus-infected cells underwent three freeze-thaw cycles at -80°C and 37°C followed by sonication to lyse cells and release infectious virus to be used for subsequent purification rounds or amplification. After 4 to 5 purifying rounds in CV-1, the same screening process was executed in HuTK<sup>-/-</sup>-143B in the presence of 25  $\mu$ g/mL BrdU. Any virus with an intact TK gene will be unable to grow in the presence of BrdU. To check purity of the recombinant viruses, virus genomic DNA was isolated (see 2.4.6) and subjected to PCR analysis with TK- primer (**Figure A.1.C**).

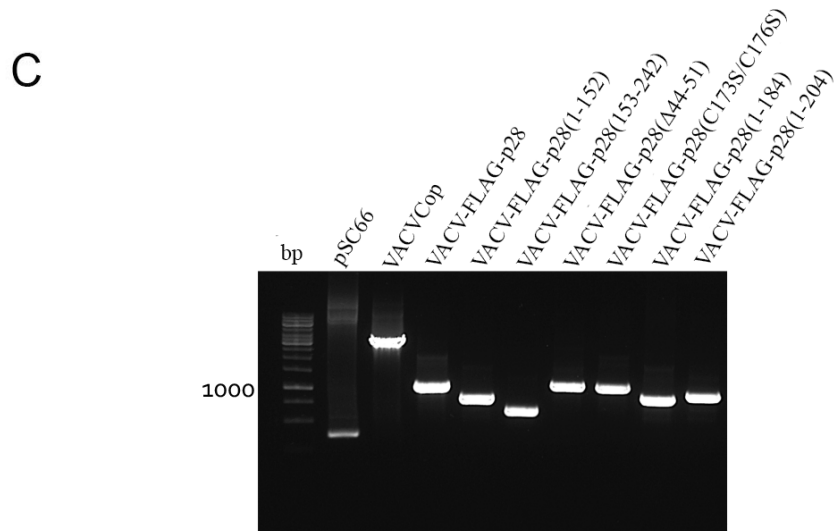
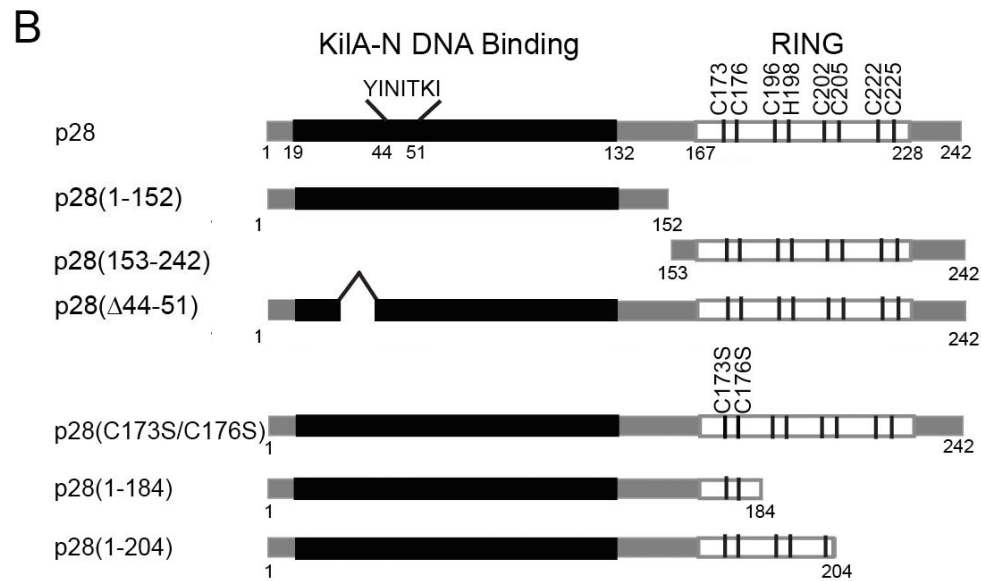
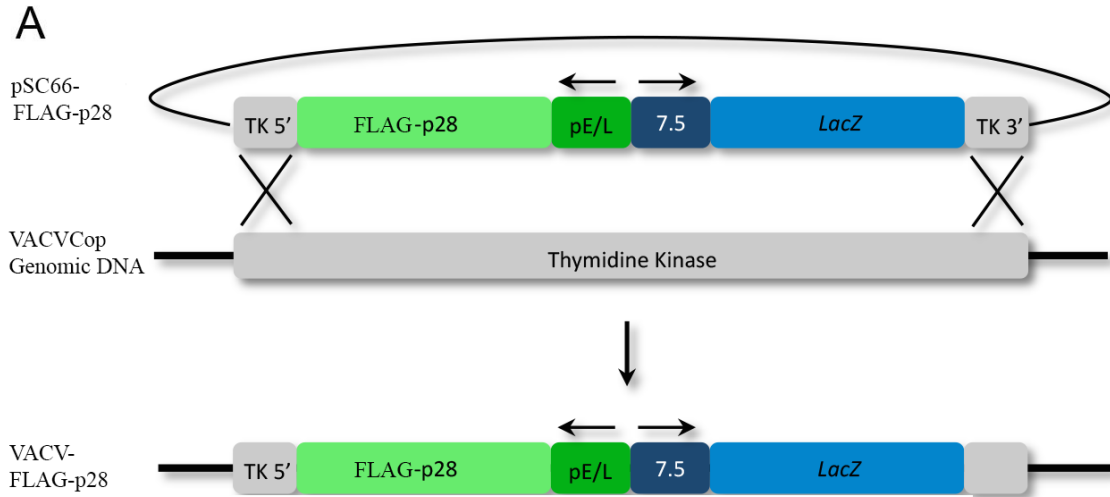


**Figure A.1 Generation of recombinant VACV strains.** To generate the VACV-FLAG-p28 mutant viruses, CV-1 cells were infected with VACVCopWhite and simultaneously transfected with pSC66-FLAG-p28(1-152), pSC66-FLAG-p28(153-242), pSC66-FLAG-p28( $\Delta$ 44-51), pSC66-FLAG-p28(1-184), and pSC66-FLAG-p28(1-204), here referred as to FLAG-p28 mutants. **(A)** The pSC66 plasmid contains the *LacZ* gene under a 7.5 poxviral promoter and the gene of interest (FLAG-p28 mutant) under control of a synthetic poxviral early/late promoter, both flanked by regions of homology to the VACVCopWhite thymidine kinase locus (289). CV-1 cells, which are infected and transfected can undergo homologous recombination, resulting in a recombinant virus expressing FLAG-p28 mutants,  $\beta$ -galactosidase, and are lacking a functional thymidine kinase. **(B)** List of p28 mutants, which were used to generate recombinant viruses. **(C)** Genomic DNA from recombinant viruses was isolated and PCR was performed with specific primers for the TK-site. Shown is a SYBR safe stained agarose gel, which shows the presence of p28 mutant genes in the recombinant virus TK-sites. pSC66 control shows TK-site without inserted gene.

## **A.2 Validation of p28 mass spectrometry hits revealed a high false positive rate.**

Chapter 5 described the main approach of mass spectrometry validation for p28 co-immunoprecipitated proteins, belonging to the major functional clusters of annotation. Here, we present further validation of p28 hits, where antibodies were readily available. These include valosin-containing protein (VCP), proliferating cell nuclear antigen (PCNA), and proteasomal subunits Rpt6 and PSMB3. We further tested if the FLAG-tagged Karyopherin (KPNA) subtypes 1-6 interacted with EGFP-tagged p28. Methodology for co-immunoprecipitation and confocal analysis was similar to Chapter 5. In brief, HeLa cells were infected with VACVCop, VACV expressing FLAG-p28, or FLAG-p28(C173S/C176S) at an MOI of 5 and cells were treated with MG132 (20 $\mu$ M) for the last 4 hours of 16 hour infection. Immunoprecipitations were performed using the anti-FLAG M2 mAB. Protein G beads were washed with 1% NP-40 lysis buffer. Immunoprecipitated proteins were then eluted from the beads by boiling in SDS-PAGE sample loading buffer. For mass spectrometry follow-up immunoprecipitations and western blotting, primary antibody staining were anti-VCP, anti-PCNA, anti-Rpt6, and anti-PSMB3 (**Figure A.2.1**). WCL of HeLa cells infected with VACVCop expressing FLAG-p28 were also included to confirm that the interacting proteins were expressed in cells. Anti-FLAG western blot shown is a representative from one immunoprecipitation and demonstrates that the anti-FLAG immunoprecipitations worked. This representative blot is also shown in Figure 5.3.2 and 5.3.1. We detected VCP, PCNA and Rpt6 in WCL, but we were unable to detect PSMB3. We could only detect weak bands for co-immunoprecipitated Rpt6 with FLAG-p28 and FLAG-p28(C173S/C176S); none of the other tested proteins co-immunoprecipitated with FLAG-p28 in lysates of VACV

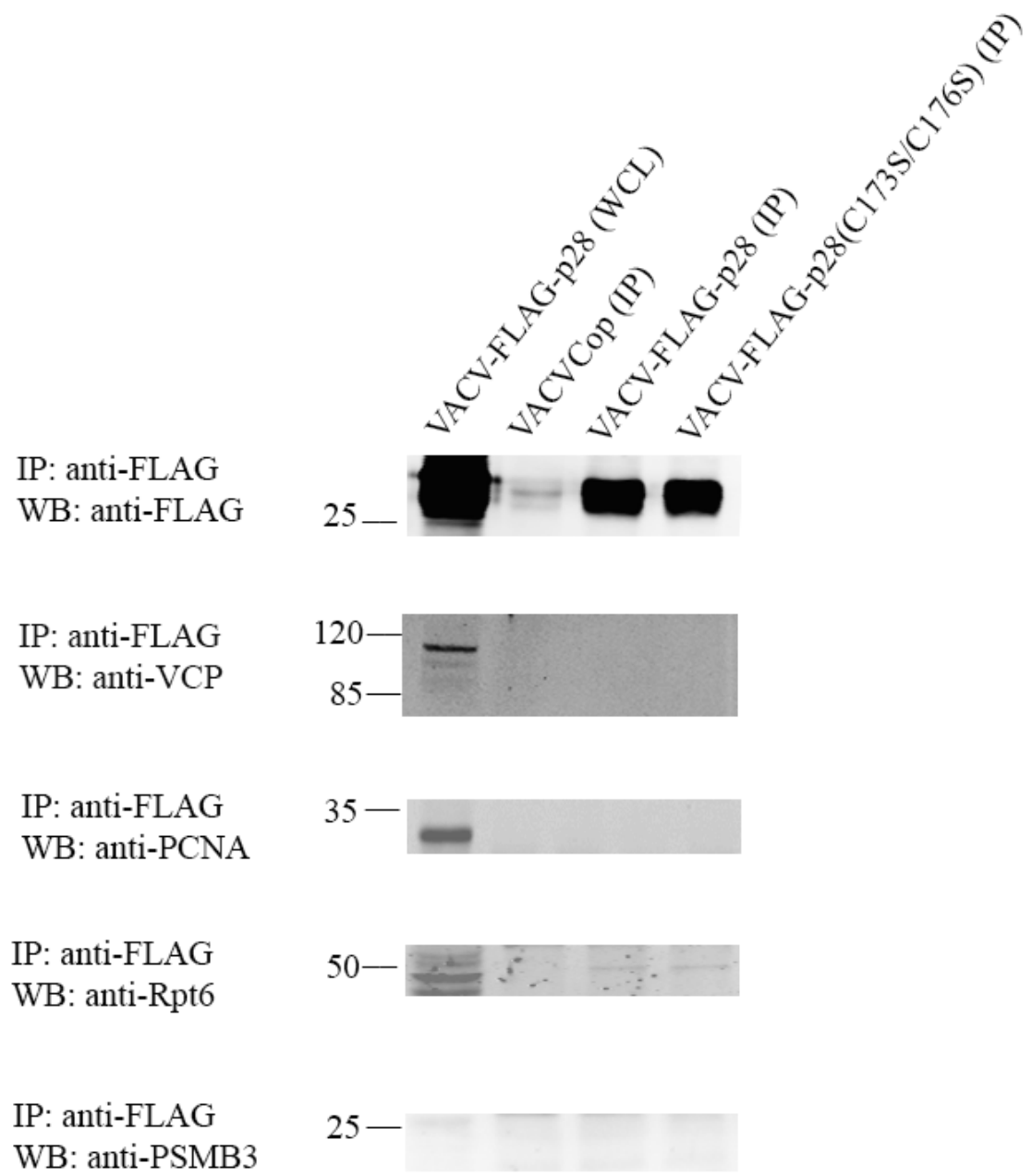


**Figure A.2.1 Validation of p28 mass spectrometry hits VCP, PCNA, Rpt6 and PSMB3 revealed no interaction in co-immunoprecipitation studies.** HeLa cells were infected with VACVCop, VACV-FLAG-p28, or VACV-FLAG-p28(C173S/C176S) at an MOI of 5 and cells were treated with MG132 (20 $\mu$ M) for the last 4 hours of 16 hour infection. Immunoprecipitations were performed using the anti-FLAG M2 mAB in with 1% NP-40 lysis buffer. For mass spectrometry follow-up immunoprecipitations and western blotting were performed with primary antibody staining for anti-VCP, anti-PCNA, anti-Rpt6, and anti-PSMB3. WCL of HeLa cells infected with VACVCop expressing FLAG-p28 were also included to confirm that the interacting proteins were expressed in cells, which was the case for VCP, PCNA and Rpt6; but we were unable to detect PSMB3. Note: All though some of these blots are from separate anti-FLAG IPs, we verified that the FLAG proteins were precipitated in all IPs. The anti-FLAG blot shown is representative from one IP. This representative blot is also shown in Figure 5.3.1 and 5.3.2.

infected cells expressing FLAG-p28. Since the KPNA subtypes 1-6 were readily available in FLAG-tagged pcDNA3 vectors (generous gift from D. Evans), we tested, if any of the subtypes co-immunoprecipitated with EGFP-p28. HeLa cells were transfected with either of the pcDNA-FLAG-tagged KPNA subtypes 1-6 and cells were co-transfected with pEGFP-p28. Sixteen hours post-transfection, cells were lysed in NP-40 lysis buffer and immunoprecipitations were performed using the anti-EGFP antibody. Protein G beads were washed with 1% NP-40 lysis buffer. Immunoprecipitated proteins were then eluted from the beads by boiling in SDS-PAGE sample loading buffer. The immunoprecipitates were analysed by western blotting using antibodies specific for EGFP to detect the pulldown EGFP-p28, and FLAG to investigate, if any KPNA subtypes co-immunoprecipitated with EGFP-p28. WCL of transfected HeLa cells with KPNA subtypes were also included to confirm their expression in cells. We were unable to detect any of the tested proteins in anti-EGFP-immunoprecipitates of cells expressing FLAG-KPNA-1, FLAG-KPNA-2, FLAG-KPNA-3, FLAG-KPNA-4, FLAG-KPNA-5, or FLAG-KPNA-6, even though all proteins were expressed and were present in the WCL (**Figure A.2.2**). We were unable to validate the interaction of KPNA subtypes with p28.

We further follow up with confocal analysis, to investigate, if VACVCop, VACVCop expressing FLAG-p28, or FLAG-p28(C173S/C176S) had an effect on the cellular distribution of PCNA, Rpt6, PSMB3, and MSH6. Unfortunately, the VCP antibody was unsuitable for immunofluorescence analysis. In brief, HeLa cells were mock-infected, or infected with VACVCop, VACVCop expressing FLAG-p28, or VACVCop expressing FLAG-p28(C17S/C176S) at an MOI of 5 for 14 hours.

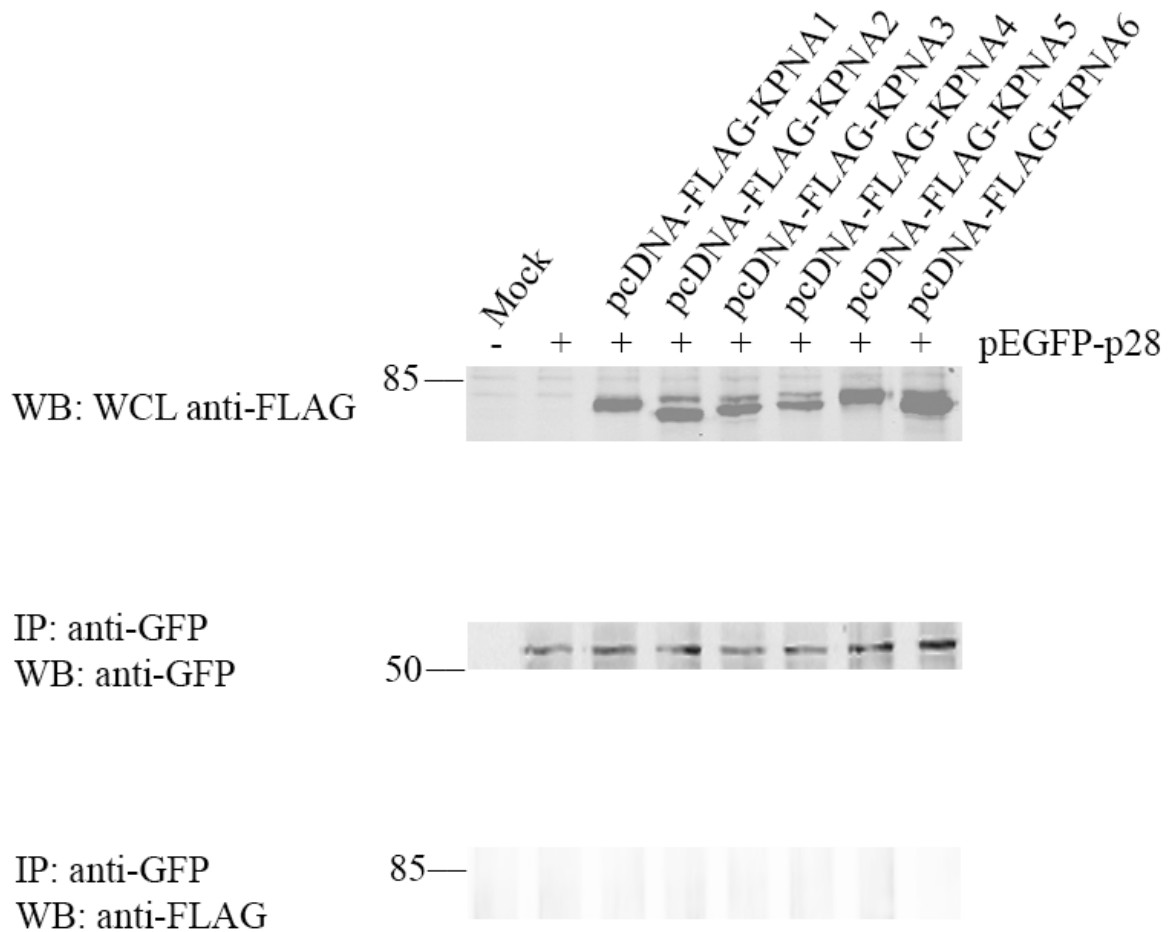


**Figure A.2.2 Karyopherin subtypes 1-6 did not co-immunoprecipitate with EGFP-p28.** HeLa cells were transfected with pcDNA plasmids expressing FLAG-tagged KPNA subtypes 1-6 and were co-transfected with pEGFP-p28 for 16 hours. Cells were lysed in NP-40 lysis buffer and immunoprecipitated with an antibody against EGFP. The immunoprecipitates were analysed by western blotting using antibodies specific for EGFP to detect the pulldown EGFP-p28, and FLAG-tagged KPNA subtypes. WCL of HeLas transfected with KPNA subtypes were included to confirm their expression. We were unable to detect any of the tested proteins in anti-EGFP-immunoprecipitates of cells expressing FLAG-KPNA-1, FLAG-KPNA-2, FLAG-KPNA-3, FLAG-KPNA-4, FLAG-KPNA-5, or FLAG-KPNA-6, even though all proteins were expressed and were present in the WCL.

Cells were stained with anti-PCNA, anti-MSH6, anti-Rpt6, or anti-PSMB3. We investigated whether p28 affected the cellular localization of the mass spectrometry hits. Both, PCNA and MSH6 localized mostly in the nucleus in mock-infected cells (**Figure A.2.3 and A.2.4**). Some of the cellular PCNA and MSH6 were re-localized from the nucleus to the virus factory during VACVCop infection. However, the presence of p28 or p28(C173S/C176S) did not change this phenotype. We were unable to demonstrate that MSH6 co-immunoprecipitates with p28 (**Figure 5.3.2**). Here we confirm with immunofluorescence that p28 has no effect of MSH6 localization to the virus factory.

Since a significant functional cluster of p28 mass spectrometry hits were parts of the 26S proteasome, we investigated the effect of the presence of FLAG-p28 on their subcellular localization, similar as seen in the sections above. We demonstrate in **Figure A.2.5** that the presence of FLAG-p28 leads to the enrichment of proteasomal subunit PSMB3 at the virus factory, but has no effect on the subunit Rpt6. This effect is similar to what was seen in previous work by the Barry group (362).

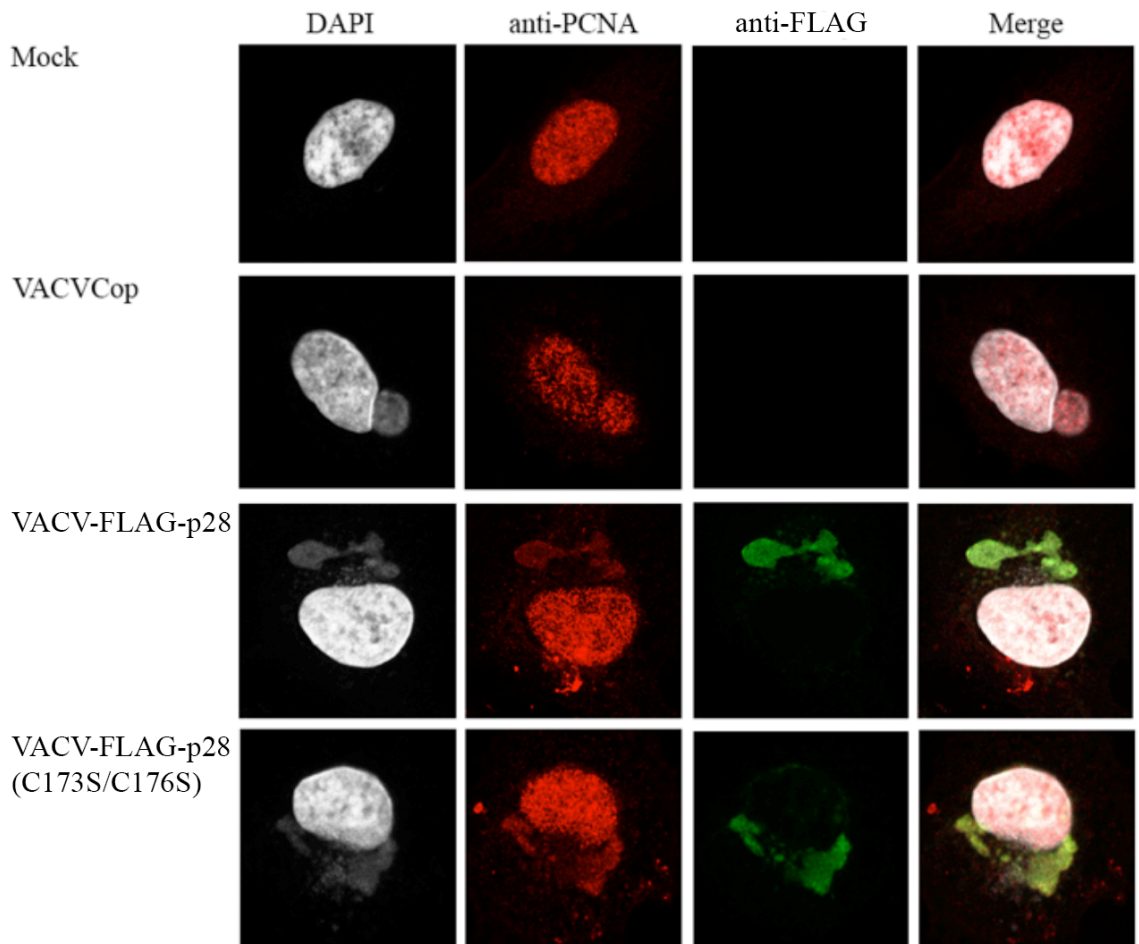


**Figure A.2.3 VACVCop infection leads to PCNA localization to the virus factories, independent on the presence of functional p28.** HeLa cells were mock-infected, or infected with VACVCop, VACV-FLAG-p28, or VACV-FLAG-p28(C173S/C176S) at an MOI of 5 for 14 hours. Cells were fixed with 4% PFA and permeabilized with 1% NP-40. Cells were stained with anti-PCNA, anti-FLAG and DAPI to visualize nuclei and cytoplasmic viral factories. Cells were examined using a Leica SP5 confocal microscope. We investigated whether p28 affected the cellular localization of the potential mass spectrometry hit PCNA. PCNA localized mostly in the nucleus in mock infected cells. Some of the cellular PCNA was re-localized from the nucleus to the virus factory during VACVCop infection. The presence of p28 or p28(C173S/C176S) did not change this phenotype.

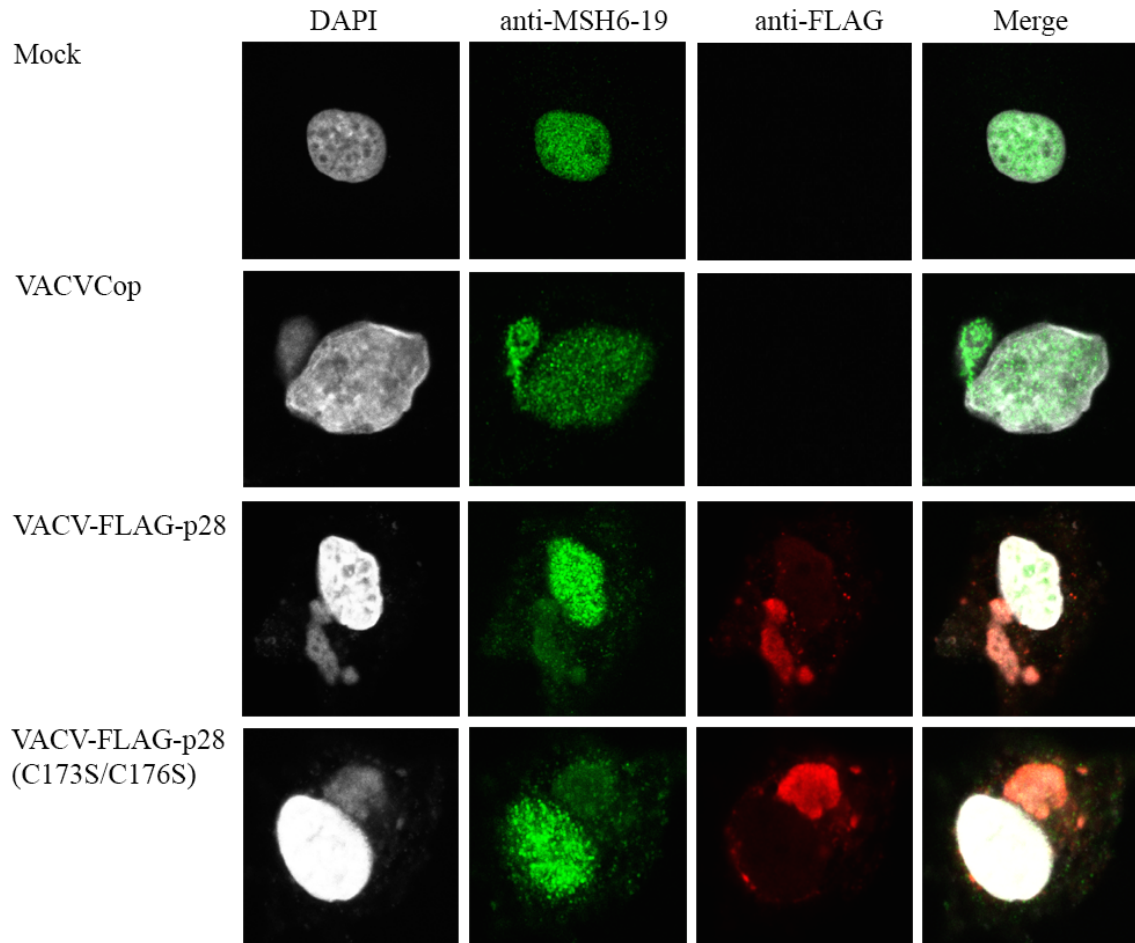
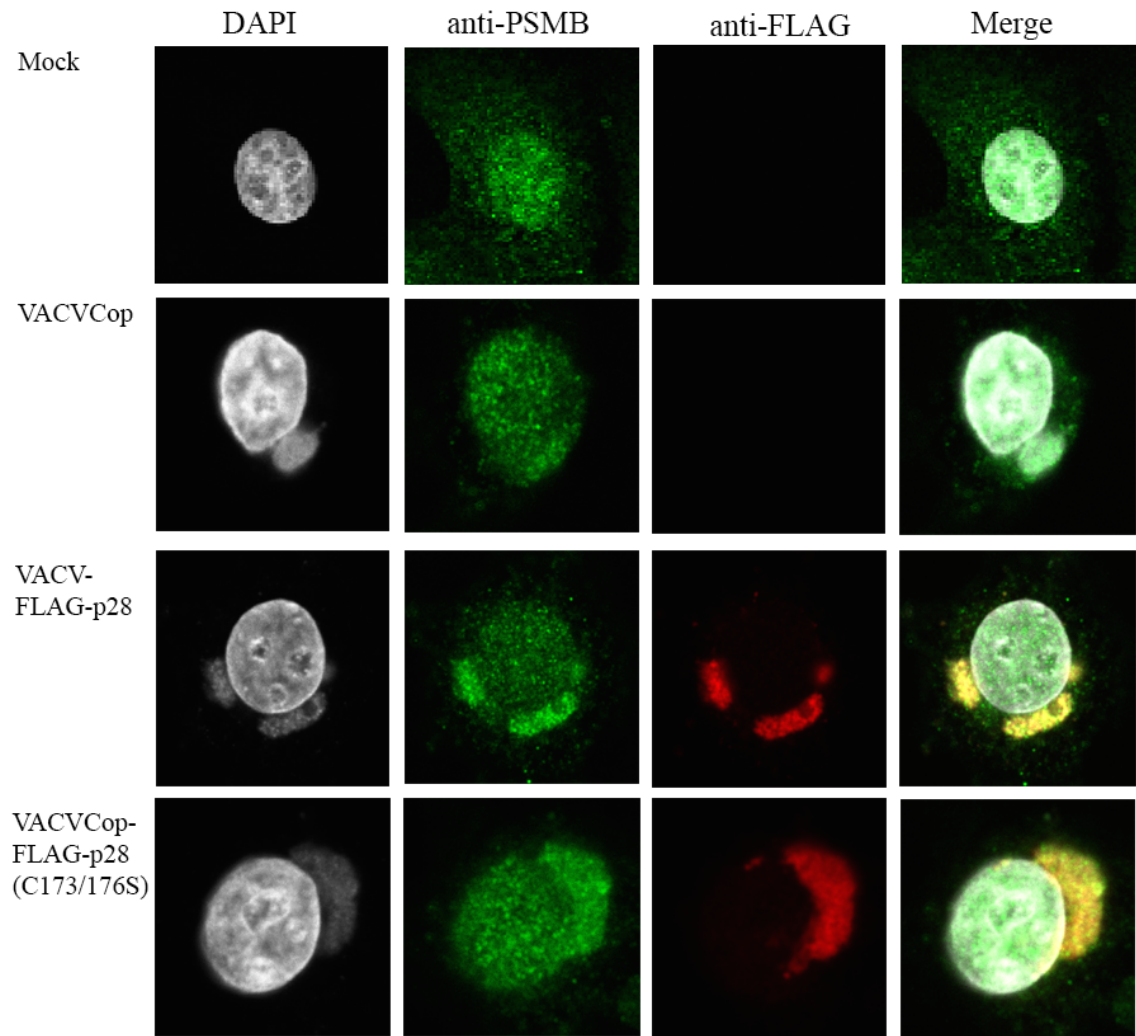


**Figure A.2.4 VACVCop infection leads to MSH6 localization to the virus factories, independent on the presence of functional p28.** HeLa cells were mock-infected or infected with VACVCop, VACV-FLAG-p28, or VACV-FLAG-p28(C173S/C176S) at an MOI of 5 for 14 hours. Cells were fixed in 4% PFA and stained for anti-FLAG, anti-MSH6, DAPI and were analyzed with confocal analysis. We compared the localization of MSH6 at the virus factory where p28 resides, which was evaluated with confocal analysis. In VACVCop infected cells, MSH6 localized to the virus factory. A similar effect was seen for VACVCop infected cells expressing FLAG-p28 or FLAG-p28(C173S/C176S). We did not further follow up on MSH6, since VACVCop infection led to MSH6 localization to the virus factories, independent on the presence of functional p28.

A



B

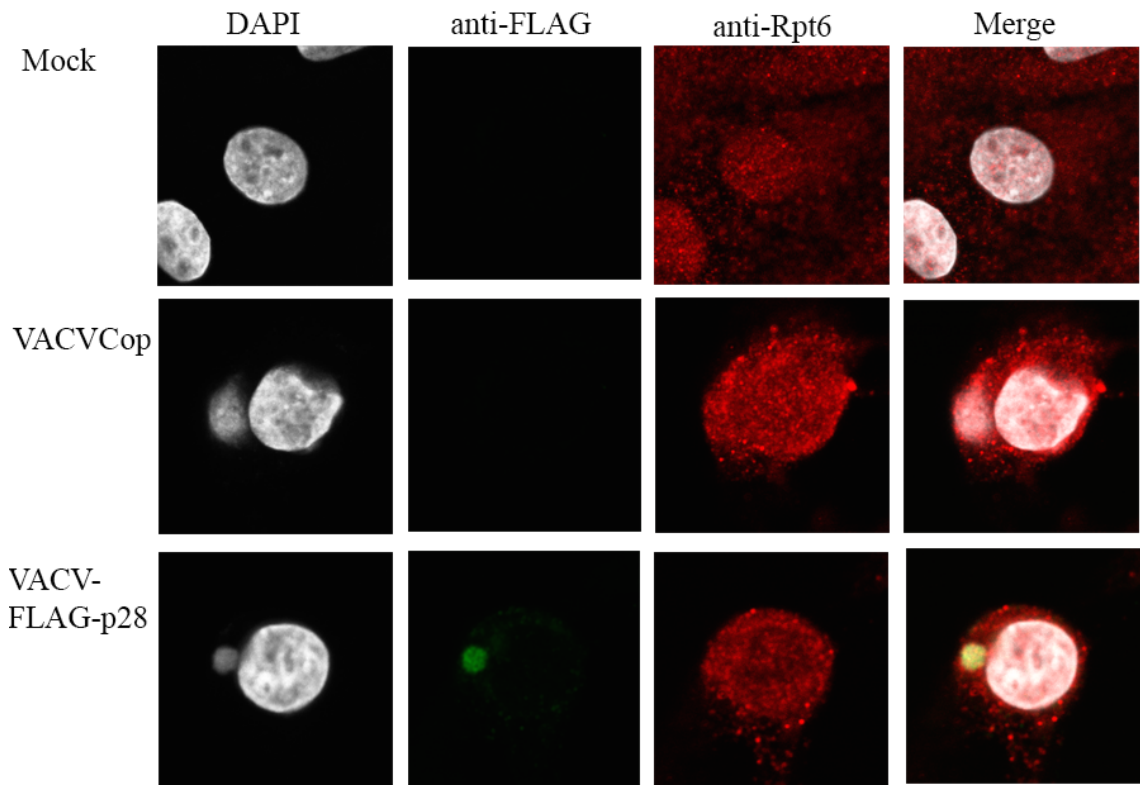


**Figure A.2.5 p28 leads to the enrichment of proteasomal subunit PSMB3 to the virus factory, but has no effect on the subunit Rpt6.** HeLa cells were infected with VACVCop, VACV-FLAG-p28, or VACV-FLAG-p28(C17S/C176S) at an MOI of 5 for 14 hours. Cells were fixed in 4% PFA and stained for mouse anti-FLAG, DAPI, and (A) rabbit anti-PSMB, or (B) anti-Rpt6 and were analyzed with confocal analysis. The presence of FLAG-p28 led to the enrichment of PSMB to the virus factory, but had no effect on Rpt6.

**Table A.1 Cellular mass spectrometry results of FLAG-p28 and FLAG-p28(C173S/C176S) pull-downs. Score: Abundance of peptides in the sample.**

**Coverage: percentage of protein recovered.**

<b>Accession</b>	<b>Description</b>	<b>Score VACV- FLAG p28 (C173S/ C176S)</b>	<b>Coverage VACV- FLAG p28 (C173S/ C176S)</b>	<b>Score VACV- FLAG- p28</b>	<b>Coverage VACV- FLAG- p28</b>
<b>P0CG48</b>	Polyubiquitin-C OS=Homo sapiens GN=UBC PE=1 SV=3 - [UBC_HUMAN ]	62.24	61.75	90.88	49.93
<b>P87607</b>	E3 ubiquitin- protein ligase p28-like OS=Cowpox virus (strain GRI-90 / Grishak) GN=p28 PE=3 SV=1 - [P28_CWPXG]	864.99	38.84	799.26	48.76
<b>P11142</b>	Heat shock cognate 71 kDa protein OS=Homo sapiens GN=HSPA8 PE=1 SV=1 - [HSP7C_HUM AN]	688.63	49.85	430.05	47.83
<b>O57224</b>	25 kDa core protein A12L OS=Vaccinia virus (strain Ankara) GN=MVA123L PE=2 SV=1 - [A12_VACCA]	16.85	34.76	48.57	47.59

<b>P23396</b>	40S ribosomal protein S3 OS=Homo sapiens GN=RPS3 PE=1 SV=2 - [RS3_HUMAN]	52.46	44.86	20.50	31.28
<b>O60884</b>	DnaJ homolog subfamily A member 2 OS=Homo sapiens GN=DNAJA2 PE=1 SV=1 - [DNJA2_HUMAN]	39.23	25.97	77.98	35.44
<b>Q49PZ0</b>	E3 ubiquitin ligase p28-like OS=Vaccinia virus (strain LC16m0) GN=p28 PE=3 SV=1 - [P28_VACC0]	904.07	38.49	883.42	37.66
<b>P35998</b>	26S protease regulatory subunit 7 OS=Homo sapiens GN=PSMC2 PE=1 SV=3 - [PRS7_HUMAN]	33.57	30.02	39.31	27.02
<b>P49411</b>	Elongation factor Tu, mitochondrial OS=Homo sapiens GN=TUFM PE=1 SV=2 - [EFTU_HUMAN]	54.80	29.87	105.03	38.05
<b>P38646</b>	Stress-70 protein, mitochondrial OS=Homo	120.85	35.20	139.19	26.66

	sapiens GN=HSPA9 PE=1 SV=2 - [GRP75_HUMAN]					
<b>P25705</b>	ATP synthase subunit alpha, mitochondrial OS=Homo sapiens GN=ATP5A1 PE=1 SV=1 - [ATPA_HUMAN]	40.63	20.07	104.39	34.36	
<b>P08107</b>	Heat shock protein 70 kDa 1A/1B OS=Homo sapiens GN=HSPA1A PE=1 SV=5 - [HSP71_HUMAN]	150.07	32.14	179.39	27.61	
<b>P60709</b>	Actin, cytoplasmic 1 OS=Homo sapiens GN=ACTB PE=1 SV=1 - [ACTB_HUMAN]	49.02	25.87	77.88	29.33	
<b>P20643</b>	Major core protein 4b OS=Vaccinia virus (strain Copenhagen) GN=A3L PE=3 SV=1 - [P4B_VACCC]	86.88	18.48	287.94	29.50	
<b>P55072</b>	Transitional endoplasmic reticulum ATPase OS=Homo sapiens GN=VCP PE=1	87.64	28.04	25.90	13.03	

	SV=4 - [TERA_HUMAN]				
<b>P05141</b>	ADP/ATP translocase 2 OS=Homo sapiens GN=SLC25A5 PE=1 SV=7 - [ADT2_HUMAN]	101.17	29.19	118.65	19.80
<b>P04792</b>	Heat shock protein beta-1 OS=Homo sapiens GN=HSPB1 PE=1 SV=2 - [HSPB1_HUMAN]	8.27	18.05	22.69	23.41
<b>Q07021</b>	Complement component 1 Q subcomponent-binding protein, mitochondrial OS=Homo sapiens GN=C1QBP PE=1 SV=1 - [C1QBP_HUMAN]	27.01	26.95		0.00
<b>P20638</b>	Envelope protein F13 OS=Vaccinia virus (strain Copenhagen) GN=F13L PE=3 SV=1 - [F13_VACCC]	55.66	26.34	40.42	23.92
<b>P31689</b>	DnaJ homolog subfamily A member 1 OS=Homo sapiens GN=DNAJA1 PE=1 SV=2 - [DNJA1_HUMAN]	32.93	23.17	68.39	26.20

	AN]				
<b>Q9NS69</b>	Mitochondrial import receptor subunit TOM22 homolog OS=Homo sapiens GN=TOMM22 PE=1 SV=3 - [TOM22_HUMAN]		0.00	10.90	26.06
<b>P12236</b>	ADP/ATP translocase 3 OS=Homo sapiens GN=SLC25A6 PE=1 SV=4 - [ADT3_HUMAN]	43.17	25.84	25.98	16.11
<b>Q9UJS0</b>	Calcium-binding mitochondrial carrier protein Aralar2 OS=Homo sapiens GN=SLC25A13 PE=1 SV=2 - [CMC2_HUMAN]	54.27	25.33	18.72	8.44
<b>P62195</b>	26S protease regulatory subunit 8 OS=Homo sapiens GN=PSMC5 PE=1 SV=1 - [PRS8_HUMAN]	37.89	22.66	40.08	22.17
<b>O95816</b>	BAG family molecular chaperone regulator 2 OS=Homo sapiens GN=BAG2 PE=1 SV=1 -	15.08	23.22	17.59	15.64

	[BAG2_HUMAN]					
<b>P62191</b>	26S protease regulatory subunit 4 OS=Homo sapiens GN=PSMC1 PE=1 SV=1 - [PRS4_HUMAN]	28.01	18.18	55.84	22.73	
<b>P43686</b>	26S protease regulatory subunit 6B OS=Homo sapiens GN=PSMC4 PE=1 SV=2 - [PRS6B_HUMAN]	21.03	9.09	43.59	22.49	
<b>P12004</b>	Proliferating cell nuclear antigen OS=Homo sapiens GN=PCNA PE=1 SV=1 - [PCNA_HUMAN]	30.71	22.22	14.66	16.48	
<b>Q92616</b>	Translational activator GCN1 OS=Homo sapiens GN=GCN1L1 PE=1 SV=6 - [GCN1L_HUMAN]	211.61	21.19	69.59	8.91	
<b>P68608</b>	DNA-directed RNA polymerase 22 kDa subunit OS=Vaccinia virus (strain Copenhagen) GN=RPO22 PE=3 SV=1 - [RP22_VACCC	7.73	10.81	13.71	21.08	

	]					
<b>Q01813</b>	6-phosphofructokinase type C OS=Homo sapiens GN=PFKP PE=1 SV=2 - [K6PP_HUMAN]	45.74	19.13	43.84	18.49	
<b>P62269</b>	40S ribosomal protein S18 OS=Homo sapiens GN=RPS18 PE=1 SV=3 - [RS18_HUMAN]	16.92	21.05	22.96	21.05	
<b>P48047</b>	ATP synthase subunit O, mitochondrial OS=Homo sapiens GN=ATP5O PE=1 SV=1 - [ATPO_HUMAN]	10.60	20.66		0.00	
<b>P21057</b>	Protein A34 OS=Vaccinia virus (strain Copenhagen) GN=A34R PE=3 SV=1 - [A34_VACCC]	8.32	13.69	8.84	14.88	
<b>P18085</b>	ADP-ribosylation factor 4 OS=Homo sapiens GN=ARF4 PE=1 SV=3 - [ARF4_HUMAN]		0.00	7.92	20.00	
<b>Q9BSD7</b>	Cancer-related nucleoside-triphosphatase		0.00	7.88	20.00	

	OS=Homo sapiens GN=NTPCR PE=1 SV=1 - [NTPCR_HUMAN]				
<b>P61204</b>	ADP-ribosylation factor 3 OS=Homo sapiens GN=ARF3 PE=1 SV=2 - [ARF3_HUMAN]		0.00	12.43	19.89
<b>Q9UNM6</b>	26S proteasome non-ATPase regulatory subunit 13 OS=Homo sapiens GN=PSMD13 PE=1 SV=2 - [PSD13_HUMAN]	9.68	10.64	15.18	17.02
<b>P51571</b>	Translocon-associated protein subunit delta OS=Homo sapiens GN=SSR4 PE=1 SV=1 - [SSRD_HUMAN]		0.00	8.11	19.65
<b>Q06830</b>	Peroxiredoxin-1 OS=Homo sapiens GN=PRDX1 PE=1 SV=1 - [PRDX1_HUMAN]	10.74	19.60	8.20	14.57
<b>P68457</b>	Late transcription elongation factor G2 OS=Vaccinia	7.76	11.36	12.49	13.64

	virus (strain Copenhagen) GN=G2R PE=3 SV=1 - [G2_VACCC]					
<b>Q92928</b>	Putative Ras- related protein Rab-1C OS=Homo sapiens GN=RAB1C PE=5 SV=2 - [RAB1C_HUM AN]		0.00	5.46	13.43	
<b>P30050</b>	60S ribosomal protein L12 OS=Homo sapiens GN=RPL12 PE=1 SV=1 - [RL12_HUMA N]	11.33	18.79	7.96	18.79	
<b>P62333</b>	26S protease regulatory subunit 10B OS=Homo sapiens GN=PSMC6 PE=1 SV=1 - [PRS10_HUMA N]	16.01	15.68	15.90	15.68	
<b>P17980</b>	26S protease regulatory subunit 6A OS=Homo sapiens GN=PSMC3 PE=1 SV=3 - [PRS6A_HUM AN]	29.34	18.68	23.68	13.21	
<b>P36404</b>	ADP- ribosylation factor-like protein 2 OS=Homo sapiens	7.68	18.48		0.00	

	GN=ARL2 PE=1 SV=4 - [ARL2_HUMAN]				
<b>P61026</b>	Ras-related protein Rab-10 OS=Homo sapiens GN=RAB10 PE=1 SV=1 - [RAB10_HUMAN]	5.27	11.50		0.00
<b>Q99653</b>	Calcineurin B homologous protein 1 OS=Homo sapiens GN=CHP1 PE=1 SV=3 - [CHP1_HUMAN]		0.00	7.89	16.92
<b>P78527</b>	DNA-dependent protein kinase catalytic subunit OS=Homo sapiens GN=PRKDC PE=1 SV=3 - [PRKDC_HUMAN]	282.16	16.25	94.79	7.10
<b>O95831</b>	Apoptosis-inducing factor 1, mitochondrial OS=Homo sapiens GN=AIFM1 PE=1 SV=1 - [AIFM1_HUMAN]	26.56	14.52	19.32	9.79
<b>O57198</b>	Late transcription factor 1 OS=Vaccinia virus (strain Ankara) GN=VLTF1	22.54	16.54	19.47	16.54

	PE=2 SV=1 - [VLTF1_VACC A]				
<b>Q9BZX2</b>	Uridine-cytidine kinase 2 OS=Homo sapiens GN=UCK2 PE=1 SV=1 - [UCK2_HUMA N]		0.00	18.21	16.48
<b>O57245</b>	3 beta- hydroxysteroid dehydrogenase/ Delta 5-->4- isomerase OS=Vaccinia virus (strain Ankara) GN=MVA157L PE=3 SV=1 - [3BHS_VACCA ]	12.19	13.87	11.71	10.12
<b>O43242</b>	26S proteasome non-ATPase regulatory subunit 3 OS=Homo sapiens GN=PSMD3 PE=1 SV=2 - [PSMD3_HUM AN]	18.63	13.67	13.33	9.74
<b>P62263</b>	40S ribosomal protein S14 OS=Homo sapiens GN=RPS14 PE=1 SV=3 - [RS14_HUMA N]			5.18	15.89
<b>Q3ZCQ8</b>	Mitochondrial import inner membrane translocase subunit TIM50	7.70	11.33	9.57	12.46

	OS=Homo sapiens GN=TIMM50 PE=1 SV=2 - [TIM50_HUMAN]				
<b>Q9NVI7</b>	ATPase family AAA domain-containing protein 3A OS=Homo sapiens GN=ATAD3A PE=1 SV=2 - [ATD3A_HUMAN]	19.37	8.20	24.09	11.83
<b>O00231</b>	26S proteasome non-ATPase regulatory subunit 11 OS=Homo sapiens GN=PSMD11 PE=1 SV=3 - [PSD11_HUMAN]	11.60	12.56	8.66	5.92
<b>P16615</b>	Sarcoplasmic/endoplasmic reticulum calcium ATPase 2 OS=Homo sapiens GN=ATP2A2 PE=1 SV=1 - [AT2A2_HUMAN]	70.72	13.63	28.24	8.83
<b>P08238</b>	Heat shock protein HSP 90-beta OS=Homo sapiens GN=HSP90AB1 PE=1 SV=4 - [HS90B_HUMAN]	30.88	13.67	32.09	13.12
<b>P20495</b>	Dual specificity protein		0.00	8.37	14.62

	phosphatase H1 OS=Vaccinia virus (strain Copenhagen) GN=H1L PE=2 SV=1 - [DUSP_VACC C]					
<b>O75832</b>	26S proteasome non-ATPase regulatory subunit 10 OS=Homo sapiens GN=PSMD10 PE=1 SV=1 - [PSD10_HUMA N]	6.07	14.60		0.00	
<b>O14980</b>	Exportin-1 OS=Homo sapiens GN=XPO1 PE=1 SV=1 - [XPO1_HUMA N]	41.90	13.54	9.32	1.87	
<b>P20642</b>	Major core protein 4a precursor OS=Vaccinia virus (strain Copenhagen) GN=A10L PE=3 SV=1 - [P4A_VACCC]	12.55	5.72	53.40	14.25	
<b>Q99460</b>	26S proteasome non-ATPase regulatory subunit 1 OS=Homo sapiens GN=PSMD1 PE=1 SV=2 - [PSMD1_HUM AN]	28.97	13.96	8.35	6.40	
<b>P53007</b>	Tricarboxylate transport	15.98	13.50	12.99	9.65	

	protein, mitochondrial OS=Homo sapiens GN=SLC25A1 PE=1 SV=2 - [TXTP_HUMAN]					
<b>P11441</b>	Ubiquitin-like protein 4A OS=Homo sapiens GN=UBL4A PE=1 SV=1 - [UBL4A_HUMAN]	5.40	13.38	17.29	13.38	
<b>Q13200</b>	26S proteasome non-ATPase regulatory subunit 2 OS=Homo sapiens GN=PSMD2 PE=1 SV=3 - [PSMD2_HUMAN]	30.27	9.36	51.97	13.33	
<b>O43175</b>	D-3- phosphoglycerate dehydrogenase OS=Homo sapiens GN=PHGDH PE=1 SV=4 - [SERA_HUMAN]	11.96	9.01	21.65	13.32	
<b>P10809</b>	60 kDa heat shock protein, mitochondrial OS=Homo sapiens GN=HSPD1 PE=1 SV=2 - [CH60_HUMAN]	10.82	5.76	20.22	11.17	
<b>O14925</b>	Mitochondrial import inner	8.92	12.92		0.00	

	membrane translocase subunit Tim23 OS=Homo sapiens GN=TIMM23 PE=1 SV=1 - [TIM23_HUMAN]				
<b>Q9UBS4</b>	DnaJ homolog subfamily B member 11 OS=Homo sapiens GN=DNAJB11 PE=1 SV=1 - [DJB11_HUMAN]	10.43	12.85		0.00
<b>Q76RA8</b>	Thymidylate kinase OS=Vaccinia virus (strain Ankara) GN=TMK PE=3 SV=1 - [KTHY_VACC A]		0.00	12.51	12.75
<b>Q9NP72</b>	Ras-related protein Rab-18 OS=Homo sapiens GN=RAB18 PE=1 SV=1 - [RAB18_HUMAN]		0.00	6.19	12.62
<b>P07477</b>	Trypsin-1 OS=Homo sapiens GN=PRSS1 PE=1 SV=1 - [TRY1_HUMAN]	33.93	12.15	35.88	12.15
<b>P20985</b>	Protein A6 OS=Vaccinia virus (strain Copenhagen)	16.12	11.83	6.54	6.45

	GN=A6L PE=3 SV=1 - [A6_VACCC]				
<b>Q75746</b>	Calcium-binding mitochondrial carrier protein Aralar1 OS=Homo sapiens GN=SLC25A12 PE=1 SV=2 - [CMC1_HUMAN]	23.93	11.80		0.00
<b>Q07020</b>	60S ribosomal protein L18 OS=Homo sapiens GN=RPL18 PE=1 SV=2 - [RL18_HUMAN]	5.11	11.70		0.00
<b>Q76RB8</b>	Protein A11 OS=Vaccinia virus (strain Ankara) GN=MVA122R PE=2 SV=1 - [A11_VACCA]	9.09	11.64		0.00
<b>Q9NX63</b>	Coiled-coil- helix-coiled- coil-helix domain- containing protein 3, mitochondrial OS=Homo sapiens GN=CHCHD3 PE=1 SV=1 - [CHCH3_HUMAN]	6.90	11.45	7.18	11.45
<b>Q9BWM7</b>	Sideroflexin-3 OS=Homo sapiens GN=SFXN3 PE=1 SV=2 -	8.90	11.38		0.00

	[SFXN3_HUMAN]			
<b>Q8WWC4</b>	Uncharacterized protein C2orf47, mitochondrial OS=Homo sapiens GN=C2orf47 PE=1 SV=1 - [CB047_HUMAN]		0.00	8.17 11.34
<b>P62826</b>	GTP-binding nuclear protein Ran OS=Homo sapiens GN=RAN PE=1 SV=3 - [RAN_HUMAN]	5.82	11.11	0.00
<b>P17844</b>	Probable ATP-dependent RNA helicase DDX5 OS=Homo sapiens GN=DDX5 PE=1 SV=1 - [DDX5_HUMAN]	19.43	10.91	0.00
<b>O93117</b>	Telomere-binding protein I1 OS=Vaccinia virus (strain Ankara) GN=MVA062L PE=2 SV=1 - [I1_VACCA]	18.38	10.90	0.00
<b>P51148</b>	Ras-related protein Rab-5C OS=Homo sapiens GN=RAB5C PE=1 SV=2 - [RAB5C_HUMAN]	5.31	10.65	0.00
<b>O94905</b>	Erlin-2 OS=Homo	9.57	10.62	0.00

	sapiens GN=ERLIN2 PE=1 SV=1 - [ERLN2_HUMAN]				
<b>P22695</b>	Cytochrome b-c1 complex subunit 2, mitochondrial OS=Homo sapiens GN=UQCRC2 PE=1 SV=3 - [QCR2_HUMAN]	9.80	10.60	6.94	7.73
<b>Q9Y3D8</b>	Adenylate kinase isoenzyme 6 OS=Homo sapiens GN=TAF9 PE=1 SV=1 - [KAD6_HUMAN]	5.28	10.47	5.45	10.47
<b>P43246</b>	DNA mismatch repair protein Msh2 OS=Homo sapiens GN=MSH2 PE=1 SV=1 - [MSH2_HUMAN]	29.37	9.31	18.51	6.21
<b>P52597</b>	Heterogeneous nuclear ribonucleoprotein F OS=Homo sapiens GN=HNRNPF PE=1 SV=3 - [HNRPF_HUMAN]	6.13	7.95	7.36	6.51
<b>O14966</b>	Ras-related protein Rab-7L1 OS=Homo sapiens		0.00	5.24	10.34

	GN=RAB7L1 PE=1 SV=1 - [RAB7L_HUMAN]				
<b>P52701</b>	DNA mismatch repair protein Msh6 OS=Homo sapiens GN=MSH6 PE=1 SV=2 - [MSH6_HUMAN]	31.63	10.22	12.39	2.72
<b>P40939</b>	Trifunctional enzyme subunit alpha, mitochondrial OS=Homo sapiens GN=HADHA PE=1 SV=2 - [ECHA_HUMAN]	6.14	3.28	12.23	6.42
<b>Q00325</b>	Phosphate carrier protein, mitochondrial OS=Homo sapiens GN=SLC25A3 PE=1 SV=2 - [MPCP_HUMAN]	71.87	9.67	36.17	7.18
<b>P50416</b>	Carnitine O-palmitoyltransferase 1, liver isoform OS=Homo sapiens GN=CPT1A PE=1 SV=2 - [CPT1A_HUMAN]	11.71	6.60	22.25	9.57
<b>O43592</b>	Exportin-T OS=Homo sapiens GN=XPOT	25.56	9.46		0.00

	PE=1 SV=2 - [XPOT_HUMAN]				
<b>O57187</b>	DNA-directed RNA polymerase 30 kDa polypeptide OS=Vaccinia virus (strain Ankara) GN=RPO30 PE=4 SV=1 - [RPO5_VACCARIA]		0.00	6.29	9.27
<b>Q96EY1</b>	DnaJ homolog subfamily A member 3, mitochondrial OS=Homo sapiens GN=DNAJA3 PE=1 SV=2 - [DNJA3_HUMAN]	5.29	5.83	6.35	6.67
<b>Q9UBX3</b>	Mitochondrial dicarboxylate carrier OS=Homo sapiens GN=SLC25A10 PE=1 SV=2 - [DIC_HUMAN]	6.74	9.06		0.00
<b>P57088</b>	Transmembrane protein 33 OS=Homo sapiens GN=TMEM33 PE=1 SV=2 - [TMM33_HUMAN]	5.47	8.91		0.00
<b>P22061</b>	Protein-L-isoaspartate(D-aspartate) O-methyltransferase OS=Homo sapiens	5.06	8.81		0.00

	GN=PCMT1 PE=1 SV=4 - [PIMT_HUMAN]				
<b>P21049</b>	Protein E8 OS=Vaccinia virus (strain Copenhagen) GN=E8R PE=2 SV=1 - [E8_VACCC]	5.13	8.79		
<b>Q9H936</b>	Mitochondrial glutamate carrier 1 OS=Homo sapiens GN=SLC25A22 PE=1 SV=1 - [GHC1_HUMAN]	6.59	8.67		0.00
<b>Q9Y4W6</b>	AFG3-like protein 2 OS=Homo sapiens GN=AFG3L2 PE=1 SV=2 - [AFG32_HUMAN]	11.28	6.15	14.44	7.53
<b>P11310</b>	Medium-chain specific acyl-CoA dehydrogenase, mitochondrial OS=Homo sapiens GN=ACADM PE=1 SV=1 - [ACADM_HUMAN]	8.69	8.55	9.32	8.55
<b>O60762</b>	Dolichol-phosphate mannosyltransferase OS=Homo sapiens GN=DPM1 PE=1 SV=1 -	6.19	8.46	6.02	8.46

	[DPM1_HUMAN]					
<b>P46379</b>	Large proline-rich protein BAG6 OS=Homo sapiens GN=BAG6 PE=1 SV=2 - [BAG6_HUMAN]	10.77	4.42	24.18	8.39	
<b>Q9H5Q4</b>	Dimethyladenosine transferase 2, mitochondrial OS=Homo sapiens GN=TFB2M PE=1 SV=1 - [TFB2M_HUMAN]	5.06	4.29	5.75	6.31	
<b>P05023</b>	Sodium/potassium-transporting ATPase subunit alpha-1 OS=Homo sapiens GN=ATP1A1 PE=1 SV=1 - [AT1A1_HUMAN]	29.44	8.31	6.59	2.74	
<b>P49368</b>	T-complex protein 1 subunit gamma OS=Homo sapiens GN=CCT3 PE=1 SV=4 - [TCPG_HUMAN]	8.58	6.24	5.55	4.04	
<b>P46781</b>	40S ribosomal protein S9 OS=Homo sapiens GN=RPS9 PE=1 SV=3 - [RS9_HUMAN]	4.99	8.25		0.00	

<b>Q92598</b>	Heat shock protein 105 kDa OS=Homo sapiens GN=HSPH1 PE=1 SV=1 - [HS105_HUMAN]	15.17	8.16		0.00
<b>Q9H3U1</b>	Protein unc-45 homolog A OS=Homo sapiens GN=UNC45A PE=1 SV=1 - [UN45A_HUMAN]	19.28	8.16	6.11	2.75
<b>P21080</b>	Protein E2 OS=Vaccinia virus (strain Copenhagen) GN=E2L PE=3 SV=1 - [E2_VACCC]	15.74	8.14	9.56	5.29
<b>Q16401</b>	26S proteasome non-ATPase regulatory subunit 5 OS=Homo sapiens GN=PSMD5 PE=1 SV=3 - [PSMD5_HUMAN]			14.20	7.94
<b>P02768</b>	Serum albumin OS=Homo sapiens GN=ALB PE=1 SV=2 - [ALBU_HUMAN]	11.61	4.43	17.89	5.91
<b>P40938</b>	Replication factor C subunit 3 OS=Homo sapiens GN=RFC3 PE=1 SV=2 -		0.00	5.31	7.87

	[RFC3_HUMAN]			
<b>P21047</b>	Protein E6 OS=Vaccinia virus (strain Copenhagen) GN=E6R PE=2 SV=1 - [E6_VACCC]	12.68	7.76	0.00
<b>P36542</b>	ATP synthase subunit gamma, mitochondrial OS=Homo sapiens GN=ATP5C1 PE=1 SV=1 - [ATPG_HUMAN]	6.72	7.72	0.00
<b>O14732</b>	Inositol monophosphatase 2 OS=Homo sapiens GN=IMPA2 PE=1 SV=1 - [IMPA2_HUMAN]	7.87	7.64	0.00
<b>Q96TA2</b>	ATP-dependent zinc metalloprotease YME1L1 OS=Homo sapiens GN=YME1L1 PE=1 SV=2 - [YMEL1_HUMAN]	13.83	7.63	0.00
<b>P55060</b>	Exportin-2 OS=Homo sapiens GN=CSE1L PE=1 SV=3 - [XPO2_HUMAN]	20.71	7.62	0.00
<b>P09651</b>	Heterogeneous nuclear ribonucleoprotei	8.65	7.53	0.00

	n A1 OS=Homo sapiens GN=HNRNPA1 PE=1 SV=5 - [ROA1_HUMAN]				
<b>P51665</b>	26S proteasome non-ATPase regulatory subunit 7 OS=Homo sapiens GN=PSMD7 PE=1 SV=2 - [PSD7_HUMAN]	8.14	7.41		0.00
<b>P62701</b>	40S ribosomal protein S4, X isoform OS=Homo sapiens GN=RPS4X PE=1 SV=2 - [RS4X_HUMAN]	5.31	7.22		0.00
<b>P21060</b>	Protein A37 OS=Vaccinia virus (strain Copenhagen) GN=A37R PE=3 SV=1 - [A37_VACCC]		0.00	5.21	7.22
<b>O57178</b>	Protein F12 OS=Vaccinia virus (strain Ankara) GN=MVA042L PE=3 SV=1 - [F12_VACCA]	13.87	7.09		0.00
<b>Q9UG63</b>	ATP-binding cassette sub-family F member 2 OS=Homo sapiens GN=ABCF2	17.96	7.06	8.30	3.85

	PE=1 SV=2 - [ABCF2_HUMAN]				
<b>Q92841</b>	Probable ATP-dependent RNA helicase DDX17 OS=Homo sapiens GN=DDX17 PE=1 SV=2 - [DDX17_HUMAN]	14.75	7.00		0.00
<b>P05388</b>	60S acidic ribosomal protein P0 OS=Homo sapiens GN=RPLP0 PE=1 SV=1 - [RLA0_HUMAN]	5.76	6.94		0.00
<b>Q86VP6</b>	Cullin-associated NEDD8-dissociated protein 1 OS=Homo sapiens GN=CAND1 PE=1 SV=2 - [CAND1_HUMAN]	11.21	4.31	15.67	4.88
<b>Q2TB90</b>	Putative hexokinase HKDC1 OS=Homo sapiens GN=HKDC1 PE=1 SV=3 - [HKDC1_HUMAN]	21.12	6.87	12.14	3.49
<b>Q15366</b>	Poly(rC)-binding protein 2 OS=Homo sapiens GN=PCBP2	5.51	6.85		0.00

	PE=1 SV=1 - [PCBP2_HUM AN]				
<b>Q92621</b>	Nuclear pore complex protein Nup205 OS=Homo sapiens GN=NUP205 PE=1 SV=3 - [NU205_HUM AN]	32.11	5.86	25.95	4.22
<b>P33810</b>	Scaffold protein D13 OS=Variola virus (isolate Human/India/Ind3/1967) GN=D13L PE=3 SV=1 - [D13 VAR67]	5.47	4.72	5.38	4.17
<b>P20700</b>	Lamin-B1 OS=Homo sapiens GN=LMNB1 PE=1 SV=2 - [LMNB1_HUM AN]	7.89	6.14		0.00
<b>P08195</b>	4F2 cell-surface antigen heavy chain OS=Homo sapiens GN=SLC3A2 PE=1 SV=3 - [4F2 HUMAN]	9.15	6.03		0.00
<b>Q8N1F7</b>	Nuclear pore complex protein Nup93 OS=Homo sapiens GN=NUP93 PE=1 SV=2 - [NUP93_HUM AN]		0.00	11.78	5.98
<b>Q96S55</b>	ATPase WRNIP1	9.56	5.86	6.10	4.06

	OS=Homo sapiens GN=WRNIP1 PE=1 SV=2 - [WRIP1_HUMAN]				
<b>P04843</b>	Dolichyl-diphosphooligosaccharide--protein glycosyltransferase subunit 1 OS=Homo sapiens GN=RPN1 PE=1 SV=1 - [RPN1_HUMAN]	5.80	3.79	10.96	5.77
<b>Q16891</b>	Mitochondrial inner membrane protein OS=Homo sapiens GN=IMMT PE=1 SV=1 - [IMMT_HUMAN]	5.81	4.35	9.17	5.54
<b>O76031</b>	ATP-dependent Clp protease ATP-binding subunit clpX-like, mitochondrial OS=Homo sapiens GN=CLPX PE=1 SV=2 - [CLPX_HUMAN]	6.16	3.63	6.38	3.95
<b>Q9Y265</b>	RuvB-like OS=Homo sapiens GN=RUVBL1 PE=1 SV=1 - [RUVBL1_HUMAN]	1 4.98	5.48		0.00

<b>P21022</b>	Metalloendopeptidase G1 OS=Vaccinia virus (strain Copenhagen) GN=G1L PE=3 SV=1 - [G1_VACCC]	7.79	5.41	8.26	3.38
<b>Q9Y230</b>	RuvB-like 2 OS=Homo sapiens GN=RUVBL2 PE=1 SV=3 - [RUVB2_HUMAN]	5.18	5.18		
<b>Q15645</b>	Pachytene checkpoint protein 2 homolog OS=Homo sapiens GN=TRIP13 PE=1 SV=2 - [PCH2_HUMAN]	5.71	5.09		0.00
<b>P28288</b>	ATP-binding cassette sub-family D member 3 OS=Homo sapiens GN=ABCD3 PE=1 SV=1 - [ABCD3_HUMAN]	8.83	4.86	11.61	3.49
<b>O00232</b>	26S proteasome non-ATPase regulatory subunit 12 OS=Homo sapiens GN=PSMD12 PE=1 SV=3 - [PSD12_HUMAN]	8.27	4.82		0.00
<b>P33993</b>	DNA replication	5.05	2.92	5.04	3.06

	licensing factor MCM7 OS=Homo sapiens GN=MCM7 PE=1 SV=4 - [MCM7_HUMAN]				
<b>P08237</b>	6-phosphofructokinase, muscle type OS=Homo sapiens GN=PFKM PE=1 SV=2 - [K6PF_HUMAN]	9.86	4.62	6.15	2.95
<b>P34932</b>	Heat shock 70 kDa protein 4 OS=Homo sapiens GN=HSPA4 PE=1 SV=4 - [HSP74_HUMAN]	8.38	4.52		0.00
<b>Q00839</b>	Heterogeneous nuclear ribonucleoprotein U OS=Homo sapiens GN=HNRNPU PE=1 SV=6 - [HNRNPU_HUMAN]	12.76	4.48		0.00
<b>P61619</b>	Protein transport protein Sec61 subunit alpha isoform 1 OS=Homo sapiens GN=SEC61A1 PE=1 SV=2 - [S61A1_HUMAN]	5.11	4.41		0.00
<b>P35637</b>	RNA-binding protein FUS	5.23	4.37		

	OS=Homo sapiens GN=FUS PE=1 SV=1 - [FUS_HUMAN]				
<b>P33053</b>	DNA-directed RNA polymerase 147 kDa polypeptide OS=Variola virus (isolate Human/India/Ind3/1967) GN=RPO147 PE=3 SV=1 - [RP147_VAR67]	8.86	2.57	17.01	4.20
<b>A0FGR8</b>	Extended synaptotagmin-2 OS=Homo sapiens GN=ESYT2 PE=1 SV=1 - [ESYT2_HUMAN]	12.53	4.13	5.13	2.82
<b>P17987</b>	T-complex protein 1 subunit alpha OS=Homo sapiens GN=TCP1 PE=1 SV=1 - [TCPA_HUMAN]	5.36	3.96		0.00
<b>Q92973</b>	Transportin-1 OS=Homo sapiens GN=TNPO1 PE=1 SV=2 - [TNPO1_HUMAN]	8.55	3.79		0.00
<b>P17474</b>	DNA-directed RNA polymerase 132 kDa polypeptide OS=Cowpox virus (strain	14.09	3.78		0.00

	Brighton Red) GN=RPO132 PE=3 SV=1 - [RP132_CWPXB]					
<b>P27708</b>	CAD protein OS=Homo sapiens GN=CAD PE=1 SV=3 - [PYR1_HUMAN]	15.55	3.06	5.59	1.21	
<b>Q15029</b>	116 kDa U5 small nuclear ribonucleoprotein component OS=Homo sapiens GN=EFTUD2 PE=1 SV=1 - [U5S1_HUMAN]	8.38	3.50		0.00	
<b>Q96P70</b>	Importin-9 OS=Homo sapiens GN=IPO9 PE=1 SV=3 - [IPO9_HUMAN]	8.80	3.46		0.00	
<b>O57207</b>	RNA polymerase-associated transcription-specificity factor RAP94 OS=Vaccinia virus (strain Ankara) GN=RAP94 PE=2 SV=1 - [RAP94_VACCINA]		0.00	9.00	3.40	
<b>O75643</b>	U5 small nuclear ribonucleoprotein 200 kDa	16.65	3.28		0.00	

	<p> helicase  OS=Homo  sapiens  GN=SNRNP200  PE=1 SV=2 -  [U520_HUMAN] </p>				
<b>P46459</b>	<p> Vesicle-fusing  ATPase  OS=Homo  sapiens  GN=NSF PE=1  SV=3 -  [NSF_HUMAN] </p>		0.00	6.35	3.09
<b>Q14974</b>	<p> Importin subunit  beta-1  OS=Homo  sapiens  GN=KPNB1  PE=1 SV=2 -  [IMB1_HUMAN] </p>		0.00	4.93	3.08
<b>Q14204</b>	<p> Cytoplasmic  dynein 1 heavy  chain 1  OS=Homo  sapiens  GN=DYNC1H1  PE=1 SV=5 -  [DYHC1_HUMAN] </p>	30.86	2.48	13.72	1.27
<b>Q66K14</b>	<p> TBC1 domain  family member  9B OS=Homo  sapiens  GN=TBC1D9B  PE=1 SV=3 -  [TBC9B_HUMAN] </p>		0.00	8.59	2.80
<b>P19338</b>	<p> Nucleolin  OS=Homo  sapiens  GN=NCL PE=1  SV=3 -  [NUCL_HUMAN] </p>	5.84	2.68		0.00

<b>Q29RF7</b>	Sister chromatid cohesion protein PDS5 homolog A OS=Homo sapiens GN=PDS5A PE=1 SV=1 - [PDS5A_HUMAN]		0.00	7.42	2.24
<b>Q15386</b>	Ubiquitin-protein ligase E3C OS=Homo sapiens GN=UBE3C PE=1 SV=3 - [UBE3C_HUMAN]	4.97	2.03		0.00
<b>O95373</b>	Importin-7 OS=Homo sapiens GN=IPO7 PE=1 SV=1 - [IPO7_HUMAN]	5.32	2.02	8.31	2.02
<b>Q9NTJ3</b>	Structural maintenance of chromosomes protein 4 OS=Homo sapiens GN=SMC4 PE=1 SV=2 - [SMC4_HUMAN]		0.00	5.18	1.86
<b>A6NKG5</b>	Retrotransposon-like protein 1 OS=Homo sapiens GN=RTL1 PE=2 SV=3 - [RTL1_HUMAN]		0.00	5.51	1.69
<b>Q9Y6D5</b>	Brefeldin A-inhibited guanine nucleotide-	5.89	1.62		0.00

	exchange protein 2 OS=Homo sapiens GN=ARFGEF2 PE=1 SV=3 - [BIG2_HUMAN N]			
<b>Q5UIP0</b>	Telomere- associated protein RIF1 OS=Homo sapiens GN=RIF1 PE=1 SV=2 - [RIF1_HUMAN I]	7.60	1.54	0.00
<b>O95071</b>	E3 ubiquitin- protein ligase UBR5 OS=Homo sapiens GN=UBR5 PE=1 SV=2 - [UBR5_HUMAN N]	5.26	0.86	0.00
<b>Q13315</b>	Serine-protein kinase ATM OS=Homo sapiens GN=ATM PE=1 SV=3 - [ATM_HUMAN N]	5.40	0.72	

**Table A.2 VACV mass spectrometry results of FLAG-p28 and FLAG-p28(C173S/C176S) pull-downs.**

<b>Accession</b>	<b>Description</b>	<b>Score VACV- FLAG p28 (C173S/ C176S)</b>	<b>Coverage VACV- FLAG p28 (C173S/ C176S)</b>	<b>Score VACV- FLAG- p28</b>	<b>Coverage VACV- FLAG- p28</b>
<b>Q6RZT3</b>	RPXV008 OS=Rabbitpox virus GN=RPXV008 PE=4 SV=1 - [Q6RZT3_9POX V]	1655.94	49.17	1875.01	57.02
<b>A9J0R8</b>	20k virion core protein OS=Vaccinia virus (strain Ankara) GN=CVA138 PE=4 SV=1 - [A9J0R8_VACC A]	16.85	33.85	50.76	46.35
<b>H2DZ22</b>	Late transcription elongation factor OS=Vaccinia virus GN=VAC_DPP1 1_091 PE=4 SV=1 - [H2DZ22_9POX V]	11.92	19.09	25.83	31.82
<b>A4GDH7</b>	Major core protein p4b OS=Vaccinia virus GN=List118 PE=4 SV=1 - [A4GDH7_9POX V]	138.32	26.40	425.45	34.16
<b>L7QJK6</b>	Core protein OS=Vaccinia virus GN=A12L PE=4 SV=1 -	16.85	34.39		0.00

	[L7QJK6_9POX V]				
<b>Q8JLG8</b>	EEV phospholipase OS=Ectromelia virus GN=EVM036 PE=4 SV=1 - [Q8JLG8_9POX V]	75.29	33.33		0.00
<b>H2DYZ1</b>	Palmytilated EEV membrane protein OS=Vaccinia virus GN=VAC_DPP2 1_062 PE=4 SV=1 - [H2DYZ1_9POX V]		0.00	54.47	31.18
<b>Q9JFD6</b>	TE4L OS=Vaccinia virus (strain Tian Tan) PE=4 SV=1 - [Q9JFD6_VACC T]	6.13	30.86		
<b>M9WG49</b>	Tyr/Ser protein phosphatase OS=Vaccinia virus GN=VACV_TT1 0_120 PE=4 SV=1 - [M9WG49_9PO XV]	6.90	12.28	14.61	26.90
<b>A0ES19</b>	Hydroxysteroid dehydrogenase OS=Vaccinia virus GN=VAC_DPP1 3_181 PE=3 SV=1 - [A0ES19_9POX V]	20.09	18.79	15.68	15.32
<b>Q89207</b>	36kD late protein (Fragment)	45.09	25.94	12.87	19.80

	OS=Vaccinia virus PE=4 SV=1 - [Q89207_9POXV ]				
<b>A9J0X0</b>	EEV membrane glycoprotein OS=Vaccinia virus (strain Ankara) GN=CVA165 PE=4 SV=1 - [A9J0X0_VACC A]	20.02	25.60	24.47	25.60
<b>Q0GNZ8</b>	HSPV087 OS=Horsepox virus PE=4 SV=1 - [Q0GNZ8_HSPV ]	26.27	23.08	27.76	20.38
<b>Q85331</b>	RNA polymerase 22 kD subunit (Fragment) OS=Vaccinia virus PE=4 SV=1 - [Q85331_9POXV ]	7.73	11.17	13.71	21.79
<b>A9J1K3</b>	Putative uncharacterized protein CVA064 OS=Vaccinia virus (strain Ankara) GN=CVA064 PE=4 SV=1 - [A9J1K3_VACC A]	35.48	20.35	23.75	13.98
<b>B9U1U2</b>	Thymidylate kinase OS=Vaccinia virus GLV-1h68 GN=GL234 PE=4 SV=1 - [B9U1U2_9POX V]	3.98	7.35	18.44	20.10

<b>O57223</b>	Major core protein P4a OS=Vaccinia virus GN=MVA121L PE=4 SV=1 - [O57223_9POXV]	30.85	9.32		0.00
<b>M9WH30</b>	Uncharacterized protein OS=Vaccinia virus GN=VAC_TP3_1 35 PE=4 SV=1 - [M9WH30_9POXV]		0.00	15.05	13.84
<b>A4GDI5</b>	Putative uncharacterized protein OS=Vaccinia virus GN=List126 PE=4 SV=1 - [A4GDI5_9POXV]	13.94	17.61		0.00
<b>A9J0Q2</b>	Core protein required for morphogenesis OS=Vaccinia virus (strain Ankara) GN=CVA131 PE=4 SV=1 - [A9J0Q2_VACC A]	21.58	16.94	8.76	9.68
<b>B9U1N1</b>	Precursor p4a of core protein 4a OS=Vaccinia virus GLV-1h68 GN=GL174 PE=4 SV=1 - [B9U1N1_9POXV]	30.85	9.32		0.00
<b>A4GDB5</b>	DNA-dependent RNA polymerase subunit rpo30 OS=Vaccinia	9.12	16.22	8.30	12.74

	virus GN=List056 PE=4 SV=1 - [A4GDB5_9POX V]				
<b>Q9JF94</b>	TA5L OS=Vaccinia virus (strain Tian Tan) PE=4 SV=1 - [Q9JF94_VACC T]		0.00	10.19	14.71
<b>A0ERU7</b>	DNA-dependent RNA polymerase subunit rpo147 OS=Vaccinia virus GN=VAC_DPP1 6_109 PE=4 SV=1 - [A0ERU7_9POX V]	31.71	11.12	34.25	8.55
<b>H2DWL6</b>	Putative uncharacterized protein OS=Vaccinia virus GN=VAC_DPP1 6_184 PE=4 SV=1 - [H2DWL6_9POX V]		0.00	14.86	13.52
<b>H2DUQ8</b>	ER-localized MP OS=Vaccinia virus GN=VAC_DPP1 2_075 PE=4 SV=1 - [H2DUQ8_9POX V]	7.28	12.82		
<b>Q80DT6</b>	A42R protein OS=Cowpox virus GN=A42R PE=4 SV=1 - [Q80DT6_COWP X]		0.00	3.29	12.73
<b>B9U1G9</b>	Myristylprotein	6.27	9.41		0.00

	OS=Vaccinia virus GLV-1h68 GN=GL113 PE=4 SV=1 - [B9U1G9_9POX V]				
<b>Q77TL1</b>	TG8L OS=Vaccinia virus (strain Tian Tan) PE=4 SV=1 - [Q77TL1_VACC T]		4.89	10.78	
<b>A0ES09</b>	VACV-DUKE- 168 OS=Vaccinia virus GN=VAC_DPP2 1_171 PE=4 SV=1 - [A0ES09_9POX V]	0.00	7.18	10.65	
<b>B9U1D4</b>	Putative uncharacterized protein OS=Vaccinia virus GLV-1h68 GN=GL079 PE=4 SV=1 - [B9U1D4_9POX V]	16.38	10.58		0.00
<b>A0ERZ3</b>	DNA-directed RNA polymerase OS=Vaccinia virus GN=VAC_DPP9 _155 PE=3 SV=1 - [A0ERZ3_9POX V]	28.31	10.40	19.11	7.56
<b>L7QJ25</b>	Core protein vp8 OS=Vaccinia virus GN=L4R PE=4 SV=1 - [L7QJ25_9POXV ]	4.74	10.36	4.49	10.36
<b>Q8JLC9</b>	EVM086	13.74	7.68	16.78	7.81

	OS=Ectromelia virus GN=EVM086 PE=4 SV=1 - [Q8JLC9_9POX V]				
<b>F1DIT6</b>	Myristylprotein OS=Monkeypox virus PE=4 SV=1 - [F1DIT6_MONP V]		0.00	5.59	7.94
<b>Q8JLG2</b>	EVM045 OS=Ectromelia virus GN=EVM045 PE=4 SV=1 - [Q8JLG2_9POX V]	6.97	8.76		0.00
<b>H2DS96</b>	Insulin metalloproteinase -like OS=Vaccinia virus GN=VAC_DPP2 1_089 PE=4 SV=1 - [H2DS96_9POX V]	11.45	8.63	16.20	7.11
<b>A0ERR7</b>	VACV-DUKE- 076 OS=Vaccinia virus GN=VACV- DUKE-076 PE=4 SV=1 - [A0ERR7_9POX V]	8.27	5.71	14.15	7.06
<b>Q80DS5</b>	DNA ligase OS=Cowpox virus GN=A53R PE=3 SV=1 - [Q80DS5_COWP X]	7.27	5.25		0.00
<b>A0ES25</b>	DNA ligase OS=Vaccinia virus		0.00	2.20	3.80

	GN=VACV- DUKE-184 PE=3 SV=1 - [A0ES25_9POX V]				
<b>Q80E18</b>	G12L protein OS=Cowpox virus GN=G12L PE=4 SV=1 - [Q80E18_COWP X]	13.87	7.10	7.06	5.68
<b>A4GDJ3</b>	DNA helicase OS=Vaccinia virus GN=List134 PE=4 SV=1 - [A4GDJ3_9POX V]	6.80	7.10		
<b>E2CZJ5</b>	M106L OS=Myxoma virus GN=m106L PE=4 SV=1 - [E2CZJ5_9POXV ]		0.00	1.82	6.91
<b>A4GDP6</b>	Serine/threonine protein kinase OS=Vaccinia virus GN=List189 PE=4 SV=1 - [A4GDP6_9POX V]	5.71	6.01		0.00
<b>B9U1H7</b>	Beta-D- galactosidase OS=Vaccinia virus GLV-1h68 GN=lacZ PE=3 SV=1 - [B9U1H7_9POX V]	4.73	2.26	17.96	5.89
<b>A0ERY5</b>	VACV-DUKE- 144 OS=Vaccinia virus GN=VACV- DUKE-144 PE=4 SV=1 - [A0ERY5_9POX V]		0.00	3.70	5.57

<b>A0ERX5</b>	VACV-DUKE- 134 OS=Vaccinia virus GN=VACV- DUKE-134 PE=4 SV=1 - [A0ERX5_9POX V]	3.62	2.82	6.04	3.94
<b>H2DY34</b>	Ankyrin-like OS=Vaccinia virus GN=VAC_DPP1 9_026 PE=4 SV=1 - [H2DY34_9POX V]			3.45	5.36
<b>B2CWP7</b>	M140R OS=Myxoma virus GN=m140R PE=4 SV=1 - [B2CWP7_9POX V]		0.00	3.34	4.16
<b>A0ERZ7</b>	Cowpox A-type inclusion protein OS=Vaccinia virus GN=VAC_DPP1 5_159 PE=4 SV=1 - [A0ERZ7_9POX V]	13.11	3.33		0.00
<b>Q80E23</b>	C3L protein OS=Cowpox virus GN=C3L PE=4 SV=1 - [Q80E23_COWP X]		0.00	1.61	2.52